Université de Montréal

PHOSPHATE HOMEOSTASIS AND TRANSPORT IN RELATION WITH THE LIVER MICROSOMAL GLUCOSE-6-PHOSPHATASE SYSTEM

par

Wensheng Xie

Département de Biochimie

Faculté de Médecine

Thèse présentée à la Faculté des études supérieures
en vue de l'obtention du grade de
Philosophiae Doctor (Ph.D.)
en Biochimie

Juillet, 2000

Université de Montréal
Faculté des études supérieures

Cette thèse intitulée:

PHOSPHATE HOMEOSTASIS AND TRANSPORT IN RELATION WITH THE LIVER MICROSOMAL GLUCOSE-6-PHOSPHATASE SYSTEM

présentée par Wensheng Xie

a été évaluée par un jury composé des personnes suivantes:

Président-rapporteur: Jurgen Sygusch

Directeur de recherche: Gérald van de Werve

Membre du jury: Daniel Lajeunesse

Examinateur externe: Ramjil Khandelwal

Thèse acceptée le:

Summary

Glucose-6-phosphatase (G6Pase), a multicomponent enzyme, plays a crucial role in glucose metabolism by hydrolyzing glucose-6-phosphate (G6P) into glucose and inorganic phosphate (P_i). G6Pase is located in the endoplasmic reticulum membrane and highly expressed in liver and kidneys. Two components of G6Pase have been cloned, the catalytic subunit (p36) and the putative G6P translocase (p46). Despite the great progress in G6Pase field, the hydrolytic mechanism of G6Pase is still in debate. Meanwhile, evidence also indicates that P_i deficiency is related to impaired glucose metabolism with an unclear mechanism. In this thesis, the effects of P_i deficiency on G6Pase and other glucoregulatory factors were investigated. Meanwhile, the hydrolytic mechanism of G6Pase was also studied in terms of its transport properties.

Results showed that compared to the rats fed with a control diet ($+P_i$), in the rats fed with a phosphate deficient diet ($-P_i$) for 48h, plasma phosphate concentration was decreased. Liver G6Pase was upregulated, gluconeogenesis key steps were stimulated, liver glycogen content was decreased and plasma glucose concentration was increased in the fed ($-P_i$) group. These changes could be accounted for by increased liver cAMP content and decreased plasma insulin concentration in the fed ($-P_i$) group. During an intravenous glucose tolerance test, although similar glucose fall rates and insulin responses were observed in overnight fasted ($+P_i$) and ($-P_i$) group, a tendency to hyperglycemia and less suppressed endogenous glucose production were obtained in the ($-P_i$) group. All of these results demonstrated that under the phosphate deficient condition, G6Pase was upregulated and glucose production was enhanced. The enhanced glucose production, potentially caused by the altered insulin/glucagon ratio, may contribute to the impaired glucose metabolism.

To further elucidate the relationship between glucose homeostasis and phosphate homeostasis, liver and kidney G6Pase system were investigated in X-linked hypophosphatemic mice, Hyp mice. Results showed G6Pase activity was increased in

Hyp mouse liver and kidney. Consistently, the protein amount and mRNA abundance of the catalytic subunit, p36, were increased in Hyp mouse liver and kidney. In contrast, the mRNA abundance and protein amount of p46 were decreased in Hyp mouse liver and kidney. These results further demonstrated that G6Pase activity was stimulated by P_i deficiency. The increased G6pase activity may enhance glucose production, probably contributing to impaired glucose metabolism.

The hydrolytic mechanism of G6Pase was investigated via transport studies. Inorganic phosphate (KH_2PO_4) transport across microsomes showed identical $T_{1/2}$ values around 23 s at different KH_2PO_4 concentrations, which were unaffected by potential inhibitors of G6Pase. Neither accelerated exchanging transport nor saturable effect was observed in this process. These results supported no specific inorganic phosphate transporter in the ER membrane. Similar phenomena were observed for the glucose transport process, which was characterized with $T_{1/2}$ values of 40 s. Tracer equilibration during [U-^{14}C]- and [^{32}P]G6P hydrolysis proceeded with $T_{1/2}$ values of 47 and 21 s, respectively. Steady state levels of tracer accumulation from [U-^{14}C]- and [^{32}P]G6P were also different from each other and had a similar ratio to that of their $T_{1/2}$ values. This result demonstrated that the accumulated radiotracer was the product, P_i or glucose, rather than the substrate G6P. Effects of unlabelled G6P and inhibitors on [^{32}P]G6P uptake demonstrated that G6P uptake and hydrolysis were tightly coupled processes. Moreover, no exchanging transport between G6P and inorganic phosphate/glucose was observed. These results are not compatible with the substrate-transport model of G6Pase. Based on these data, a new combined-conformational model is proposed to explain the G6Pase system. In this model, G6P transport/hydrolysis are tightly coupled processes whereas glucose and phosphate share with water and a variety of other organic and inorganic solutes a common pore-like structure accounting for their transport through the ER membrane. The p46 protein may be more like a G6P sensor than a G6P transporter. The binding of G6P to p46 may affect the conformation of p46 and p36 via their coupling interaction. The conformational change may account for the specificity and latency of G6Pase.

Résumé

La production hépatique de glucose dérive du glucose-6-phosphate (G6P) produit par la glycogénolyse et la néoglucogénèse et son hydrolyse subséquente par la glucose-6-phosphatase (G6Pase). C'est pourquoi la G6Pase joue un rôle crucial dans le maintien de la glycémie. La G6Pase est un système enzymatique à plusieurs composantes, situé dans le réticulum endoplasmique (RE) et est exprimé dans les deux organes néoglucogéniques, foie et rein, ainsi que dans l'intestin. Jusqu'à maintenant, deux composantes du système ont été clonées, l'unité catalytique qui est une protéine de 36 kDa (p36) et un transporteur putatif de G6P de masse moléculaire de 46 kDa (p46). Depuis le clonage du gène et de l'ADNc de p36, la régulation de l'expression de p36 a été étudiée en détail. Des effecteurs positifs qui augmentent l'ARNm de p36 comprennent le glucose, l'AMP cyclique, les glucocorticoïdes et les acides gras, tandis que l'insuline diminue l'abondance de l'ARNm de p36. Le glucose, l'AMP cyclique et les glucocorticoïdes ont également un effet positif sur l'ARNm de p46, tandis que l'insuline contrecarre ces effets. Deux modèles ont été proposés pour expliquer le mécanisme fonctionnel du système G6Pase : le modèle de transport du substrat et le modèle conformationnel. Le premier propose que la G6Pase est un système à plusieurs composantes, comprenant une unité catalytique dont le site actif est orienté vers la lumière du RE, un transporteur de G6P appelé T1, un transporteur de phosphate inorganique (P_i) appelé T2 et un transporteur de glucose appelé T3. T1 serait l'étape limitante de la conversion de G6P en glucose et P_i. Il a été proposé que des mutations dans les gènes de ces quatres composantes causent des glycogènoses de type Ia, Ib, Ic, and Id, respectivement. Le modèle conformationnel propose que la G6Pase est une protéine formant un canal dans la membrane du RE, où le site actif est enfoui dans une poche hydrophile. Le substrat a accès au site actif via le canal. Le processus hydrolytique a lieu dans la poche hydrophile et les produits sont délivrés dans la lumière et exportés dans le cytoplasme par l'intermédiaire du

canal. Les cinétiques rapides d'hydrolyse du G6P indiquent une transition hystérétique dans le processus catalytique qui réduit la vitesse de la réaction au profit d'une spécifité accrue pour le G6P.

Le phosphate inorganique (P_i) est une composante fondamentale de l'organisme par son implication dans de nombreuses fonctions physiologiques. L'homéostasie du Pi est règlée au niveau du rein par sa réabsorption par un co-transporteur de sodium et de phosphate (NaP_i), essentiellement l'isoforme NaP_i-2. Le contenu en P_i dans la diète, qui est important pour le maintien de la phosphatémie normale, affecte l'expression de la NaP_i-2, de l'hormone parathyroïdienne, du P_i et du calcium sérique. L'hypophosphatémie liée au chromosome X est causée par une mutation dans le gène PHEX (pour : Phosphate-regulating gene with Homologies to Endopeptidase located on the X chromosome).

Des travaux établissant que des perturbations dans l'homéostasie du phosphate pouvaient causer une intolérance au glucose et une résistance à l'insuline suggèrent une association entre l'homéostasie du glucose et du phosphate. La nature même de cette association est néanmoins encore inconnue. Nous avons donc investigué le métabolisme du glucose hépatique lors d'une diète déficiente en phosphate ainsi que chez un modèle animal d'hypophosphatémie liée au chromosome X, la souris Hyp. Les résultats montrent que le phosphate plasmatique était diminué chez des rats nourris pendant 48h avec une diète déficiente en P_i ($-P_i$) comparés à une diète contrôle ($+P_i$). Dans le groupe ($-P_i$), l'activité de la G6Pase hépatique était augmentée lorsque mesurée dans des microsomes intacts ou perméabilisés au moyen de détergent, à des concentrations de substrat physiologiques ou saturantes. Cette activité accrue était due à une stimulation de l'expression de l'unité catalytique, comme en témoigne l'augmentation de l'abondance de l'ARNm et de l'immunoréactivité de p36. L'ARNm de p46 était également augmentée dans le groupe ($-P_i$), mais sans changement dans la quantité de protéine. Nos études subséquentes montrèrent que dans le foie des animaux du groupe ($-P_i$), la pyruvate kinase était inactivée et le phosphoenolpyruvate augmenté, et que le fructose-2,6-bisphosphate, un inhibiteur de la néoglucogénèse, était réduit de moitié. L'activité de

la glucokinase n'était pas modifiée et celle de la phosphoenolpyruvate kinase était marginalement augmentée par la diète ($-P_i$). L'ensemble de ces résultats peuvent s'expliquer par l'augmentation de la concentration de l'AMP cyclique observée dans le foie des rats nourris avec la diète ($-P_i$). Ces résultats suggèrent que la néoglucogénèse hépatique pourrait être stimulée dans des conditions d'hypophosphatémie et qu'une production accrue de glucose pourrait contribuer à une altération du métabolisme du glucose. Cette possibilité est renforcée par l'observation que la glycémie des rats nourris avec la diète ($-P_i$) était nettement augmentée, tandis que la concentration de l'insuline plasmatique était diminuée. Un test de tolérance intravéneuse au glucose n'a pas permis d'observer de différence au niveau de la normalisation de la glycémie, mais a cependant indiqué une légère intolérance au glucose dans la mesure ou le pic de glucose atteint après le test était plus élevé dans le groupe ($-P_i$). Par ailleurs, la production endogène de glucose était nettement moins inhibée après un bolus de glucose au cours du test de tolérance intravéneuse au glucose.

Afin d'élucider d'avantage la relation entre homéostasie du glucose et du P_i, le système G6Pase de foie et de rein furent examinés chez la souris Hyp. Les résultats montrent que l'activité de la G6Pase était augmentée dans ces organes des souris Hyp, semblablement à l'augmentation observée chez les rats nourris avec la diète ($-P_i$). Cette activité accrue de la G6Pase chez la souris Hyp s'explique par une plus grande quantité d'ARNm et de protéine p36, aussi bien dans le foie que dans le rein. Contrairement au modèle diététique d'hypophosphatémie, chez la souris Hyp l'abondance de l'ARNm et l'immunoréactivité du p46 hépatique et rénal sont nettement diminués.

Globalement, l'hypophosphatémie résultant soit d'une carence alimentaire ou due à un défaut génétique a pour effet d'augmenter de façon consistante l'activité de la G6Pase, elle-même causée par une stimulation de l'expression de son unité catalytique, p36. L'expression de p46 est différemment règlée par la diète déficiente en P_i ou dans le modèle génétique, indicant que d'autres facteurs que

l'hypophosphatémie affectent ce gène dans ces conditions. Il apparaît que la régulation de l'expression de p36 et de p46 est distincte.

Bien que le système G6Pase a été étudié depuis voici cinquante ans, son organisation et son mécanisme fonctionnel restent à être définis. Les propriétés cinétiques de transport du substrat, le G6P, et des produits, le glucose et le P_i, ne sont pas encore élucidés. Ces propriétés ont été investiguées au moyen d'un appareil à collection et filtration rapide (FSRFA). Le transport microsomal du Pi montre des valeurs identiques de $T_{½}$ à différentes concentrations de KH_2PO_4. Le $HgCl_2$ et des inhibiteurs potentiels de la G6Pase n'affectent pas les propriétés cinétiques du transport de P_i. On n'a également pas trouvé d'échange accéléré de P_i ou de saturation du transport de celui-ci. Ces résultats ne sont pas compatibles avec l'existence d'un transporteur spécifique pour le P_i dans la membrane du RE. Des conclusions similaires ont été tirées d'études du transport microsomal du glucose.

L'accumulation intramicrosomale de radioactivité à partir de [U-^{14}C]G6P ou de [^{32}P]G6P correspond à des paramètres cinétiques différents, indicant que les substances accumulées dans les microsomes à partir de G6P sont les produits de la réaction de la G6Pase plutôt que le substrat. Cette observation suggère que l'étape de transport du G6P, si tant est qu'elle existe, n'est pas l'étape limitante au cours de la conversion du G6P en glucose et P_i. Les paramètres cinétiques d'accumulation de radioactivité à partir de [^{32}P]G6P et les effets des inhibiteurs de la G6Pase démontrent que cette accumulation est étroitement couplée à l'activité hydrolytique de la G6Pase. De plus, nous n'avons pas observé d'échange de transport entre le G6P et le P_i ou le glucose, en accord avec l'absence présumée de transporteur spécifique pour le P_i ou le glucose. Globalement, ces données sont compatibles avec le modèle conformationnel de la G6Pase. Une nouvelle version de ce modèle, intégrant les résultats concernant le transport de P_i et de glucose, propose qu'un pore dans la membrane du RE puisse remplir la fonction d'influx/efflux des produits de la G6Pase.

Table of contents

List of tables

List of figures

Figures in articles

Article 1:

Article 2:

Article 3:

Article 4:

Article 5:

Abbreviations

ATP:	adenosine triphosphate
CHL:	chlorogenic acid
Cyclic AMP (cAMP):	adenosine 3': 5'-cyclic monophosphate
ER:	endoplasmic reticulum
Fru-1,6-P_2:	fructose-1,6-bisphosphate
Fru-2,6-P_2	fructose-2,6-bisphosphate
Fru-2,6-P_2ase:	fructose-2,6-bisphosphatase
Fru-6-P:	fructose-6-phosphate
FSRFA:	fast-sampling, rapid-filtration apparatus
GK:	glucokinase
GLUT:	the facilitative glucose transporter family
G6P:	glucose-6-phosphate
G6Pase:	glucose-6-phosphatase
GSD:	glycogen storage disease
HK:	hexokinase
Hyp mice:	X-linked hypophosphatemic mice
IVGTT:	intravenous glucose tolerance test
M6P:	mannose-6-phosphate
NaP_i cotransport:	sodium-dependent phosphate cotransport
1,25$(OH)_2$-D_3 :	1,25-dihydroxyvitamin D_3
P:	phosphorus
p36:	the catalytic subunit of glucose-6-phosphatase
p46:	the putative glucose-6-phosphate translocase
PEP:	phosphoenolpyruvate
PEPCK:	phosphoenolpyruvate carboxykinase
6-PF-1-K:	6-phosphofructo-1-kinase

6-PF-2-K/Fru-2,6-P_2ase:	6-phosphofructo-2-kinase/fructose-2,6-bisphosphatase
PHEX:	a phosphate-regulating gene with homologies to endopeptidase located on the X-chromosome
P_i:	inorganic phosphate
(-P_i) group:	rats fed with P_i deficient diet for 48h
(+P_i) group:	rats fed with control diet for 48h
PI3K:	phosphatidylinositol 3-kinase
PK:	pyruvate kinase
PKA:	protein kinase A
PP_i:	inorganic pyrophosphate
PTH:	parathyroid hormone
SGLT:	sodium-dependent glucose transporter family
T1:	G6P translocase in ER membrane
T2:	P_i, PP_i and carbamyl-P translocase in ER membrane
T3:	glucose translocase in ER membrane
UhpC:	upper hexose phosphate ester receptor
UhpT:	upper hexose phosphate ester transporter
XLH:	X-linked hypophosphatemic rickets

ACKNOWLEDGEMENT

This thesis is done for my daughter, Ranran! There are three years in her childhood without her mother. Ranran, Mom love you and wish you happy in your whole life.

Here, I express my deep gratitude to Prof. Gérald van de Werve for his scientific guiding during the course of my Ph.D. study, for his encouraging and helping in my foreign-student's life, and for his understanding at the difficulties of my studying and living in a foreign country.

I would like to express a heartfelt thank to Dr. Alfred Berteloot for his helping and guiding in my studies. His knowledge and strict scientific spirit showed me how to become a good scientist.

I would also like to thank Dr. Diane T. Finegood for her big help in the experiments and manuscript correction. Because of her welcome, I had a chance to learn a number of new things, and spent a wonderful three weeks in her laboratory.

A heartfelt thank to Dr. Marc Prentki for his help in the experiments and in my career.

A heartfelt thank to Dr. Jiang-Ping Wu for his help in my studies and many other aspects.

I would also like to say thank you to Drs. Marie-Claire Méchin and Yazhou Li for sharing the enjoyment in G6Pase research. We spent a common period in the 8th floor, Pavillon Mailloux. And also, Marie-Claire, you are the first person I met in Montreal. Wish both of you a successful career and a happy life.

A special thank to T. Luong Tran for his big help in the IVGTT experiments. Without his participation, this experiment would have been unable to be performed.

Thanks to Dr. Daniel Lajeunesse and Stephanie Dubois for help in the experiments and discussion.

A special thank to Guylaine Gévry for the absolutely-necessary help in the laboratory stuff and thesis graphics.

Many thanks to Drs. Hong-Yu Luo, Xing-Zhen Chen, Xiang-Jiao Yang and Xiao-Chun Wan, and Mr. and Mrs. Xi-Lin Zhang, for their friendship and help.

Thanks to others who helped me and encouraged me during my years in Canada.

Finally, a heartfelt thank to my family, my husband and my mother, for their supports for my far-away studying.

Chapter I Liver Glucose-6-phosphatase System

I.1 Introduction

Glucose-6-phosphatase (EC 3.1.3.9, G6Pase) is a key enzyme in gluconeogenesis and glycogenolysis by hydrolyzing glucose-6-phosphate (G6P) into glucose and inorganic phosphate (P_i). It is also capable of catalyzing the hydrolysis of inorganic pyrophosphate (PP_i) as well as the synthesis of G6P from carbamyl-P or PP_i and glucose. These reactions are shown below:

$$G6P + H_2O \longrightarrow Glucose + P_i \quad (1)$$

$$PP_i + H_2O \longrightarrow 2\,P_i \quad (2)$$

$$PP_i + Glucose \longrightarrow G6P + P_i \quad (3)$$

$$Carbamyl\text{-}P + Glucose \longrightarrow G6P + NH_3 + CO_2 \quad (4)$$

Reaction (1) is the main physiological function of G6Pase. Although, evidence indicates the *in vivo* phosphotransferase activity of G6Pase, as reactions (2), (3) and (4), the physiological significance of this activity has not yet been determined [Foster et al., 1997].

G6Pase is a multicomponent system, located in the endoplasmic reticulum (ER) membrane. Until now, two components of G6Pase have been cloned. The cDNA coding the catalytic subunit, a 36 kDa protein (p36), was first isolated in mouse

[Shelly et al., 1993], and later on, in human [Lei et al., 1993] and rat [Argaud et al., 1996]. From its primary sequence, p36 was characterized as a hydrophobic protein of 357 amino acids. Recently, cDNA of another component of G6Pase, a 46 kDa protein (p46) which was proposed to have G6P transport function, was cloned [Gerin et al., 1997]. G6Pase system is highly expressed in the two gluconeogenic organs, liver and kidneys. Even though they have almost the same characteristics, the liver and the kidney G6Pase have specificities in their regulations as detailed below. G6Pase also exists in pancreas and small intestine [Foster et al., 1997]. The function of G6Pase in pancreas and intestine is still unclear. In pancreas, which contains a G6Pase related protein, the function of G6Pase might be linked to the insulin secretion signalling by controlling the G6P level [Arden et al., 1999].

Catalyzing the last step in gluconeogenesis and glycogenolysis, G6Pase is important for the regulation of blood glucose concentration and glycogen metabolism. Together with glucokinase, G6Pase controls the G6P/glucose cycle, where G6P and glucose themselves can regulate a number of metabolic processes, such as glycogen synthesis. The crucial role of G6Pase in the whole body metabolism is demonstrated via its dysfunction which causes glycogen storage disease type I (GSD I). GSD I is characterized by abnormal glycogen storage, severe hypoglycemia, growth retardation, hepatic steatosis, renal failure, lactic acidosis, and hyperlipidaemia [Burchell 1998a; Chou & Mansfield, 1999]. On the other hand, increased G6Pase activity is thought to play an important role in hyperglycemia in diabetes. Although major advances have been made in the G6Pase research field

through the last couple of years and the understanding of the G6Pase system has been improved greatly at the biochemical and molecular levels [van de Werve et al., 2000], the hydrolytic mechanism, the components and their functions, as well as the regulation of G6Pase system still have to be elucidated.

I.2 The G6Pase system

The G6Pase system is located in the ER membrane so that microsomes, i.e. membrane vesicles enriched in ER membrane, are generally used as an *in vitro* material to study structure and function properties of G6Pase. Currently there are two models describing the structure-function relation of G6Pase: the substrate-transport model and the combined-conformational flexibility model. Their principles and experimental basis will be detailed in the following sections.

I.2.1 The substrate-transport model

The substrate-transport model was proposed by Arion based on the kinetic parameters of G6Pase hydrolysis [Arion et al., 1975, 1976, 1980]. As shown in Fig.1, this model proposes that G6Pase is a multicomponent system, including (i) a non-specific catalytic subunit with the active site oriented towards the intramicrosomal space (the luminal side of the ER membrane); (ii) a G6P transporter designated as T1, which specifically recognizes and transports G6P across the ER membrane; (iii) a phosphate transporter (T2) which can transport the product inorganic phosphate, PP_i and carbamyl-P across the ER membrane; and (iv) a glucose transporter (T3) which transports glucose across the ER membrane. The mutations of these components are

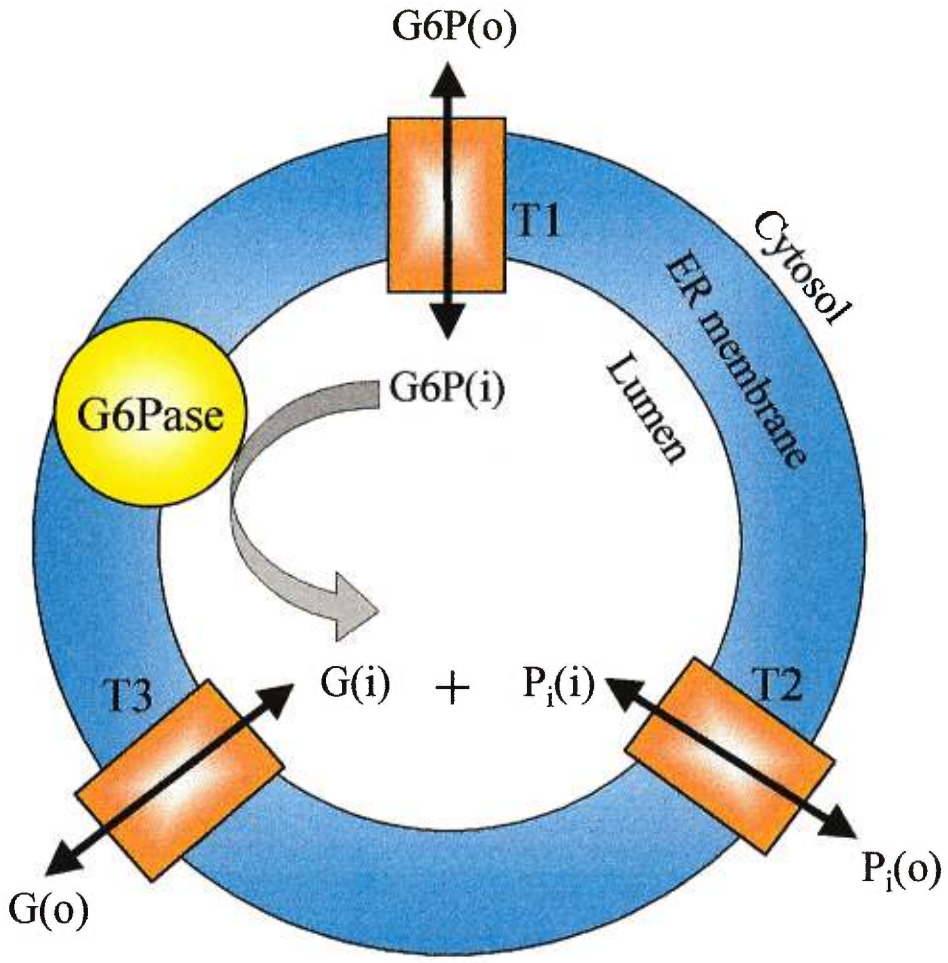

Figure 1 Substrate transport model of G6Pase

In this model, the catalytic subunit of G6Pase is located in the ER membrane with the active site oriented toward the luminal side. T1 is responsible for the G6P transport from the cytosol to the lumen, T2 and T3 are responsible for the export of the products, inorganic phosphate and glucose, respectively. The indices o and i refer the cytosol side and luminal side, respectively.

proposed to cause GSD Ia, Ib, Ic and Id, respectively. According to this model, G6P has to be transported into the lumen of the ER membrane to be hydrolyzed by the catalytic subunit, and the G6P transport step is the rate-limiting step in the G6Pase system. The first basis of this model is the latency of G6Pase, namely, the activity almost doubles after detergent treatment of microsomes [Nordlie & Jorgenson, 1981]. It was interpreted that the disruption of microsomal membrane by detergent abolishes the constraint of substrate availability so that the substrate is fully accessible to the active site. The second basis of this model is a loss of the specificity of the enzyme for G6P in permeabilized vesicles. Intact microsomes only catalyze G6P hydrolysis, but after detergent treatment of microsomes, the enzyme can hydrolyze not only G6P, but also mannose-6-phosphate (M6P) and other substrates [Arion et al., 1976]. This was also explained by the free access of the active site to these substrates after the membrane was disrupted by detergents. Effects of some inhibitors of G6Pase also meet the concept of this model because they inhibit G6Pase activity in intact microsomes, but have no effects after microsomes are treated with detergents. One representative of these inhibitors is chlorogenic acid (CHL). CHL is a competitive inhibitor of G6P in intact microsomes, but has no effect on the enzyme of fully disrupted microsomes or the inorganic pyrophosphatase activity of G6Pase [Arion et al., 1997]. It is supposedly because CHL interacts with the G6P translocase (T1) and prevents the access of the substrate to the catalytic subunit. After detergent treatment, the substrate can bind to the active site directly so that CHL has no effect. Using a synthetic analogue of CHL, it was further demonstrated that two G6P binding sites

were involved in the hydrolytic process of G6P in intact microsomes [Arion et al., 1998], indicating the existence of a G6P binding protein other than the catalytic subunit. Data from these biochemical studies are compatible with the concept of a specific G6P translocase. Meanwhile, the topology study of the catalytic subunit also backs up this model. A new transmembrane model of p36, which is different from the former six transmembrane domain model of p36 [Lei et al., 1995a], was proposed by comparing the active site of vanadate-containing chloroperoxidase with that of G6Pase [Hemrika & Wever, 1997]. This new model was confirmed by immunodetection of flagged protein and partial proteolysis [Pan et al., 1998]. Using N- and C-terminal tagged p36 transient expression, Pan et al [1998] found that in intact microsomes from the transfected cells, the N-terminus of p36 was resistant while the C-terminus was sensitive to protease digestion. This result implied that p36 possessed an odd number of transmembrane helices with its N- and C- terminus facing the ER lumen and the cytoplasm, respectively. It has been demonstrated that during catalysis, a phosphoryl-enzyme intermediate (E-P) is formed between the imidazolium group of a histidine residue on the enzyme and the phosphate moiety of G6P [Nordlie & Lygre, 1966; Feldman & Butler, 1972]. On the basis of sequence alignment of p36, lipid phosphatases, acid phosphatase, and a vanadium-containing chloroperoxidase, Pan et al [1998] also characterized this E-P complex in that Arg-83, His-119, and His-176 in p36 contributed to the active site and that His-176 covalently bound the phosphoryl moiety of G6P during catalysis. Based on these

data, they predicted a nine transmembrane helical structure of G6Pase with the active site oriented towards the luminal side.

Besides these biochemical studies, gene cloning provides more and more information about the G6Pase system at molecular level. The cDNA encoding the G6Pase catalytic subunit was cloned first from mouse by taking advantage of an albino mouse which had markedly reduced G6Pase activity [Shelly et al., 1993]. Right after that, human p36 cDNA was cloned and mutations were found in GSD Ia patients [Lei et al., 1993], further demonstrating the function of p36 in the G6Pase system. From then on, more than 40 mutations have been discovered in GSD Ia patients [Foster et al., 1997; Keller et al., 1998; Lam et al., 1998; Bruni et al., 1999; Rake et al., 1999; Stroppiano et al., 1999; Trioche et al., 1999;]. These mutations include homozygous, heterozygous site mutations, insertions or deletions, resulting in unfunctional protein or no protein expression. Among all of these mutations, the R83C/H is more prevalent [Lei et al., 1995b; Chevalier et al., 1996; Lee et al., 1996]. These studies not only elucidated the molecular properties of G6Pase, but also established the molecular basis and precise diagnosing methods for GSD Ia. It also set up molecular data for gene therapy for this most prevalent form of GSD I. In a recent study, the adenoviral vector containing the murine p36 gene was infused into G6Pase-deficient ($G6Pase^{-/-}$) mice that manifested symptoms of human GSD Ia [Zingone et al., 2000]. It was found that liver G6Pase activity was restored to 70% of normal level in infused $G6Pase^{-/-}$ mice, and 100% infused mice survived as compared to a 15% survival rate of $G6Pase^{-/-}$ mice, furthermore, all the symptoms were reduced

to near normal level. This result demonstrated that dysfunction of p36 was the primary cause for GSD Ia.

Taking advantage of the weak homology to the gene of bacterial upper hexose phosphate ester transporter (UhpT), the putative G6P transporter (p46) cDNA was cloned from the human liver and mutations were found in two GSD Ib patients [Gerin et al., 1997]. Based on the homology to UhpT and the mutations in GSD Ib patients, p46 was proposed to represent the G6P translocase, T1. The p46 cDNA was subsequently cloned in the liver of rat and mouse [Lin et al., 1998a], and the human p46 gene was characterized [Ihara et al., 1998; Marcolongo et al., 1998]. Besides in liver and kidney, p46 is expressed in heart, brain and leucocytes [Middleditch et al., 1998; Lin et al., 1998a]. From its cDNA sequence, p46 was characterized as a membrane protein with 429 amino acids containing an ER transmembrane protein retention signal at its C-terminus [Gerin et al., 1997]. Using transient expression of N- and C-terminal tagged p46 and alignment analysis, it has been reported that p46 has ten transmembrane domain with both N-and C-terminus towards the cytoplasm [Pan et al., 1999; Méchin & van de Werve, 2000a].

The function of p46 was investigated through its expression in cells. When p46 cDNA alone was transfected into COS-1 cells, a significant but very small amount of radioactivity uptake from [^{14}C]G6P was observed, whereas no uptake occurred with the transfection of p36 cDNA alone, while, a much higher amount of radioactivity uptake from [^{14}C]G6P occurred when p46 and p36 were expressed together in COS-1 cells [Hiraiwa et al., 1999]. These results were consistent to those observed in p36

knockout mice. The p36 gene was experimentally disrupted in mice, and these animals manifested essentially the same pathophysiology as human GSD Ia patients [Lei et al., 1996]. Interestingly, liver microsomes from p36 knockout mice had no G6P uptake at all, suggesting that either G6Pase activity was required for G6P transport into the microsomes or that G6Pase was its own substrate transporter [Lei et al., 1996]. The low G6P transport function of p46 in the absence of p36 suggests that there might be a coupling interaction between p46 and p36, which could affect the conformation and function of each other. With regard to the function of p46, another point worthy to remember is that p46 is expressed in tissues such as brain, heart, netrophils and monocytes, where p36 is not expressed [Middleditch et al., 1998; Lin et al., 1998a]. In addition, GSD Ib patients have neutropenia and impaired neutrophil function which are distinct from GSD Ia patients [Bashan et al., 1993]. From these facts, one may consider that p46 could have other function(s) than G6P transport. Studies on the ontology of p46 and p36 are also consistent with this suggestion. Unlike the adult G6Pase system, liver microsomes from a mouse (before one day of age) had G6Pase activity, but no intravesicular radioactivity accumulation from labelled G6P was observed [Annabi & van de Werve, 1997]. It was demonstrated later using immunodetection that liver p36 immunoreactivity was low in rats of 20th and 21st days of gestation, as well as 6 hours after birth, but sharply increased at 1 day postpartum [Méchin et al., 2000b]. Unlike p36, p46 protein was already present in fetal rat liver microsomes at levels similar to those found in 7-day-old rat liver microsomes. Corresponding to p36 immunoreactivity, liver G6Pase activity was low

in fetal rat and 6 hours after birth rat, but increased to maximal activity at 1 day postpartum. In contrast, G6P uptake was undetectable before birth and up to 6 hours after birth, but appeared at 1 day postpartum [Méchin et al., 2000b]. These data clearly showed that there was G6Pase activity in the absence of G6P uptake. Another group also showed that p36 was present in 18-day fetal rat liver and G6Pase activity was also present [Puskàs et al., 1999]. But fetal rat liver microsomal G6Pase activity was not latent, namely, disruption of microsomes did not increase the activity, even though radioactivity accumulation was observed in the presence of labelled G6P, P_i or glucose [Puskàs et al., 1999]. From these observations, one would consider that p46 may not necessarily be responsible for G6P transport for operative G6pase.

The other two transporters, T2 and T3, have neither been identified nor characterised. Studies on them will be detailed below.

I.2.2 The combined- conformational flexibility model

The conformational model was first introduced by Schulze [Schulze et al., 1986], and later on developed based on the rapid kinetic studies [Berteloot et al., 1991a, 1995]. As shown in Fig.2, in the modified conformational model, G6Pase is interpreted as an intrinsic membrane protein spanning the entire microsomal membrane and forming a channel like structure for the flux of the substrate and products. The catalytic site is embedded to some extent within the membrane and forms a hydrophilic pocket, which is accessible for the substrate and where the hydrolysis takes place. Glucose released at that site could be either exported to the

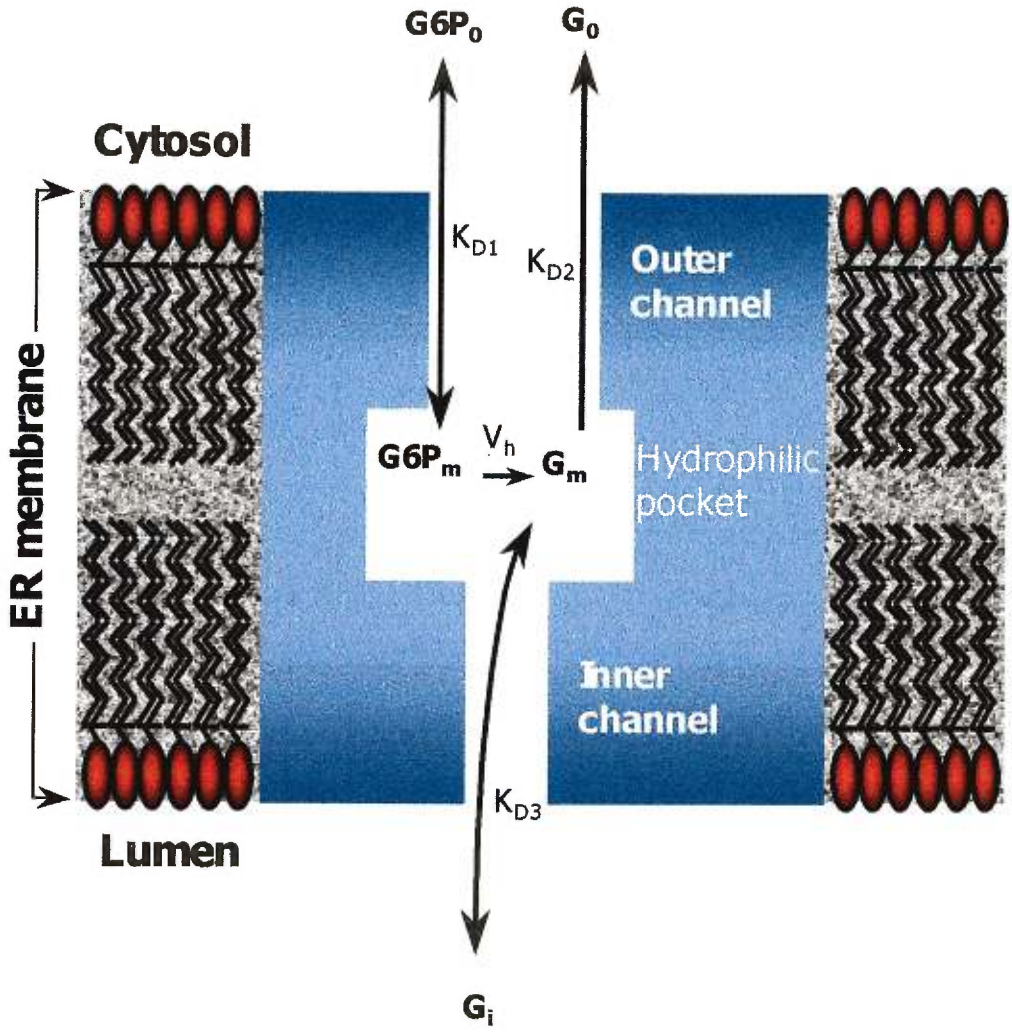

Figure 2 Combined-conformational flexibility model of G6Pase

In this model, G6Pase is depicted as a membrane protein with the active site lying in a hydrophilic pocket deep inside of the protein where G6P hydrolysis occurs. Outer and inner channels, which are responsible for the transport of G6P and glucose, have different intrinsic permeabilities to G6P and glucose. Through the outer channel, most of the product, glucose, goes to the external medium directly. Indices o, m, and i refer to the cytosol side, the hydrophilic pocket and the luminal side, respectively.

external medium through the outer channel or accumulated in the lumen via the inner channel. The outer channel allows the substrate and glucose transport but has some specificities so that intact microsomal G6Pase shows substrate and inhibitor specificities. A hysteretic transition from presteady-state to steady-state occurs during the binding and hydrolysis process. According to this model, the latency of G6Pase is due to the G6Pase transformation from a form with high affinity and low specificity to a form with low affinity but high specificity, while the detergent treatment affects membrane status and keeps the enzyme in the form with high affinity but low specificity. This model was supported by the following results: 1. A presteady-state burst in the rate of G6P hydrolysis was observed [Berteloot et al., 1991a]; 2. No radioactivity compound (G6P and/or glucose) from [U-^{14}C]G6P was taken up by liver microsomes from a GSD Ia patient [St-Denis et al., 1994]; 3. Glucose influx from hydrolysis of G6P into microsomes was tightly linked to G6Pase activity, and occurred via a diffusion process [St-Denis et al., 1995a], 4. Histone II-A stimulated G6Pase without permeabilization of microsomes [St-Denis et al., 1995b]. The presteady-state burst in the rate of G6P hydrolysis in intact microsomes was found identical to the hydrolysis rate in the presence of detergent, which is not compatible to the substrate-transport model. This burst was observed in another study of our laboratory [Vidal et al., 1992] showing that pre-incubation of G6P or M6P with intact microsomes suppressed the burst in G6Pase activity, but the burst was recovered after the substrate was completely hydrolysed. This observation further indicated the hysteretic transition during the hydrolysis process. The burst was also confirmed by another laboratory [Ajzannay et al., 1996], which found that G6Pase was able to

hydrolyze both G6P and M6P at similar high rates during the presteady-state/hysteretic transition period. This result suggested that G6P and M6P are similarly accessible to the active site in intact microsomes and the active site is oriented towards the cytoplasmic side. Meanwhile, this group also showed that G6Pase of detergent-treated microsomes was able to hydrolyze preferentially G6P rather than M6P when both were present together [Ajzannay et al., 1994]. This result demonstrated that G6Pase of disrupted microsomes still exhibited a specific, albeit limited kinetic behaviour to G6P even both G6P and M6P were hydrolyzed with the same affinities and rates when present alone. Hence it was suggested that the role of the membrane toward G6Pase in intact microsomes appeared to be to potentiate the preexisting specificity of the enzyme [Ajzannay et al., 1994]. Further studies showed that glucose accumulation was tightly linked to G6Pase hydrolytic activity and the first rapid radioactivity uptake from [U-^{14}C]G6P is an exchangeable glucose pool rather than G6P [Berteloot et al., 1995]. Furthermore, the steady-state rate of G6P hydrolysis in intact microsomes is 10-fold higher than the glucose uptake, indicating more than 90% glucose product is directly output to the cytoplasm. Besides these kinetic studies, another important support for the conformational model was the effect of histone II-A on G6Pase. As mentioned previously, the substrate-transport model proposes that the detergent treatment of microsomes permeabilizes the vesicles so that it stimulates G6Pase activity by allowing free access of G6P to the active site. In contrast, the effect of histone II-A on G6Pase activity does not support that microsomes have to be permeabilized in order to increase the activity. Histone II-A

stimulates G6Pase to the same extent as detergents, but the radioactivity accumulation from [U-^{14}C]G6P was increased in histone II-A treated microsomes, demonstrating that histone II-A did not permeabilize the vesicles [St-Denis et al., 1995b]. The effect of histone II-A was further confirmed by other studies [Pederson et al., 1998a/b]. All of these data suggest that histone II-A stimulate G6Pase activity by a different mechanism from permeabilizing the vesicles to allow free access of G6P to the active site. It is likely that histone II-A and other detergents affect the membrane structure so that the conformation of G6Pase is also affected, resulting in stimulated hydrolytic activity.

I.3 Glucose transport

There are two classes of glucose transporters, the Na^+-dependent glucose transporter family (SGLT) and the facilitative glucose transporter family (GLUT). SGLT is an active, Na^+-dependent glucose transport protein, mainly located in intestinal brush border membranes and renal proximal convoluted tubules. They are responsible for the absorption and reabsorption of glucose. SGLT is generally constitutively expressed and not subjected to hormonal regulation. GLUT is energy independent, driven by glucose concentration gradient across the plasma membrane. Six GLUT genes in mammalian cells have been identified and characterized. GLUT1 is highly expressed in erythrocytes and the blood brain barrier, GLUT2 is in hepatocytes and pancreatic β-cells, GLUT3 is responsible for glucose supply to neurones, GLUT4 is in adipose tissue and muscle, GLUT5 is a fructose transporter

and GLUT6 is a pseudo gene [Olsen & Pessin, 1996]. Recently, a previously unidentified member of GLUT was reported as GLUT8, which was expressed in blastocysts, subjected to insulin regulation, and might be responsible for blastocyst development [Carayannopoulos et al., 2000]. In the hepatocyte plasma membrane, GLUT2 is the major form (more than 90%) responsible for glucose transport, with about 10% of GLUT1. These two glucose transporter are constitutively expressed and in contrast to GLUT4, not subjected to insulin regulation [Olson & Pessin, 1996].

It is proposed in the substrate-transport model that the product glucose of G6Pase is transported out of the ER membrane via a transport protein T3. The theoretical dysfunction of T3 is proposed to cause GSD Id. Only one GSD Id case has been reported so far [Veiga-da-Cunha et al., 1999]. A 52 kDa protein was isolated from rat liver ER membrane, which was claimed to represent T3 [Waddell et al., 1991], and a rat liver cDNA (GLUT7) was cloned via screening using an antibody raised against GLUT2 [Waddell et al., 1992]. But GLUT7 turned out to be a cloning artefact [Burchell, 1998b]. Therefore, the molecular basis for glucose transporter in ER is still uncertain and glucose transport studies rely mainly on kinetic studies using liver microsomal preparations. Using a fast-sampling, rapid-filtration apparatus (FSRFA) [Berteloot et al., 1991b], it was observed that [U-^{14}C]glucose accumulated into microsomes with a $T_{1/2}$ around 35 sec in the presence of zero-trans concentration of [U-^{14}C]G6P [St-Denis et al., 1995a]. [U-^{14}C]glucose efflux from pre-loaded microsomes with [U-^{14}C]G6P also initiated by the addition of cold G6P to the microsomal incubation medium. Consistently, the efflux $T_{1/2}$ value was in the range

of 30-50 sec and was insensitive to intramicrosomal glucose concentration up to 20 mM. It was concluded that glucose equilibration through microsomes occurred by diffusion over a physiological range of glucose concentration. In contrast, using a light-scattering technique, Marcolongo et al [1996] reported a facilitative glucose transport process based on their observation of a rapid glucose influx into rat liver microsomes, which was saturable at [glucose] $\geq$ 100 mM. But a similar permeation of ascorbic acid, L-glucose and other monosaccharides was also observed in that study, hence, lessening the argument of a facilitative transporter which should be stereospecific. Another study showed, using [^{14}C] labelled glucose and rapid filtration technique, that glucose was accumulated into microsomal vesicles with an almost linear correlation of its rate with glucose concentration up to 100 mM [Bànhegyi et al., 1998]. Neither cytochalasin B nor phloretin inhibited the glucose accumulation, and a glucose efflux was also observed from G6P preloaded microsomes. All of these data from these two reports are not unequivocally compatible with a facilitative transporter, although the authors concluded that it was a facilitative glucose transport process with a saturable glucose concentration above 100 mM. From all described above, the nature of glucose transport in the ER membrane is still controversial and deserves more studies.

I.4 Phosphate transport

In the intestine and the kidneys, both anion exchange phosphate transport and sodium phosphate (NaP_i) cotransport are responsible for phosphate absorption and

reabsorption. However, the renal NaP_i cotransport appears to be more significant to the regulation of phosphate homeostasis, therefore, it has been more profoundly studied and better characterized. The renal NaP_i cotransporters identified so far are classified into type I and type II NaP_i cotransporter [Biber et al., 1996]. Type I NaP_i cotransporter is also expressed in liver plasma membrane [Ghishan et al., 1993]. It was shown in this study that the liver plasma membrane P_i transporter was sodium dependent, with a V_{max} of 0.58 and 0.22 nmol/mg protein, a K_m of 0.39 mM and 0.25 mM, at pH 6.1 and 7.4, respectively. Type II NaP_i cotransporter mRNA is exclusively found in kidney cortex, and it has several subtypes according to their species' specificity. Its activity and mRNA are regulated by both nonhormonal and hormonal factors, such as by changes in the dietary phosphate content [Boyer et al., 1996] and parathyroid hormone [Dousa et al., 1996]. The classification, protein characteristics and regulation of NaP_i cotransporter will be detailed in Chapter II.

Almost in all tissues, there is a phosphate carrier in the inner membrane of mitochondria. The mitochondrial phosphate carrier is sensitive to SH-reagent and driven by a pH-gradient [Kramer et al., 1996]. In the ER membrane, G6Pase hydrolyzes G6P into glucose and inorganic phosphate. According to the substrate-transport model, P_i is transported out of the lumen of ER by a P_i transport protein T2, and the theoretical deficiency of T2 causes GSD Ic. T2 was further classified into two forms with different substrate specificity, termed T2α and T2β [Nordlie et al., 1983, 1992]. T2α was suggested to transport P_i solely, while T2β could transport P_i, PP_i and carbamyl-P. Compared to the dominant GSD Ia cases, only a few cases of GSD Ic

have been reported [Nordlie et al., 1983; Lin et al., 1999]. In GSD Ic patients, inorganic pyrophosphatase, PP_i/glucose phosphotransferase, and carbamyl-P/glucose phosphotransferase activities of liver G6Pase were totally latent, but these activities were fully manifested with detergent-disrupted microsomes [Nordlie et al., 1983; Burchell & Gibb, 1991]. It has been claimed that the hepatic microsomal phosphate/pyrophosphate translocase was identified and purified using antibodies raised against the rat mitochondrial phosphate/hydroxyl ion antiport protein [Waddell et al., 1988]. Based on this, a 2.5-fold increase in quantity of the P_i translocase T2 was observed in the Ehrlich-ascites-tumour-bearing mice [Lucius et al., 1993]. From the kinetic properties of the G6Pase, the tumour-stressed mice appeared to have an altered T2β with an increased K_m for P_i [Lucius et al., 1995]. However, except these, no other results are available for the characteristics and molecular properties of T2.

The understanding at phosphate transport in microsomal preparations is limited due to the experimental difficulties because of the small volume of microsomes and the rapid rate of this process. Using a fasting-sampling, rapid-filtration apparatus, inorganic P_i transport into liver microsomes was observed, and this transport was still observable in microsomes from a GSD Ia patient [St-Denis et al., 1994]. However, the kinetic properties of this process have not been well defined so far. In addition, with the advantage of cloning of p46 cDNA and gene, similar mutations of the p46 gene were found in GSD Ib and Ic patients [Veiga-da-Cunha et al., 1999], initiating the hypothesis that GSD Ic has the same molecular basis as GSD Ib. However, in a recent study [Lin et al., 1999], it was reported that the p46 gene was normal in a GSD

Ic patient, hence suggesting a distinct GSD Ic locus. Therefore, the phosphate transporter (T2) concept may have to be reconsidered.

I.5 Regulation of the G6Pase system and its genetic engineering

I.5.1 Short-term regulation

Generally, *in vivo*, G6Pase activity is correlated to its substrate concentration because its K_m for G6P (2-5 mM) is greater than the intracellular G6P concentration (70-500 nmol/g liver). However, other acute regulatory mechanisms may exist, too. It has been demonstrated that fatty acids affected microsomal G6Pase activity *in vitro*. Although the short-chain fatty acyl-CoA (less than 9 carbons) had no effect on liver microsomal G6Pase activity, the medium- and long-chain fatty acyl-CoA esters inhibited G6Pase activity in intact microsomes [Mithieux & Zitoun, 1996]. It was further shown that unsaturated fatty acids associated with glycogen could inhibit rat liver G6Pase *in vitro* [Daniele et al., 1997]. The mechanism for the inhibition of G6Pase by fatty acids appears to be more complex than only a competitive inhibition. They may insert into the lipid layers and affect the physic status of membrane, resulting in a conformational change of G6Pase. Arachidonic acid also inhibited G6Pase activity in a dose-dependent manner, likely either by binding directly to the enzyme or by affecting membrane environment and changing the enzyme conformation [Mithieux et al., 1993]. Insulin has been reported to inhibit G6Pase *in vitro* and in cultured hepatocytes [Gardner et al., 1993; Spagnoli et al., 1983] through

a mechanism that might involve phosphatidylinositol 3-kinase (PI3K) activity. It was indeed recently reported that the translocation of PI3K was associated to the inhibition of G6Pase during refeeding [Daniele et al., 1999], and G6Pase was competitively inhibited in the presence of phosphoinositides in a dose-dependent manner within a range of concentration 0.15-10 μM [Mithieux et al., 1998]. These properties have been suggested to be of special importance with regard to insulin's inhibition of hepatic glucose production. Amino acids affect the cell volume and change the cytosolic ionic strength which could affect G6Pase activity. It has been reported that physiological anions, such as chloride, phosphate and sulfate, inhibited G6Pase activity [Nordlie & Jorgenson, 1981; Pederson et al., 1998c].

I.E.2 Long-term regulation

It has been reported that G6Pase activity changes in different nutritional and endocrine states. The isolation and characterization of cDNA and gene of p36 have made it possible to study the regulation at the transcriptional level. In FAO hepatoma cells, cAMP increased p36 mRNA fourfold but decreased p36 mRNA to 50% of control values after 3h and 24h exposure, respectively; dexamethasone (an analogue of glucocorticoids) resulted in a slow response with a 3.3-fold increase after 48h treatment. Insulin greatly suppressed the mRNA level and has a dominant negative effect on glucocorticoid stimulation of p36 mRNA levels [Lange et al., 1994; Argaud et al., 1996]. Both p36 mRNA level and activity of G6Pase were elevated in fasting and diabetic rats, refeeding and insulin administration reduced both p36 mRNA level

and activity of G6Pase [Argaud et al., 1996]. Increased p36 mRNA were also observed in FAO cells in the presence of 25mM glucose [Lange et al., 1994]. This effect was confirmed by studies in primary hepatocytes [Argaud et al., 1997] and *in vivo* [Massillon et al., 1996], showing that p36 mRNA was regulated by glucose independently from insulin. The effect of glucose on G6Pase is dependent on glucose metabolism, as reflected by the correlation of stimulating degree with glucokinase activity, namely, the stimulatory effect of glucose was greater at high levels of glucokinase [Argaud et al., 1997]. This suggests that a metabolite derived from glucose, rather than glucose itself, may affect G6Pase expression. One metabolite in glucose metabolism pathway, fructose-2,6-bisphosphate (Fru-2,6-P_2), has a marked effect on p36 mRNA in FAO cells. When Fru-2,6-P_2 was increased 15-fold by an overexpression of 6-phosphofructo-2-kinase/fructose-2,6-bisphosphatase (6-PF-2-K/Fru-2,6-P_2ase) whose bisphosphatase activity was abolished through a mutation, G6Pase mRNA level was increased six-fold in FAO cells, consistently, overexpression of wild-type 6-PF-2-K/Fru-2,6-P_2ase with intact bisphosphatase activity decreased Fru-2,6-P_2 content, resulting in a decrease of G6Pase mRNA [Argaud et al., 1997]. The stimulatory effects of glucose and Fru-2,6-P_2 on G6Pase seems paradoxical since a high G6Pase activity will produce more glucose. However, it could be related to other metabolic processes, such as the G6P/glucose cycle and the glucose-stimulated insulin secretion. The auto-regulatory function of glucose, which is independent of insulin, may be another explanation because glucose will impose effects on many enzymes other than G6Pase. The effects on these enzymes

may compensate for the G6Pase effect. Besides the regulation of hormones and glucose metabolites, free fatty acids also increase mRNA level and protein amount of p36 independently from hormones [Massillon et al., 1997], suggesting that the prolonged hyperlipidemia may contribute to enhanced hepatic glucose production via increased G6Pase activity.

The mechanism of these hormonal effects on G6Pase expression is not defined. A luciferase report gene containing the 5' region of the human p36 gene was constructed and transfected into H4IIE cells, a rat hepatoma cell line that is very sensitive to insulin [Vargas et al., 1994]. In the presence of dexamethasone (an analogue of glucocorticoids), luciferase activity was increased 10-fold in transfected cells, in contrast, dibutyryl cAMP alone did not affect the luciferase activity but reduced the stimulatory action of dexamethasone. These results elucidated hormonal response elements in the 5' region of p36. A multicomponent insulin response sequence has been identified in the proximal 5' flanking region of the murine p36 gene [Streeper et al., 1997]. Deletion of the murine p36 gene sequence between –198 and –159 completely abolished the insulin response. The *cis*-elements were more detailed through the G6Pase transient expression studies [Lin et al., 1997]. DNA elements essential for optimal and liver-specific expression of G6Pase were contained within nucleotides –234 to +3, including binding sites for hepatocyte nuclear factors 1, 3, 4, and a cAMP-response element. The cAMP response element was further identified in the range from –161 to –152 through gel-electrophoretic-mobility shift assay [Schmoll et al., 1999]. Effects of *trans*-factors were also studied through the

transient expression of p36 in HepG2 cells [Lin et al., 1997] and H4IIE cells [Lin et al., 1998b]. HNF1α and HNF3γ are liver-enriched factors that bind to the G6Pase promoter and transactivate G6Pase expression. Further study showed that HNF1α is an accessory factor for the effects of glucocorticoids on G6Pase gene expression [Lin et al, 1998b].

Kidney G6Pase has a distinct regulation from liver G6Pase as shown in the work of Minassian et al [1996]. In the liver, G6Pase mRNA abundance was increased in the 24h and 48h fasted rats, and returned to the level of fed state after 72h and 96h fasting. While in the kidney, G6Pase was increased 2.7-fold after 24h fasting, 5-fold after 48h and sustained at this level at 72h and 96h fasting. The differential regulation of liver and renal G6Pase gene expression can be also reflected during development. The activation of rat liver G6Pase at 3-5 days after birth does not happen with the rat renal G6Pase, and in adult rats, the specific activity of G6Pase is higher in kidney than that in liver [Voice et al., 1996]. The differential regulation of G6Pase in these two organs may be linked to their different functions. Liver is responsible for acute glucose homeostasis, while kidney may be responsible for the prolonged glucose requirement.

The putative G6P transporter, p46, appears to have a distinct regulation from p36. As shown in our laboratory [Li et al., 1999], a two-fold increase of p46 mRNA was observed in liver, kidney, and intestine from streptozotocin-diabetic rats. A dose-dependent increase of p46 mRNA, but a lesser increase in p46 protein, by glucose was also observed in HepG2 cells with a maximal effect at 15 mM glucose, while

optimal p36 mRNA was observed at 25 mM glucose. Cyclic AMP increased p46 mRNA 1.5 fold, but not protein level, whereas, insulin reduced p46 mRNA by half and p46 protein by 33%. In a more recent report [Li & van de Werve, 2000], it was demonstrated that, in HepG2 cells, physiological concentration of insulin (0.1-1 nM) totally suppressed p36 mRNA but barely reduced p46 mRNA. Cyclic AMP (0.01-100 μM) caused a 2.7-fold increase in p36 mRNA but only slightly affected p46 mRNA. Thapsigargin (1-100 nM), an inhibitor of the endoplasmic reticulum Ca^{2+}-ATPase, increased p36 mRNA by two fold but not p46 mRNA. In contrast, dexamethasone (0.1-100 nM) increased both p36 and p46 mRNA by more than threefold, which was counteracted by 1 μM insulin. Taken together, it was documented that hormonal changes compatible with increased hepatic glucose production essentially modify the expression of the catalytic subunit of G6Pase, p36, without any significant effect on that of p46.

I.5.3 Genetic engineering of the G6Pase system

The metabolic impact of overexpression of p36 has been studied using gene delivery via a recombinant adenovirus containing p36 cDNA to primary hepatocytes and liver of normal animals [Trinh et al., 1998; Seoane et al., 1997], as well as insulinoma cell line INS-1 cells [Trinh et al., 1997].

Overexpression of p36 in primary hepatocytes resulted in a ninefold increase in G6Pase activity, 25% reduction in intracellular G6P levels, a substantial decrease in glycolytic flux and glycogen deposition and an increase in gluconeogenesis [Seoane

et al., 1997]. In rats infused with the recombinant adenovirus containing p36 cDNA, liver G6Pase activity and immunodetectable p36 protein were increased [Trinh et al., 1998]. Meanwhile, these animals exhibited the abnormalities associated in early stage NIDDM, including glucose intolerance, hyperinsulinemia, decreased glycogen content, increased muscle triglyceride stores. The rats also had hypolipidemia, which is normally not associated with NIDDM [Trinh et al., 1998].

Overexpression of p36 in INS-1 cells caused a fourfold increase in G6P hydrolysis, 32% decrease in glycolysis, and a proportional decrease in glucose-stimulated insulin secretion [Trinh et al., 1997].

Chapter II Phosphate homeostasis in relation with glucose metabolism

II.1. Distribution and general function of phosphate

Phosphorus (P) approximately constitutes 1% of the whole body weight and is the sixth most abundant element in the human body. Around 85% of phosphorus is in bone as hydroxyapatite crystals, 14% in cells in soft tissues as phosphate, and 1% in extracellular fluids [Berner & Shike, 1988]. About 70% of blood phosphate is in the organic form, such as phospholipids, the remainder, 30%, is inorganic phosphate (P_i), which circulates either binding to proteins or as free phosphate. The normal plasma levels of phosphate range between 0.85-1.45 mM, which also depends on the assay methods. The intracellular inorganic phosphate concentration is higher than in the plasma. Most NMR estimates of cellular (cytosolic) phosphate concentration seem to lie in the range of 0.5-5 mM [Bevington et al., 1992]. The distribution of intracellular inorganic phosphate are compartmentalized and influenced by separate phosphate transporters in mitochondria, lysosomes, ER, and nucleus membranes. Mitochondria store a large amount of phosphate, which is the major part of the measured phosphate concentration. In the whole human liver biopsy, the inorganic P_i concentration is about 3.5 μmol/g wet liver in fasted condition. For rat liver, it is around 3.5 and 6-7 μmol/g liver in fed and fasted conditions, respectively, while reported total phosphate concentration was around 4-5 mM in hepatocytes and around 1.8 mM in kidney cells

[Sestoft et al, 1981; Bevington et al., 1992]. Relatively, the intracellular P_i concentration is more stable, while the plasma P_i concentration is subjected to dietary and hormonal regulation, and provides an exchangeable P_i pool to intracellular P_i requirements. The relative stability of intracellular P_i concentration is reflected in the case of hypophosphatemia. In this case, the intracellular P_i seems to be buffered or regulated in the face of changes in extracellular P_i concentration. Even in mammals subjected to sever phosphorus depletion, total phosphate measured chemically in skeletal muscle may decrease no more than 50% of control [Brautbar et al., 1983; Horl et al., 1983], and negligible changes in tissue P_i have been reported from renal cortex of rats after 4 days of dietary phosphorus deprivation [Gray et al., 1983].

Phosphate has multiple physiological functions. First of all, it is an essential component for bone mineralization. Besides this, it is a vital component of many intracellular compounds including phospholipids, nucleic acids, nucleoproteins and enzymatic cofactors such as nicotinamide diphosphate. Moreover, it is the source of the high-energy phosphate bonds of adenosine triphosphate (ATP), and a component of 2,3-diphosphoglycerate in the supply of oxygen to the tissues. Other important roles of phosphate are to participate in the metabolism of second intracellular messengers (cAMP, cGMP), and to maintain the plasma and urinary acid-base balance [Bugg & Jones, 1998]. Now it has been demonstrated that a number of enzymes in glycogen metabolism, glycolysis and gluconeogenesis are also sensitive to changes of P_i concentration, as shown in Table 1.

Table 1 Effects of P_i on enzymes

Biological process	Enzyme	Tissue	Effect	Reference
a. Glycolysis	Hexokinase (2.7.1.1)	Rat brain	Activation	White & Wilson, 1990
	6-Phospho fructokinase (2.7.1.11)	Human erythrocyte	Activation	Tsuboi et al., 1965
	6-Phosphofructo-2-kinase (2.7.1.105)	Rat liver	Activation	Kountz et al., 1986
	Fru-2,6-P2ase (3.1.3.46)	Rat liver	Activation	Kountz et al., 1986
	Pyruvate kinase (2.7.1.40)	Ox heart	Activation	Baranowska et al., 1984
b. Glycogen metabolism	Glycogen phosphorylase a phosphatase (3.1.3.16)	Rabbit liver	Inhibition	Khandelwal & Kasmani 1980
	Glycogen synthetase b phosphatase (3.1.3.16)	Rabbit muscle	Inhibition	Kato & Bishop, 1972
	Glycogen phosphorylase a (2.4.1.1)	Human muscle	Activation	Chasiotis, 1983
		Dog liver		van den Berghe et al., 1973
	Glycogen synthetase a (2.4.1.11)	Rat liver	Activation	Mersmann & Segal, 1967
c. Gluconeo-genesis	Fru-1,6-P_2ase (3.1.3.11)	Rabbit liver	Inhibition	Dudman et al., 1978

In summary, the ATP-producing pathways are stimulated by increasing phosphate concentration, while ATP-utilizing enzymes are generally inhibited by physiological P_i concentration. Glycolysis appears to be increased by P_i according to its effect on the isolated enzymes in this pathway. It is also considered that glycogenolysis is directly proportional to P_i concentration because it is one substrate of phosphorylase.

It is now widely recognized that disturbances in phosphate homeostasis, usually hypophosphatemia, are serious disorders of metabolism. The clinical consequences of severe hypophosphataemia include haemolysis, skeletal muscle myopathy, cardiomyopathy, neuropathy, and osteomalacia. Hypophosphatemia is generally subdivided into two categories. Providing normal inorganic serum phosphate is 0.8-1.3 mM, moderate hypophosphatemia is arbitrarily defined as 0.32-0.65 mM, and severe hypophosphatemia is less than 0.32 mM. Their incidences in human are around 2.5-3.1% and 0.24-0.42%, respectively [Bugg et al, 1998].

II.2 Phosphate homeostasis

II.2.1 Regulation of phosphate homeostasis

Phosphate is absorbed in intestine and reabsorbed in kidney. Uptake of phosphate from diet occurs along the length of the intestinal tract with the jejunum being the main site of absorption. It is generally thought that, in intestine, there are two mechanisms for P_i transport. The first involves the passive diffusion of phosphate across the plasma membrane. This process is related to the concentration gradient of phosphate so that the dietary content of phosphate affects phosphate uptake. The

other one is a sodium-dependent P_i transport mechanism, which is regulated by dietary P_i and 1,25-dihydroxyvitamin D_3 (1,25 $(OH)_2$-D_3). For the normal P_i content diet, the first mechanism predominates; when P_i content is low in diet, the active transport is upregulated and accounts for the major P_i uptake. Dietary P_i deprivation occurs rarely so that the P_i intake process in the intestine is not the crucial point in P_i homeostasis regulation. On the contrary, the P_i reabsorption in kidney is the modulating point. In a normal, healthy human, renal P_i excretion matches net intestinal absorption, thereby achieving a zero balance. The renal P_i reabsorption also occurs via a sodium-dependent P_i transport (NaP_i cotransport) process which exists in the proximal tubular brush border membrane. According to amino acid homology, tissue distribution and regulation, NaP_i cotransporters identified thus far have been classified into three groups: type I (NaP_i-1 related), type II (NaP_i-2 related), and type III. Type I and type II NaP_i cotransporters share 20% overall amino acid identity. Type I NaP_i cotransporters have approximately 465 amino acids with 60-64 kDa molecular weight [Werner et al., 1991]. The predicted secondary structure has seven transmembrane domains [Biber et al., 1996]. Type II NaP_i cotransporters have around 635 amino acids with a 80-90 kDa molecular weight. They have 8 predicted transmembrane domains [Biber et al., 1996; Murer et al., 1999]. Type I NaP_i cotransporters are predominantly expressed at the brush border membrane of proximal tubule cells, but also expressed in hepatocyte plasma membrane [Gishan et al., 1993]. Until now, no evidence has been reported about the exact physiological role of type I NaP_i cotransporter, nor its regulation. However, the amount of type I NaP_i cotransporter mRNA in liver and kidney was reported to be affected by fasting

and streptozotocin-induced diabetes [Li et al, 1996], suggesting a possible role in glucose metabolism. Type II NaP_i cotransporter was originally found exclusively in kidney cortex, while recently an isoform of type II NaP_i cotransporter (type IIb) cDNA was cloned from mouse small intestine and its mRNA was found in a variety of tissues [Hilfiker et al., 1998]. The subclassification of type IIa and type IIb is based on differences of their C-terminal amino acid sequence [Murer et al., 1999]. In addition to type I and type II NaP_i cotransporters, another type of NaP_i cotransporter, type III, are widely expressed in mouse, rat and human tissues [Kavanaugh et al, 1996]. Type III NaP_i cotransporters were isolated as receptors for gibbon ape leukaemia virus in mice and humans and amphotropic murine retrovirus in rats. Among these three types of NaP_i cotransporters, the roles of type I and III are currently unclear, while it is widely accepted that type II NaP_i cotransporter is largely involved in proximal tubular P_i reabsorption and represents, as detailed below, a target for physiological regulation of proximal tubular P_i reabsorption.

Two main modulating factors of type II NaP_i cotransport are dietary P_i content and parathyroid hormone (PTH). It has been well studied that restriction of dietary phosphate is associated with an increase of the overall proximal tubular capacity to reabsorb P_i. It has been demonstrated that both mRNA and protein levels of NaP_i-2 cotransporter were increased due to the low P_i diet [Collins et al., 1995a]. Moreover, the increase in NaP_i-2 protein far exceeds the increase in NaP_i-2 mRNA, indicating besides the transcriptional regulation, translational and/or post-translational mechanism play a significant role in the adaptive response to P_i restriction [Tenenhouse et al., 1995]. This is consistent with the observation that, in rats fed 2h a

low P_i diet, the NaP_i cotransport rate was increased 1.5-fold with a 1.8-fold increase in NaP_i-2 protein but no change in its mRNA [Levi et al., 1994; Katai et al., 1997].

PTH acts on both bone and kidney to affect phosphate homeostasis. In the kidney, PTH downregulates the P_i tubular reabsorption due to its inhibitory effect on the NaP_i-2 cotransporter. The potential mechanism is through its binding on receptors outside on the cell membrane and via intracellular signalling system, such as cAMP-protein kinase A and/or phosphatidyl inositol phospholipase C pathway. It has been demonstrated that the activation of a regulatory cascade involving protein kinase A and C mediates the inhibition of type II NaP_i cotransporter [Murer et al., 1991]. Besides the phosphorylating effect, it was also reported that both the type II NaP_i cotransport rate and the immunoreactivity of NaP_i-2 were increased in the parathyroidectomized (PTX) rats and could be reduced to control levels by PTH treatment [Kempson et al., 1995]. The mechanism may be related to the degradation of NaP_i-2 cotransport protein. When NaP_i-2 cotransporter was expressed in opossum kidney cells by the transfection of its cDNA, it was found that the NaP_i cotransport rate in transfected cells was inhibited by PTH, and the cotransport protein was internalized and rapidly degraded in the presence of PTH. These results indicated that PTH led to a removal of type II NaP_i cotransporters from the apical membrane and to their subsequent degradation [Pfister et al., 1997, 1998]. Further studies showed that the response of NaP_i-2 to PTH involved a rapid endocytic process, in which the transporters were delivered to degradative organelles by a taxol-sensitive rearrangement of microtubules [Lotscher et al., 1999].

Vitamin D is another regulator for P_i homeostasis. In contrast to the intestinal NaP_i cotransport, which is well known to be induced by 1,25 $(OH)_2$ D_3 [Katai et al., 1999], the effect of vitamin D_3 on renal NaP_i cotransport is far less clear, even controversial in some studies. It was shown that 1,25 $(OH)_2$ D_3 dose-dependently inhibited NaP_i transport in osteoblastic cells [Green et al., 1993], while it was shown recently that the administration of 1,25 $(OH)_2$ D_3 to vitamin D-deficient rats increased the initial rate of P_i uptake as well as the amounts of NaP_i-2 mRNA and protein in the juxtamedullary cortex [Taketani et al., 1998].

Another hormone, stanniocalcin (STC) may regulate phosphate homeostasis. STC was first identified in fish with a primary function to prevent hypercalcemia [Lu et al, 1994]. Two mammalian homologues of STC have been identified, STC 1 [Olsen et al., 1996] and STC 2 [Ishibashi et al., 1998]. STC 1, expressed in various tissues such as kidney and bone [Olsen et al., 1996; Yoshiko et al., 1999], could inhibit calcium uptake by goldfish gills and stimulate phosphate reabsorption by rat kidneys [Olsen et al., 1996; Wagner et al., 1997]. STC 2 was recently reported to be expressed in pancreatic islets and may play a role in glucose homeostasis [Moore et al., 1999].

More or less and by a yet-unclear mechanism, other hormones such as insulin, IGF-1 and thyroid hormone, stimulate NaP_i cotransport, while glucocorticoids potentially inhibit NaP_i cotransport [Dousa et al., 1996; Essig & Friedlander, 1998].

II.2.2 Consequence of dietary phosphate deficiency

As described above, it has been well known that dietary P_i deprivation upregulates NaP_i-2 cotransport activity and the expression of NaP_i-2 gene. Besides

this well documented effect, dietary phosphate deficiency also affects the expression of PTH, serum calcium concentration, and serum $1,25(OH)_2$ D_3 content. It has been reported that PTH mRNA levels were decreased by a low P_i diet, and its serum immunoreactivity was also decreased compared to a control normal P_i diet [Kilav et al., 1995]. Later studies showed that the effect of a low P_i diet on PTH mRNA was post-transcriptional based on the decreased mRNA stability [Moallem et al., 1998]. In addition to these effects, dietary P_i restriction also increases serum 1,25 (OH)2 D_3 [Gray et al., 1983] by stimulating its production, and also by reducing its catabolic metabolism through the suppression of vitamin D-24-hydroxylase, the first enzyme in the catabolic pathway for vitamin D compounds [Wu et al., 1996].

It has been shown that phosphate depletion in the growing and adult rat produces hypercalcemia and hypercalciuria [Jara et al., 1999]. This is probably due to the increased bone reabsorption or the indirect effect of stimulated vitamin D content on calcium absorption.

II.2.3 X-linked hypophosphatemia

Among all the hereditary renal phosphate wasting disorders, including X-linked hypophosphatemic rickets (XLH), autosomal dominant hypophosphatemic rickets (ADHR), and hereditary hypophosphatemic rickets with hypercalcuria (HHRH), XLH is the most common inherited disorder of renal phosphate wasting. XLH, also known as familial hypophosphatemic or vitamin D-resistant ricket, has a prevalence of around 1:20,000. It has clinical characteristics of lower extremity deformities, rickets, short stature, bone pain, dental abscesses, enthesopathy, and osteomalacia, as

well as biochemical characteristics of hypophosphatemia, elevated serum alkaline phosphatase activity, and inappropriately normal $1,25(OH)_2$-D_3 levels [Hruska et al., 1995]. Human XLH has two murine homologues, the Hyp mice [Eicher et al., 1976] and the Gy mice [Lyon et al., 1986]. Hyp mutations occur spontaneously, while Gy mutations are experimentally induced by irradiation. Although both of them exhibit similar phenotypic features of human XLH patients except the inner ear abnormalities of Gy mice, more experiments have been performed with Hyp mice. Studies on Hyp mice have demonstrated a remarkable renal phosphate wasting, a result of decreased NaP_i cotransport in the brush border membrane [Tenenhouse et al., 1978]. Studies on the molecular mechanism for the reduced P_i transport showed that Hyp mice have a 50% decrease in NaP_i-2 mRNA and protein [Collins et al., 1995b; Tenenhouse et al, 1994]. With regard to the molecular basis of Hyp, the possibility that reduced expression of NaP_i-2 is the primary cause of Hyp is precluded by several evidences. First of all, human NaP_i-2 gene is mapped to chromosome 5 in the 5q35, indicating it is not the candidate gene for the genetic defect of XLH [Kos et al., 1994]. Secondly, experiments of parabiosis suggested that a humoral factor(s) might be responsible for the Hyp abnormalities. The normal mice joined to Hyp mice showed a progressive diminution of plasma phosphate over the next 3 weeks to approach the level of the Hyp mice, and this reduced plasma phosphate recovered to normal level after the separation from Hyp mice [Meyer et al., 1989]. This was supported by the renal crosstransplantation between normal and Hyp mice. The kidney from Hyp mouse had a normal NaP_i cotransport function when transplanted to normal mouse, while the normal kidney developed a reduced NaP_i cotransport in Hyp mice [Nesbitt et al.,

1992]. These results indicated that the kidney of Hyp mouse had a normal function, and other factors induced its *in vivo* abnormality. Of interest is that immortalized cell cultures from the kidney of Hyp mouse showed a normal *in vitro* phosphate transport [Nesbitt et al., 1995]. All of these observations demonstrated that the primary cause for Hyp is the abnormality of a humoral factor rather than an intrinsic renal defect. Since PTH is known to inhibit renal NaP_i cotransport, one might expect it to be involved in the pathogenesis. However, PTH level is normal in XLH patients [Arnaud et al., 1971], and parathyroidectomy does not alleviate phosphate wasting in Hyp mice [Cowgill et al., 1979]. These two results exclude the responsibility of PTH for hypophosphatemia in Hyp mice. According to all of these results, it is proposed that a new humoral factor(s) regulate(s) the expression of NaP_i-2 and control(s) the phosphate homeostasis. In addition, based on the fact that Hyp bone cells failed to produce normal bone when transplanted into normal mice, it was proposed that Hyp mice had a primary osteoblast defect and osteoblasts played an important role in the pathogenesis of the Hyp defect [Ecarot-Charrier et al., 1988; Ecarot et al., 1992]. These suggestions are strongly supported by the studies of Lajeunesse et al. [1996], in which it was found that the addition of Hyp mouse serum, not the normal mouse serum, to the culture medium for at least 24h specifically impaired NaP_i cotransport in primary mouse proximal tubular cultures. Moreover, when primary mouse proximal tubular cells were treated for 48h with Hyp mouse bone cell medium conditioned for at least 48h of culture, P_i uptake was specifically inhibited. The existence of a humoral factor that can impair renal NaP_i cotransport and the proposition that osteoblasts play an important role in maintenance of Pi homeostasis

are further supported by the studies on the tumour-induced osteomalacia. The oncogenic osteomalacia has similar characteristics to XLH, such as hypophosphatemia, low or inappropriately normal serum concentration of $1,25(OH)_2D_3$. Strong evidence has been raised that a humoral factor produced by the tumour is responsible for oncogenic osteomalacia. If the tumor can be located and completely removed, all the symptoms are alleviated, moreover, tumor extracts or conditioned medium from cultured osteomalacia caused abnormal P_i transport [Popovetzer et al., 1981; Nelson et al., 1996], indicating the tumor produces one or more factors that impair both renal phosphate reabsorption and $1,25(OH)_2D_3$ synthesis. This new humoral factor(s), termed as phosphatonin [Econs et al., 1994], may represent a peptide hormone or a family of hormones, with a broad molecular weight of 8-40 kDa [Cai et al., 1994; Chalew et al., 1996]. Although no direct evidence show that phosphatonin is parathyroid hormone or parathyroid hormone-related protein, some observations suggest that parathyroid hormone/parathyroid hormone-related protein receptors may modulate the activity of the factor [Drezner et al., 2000].

With great efforts to elucidate the genetic basis of XLH, an International Consortium identified the responsible gene for XLH by genetic linkage analysis, using highly polymorphic microsatellite markers and DNA samples from 150 unrelated families with XLH [HYP Consortium, 1995; Econs, 1996]. This gene was designated PHEX (PEX formerly) to depict a phosphate-regulating gene with homologies to endopeptidase located on the X chromosome. Its predicted amino acid sequence suggests that it is a membrane protein with a short N-terminal cytoplasmic

domain, a single transmembrane domain and a large extracellular domain, of more interest, it contains significant homology to a family of metalloprotease [Francis et al., 1997]. Subsequent studies determined that human PHEX gene has 22 exons that encode a 749 amino acid protein which is highly expressed in bone cells, but not in kidney [Beck et al., 1997; Lipman et al., 1998]. A study demonstrated for the first time that the Phex gene encoded for a 97 kDa protein which was present in the membrane extracts of cultured osteoblasts derived from newborn mouse calvaria [Ecarot & Desbarats, 1999]. This 97 kDa protein was undetectable in the kidney of normal and Hyp mice, nor in bone of Hyp mice, but in bone of normal mice. Another study showed that cell membrane from cultured COS cells transiently expressing Phex gene efficiently degraded exogenously added parathyroid hormone-derived peptides [Lipman et al, 1998]. After the human PHEX gene and cDNA clone, mouse Phex was rapidly cloned [Du et al., 1996]. Subsequent to the cloning, mutations of PHEX/Phex gene have been discovered in XLH patients, Hyp mice and Gy mice [Holm et al., 1997; Strom et al., 1997; Tyynismaa et al., 2000]. These mutations further demonstrated the association of PHEX/Phex to XLH, while the function and mechanism of PHEX/Phex protein is not clear. Given its homologue to endopeptidase, one hypothesis emerged that PHEX/Phex is involved in the inactivation of a phosphaturic hormone or the activation of a P_i-conserving hormone. Because it codes a membrane-bound protein, it is clear that the PHEX/Phex protein is not phosphatonin. However, phosphatonin is its potential substrate. In healthy conditions, PHEX/Phex is expressed at a normal level in bone cells, it directly or indirectly regulates the expression or function of phosphatonin and keeps the renal

NaP_i cotransport function to maintain a normal serum P_i concentration. Mutations produce dysfunctional PHEX/Phex protein or no protein expression, resulting in excessive concentrations of phosphatonin which would inhibit the renal NaP_i cotransport [Rowe, 1998; Tenenhouse, 1999; Econs, 1999; Drenzner, 2000].

II.3 Effects of hypophosphatemia on glucose metabolism

II.3.1 Glucose metabolism

Glucose is the main energy source in most tissues, and the only energy substrate in some tissues, such as in brain and erythrocyte. Glucose homeostasis is such of importance that it is controlled within a strict range by hormones. Glucose is mainly produced in liver through gluconeogenesis and glycogenolysis, utilized through glycolysis, and deposited via glycogenesis.

Gluconeogenesis and glycolysis have all enzymes in common except those that catalyze the irreversible steps that ensure a unidirectional flux from pyruvate to glucose: pyruvate carboxylase, phosphoenolpyruvate carboxykinase (PEPCK), fructose-1,6-bisphosphatase (Fru-1,6-P_2ase), and glucose-6-phosphatase (G6Pase). Gluconeogenesis is under hormonal regulation. Stimulating factors include glucagon (acting via cAMP), epinephrine, glucocorticoids, thyroid hormones, and vasopressin, while insulin is the physiological counterregulatory hormone [Kraus-Friedmann et al., 1984]. Gluconeogenesis is controlled at several steps which are the PEP/pyruvate

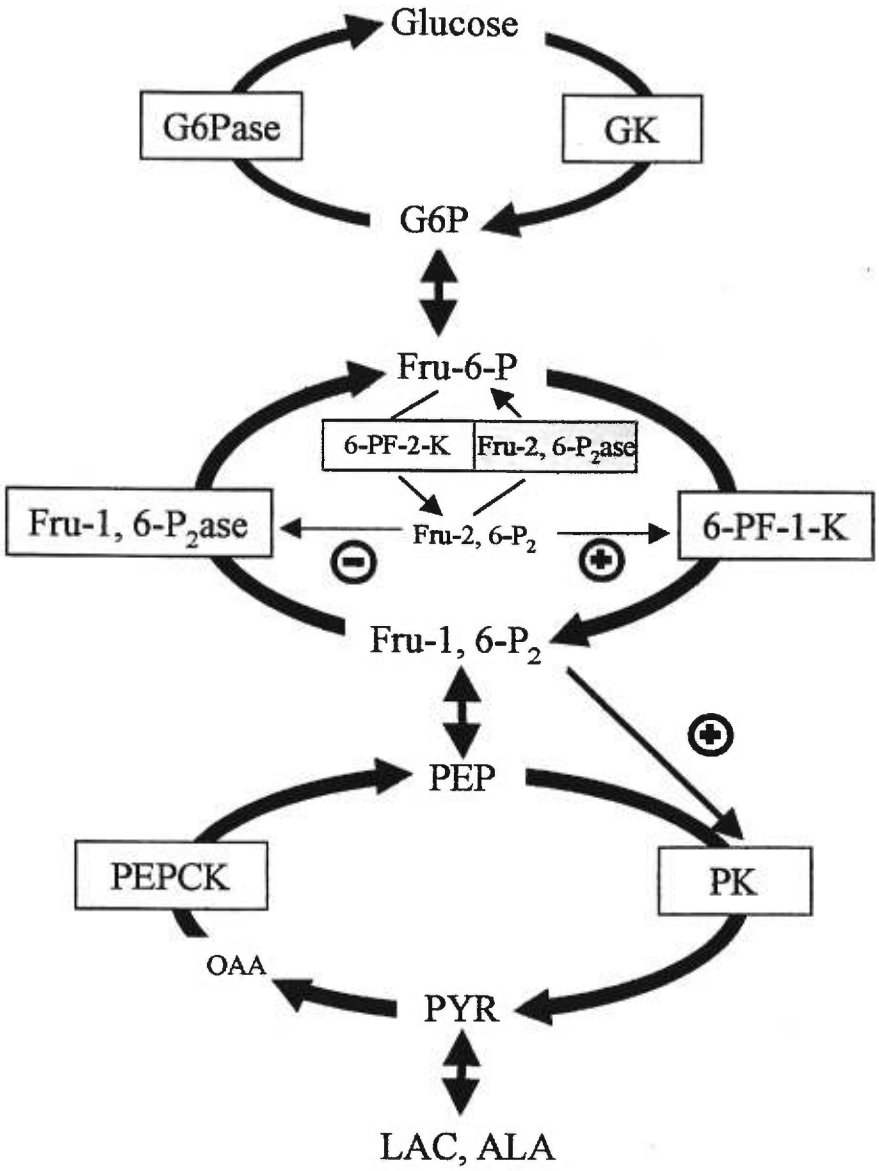

Figure 3 Substrate cycles in the gluconeogenesis and glycolytic pathway

The three cycles are PEP/pyruvate cycle, Fru-6-P/Fru-1,6-P_2 cycle and G6P/glucose cycle. The enzymes of these three cycles, which are subjected to hormonal regulations, are PK, PEPCK, Fru-1,6-P_2ase, 6-PF-1-K, 6-PF-2-K/Fru-2,6-P_2ase, GK and G6Pase. Fru-2,6-P_2 is an activator of 6-PF-1-K and an inhibitor of Fru-1,6-P_2ase.

cycle, fructose-6-phosphate/fructose-1,6-bisphosphate (Fru-6-P/Fru-1,6-P_2) cycle, and G6P/glucose cycle (as shown in Figure 3).

In the PEP/pyruvate cycle, pyruvate is converted to oxaloacetate by pyruvate carboxylase which is located in mitochondria. Oxaloacetate is converted to PEP by PEPCK. In the glycolytic pathway, pyruvate kinase (PK) converts PEP to pyruvate. Some studies showed that pyruvate carboxylation was the limiting and flux-generating steps [Ochs & Lardy, 1983], while others suggested the futile cycling at the pyruvate kinase level was a regulated point for the metabolite flux [Groen et al., 1983]. Liver type PK is an allosteric enzyme. The phosphorylation of PK by cAMP dependent protein kinase increases the apparent K_m for PEP without effect on activity in the presence of a saturating concentration of substrate. Cyclic AMP also inhibits the transcription level of L-type PK, whereas insulin stimulates PK transcription [Decaux et al., 1989; Noguchi et al., 1985]. In diabetic and fasting subjects, PK activity and mRNA decreased, which could be restored by insulin administration or refeeding [Vaulont et al., 1986]. PEPCK, mainly located in cytosol in rat and mouse liver, is generally considered to be the first committed step in gluconeogenesis in hepatic and renal cells. PEPCK activity is determined by its protein amount because no allosteric modifiers have been described. Its gene expression is decreased by insulin, increased by cAMP, glucocorticoids and thyroid hormones [Hanson & Reshef, 1997].

The Fru-6-P/Fru-1,6-P_2 cycle is a pivotal crossroad for glycolytic/ gluconeogenesis flux in liver. Fru-1,6-P_2 level is controlled by the activities of the gluconeogenic enzyme Fru-1,6-P_2ase and by 6-phosphofructo-1-kinase (6-PF-1-K),

the opposing glycolytic enzyme. The activities of these two enzymes are affected by a metabolite Fru-2,6-P_2, an allosteric activator of 6-PF-1-K and competitive inhibitor of Fru-1,6-P_2ase. Its level is controlled by a unique bifunctional enzyme, 6-phosphofructo-2-kinase/fructose-2,6-bisphosphatase (6-PF-2-K/Fru-2,6-P_2ase), the activity of which is subjected to phosphorylation and dephosphorylation. In liver, cyclic AMP dependent protein kinase can phosphorylate 6-PF-2-K/Fru-2,6-P_2ase and result in the inhibition of its kinase and stimulation of its phosphatase activity, hence a decrease in Fru-2,6-P_2 [Kurland & Pilkis, 1995]. Because of the activating effect of Fru-1,6-P_2 on pyruvate kinase, these two cycles of PEP/pyruvate and Fru-6-P/Fru-1,6-P_2 are linked together. All the regulatory factors which favour the increase of Fru-1,6-P_2 could also stimulate pyruvate kinase and affect the flux towards the direction of glycolysis.

The G6P/glucose cycle is at the final step of glucose production and controls the fate of G6P. Both G6Pase and glucokinase (GK) are involved in this cycle. The detailed information of G6Pase is discussed in the previous chapter. GK, one member of the hexokinase (HK) family, is highly expressed in hepatocytes and β-cells. GK is important for glycolysis and glucose-stimulated insulin secretion. Hepatic GK activity is allosterically inhibited by its regulatory protein [van Schaftingen et al., 1992]. Fru-6-P potentiates the binding of GK to its regulatory protein while fructose and Fru-1-P inhibit this reaction, hence increase GK activity. GK gene expression is increased by hyperinsulinemia in rats [Matschinsky et al., 1996], while cAMP could repress the transcription of GK [Nouspikel & Iynedjian, 1992]. In fasting or diabetic

subjects, GK mRNA and activity was reduced, when refeeding or injecting insulin, GK transcription was induced rapidly.

Glycogen phosphorylase (1,4-α-D-glucan:orthophosphate α-D-glucosyltransferase) phosphorolytically removes single glucose residues from α-(1,4)-linkages within the glycogen molecules. The product of this reaction is glucose-1-phosphate. Liver phosphorylase activity is tightly controlled by phosphorylation. Cyclic AMP activates phosphorylase kinase and phosphorylase, glucose itself competitively inhibits the activity of phosphorylase.

II.3.2 Relation between hypophosphatemia and glucose metabolism

As previous described, inorganic phosphate plays a crucial role in cellular metabolism and disturbances of phosphate homeostasis cause a number of abnormalities in body metabolism. Poorly controlled diabetes is one of the clinical situations to which hypophosphatemia may be associated. One can see this situation clearly from a case report. One woman was hospitalized because of hyperglycemia, insulin resistance and hypophosphatemia. Her hyperglycemia could not be reduced by insulin administration and other regular diabetic therapy methods, but quickly returned to normal level after inorganic phosphate infusion [Ravenscroft et al., 1999]. Other studies have also been reported on the relation between hypophosphatemia and glucose metabolism. It was reported that, as early as in 1980 [DeFronzo & Lang, 1980], hypophosphatemic patients had reduced glucose metabolizing rate, but similar insulin response and insulin clearance rate, indicating tissue insensitivity to insulin in

hypophosphatemic conditions. Similarly, when plasma phosphate concentration was elevated by phosphate infusion in healthy subjects, the glucose disposal rate was higher than that of control (sham infusion, inducing low plasma phosphate) while insulin secretion was similar [Nowicki et al., 1996], indicating a tissue insulin insensitivity in the sham infusion individuals. This was further supported by the study of Paula et al [1998] which showed that hypophosphatemic patients had the same glucose tolerance, but significantly higher insulin secretion during the oral and intravenous glucose tolerance test. In contrast, it was reported that the glucose stimulated insulin secretion in pancreatic islets was lower in the P_i-depleted rats [Zhou et al., 1991]. It was also reported that, when glutamine and α-ketoglutarate were used as substrate, a higher glucose production was found in cultured proximal tubule cells from Hyp mice [Capparelli et al., 1992]. It is of interest to notify that an altered gluconeogenesis was also observed in the cultured osteoblast from Hyp mice when fructose, glutamine, and malate were used as gluconeogenic precursor, but not with α-ketoglutarate, and this was associated with a depressed intracellular pH [Rifas et al., 1995]. From these evidences, it is clear that hypophosphatemia affects glucose and insulin metabolism. On the other hand, glucose and insulin also affect phosphate homeostasis. In the presence of hyperglycemia, especially when accompanied with polyuria and acidosis, phosphate is lost through the urine in excess [Berner et al., 1988]. As reported [Li et al., 1996], fasting downregulated, while streptozotocin-induced diabetes increased the NaP_i-1 mRNA in both rat kidney and liver, insulin upregulated the NaP_i-1 mRNA in primary cultures of rat hepatocytes.

Chapter III Objectives and experimental hypothesises

The objectives of this thesis are to investigate the hydrolytic mechanism of G6Pase, the function of the two components of the G6Pase system, as well as the relation between glucose metabolism and phosphate deficiency, caused either by a P_i-deficient diet or genetic mutations.

The hypothesis about the relation of glucose and P_i deficiency is that hypophosphatemia affects G6Pase and impair glucose metabolism. In order to testify this hypothesis, G6Pase was studied in rats fed with a P_i-deficient diet or a control diet. Other glucoregulatory factors were also investigated under these conditions. G6Pase was also studied in a genetic hypophosphatemic animal model – Hyp mice.

In order to study the hydrolytic mechanism of G6Pase and to investigate the function of p46 in the G6Pase system, kinetic characteristics of inorganic phosphate and glucose transport were investigated in rat liver microsomes. Moreover, kinetic characteristics of G6P transport/hydrolysis were also studied in rat liver microsomes.

Chapter IV Methods

IV.1 Animal handling

IV.1.1 Feeding condition

Spragle-Dawley male rats (around 300g) from the Charles Rivers Company were housed in plastic cages under 12h:12h day and night conditions with free access to water all the time. They were fed *ad libitum* with regular rodent diet (LabDiet, Oakville, ONT) for one week and switched to a P_i-deficient diet (No. 86128, Teklad, Madison, WI) ($-P_i$) or a control (No.86129) ($+P_i$) diet for 48h with or without overnight fasting. They were sacrificed on the morning of the third day for liver or blood sampling. According to these conditions, 4 groups of rats were obtained: 1. Fed ($-P_i$); 2. Fed ($+P_i$); 3. Fasted ($-P_i$); 4. Fasted ($+P_i$). These rats were used as the liver and kidneys donors ($n = 5$-6) or for the intravenous glucose tolerance test ($n = 4$-5).

IV.1.2 Animal surgery for intravenous glucose tolerance test

Spragle-Dawley rats (around 300g) were fed with the regular rodent diet for one week to get used to the environment before the surgery. The rat was anaesthetized with pentobarbital sodium (50mg/kg body weight) and given atropine to minimize respiratory secretions during anaesthesia. They also received one dose of antibiotic (Baytril, 5mg/kg body weight) and analgesic postoperatively (0.1mg/kg body

weight). Sterile catheters (Intramedic PE-50 with around 3cm beveled Silastic tips) were placed in the left carotid artery (for blood sampling) and the right jugular vein (for tracer infusion and bolus injection). The distal ends of all catheters were tunneled subcutaneously, exteriorized, and anchored at the nape of the neck. The catheters were backfilled with heparinized (20 units/ml) saline and sealed, and flushed every other day with normal saline and refilled with heparinized saline to maintain patency.

After the surgery, rats were recovered for one week, then fed with the ($-P_i$) diet or the ($+P_i$) diet for 48h and fasted overnight for the glucose tolerance experiments.

IV.1.3 Hyp mice

Male mice (4-6 weeks old) of the C57BL/6J strain, both normal (C57BL/6J +/Y) and Hyp (C57BL/6J Hyp/Y) were obtained from the laboratory of Dr. Lajeunesse at University of Montreal. Hyp mice were identified by the shorter body length and tail length, lower weight and reduced serum phosphorus levels [Lajeunesse et al., 1996]. The mice were fed with regular rodent diet RMH 2500 from PROLAB (Mexico, MX) and anaesthesized with Nembutal (75mg/kg body weight) before the livers and kidneys were taken for homogenization or frozen in liquid nitrogen pending further analysis. Five Hyp mice and four age matched control mice were used.

IV. 2 Preparation of microsomes

The livers from the rats described above were homogenized at 4°C with a Yamato homogenizer in 50 mM Hepes-Tris buffer, pH 7.3, including 250 mM sucrose. The

homogenate was centrifuged at 1,000g for 10 min at 4°C. The supernatant was centrifuged at 12,000g for 10 min at 4°C. The second supernatant was centrifuged at 100,000g for 60 min at 4°C. The pellet was resuspended in the same buffer (around 20 mg protein/ml) and kept at -80°C. This microsomal preparation was for G6Pase hydrolytic activity and transport measurements. The last supernatant was aliquated and kept at –80°C for the assay of glucokinase, pyruvate kinase and PEPCK activity.

Microsomal preparations from mouse organs and primary cultured hepatocytes were performed similarly except a glass homogenizer was used.

IV.3 Enzyme activity measurement

IV.3.1 G6Pase hydrolytic activity

G6Pase hydrolytic activity was measured at 30°C or room temperature in 50 mM Hepes-Tris, pH 7.3, including 250 mM sucrose at different concentration of G6P with a constant [U-^{14}C]G6P around 8 nCi. The reaction volume was 100 µl, including 10 µl microsomes, the indicated concentration of G6P and buffer. After 2 min incubation, 500 µl 0.3 N $ZnSO_4$ was added to stop the reaction. 500 µl saturated $Ba(OH)_2$ was added to precipitate the unhydrolyzed G6P. The mixture was centrifuged at 1000g for 2 min and 500 µl of the supernatant containing the released glucose was counted. The activity was defined as units/mg protein. One unit styands for the enzyme amount to release one µmol glucose in one minute. Detergent treated microsomes were treated with 0.8% chapso at 4°C for 5 min before the activity assay.

IV.3.2 Glucokinase activity

Glucokinase activity was measured according to Bontemps et al. [1978]. Glucokinase has a higher K_m and V_{max} than other hexokinases. Glucokinase phosphorylates glucose to G6P which is, by other enzymes, converted to ribulose-5-phosphate with the conversion of two NADP to NADPH. The difference of activity between 100 and 0.5 mM glucose represents the activity of glucokinase. The reaction was performed at 30°C in 50 mM triethanolamine buffer, pH 7.5, including 5 mM ATP, 5 mM $MgCl_2$, 1 mM NADP, 1 μg/μl G6PDH, 0.5 or 100 mM glucose. The blank was scanned with 800 μl of prewarmed buffer. 100 μl sample was added and the increase in the absorbance at 340nm was recorded. The glucokinase activity was calculated according to the molar absorptivity of NADH which is 6300 L/mol/cm, and expressed as μmol/min/mg protein.

IV.3.3 Pyruvate kinase activity

It was performed according to Feliu et al. [1976]. In the presence of ADP-Mg, pyruvate kinase converts PEP into pyruvate which is converted into lactate by lactate dehydrogenase with the oxidation of NADH to NAD. The activity is reflected by the decrease of NADH. The assay buffer was 50 mM imidazol, pH 7.5, including 100 mM KCl, 5 mM $MgCl_2$. The blank was scanned with 835 μl of the assay buffer, 20 μl of lactate dehydrogenase (25 mg/5 ml), 20 μl of 7.3 mM NADH, 25 μl of 50 mM ADP-Mg, 50 μl of sample. 50 μl of 3 or 100 mM (0.15 or 5 mM at final, respectively) PEP was added to initiate the reaction. The absorbance at 340nm was

recorded. The activity at 0.5 or 5mM PEP represented the activity of the active form or the total activity, respectively. The activity was calculated similarly to that of glucokinase.

IV.3.4 Phosphoenolpyruvate carboxykinase activity assay

PEPCK activity was assayed according to its carboxylation activity [Change & Lane, 1966]. The assay buffer was 100 mM imidazole, pH 7.0, including 50 mM $KHCO_3$, 1 mM $MnCl_2$ and 2 mM GSH. The blank was scanned with 880 µl of the assay buffer, 20 µl of 7.3 mM NADH, 25 µl of 50 mM IDP, 5 units of malate dehydrogenase and 50 µl of sample. 25 µl of 50 mM PEP was added and the absorbance at 340nm was recorded. The activity was calculated as in III.3.3.

IV.4 Metabolite assays

IV.4.1 cAMP

Around 100 mg frozen liver was homogenized in 1 ml cold 6% TCA at 4°C. 100,000 cpm of [^{3}H]cAMP was added to the homogenate as an internal control. The homogenate was centrifuged at 2,000g for 15 min at 4°C. The supernatant was recovered and washed 4 times with 5 volumes of water-saturated ether. This preparation was kept at –20°C for the assay of cAMP, pyruvate and PEP.

The cAMP was measured according to the instructions of a cAMP assay kit from Amersham Pharmacia Biotech (Baie d'Urfé, QC).

IV.4.2 Pyruvate and PEP

The assay for pyruvate and PEP was performed according to Czok & Lamprecht [1983] with the same principal to pyruvate kinase assay. The oxidation of NADH is proportional to the converted substrate.

The TCA extracts were used for the assay of pyruvate and PEP. The assay buffer was 500 mM triethanolamine, pH 7.6, including 5 mM EDTA. The blank was scanned with 800 µl of the assay buffer, 200 µl of TCA extracts and 20 µl of 6 mM NADH. 10 µl of lactate dehydrogenase (2.75 units/ml at final) was added and the absorbance at 340nm was recorded until it was stable. The change in the absorbance represented the amount of pyruvate. For the assay of PEP, 10 µl of 125 mM ADP, 20 µl of 500 mM $MgSO_4$ and 10 µl of 3.7 M KCl were added and the blank was scanned again. 20 µl of pyruvate kinase (2 units/ml at final) was added and the absorbance at 340nm was recorded until it was stable. This change represents the amount of PEP.

IV.4.3 Inorganic phosphate

Inorganic phosphate was measured according to the classical acidified molybdate colorimetric phosphate assay. The TCA extracts were used for liver P_i content assay. For blood sample, 50 µl of plasma was deproteinized by adding 1 ml 6% TCA. The mixture was centrifuged to precipitate the protein. 0.2 ml of TCA tissue extracts or 1 ml of TCA plasma extracts were added into a glass tube. The final volume was made up to 4.3 ml with water. 0.5 ml molybdate and 0.2 ml AANS were added. The

mixture was incubated for 30 min at room temperature and the absorbance at 660nm was read. The P_i content was calculated by comparing the absorbance with that of 0.5 μmol of H_3PO_4. The composition of AANS was 14.6% (w/v) $NaHSO_3$, 0.25% 1,2,4-amino-naphtolsulfonic acid, 0.5% Na_2SO_3.

IV.4.4 Fru-2,6-P_2

Fru-2,6-P_2 was assayed by its property to stimulate liver phosphofructokinase [van Schaftingen et al., 1982]. Since it is acid liable, Fru-2,6-P_2 was extracted from frozen tissue in 50 mM NaOH. Around 100 mg frozen tissue was homogenized in 1 ml of 50 mM NaOH. The homogenate was incubated at 80°C for 10 min and kept at 4°C for the assay. The assay buffer was 500 mM Tris-acetate, pH 8.0, including 25 mM $MgCl_2$, 10 mM F6P, 30 mM G6P, 2mM NADH. The traces of Fru-2,6-P_2 in the product of Fru-6-P was destroyed through the following treatment. 5 ml of 50 mM Fru-6-P solution was treated with 335 μl of 45% $HCLO_4$ for 20 min at room temperature, then neutralized with 250 μl saturated K_2CO_3. The mixture was centrifuge at 5000g for 5 min and 5 ml of supernatant was taken to obtain a final concentration of 100 mM with H_2O. Anions which can counteract the effect of Fru-2,6-P_2 was removed from auxiliary enzyme by gel filtration as below. The mixture of 5 mg muscle aldolase (9 units/mg), 1 mg glycerol-3-P-dehydrogenase (170 units/mg) and 0.1 mg triose-phosphate isomerase (5000 units/mg) was centrifuged at 5000g for 5 min. The pellet was dissolved in 0.4 ml water and loaded onto a 20 ml column of Sephadex G-25 (fine) equilibrated with 50 mM NaCl, 25 mM Tris/acetate, pH 8.0.

The filtered enzyme fraction (1 ml) was combined with 1 ml 2% bovine serum albumin and 1 unit of phosphofructokinase. The mixture was made up to 10 ml and kept for no longer than 1 day at 4°C.

For the standard curve, the reaction solution contained 50 µl of 50 mM NaOH, 100 µl of the assay buffer, 50 µl of combined enzyme solution, and 0, 10, 15, 20, 25, or 30 µl of 0.1 µM Fru-2,6-P_2, respectively, with H_2O to a total volume of 950 µl. After scanning the blank, 50 µl of 20 mM sodium pyrophosphate was added and the absorbance at 340nm was recorded every minute for 10 min. The standard curve was obtained from the $\Delta A/\Delta t$ values versus the corresponding concentration of Fru-2,6-P_2.

For the sample assay, Fru-2,6-P_2 was replaced by 20 µl of sample. The concentration was obtained from the standard curve according to the $\Delta A/\Delta t$ values.

IV.4.5 Glycogen

Liver or microsomal bound glycogen content was assayed according to Hue et al. [1975]. The NaOH extracts for Fru-2,6-P_2 assay were used for liver glycogen content measurement. The alkaline extracts were neutralized with 1.5 N acetic acid until pH 5.5, and centrifuged 20 min at 4°C at 10,000g. 500 µl supernatant was taken to incubate with 100 µl amyloglucosidase (1 mg/ml in 100 mM acetate buffer, pH 5.5) at 37°C for 90 min. The produced glucose from glycogen was measured by the appearance of NADH through the combined reaction of hexokinase and G6PDH. The assay buffer was 250 mM triethanolamine, 2.5 mM $MgSO_4$, 10 mM ATP, 10 mM NADP, pH 7.3, including 7 µl/ml G6PDH (1 mg/ml). The blank was scanned with

850 μl assay buffer and 50 μl sample. 5 μl hexokinase (10 mg/ml) was added and the absorbance at 340nm was recorded until it was stable. The ΔA340nm was transformed to glucose amounts by comparison with the values of glucose standards.

IV.5 Intravenous glucose tolerance test

The rat IVGTT was done as described in [McArthur et al., 1999]. After the surgery, rats were allowed to recover for one week, fed with the special diet for 48h, and fasted for overnight. On the morning, after weighted and 30cm saline-filled PE-50 extensions were connected to the exteriorized catheters, the rat was placed into a Plexiglas experimental chamber (floor area around 600 cm^2) and left to settle for 20-30 min. The first blood sample was taken when the rat was settled calmly. 10 min later (regarded as time point 0), a primed, continuous infusion of [3-^{3}H]glucose was started via the jugular vein catheter with a peristaltic pump. The priming dose (9 μCi in 0.9 ml) was given within 60 s, and the continuous infusion (10 μCi/ml) was infused at a rate of 0.015 ml/min (0.15 μCi/min) throughout the experiment. Blood samples were taken at 120, 130, 140, 150, and 155 min. At 160 min, a glucose bolus (0.3 g/kg) mixed with tracer glucose (13 μCi) was given via the jugular catheter within 1 min. Blood samples were taken at 162, 165, 170, 175, 180, 190, 220, and 250 min. Hematocrit was measured before and after the experiment. Blood samples were centrifuged for 5 min at 10,000g. The plasma was taken for glucose, insulin and tracer radioactivity assay as following.

Plasma glucose was assayed with glucose oxidase method (microplate assay).

Plasma insulin was assayed according to the rat insulin ELISA kit from Crystal chem Inc (Chicago, IL).

To determine the plasma specific radioactivity, 20 μl plasma were deproteinized by addition of 40 μl of 0.3 N $Ba(OH)_2$ and 40 μl of 0.3 N $ZnSO_2$. The mixture was centrifuged and 100 μl of supernatant was transferred into a scintillation vial which were dried at 37°C overnight to remove $[^3H]H_2O$. 100 μl distilled water and 10 ml scintillation liquid were added to the vials which were counted for 10 min.

IV.6 Northern blot

Total RNA was extracted from frozen tissue (Liver or kidney) or primary cultured hepatocytes using TRIzol Reagent. 15 or 20 μg total RNA was separated in 1% agarose gel containing 1.5 M formaldehyde for 2.5 h at 72 V. RNA was transferred to Nylon membrane by a capillary technique in 20× SSC (1× SSC is 0.15 M NaCl, 0.015 M sodium citrate, pH 7.0) solution, and immobilized to the membrane by 5 min exposure to UV. The membrane was prehybridizated in 1 ml prehybridization/ hybridization solution per 10 cm^2 membrane at 68°C for 3 h, then hybridized overnight at 68°C with the specific probe at a total radioactive specificity of 6×10^6 CPM in 6 ml hybridization solution. The membrane was then washed with 2× SSC/0.1% SDS, 0.5× SSC/0.1% SDS, and 0.1×SSC/0.1% SDS solution for 10 min at 50°C, respectively. Autoradiography was performed.

The recombinant cDNA template of p36 and p46 were prepared according to Qiagen Mini plasmid purification method. The purified cDNA fragments were labelled randomly with [^{32}P]dCTP.

IV.7 Western blot

50 μg microsomal protein was run in a 12% SDS-PAGE for 1h at 100 voltage and transferred onto a nitrocellulose membrane. The membrane was saturated in 10% milk in 100 mM Tris, 0.9% NaCl (TBS), pH 7.5, for 1 hour at room temperature and incubated overnight at 4°C with the primary antibody solution (diluted to 1:500 for anti-p36 or 1:200 for anti-p46). After washing in TBST for 2× 5min and 1× 15 min, the membrane was incubated with the secondary antibody (Anti-rabbit IgG AP conjugated) for 2 h at room temperature. After washing with TBST for 2× 5 min and 1× 15 min, the immunoreaction was detected by the BCIP/NBT system. The specific band was analysed using a Dual Light TM Transilluminator.

The antiserum against p36 was prepared against the recombinant p36, which was kindly given by Dr. J.Y. Chou in National Institutes of Health, Bethesda, MD, USA.

The antiserum against p46 was produced against the N-terminus of p46 (5-GYGYYRTVIFSAMFGGY-21) in our laboratory.

IV.8 Hepatocyte primary culture

Young Wistar male rats (around 200 g body weight) were used for liver perfusion. The rat was anaesthetized with pentobarbital (50 mg/kg body weight). One canula

was connected to the portal vein for the perfusat influx. Another canula was connected to the inferior vena cava for the perfusat efflux. The liver was first perfused with 200 ml of 119 mM NaCl, 6.7 mM KCl, 10 mM Hepes, pH 7.4 at a rate of 20 ml/min for 10 min, at 37°C. The solution was then changed into 100 ml of the same content buffer but including 4 mM $CaCl_2$ and 50 mg collagenase. The perfusate was circulated for 15-20 min at 37°C until the hepatocytes were separated effectively. Hepatocytes were released into Lebovits' medium, including 0.2% albumin and 1 ml/L gentamicine. After three times washing, the cells were diluted to 1×10^6 cells/ml with MEM supplemented with 10% fetal bovine serum and 1 ml/L gentamicine, and added to collagen coated dishes (4 $\mu g/cm^2$) in a density of 1×10^5 cells/cm^2. Cells were incubated at 37°C, with 5% CO_2 in a humidfied incubator for 1.5 to 3h. The medium was then changed into P_i depleted MEM or control MEM which was supplemented with 10% fetal bovine serum and 1 ml/L gentamicine. After 24h incubation, cells were harvested for microsomal preparation or RNA extraction.

IV.9 Transport experiments

IV.9.1 Inorganic phosphate and glucose uptake into rat liver microsomes

Uptake of inorganic phosphate or glucose into rat liver microsomes was performed at room temperature with a fast sampling, rapid filtration apparatus (FSRFA, US patent No. 5,330,717). Basically, the substrate (glucose or KH_2PO_4, at different concentrations with a constant radioactivity) was included in the incubation medium (50 mM Hepes-Tris, 250 mM sucrose, pH 7.3) with or without potential inhibitors at

a final volume of 960 µl, and loaded into the chamber of the machine. 40 µl microsomes (around 20 mg protein /ml) were injected into the chamber to initiate the uptake. The mixed solution was sequentially sampled at different time points and filtered through 0.65 µm cellulose nitrate filters. The filters were washed three times with 1 ml ice-cold buffer and counted for the radioactive content. When 100 mM unlabelled glucose was used, the same osmolarity was kept by adjusting the sucrose concentration to 150 mM. For the phosphate transport, 2 mM EGTA was included in the incubation solution. For the glucose uptake, the washing solution was 50 mM Hepes-Tris, 250 mM sucrose, with or without 0.25 mM phloretin.

IV.9.2 [U-^{14}C] or [^{32}P]G6P uptake and efflux across rat liver microsomes

[^{32}P]G6P was prepared through the reaction of glucose with [γ-^{32}P]ATP catalyzed by hexokinase [Berteloot et al., 1991a]. The reaction was performed with 2 mM [[γ-^{32}P]ATP-Mg (10 µCi/µl), 10 mM glucose and 10 µg hexokinase in a total volume of 500 µl for 4 h at 30°C. The remained ATP was taken out by the treatment of 2% activated charcoal. The supernatant was loaded onto a Dowex column and G6P was collected according to the radioactivity peak. The concentration and specific activity of G6P were calculated according to its counted DPM compared to that of the original [γ-^{32}P]ATP.

The uptake experiments of G6P were performed with the FSRFA at room temperature. Different concentrations of G6P with 10 µM [U-^{14}C] or [^{32}P]G6P were added to the incubation medium (50 mM Hepes-Tris, 250 mM sucrose, pH 7.3) and

loaded into the chamber. Microsomes were injected into the chamber to initiate the uptake. Other steps were similarly performed as above.

For efflux experiments, microsomes were incubated with 10 μM [^{32}P]G6P, or 0.2 mM G6P including 10 μM [U-^{14}C] or [^{32}P]G6P, for 3 min at room temperature and loaded into the chamber. Efflux was initiated by the injection of 0.5 mM vanadate, unlabelled G6P or KH_2PO_4 into the chamber.

IV.9.3 Exchanging transport measurements

The exchanging transport between G6P and phosphate/glucose was performed using the FSRFA. Microsomes were preincubated with 50 mM glucose or KH_2PO_4 for 3 min at room temperature, then injected into the chamber containing 50 mM Hepes-Tris, 250 mM sucrose, pH 7.3 and 10 μM [U-^{14}C] or [^{32}P]G6P. Other steps were performed similarly as above.

In order to suppress the hydrolytic activity of G6Pase, microsomes were treated with 200 μM vanadate for 3 min at room temperature, then preloaded with 50 mM glucose or phosphate. Similar steps were subsequently performed as above.

IV.10 Data analysis

IV.10.1 Calculation of endogenous glucose production

Endogenous glucose production (Ra) during the IVGTT was calculated from the plasma specific activity of [^{3}H]glucose according to the following equation as described in [Finegood & Bergman, 1983]:

$$Ra = (Ra^{*} - V \cdot G \cdot dSA/dt)/SA$$

in which V stands the effective glucose distribution volume which is equal to 25% · Body weight · 0.45, Ra^{*} is the tracer infusion rate, SA is the tracer specific activity, dSA/dt is obtained from smoothing the curve of SA data against time points using Optimal Segments software [Finegood et al., 1983].

IV.10.2 Glucose disappearance rate

Glucose disappearance rate K_G was calculated according to [McArthur et al., 1999]. A double-exponential curve fit to the plot of ^3H counts (DPM) against time (t) was applied to calculate the rate of [^3H]glucose disappearance. The slope of the $\log_e$ of plasma glucose against time between the 162 and 180 min time points during the IVGTT was regarded as K_G.

IV.10.3 Transport kinetic parameters

Transport kinetic parameters, $T_{1/2}$ and the steady-state levels were calculated as described in the papers.

Chapter IV Articles and other results

IV.1 Article 1

Up-regulation of liver glucose-6-phosphatase in rats fed with a P_i-deficient diet

Wensheng XIE, Yazhou LI, Marie-Claire MÉCHIN and Gérald VAN DE WERVE*

Departments of Nutrition and Biochemistry, Centre de Recherche du CHUM, University of Montreal, Montreal, QC, H3C 3J7, Canada

* Corresponding author. Tel: +1 (514) 2816000 ext.7237; Fax: +1 (514) 8964701.
E-mail: vandeweg@mdnut.umontreal.ca

Key words: Phosphate deficiency, glucose-6-phosphatase, rat liver microsomes

Running title: Up-regulation of liver glucose-6-phosphatase by a Pi-deficient diet

Abbreviations used: G6P, glucose-6-phosphate; G6Pase, glucose-6-phosphatase; p36, G6Pase catalytic subunit; p46, putative G6P translocase protein; BCIP, 5-bromo-4-chloro-3-indolyl-phosphate; NBT, nitro blue tetrazolium; EQU, tracer accumulation inside microsomes at transport equilibrium stage.

SYNOPSIS

Because phosphate (P_i) deprivation markedly affects the NaP_i cotransporter in kidney and has been related to insulin resistance and glucose intolerance, the effect of a P_i-deficient diet on the liver microsomal glucose-6-phosphatase (G6Pase) system was investigated. Rats were fed with a control diet ($+P_i$) or a diet deficient in phosphate ($-P_i$) during two days and sacrificed on the morning of the third day, after an overnight fast (fasted) or not (fed). Kinetic parameters of P_i transport ($t_{½}$ and equilibration) into liver microsomes were not changed by the different nutritional conditions. In contrast, it was found that G6Pase activity was significantly increased in the ($-P_i$) groups. This was due to an increase in the V_{max} of the enzyme, without change in the K_m for G6P. There was no correlation between liver microsomal glycogen content and G6Pase activity, but both protein abundance and mRNA of liver 36 kDa catalytic subunit of G6Pase (p36) were increased. The mRNA of the putative G6P translocase protein (p46) was changed in parallel with that of the catalytic subunit, but the p46 immunoreactive protein was unchanged. These findings indicate that dietary P_i-deficiency causes increased G6Pase activity by upregulation of the expression of the 36 kDa catalytic subunit gene.

INTRODUCTION

The liver glucose-6-phosphatase (G6Pase) is a multiprotein complex, which resides in the endoplasmic reticulum membrane and plays an important role in the regulation of blood glucose concentration [1]. Until now, two components have been cloned: a 36 kDa catalytic subunit (p36) [2] and more recently a 46 kDa protein (p46) [3], that has been proposed to be a G6P transporter. P36 gene expression has now been well studied, positive effectors that increase p36 mRNA include glucose, fatty acids, cyclic AMP and glucocorticoids, whereas insulin decreases p36 mRNA [4]. Accordingly, in fasting and diabetes, when the insulin/glucagon ratio is low, p36 mRNA, protein and activity are high [5]. Hormonal control of p46 has not yet been reported. Inorganic phosphate imbalance leads to a number of disorders [6,7]. Hypophosphatemia in several diseases (hypophosphatemic rickets, adult-onset hypophosphatemic osteomalacia, renal P_i leak) is associated with insulin resistance and glucose intolerance [8], but this association depends on the severity of hypophosphatemia [9]. A P_i-deficient diet causes upregulation of the expression of the rat kidney NaP_i-2 cotransporter [10-12], while a potential effect of P_i deprivation on the liver endoplasmic reticulum G6Pase complex, which includes a P_i transport system, has not been investigated.

Our results show that a P_i-deficient diet upregulates rat liver microsomal G6Pase activity by increased expression of the p36 catalytic subunit gene, but without significant change in the abundance of the putative G6P translocase p46 protein.

EXPERIMENTAL

Materials

[^{32}P]KH_2PO_4 and [U-^{14}C]glucose-6-phosphate were from ICN Biomedicals (Montreal, QC) and [α-^{32}P]dCTP was from Pharmacia Biotech (Baie d'Urfé, QC). Bovine serum albumin, glucose-6-phosphate and amyloglucosidase were from Sigma (St Louis, MI). Hexokinase and glucose-6-phosphate dehydrogenase were purchased from Boehringer (Laval, QC). Molecular markers were purchased from Bio-Rad (Mississauga, ONT). The rabbit polyclonal antiserum against the recombinant G6Pase catalytic subunit (antibody against p36) was a kind gift of Dr. J.Y. Chou (N.I.H., Bethesda). The rabbit antiserum against N-terminal of p46 (GYGYYRTVIFSSAMFGGY) was produced in our laboratory. The BCIP/NBT stock solutions and the anti-rabbit IgG-AP conjugate were from the Promega Co (Madison, WI). TRIZOL LS Reagent was from Gibco BRL (Burlington, ONT).

Animals

Male Sprague-Dawley rats (300-350 g body weight) were used as the liver donor. Rats were fed for 48 hours with either a P_i-deficient diet (No. 86128) (-P_i) or a control (No. 86129) (+P_i) diet (Teklad, Madison, WI) containing 0.03% (w/w) or 1% (w/w) phosphate, respectively. All other components are the same in both diets. The fasted group had food removed 18 hours before sacrifice by decapitation while the fed group had constant access to food. According to these conditions, rats were classified into 4 groups: 1. Fed (-P_i); 2. Fed (+P_i); 3. Fasted (-P_i); 4. Fasted (+P_i). There were 5 rats in groups 1 to 3, and 6 rats in group 4.

Preparation of rat liver microsomes and G6Pase assay

Rat liver microsomes were isolated individually as described previously [13], except that the buffer was 250mM sucrose, 50mM Hepes-Tris at pH 7.3. G6Pase activity was assayed as in [14], before and after detergent (Chapso 0.8%) treatment.

Glycogen

Glycogen was asssayed in liver microsomes with the amyloglucosidase assay [15].

Phosphate transport

Zero-trans phosphate transport across the microsomal membrane was measured as described before [13].

Western blot analysis

Rat liver microsomes (50μg) were subjected to a 12% SDS-PAGE at 100V for about 1 hour in the Laemmli buffer. Then proteins were electro-transferred to a nitrocellulose membrane at 100V for 1 hour. The membrane was saturated for 30min in 100mM TBS, pH7.5, containing 10% milk. Membranes were incubated in the primary antibody solution (diluted to 1/500 for anti-p36 or 1/200 for anti-p46). The membrane was washed and incubated in the alkaline phosphatase conjugated anti-rabbit IgG solution (diluted as specified) for 1 hour. The membrane was washed again and detected in BCIP/NBT substrate system. The membrane was scanned and the quantification of each specific band was analyzed by using a Dual Light™ Transilluminator.

Northern blot analysis

Total liver RNA was individually extracted with TRIZOL LS Reagent. The same amount of RNA was fractionated by 1% agarose-formaldehyde gel electrophoresis, then transferred to a nylon membrane by a capillary technique in 20×SSC solution. The membrane was rinsed in 2×SSC solution, dried and immobilised under UV light. The hybridization was performed with [α-^{32}P]dCTP labelled probe (full length cDNA of p36 or p46) overnight at 68°C. The membrane was washed properly and exposed to a film for a certain time. The intensities of the mRNA bands were determined using a densitometer (Dual Light™ Transilluminator).

Data analysis

Phosphate transport kinetic analysis was done according to Equation 1:

$$A = EQU\ (1\text{-}e^{-kt}) + A_o \qquad \text{(Equation 1)}$$

in which A represents the tracer accumulation into microsomes at time t, EQU is the tracer accumulation at equilibrium, k is the rate constant and A_o the radioactive background.

The parameter $t_{1/2}$, the time at which 50% of a process has been completed, was calculated using Equation 2:

$$t_{1/2} = Ln2 / k \qquad \text{(Equation 2)}$$

Statistical analysis was performed according to Students' T test. Differences were considered significant when the p value was less than 0.05.

RESULTS AND DISCUSSION

P_i transport

Renal NaP_i cotransport is markedly upregulated by dietary phosphate deprivation [10-12], but it is not known whether liver microsomal phosphate transport is also affected by this diet. Liver microsomes were prepared individually from each rat in the 4 experimental groups. Table I shows that the $t_{1/2}$ of tracer [^{32}P]KH_2PO_4 (10μM) uptake into microsomes was about 23 seconds and did not change with the nutritional conditions (fasted or fed, + P_i or - P_i). The transport process reached an equilibrium after about 2min, as we documented before [13], and the tracer accumulation at that time (EQU) was about 9 pmol/mg. Similarly to the $t_{1/2}$, EQU values were not statistically different for the four experimental groups. These results show that the transport rate and the phosphate accessible space of liver microsomes were unaffected either by fasting or by a (-P_i) diet.

G6Pase activity

The reported association of phosphate deprivation and glucose intolerance [8,9] lead us to further investigate the liver G6Pase system in our experimental conditions, since G6Pase is responsible for hepatic glucose production and the maintenance of euglycemia. Fig.1 shows that the activity of G6Pase, measured in liver microsomes with 0.2mM G6P before and after detergent treatment, was increased in both fed and fasted groups of (-P_i) rats compared to controls (+P_i). It can be seen that this diet-induced increase in activity was additive with the well-documented proper effect of

fasting [16] as well as with that resulting from detergent treatment. The increase in G6Pase activity due to the ($-P_i$) diet was caused by an increase in V_{max} rather than a change in the K_m of G6Pase for G6P (Table II). Also shown in Table II, is that fasting increased significantly the V_{max} of G6Pase and that the K_m of G6Pase for G6P decreased in the presence of detergent, as has been shown before. From these results, it could be deduced that the ($-P_i$) diet upregulates G6Pase activity in liver.

It has been reported that glycogen-bound fatty acids regulate G6Pase activity and might be responsible for changes in this enzyme activity in the fasting-refeeding period [17]. We thus explored the possibility that increased G6Pase activity was due to a lower liver microsomal glycogen concentration in the ($-P_i$) group. This was however not the case. As shown in Fig.2, the microsome glycogen content decreased to a large extent by fasting, but there was no obvious correlation between glycogen content and G6Pase activity.

We further verified if upregulation of G6Pase activity by dietary P_i deprivation was caused by changes in the protein amount of G6Pase p36 catalytic subunit and/or of p46 putative G6P transporter.

Western analysis of p36 and p46 G6Pase protein

The abundance of immunoreactive microsomal protein was measured with a polyclonal antibody against the catalytic subunit of G6Pase. The visualized band was at a position corresponding to a M*r* of about 36kDa (Fig.3A). The corresponding density scan results are shown in Fig.3C. One can see that the effect of the ($-P_i$) diet on G6Pase activity was accompanied by a parallel increase in p36 catalytic subunit

abundance and that, as for G6Pase activity, there was an additive effect of ($-P_i$) diet and fasting on this parameter.

The 46kDa component of G6Pase is a putative glucose-6-phosphate transporter, which may also be a regulator of the G6Pase catalytic subunit. It was thus possible that a ($-P_i$) diet has some effect on this protein, resulting in the change in G6Pase activity. An antibody against the N-terminal part of p46 was used to detect p46 protein abundance. The scan results of the specific band are shown in Fig.3B. It is apparent that unlike p36, the p46 protein associated to microsomes was not significantly changed in the present experimental conditions (Fig.3C).

Northern blot analysis of p36 and p46 G6Pase mRNA

In order to know if the increased p36 protein was due to increased synthesis or decreased degradation, the p36 mRNA abundance was measured. Northern blots of p36 mRNA and p46 mRNA were performed with the full length cDNA of p36 or p46 as a probe, respectively. Fig.4A shows a representative blot for p36 in the four experimental groups and Fig.4C shows the quantification of the bands. It can be seen that fasting increases p36 mRNA, a result consistent with the corresponding Western blot and that has been reported previously [16]. Also in agreement with the immunoreactivity, p36 mRNA increased significantly in the ($-P_i$) diet groups as compared to the ($+P_i$) diet groups, showing that alimentary P_i deficiency affects p36 gene expression. The liver p46 mRNA changes were parallel to those of p36. Fig.4 shows indeed that p46 mRNA abundance was increased with fasting, as documented before [18], as well as with the ($-P_i$) diet in the fed and fasted groups. The fact that these changes in mRNA were not associated with changes in protein (see Fig.3),

suggests either increased degradation of p46 or less translation of p46 mRNA. Interestingly, a low phosphate diet induces a post-transcriptional effect on parathyroid hormone gene expression that is related to the binding of parathyroid proteins to the 3'-untranslated region of parathyroid hormone mRNA, this low phosphate diet results in decreased stability of the transcript [19].

CONCLUSIONS

Contrary to kidney, where dietary P_i deprivation markedly induces overexpression of the NaP_i-2 cotransporter, this diet does not affect liver microsomal P_i transport. The present results show for the first time that P_i deprivation *in vivo* causes microsomal liver G6Pase upregulation. In our experimental conditions, an increase in the p36 catalytic subunit alone is sufficient to enhance G6Pase activity. This could in turn favor increased hepatic glucose production and be partially causal in the association found between hypophosphatemia and glucose intolerance.

We do not know how P_i deficiency leads to increased gene expression. Studies using cultured cells, in which the extracellular parameters can be controlled better than *in vivo* could give us that information. It will also be interesting to see if other enzymes, besides G6Pase, involved in glucose production by the liver are also affected by P_i deprivation. The candidate genes to be affected by Pi-deficiency are glucokinase, pyruvate kinase (that are expected to be down-regulated) and phosphoenolpyruvate carboxykinase (that is expected to be upregulated). This work is in progress.

Acknowledgement: This work was supported by Grant MT-10804 from the Medical Research Council of Canada. Dr Richard Béliveau (UQAM) is gratefully acknowledged for providing the diets and animal care.

REFERENCES

1. Foster, J.D.F., Pederson, B.A. and Nordlie, R.C. (1997) Proc. Soc. Exp. Biol. Med. **215**, 314-332
2. Lei, K.J., Shelly, L.L., Pan, C.J., Sidbury, J.B. and Chou, J.Y. (1993) Science **262,** 580-583
3. Gerin, I., Veiga-da-Cunha, M., Achouri, Y., Collet, J.F. and van Schaftingen, E. (1997) FEBS Lett. **419**, 235-238
4. Lange, A.J., Argaud, D., El-Maghrabi, M.R., Pan, W., Maitra, S.R. and Pilkis, S.J. (1994) Biochem. Biophys. Res. Commun. **201**, 302-309
5. Liu, Z., Barrett, E.J., Dalkin, A.C., Zeart, A.D. and Chou, J.Y. (1994) Biochem. Biophys. Res. Commun. **205,** 680-686
6. Bevington, A., Kemp, G.T., Graham, R. and Russell, R.G.G. (1992) Clin. Chem. Enzym. Commun. **4**, 235-237
7. Berner, Y.N. and Shike, M. (1988) Annu. Rev. Nutr. **8**, 121-148
8. DeFronzo, R.A. and Lang, R. (1980) N. Engl. J. Med. **303**, 1259-1263
9. Paula, F.J.A., Plens, A.E.C.M. and Foss, M.C. (1998) Horm. Metab. Res. **30**, 281-284
10. Tenenhouse, H.S., Martel, J., Biber, J. and Murer, H. (1995) Am. J. Physiol. **268**, F1062-F1069
11. Boyer, C.J.C., Xiao, Y., Dugré, A., Vincent, É., Delisle, M.C. and Béliveau, R. (1996) Biochim. Biophys. Acta. **1281**, 117-123

12. Seifert, S.A., Hsiao, S., Murer, H., Biber, J. and Kempson, S.A. (1997) Cell Biochem. Funct. **15**, 9-14

13. St-Denis, J.-F., Comte, B., Nguyen, D.K., Seidman, E., Paradis, K., Levy, E. and van de Werve, G. (1994). J. Clin. Endo. Metabol. **79**, 955-959

14. St-Denis, J.-F., Berteloot, A., Vidal, H., Annabi, B. and van de Werve G. (1995) J. Biol. Chem. **270**, 21092-21097

15. van de Werve, G., Sestoft, L., Folke, M. and Kristensen, L. Ø. (1984) Diabetes, **33**, 944-949

16. Minassian, C., Zitoun, C. and Mithieux, G. (1996) Mol. Cell. Biochem. **155**, 37-41

17. Mithieux, G. and Zitoun, C. (1996) Eur. J. Biochem. **235**, 799-803

18. Middleditch, C., Clottes, E. and Burchell, A. (1998) FEBS Lett. **433**, 33-36

19. Moallem, E., Kilav, R., Silver, J. and Naveh-Many, T. (1998) J. Biol. Chem. **273**, 5253-5259

FIGURE LEGENDS

Figure 1. Effect of fasting and a P_i-deficient diet on microsomal G6Pase activity

G6Pase activity was measured with 0.2mM glucose-6-phosphate at 30°C for 2min. Results are mean values ± S.E.M. for each group (n = 5-6). Bars headed by same letters are statistically different from each other by : *a* $p< 0.001$; *b* $p< 0.02$; *c* $p< 0.01$; *d* $p< 0.01$ (Unpaired Student's *t* test).

Figure 2. Comparison of microsomal glycogen content and G6Pase activity

Glycogen content was measured in microsomes as described in the Methods section. G6Pase activity was measured at 0.2mM G6P in intact microsomes at 30°C for 2min.

Figure 3. Immunoblot analysis of p36 and p46

(A, B) One representative visualization of specific bands of p36 and p46 respectively in the four experimental groups. (C) Quantification of specific bands for each group. The fed (+Pi) group was taken as control (100%). Results are mean values ± S.E.M. for each group (n = 5-6). Bars headed by same letters are statistically different from each other by : *a* $p< 0.02$; *b* $p< 0.02$ (Unpaired Student's *t* test).

Figure 4. Northern blot of mRNA of p36 and p46

(A, B) One representative visualization of p36 and p46 mRNA levels respectively in the four experimental groups. (C) Quantification of p36 mRNA and p46 mRNA of each group. The fed (+Pi) group was taken as control (100%). Results are mean values ± S.E.M. (n = 3-4). Bars headed by same letters are statistically different from each other by : *a* $p< 0.05$; *b* $p < 0.05$; *c* $p< 0.05$; *d* $p< 0.05$ (Unpaired Student's *t* test).

Table I Kinetic parameters for phosphate transport in microsomes. Effect of fasting and of a P_i-deficient diet.

Groups of rats	$t_{1/2}$ (sec)	EQU (pmol/mg protein)
Fed ($-P_i$)	23 ± 1.4	8.7 ± 0.3
Fed ($+P_i$)	22 ± 1.3	10.0 ± 0.4
Fasted ($-P_i$)	24 ± 0.9	9.0 ± 1.1
Fasted ($+P_i$)	22 ± 1.7	10.0 ± 1.7

Phosphate transport in intact microsomes was measured with tracer (10μM) $[^{32}P]KH_2PO_4$ for different times up to 2min at which equilibrium of uptake was reached. Results are means ± S.E.M for each group (n = 4-5). $t_{½}$ and EQU values are not statistically different from each other respectively in the four groups.

Table II Kinetic parameters for G6P hydrolysis in microsomes. Effect of fasting and of a P_i-deficient diet.

Group of rats	V_{max} (munits/mg)		K_m (mM)	
	Intact	detergent-treated	Intact	etergent-treated
Fed (-P_i)	176 ± 8 [a]	330 ± 10 [c]	2.66 ± 0.14	2.15 ± 0.19
Fed (+P_i)	132 ± 4 [a]	194 ± 8 [c]	2.68 ± 0.13	2.13 ± 0.08
Fasted (-P_i)	214 ± 3 [b]	381 ± 11 [d]	2.90 ± 0.10	2.26 ± 0.15
Fasted (+P_i)	158 ± 5 [b]	321 ± 9 [d]	2.70 ± 0.11	2.35 ± 0.47

The G6Pase activity of intact or detergent-treated microsomes was measured with 0.2, 0.5, 1, 2 and 5mM G6P for 2min at 30°C. V_{max} and K_m were calculated by non-linear regression of Michaelis-Menten kinetics. Results are mean values ± S.E.M for each group (n = 5-6). Values headed by same letters are statistically different from each other by $p < 0.02$ (Unpaired Student's *t* test).

Figure 1

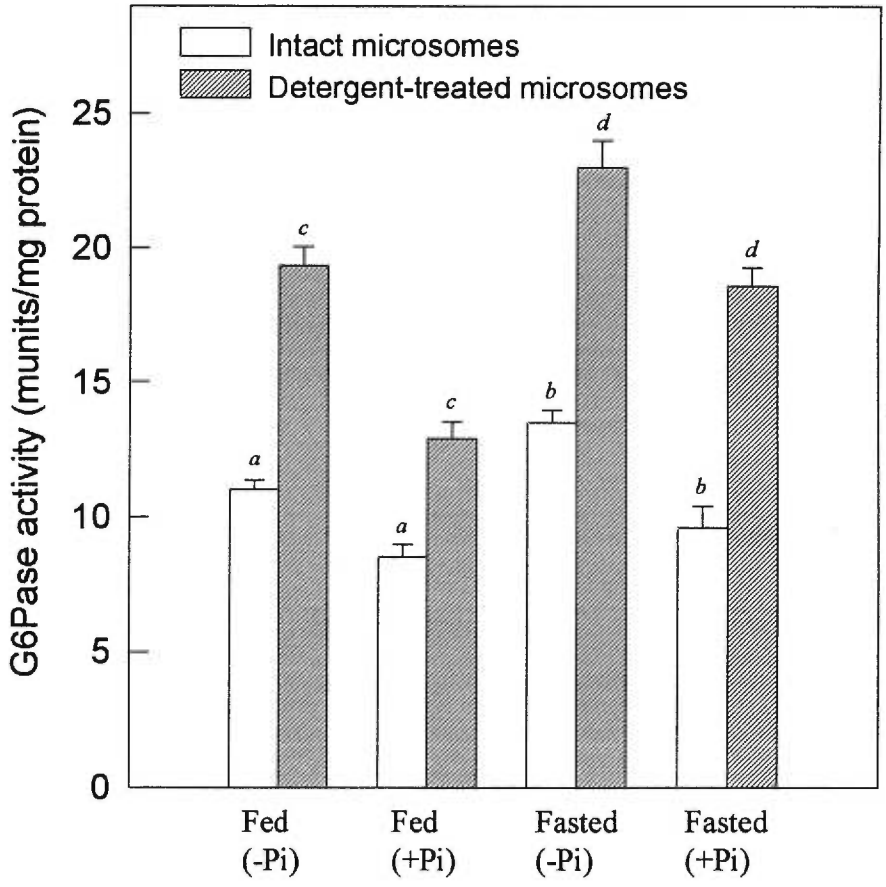
Intact microsomes
Detergent-treated microsomes
G6Pase activity (munits/mg protein)
0
5
10
15
20
25
a
c
a
c
b
d
b
d
Fed (-Pi)
Fed (+Pi)
Fasted (-Pi)
Fasted (+Pi)

Figure 2

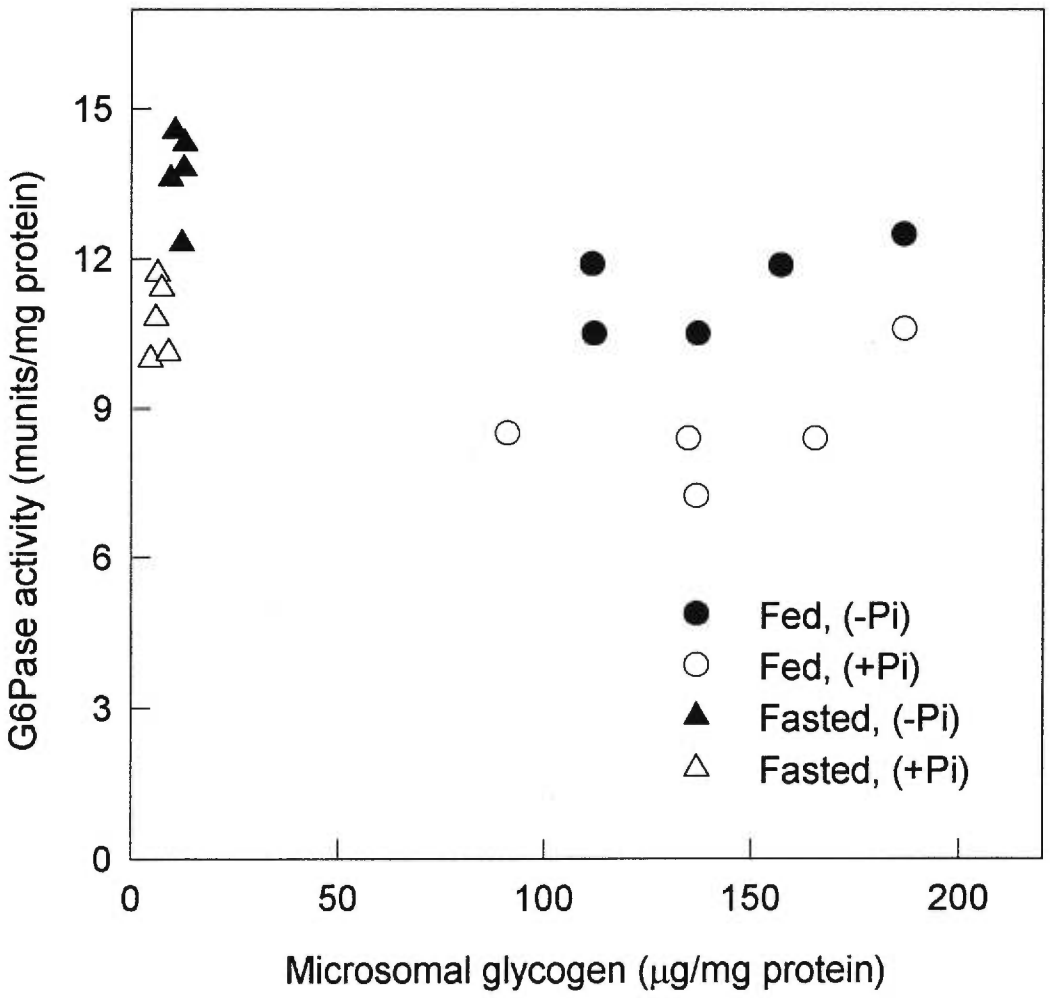
G6Pase activity (munits/mg protein)
15
12
9
6
3
0
0
50
100
150
200
Microsomal glycogen (μg/mg protein)
Fed, (-Pi)
Fed, (+Pi)
Fasted, (-Pi)
Fasted, (+Pi)

Figure 3

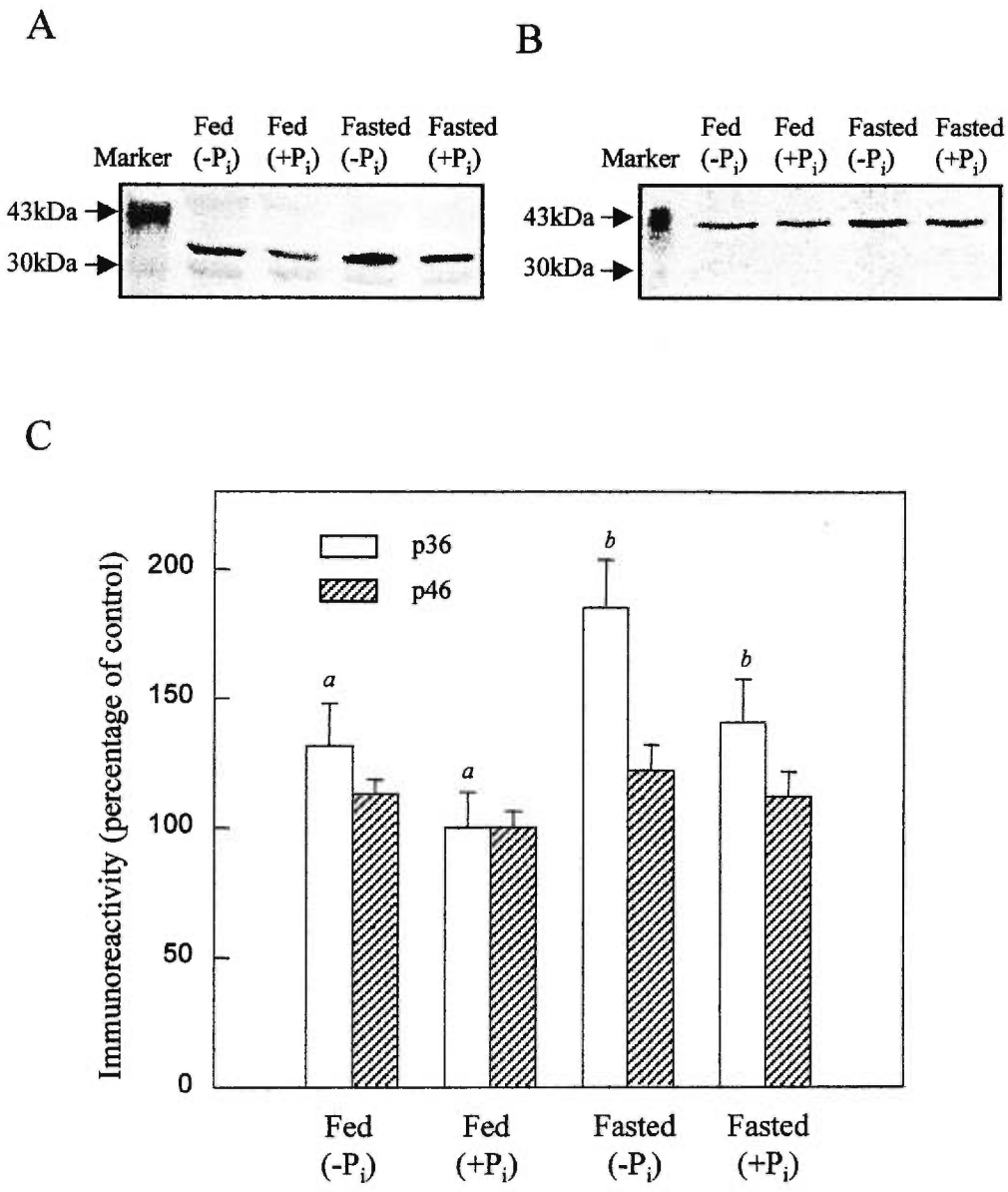
A
B
Marker
Fed (-Pi)
Fed (+Pi)
Fasted (-Pi)
Fasted (+Pi)
43kDa
30kDa
C
p36
p46
Immunoreactivity (percentage of control)
200
150
100
50
0
a
a
b
b
Fed (-Pi)
Fed (+Pi)
Fasted (-Pi)
Fasted (+Pi)

Figure 4

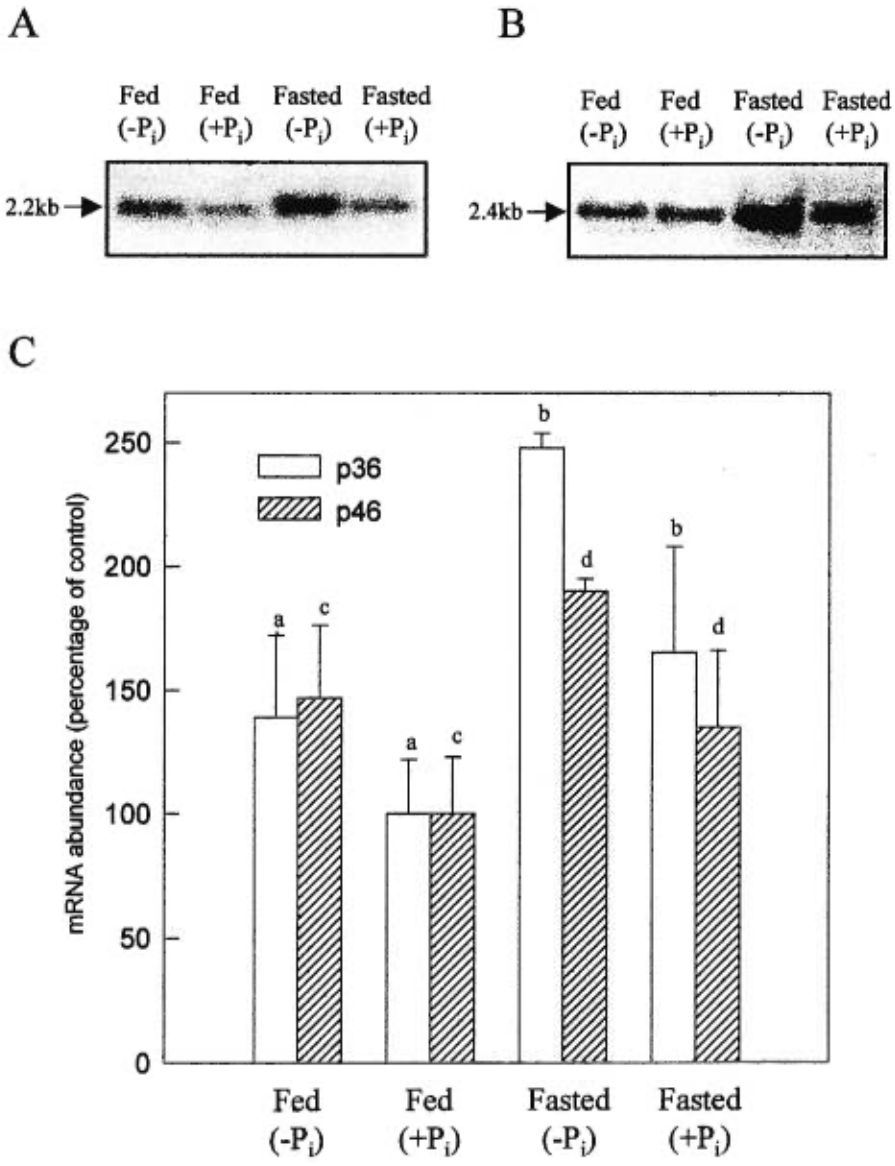
A
Fed (-Pi)
Fed (+Pi)
Fasted (-Pi)
Fasted (+Pi)
2.2kb
B
Fed (-Pi)
Fed (+Pi)
Fasted (-Pi)
Fasted (+Pi)
2.4kb
C
mRNA abundance (percentage of control)
p36
p46
0
50
100
150
200
250
a
c
a
c
b
d
b
d
Fed (-Pi)
Fed (+Pi)
Fasted (-Pi)
Fasted (+Pi)

IV.2 Article 2

Dietary phosphate deprivation in rats affects liver cyclic AMP, glycogen, key steps of gluconeogenesis and glucose production

Wensheng XIE [§], T. Luong TRAN [‡], Diane T. FINEGOOD[‡] and Gérald VAN DE WERVE [§*]

[§] Departments of Nutrition and Biochemistry, Centre de Recherche du CHUM, University of Montreal, Montreal, QC, H3C 3J7, Canada, [‡] School of Kinesiology, Simon Fraser University, 8888 University Drive, Burnaby, BC, V5A 1S6, Canada

* Corresponding author. Tel: +1 (514) 2816000 ext.7237; Fax: +1 (514) 8964701.
E-mail: [redacted]

Key words: Phosphate deficiency, cyclic AMP, gluconeogenesis, glycogen, intravenous glucose tolerance, endogenous glucose production, rat liver

Running title: Stimulation of liver glucose production by a P_i-deficient diet

Abbreviations used: G6P, glucose-6-phosphate; PK, pyruvate kinase; PEP, phospho*enol*pyruvate; PEPCK, phospho*enol*pyruvate carboxykinase; G6Pase, glucose-6-phosphatase; GK, glucokinase; F-2,6-P_2, fructose-2,6-bisphosphate; IVGTT, intravenous glucose tolerance test.

SYNOPSIS

We previously reported (Biochem. J., 1999, 343, 393-396) that dietary phosphate deprivation up-regulated both the catalytic subunit and the putative glucose-6-phosphate translocase of the rat liver microsomal glucose-6-phosphatase (G6Pase) system, suggesting that increased hepatic glucose production might be responsible for the frequent clinical association of hypophosphatemia and glucose intolerance. We now show that liver cyclic AMP (cAMP) was increased in rats fed with a diet deficient in phosphate ($-P_i$) compared to rats fed with a control diet ($+P_i$). Accordingly, in the ($-P_i$) group pyruvate kinase (PK) was inactivated, the concentration of phospho*enol*pyruvate (PEP) was increased and fructose-2,6-bisphosphate (F-2,6-P_2) concentrations were reduced by half. Phospho*enol*pyruvate carboxykinase (PEPCK) activity was marginally increased and glucokinase (GK) activity was unchanged by phosphate deprivation. The liver glycogen concentration decreased in the ($-P_i$) group. In the fed state, plasma glucose concentration was increased and plasma insulin concentration was substantially decreased in the ($-P_i$) group. The plasma glucose level was elevated in ($-P_i$) group immediately after the glucose bolus during the intravenous glucose tolerance test (IVGTT), although there was no significant difference in the rate of glucose fall. The elevated plasma glucose in the ($-P_i$) group was due to reduced suppression of endogenous glucose production following the glucose bolus. Taken together, these changes are compatible with a stimulation of liver gluconeogenesis and glycogenolysis by the ($-P_i$) diet and further

indicate that the liver might contribute to impaired glucose homeostasis in P_i-deficient states.

INTRODUCTION

Liver glucose production stems from glycogenolysis and gluconeogenesis to glucose 6-phosphate (G6P) and its subsequent hydrolysis by the glucose-6-phosphatase (G6Pase) complex in the endoplasmic reticulum membrane [1]. G6Pase comprises at least two proteins, a 36 kDa catalytic subunit (p36) [2] and a 46 kDa protein (p46) [3], that has been proposed to be a G6P transporter. We have recently shown that a P_i-deficient (-P_i) diet upregulates rat liver microsomal G6Pase activity by increased expression of both the p36 and p46 genes, and protein abundance of p36 only [4]. This finding suggests that overproduction of glucose by the liver may contribute to glucose intolerance and insulin resistance that were documented in several diseases (hypophosphatemia rickets, adult-onset hypophosphatemia osteomalacia, renal P_i leak) characterized with hypophosphatemia [5]. It was indeed reported that changes in plasma phosphate levels influenced insulin sensitivity [6] and gluconeogenesis was altered in kidney proximal tubules and osteoblasts from X-linked hypophosphatemia mice [7, 8]. Except for these data, it is uncertain, even controversial, whether and how hypophosphatemia affects glucose metabolism *in vivo*. In the present study, we have also investigated the cause(s) for the upregulation of G6Pase by the (-P_i) diet and found that liver cAMP, which enhances G6Pase gene expression [9,10], was increased. In parallel, pyruvate kinase was inactivated, PEP was elevated, F-2,6-P_2 was decreased, and glycogen was also decreased. In the fed state, the plasma glucose concentration was increased and the plasma insulin concentration was decreased in the (-P_i) group. After an overnight fast, there was less suppression of endogenous

glucose production by a glucose bolus in the ($-P_i$) group, resulting in higher plasma glucose levels. Taken together, these data support a role for enhanced glucose production in the ($-P_i$) group from elevation of liver gluconeogenesis and glycogenolysis by the ($-P_i$) diet.

EXPERIMENTAL

Materials

Glucose, triethanolamine, adenosine 5'-trisphosphate, adenosine 5'-diphosphate, imidazole, glutathione, fructose-6-phosphate disodium salt, sodium pyrophosphate, F-2,6-P_2 tetrasodium salt, inosine 5'-diphosphate, glucose 6-phosphate, amylo-1,4-1,6-glucosidase, PPi-phosphotransferase and glucose oxidase were from Sigma (St Louis, MI). NADP, NADH, PEP, PK, malate dehydrogenase, lactate dehydrogenase, hexokinase, glucose-6-phosphate dehydrogenase, aldolase, glyceraldehyde-3-phosphate dehydrogenase, triose-3-phosphate isomerase were purchased from Boehringer (Laval, QC). [^{3}H]cAMP was from NEN (Boston, MA). [3-^{3}H]glucose was purchased from Mandel Scientific Company (Guelph, Ont). A cAMP assay kit was purchased from Amersham (Baie d'Urfé, QC). Rat Insulin ELISA kit was from Crystal chem Inc (Chicago, IL).

Animals

Male Sprague-Dawley rats (around 300g body weight) were used for all of the experiments. Rats used for liver sampling were fed for 48 hours with either a P_i-deficient diet (No. 86128) (-P_i) or a control (No. 86129) (+P_i) diet (Teklad, Madison, WI) containing 0.03% (w/w) or 1% (w/w) phosphate, respectively. All other components were the same in both diets. Five rats were used in each group (-P_i and +P_i). To sample the livers, rats were decapitated on the morning of the third day.

For rats undergoing an IVGTT, catheters were inserted as described in [11]. Briefly, the animal was anesthetized and sterile catheters were placed in the left carotid artery (for blood sampling) and the right jugular vein (for tracer infusion and bolus injection). After one week of recovery, the rats were fed with ($-P_i$) or ($+P_i$) diet for 48h, then fasted overnight before the IVGTT was performed. Four rats were used in the ($-P_i$) group and five in the ($+P_i$) group.

In a separate group of animals fed with the ($-P_i$) or ($+P_i$) diet for 48h (n = 5 for each diet), blood samples were taken at 9:00AM on the morning of the third day for the measurement of fed state plasma glucose and insulin.

Intravenous glucose tolerance test

The IVGTT was performed as described in [11]. 10 min after the first blood sample (regarded as time point 0 min), a primed, continuous infusion of [3-^{3}H]glucose was started. The priming dose (9 μCi/ml) was given within 60 s, and the continuous infusion (10 μCi/ml) was infused at 0.015 ml/min (0.15 μCi/min). Blood samples were taken at 120, 130, 140, 150, and 155 min. At 160 min, a glucose bolus (0.3g/kg body weight) mixed with tracer glucose (13μCi) was given within 1min. Blood samples were taken at 162, 165, 170, 175, 180, 190, 220, 250 min. Hematocrit was measured before and after the experiment. Blood sample handling, plasma glucose and plasma specific radioactivity determination were performed as described in [11]. Plasma insulin was assayed using a Rat Insulin ELISA kit.

Liver treatment

Livers were homogenized in 50 mM Hepes-Tris, 250 mM sucrose, pH 7.3 and further processed at 4°C. The homogenates were centrifuged at 1,000g for 10min, the first supernatant was recovered and further centrifuged at 12,000g for 10min. The second supernatant was centrifuged at 100,000g for 60min. This last high-speed supernatant was used for the assay of GK, PK and PEPCK. Prior to homogeneization, part of the liver from each rat was freeze-clamped in liquid nitrogen and kept at -80°C pending other assays.

Liver cAMP

About 100mg of frozen liver was homogenized in 1ml cold 6% TCA containing a tracer amount of [^{3}H]cAMP as internal control. Denatured proteins were removed by centrifugation and the TCA was extracted from the supernatant 4 times with 5 vol. of water-saturated-ether. Cyclic AMP was assayed in the aqueous phase according to the instructions of the assay kit. Recovery was calculated from the carry-over of [^{3}H]cAMP in the assay samples.

Enzyme assays

GK activity was assayed as described before [12]. PK and PEPCK activities were measured at room temperature as detailed previously [13,14]. The active form of PK was measured in the presence of 0.15 mM PEP and the total activity at 5.0 mM PEP [13].

Metabolite assays

Pyruvate, Pi and PEP were measured in neutralized TCA extracts by classical procedures [15]. Glycogen [15] and F-2, 6-P_2 [16] were measured in neutralized NaOH extracts.

Data analysis

The rate of glucose disappearance during IVGTT (K_G) was calculated as the slope of the $\log_e$ of plasma glucose against time between the 162 and 180 min time points as described in [11]. Endogenous glucose production was calculated as described in [17]. Statistical analysis was performed according to Students' T test. Differences were considered significant when the p value was less than 0.05.

RESULTS AND DISCUSSION

Our previous report demonstrated that a (-P_i) diet upregulates liver G6Pase activity [4]. This finding suggested that hepatic glucose production might be enhanced in this condition. We have therefore investigated whether glycogen and key regulatory steps of gluconeogenesis were affected by dietary P_i deprivation. These steps are at the PEP/pyruvate, fructose 6-phosphate/fructose 1,6-bisphosphate and glucose/glucose 6-phosphate cycles [18]. We also measured the fed and fasted plasma glucose and insulin concentrations, endogenous glucose production as well as intravenous glucose tolerance in rats fed with (-P_i) or (+P_i) diet.

The PEP/pyruvate cycle

We show that feeding rats for two days with a (-P_i) diet substantially decreased plasma phosphate concentration but did not affect liver P_i concentration (Table I). (-P_i) diet resulted in a 50% increase in cAMP concentration (Table I). PK, measured at 0.15 mM PEP, was found to be inactivated (Fig. 1A) whilst the total PK activity, measured at 5.0 mM PEP, was unchanged by P_i deprivation (Fig. 1B). Fig. 2 shows that there was a linear negative correlation between the active form of PK and cAMP and that all individual values of cAMP and PK were different between the two groups. These results suggest that the inactivation of PK in the (-P_i) group is the consequence of increased liver cAMP and activation of cAMP-dependent protein kinase (PKA). PKA has indeed been well documented to phosphorylate and inactivate PK *in vitro* [19], an effect mediated by glucagon in the perfused liver [20] and in isolated hepatocytes [13]. In the latter [13], the dose-dependent stimulation of gluconeogenesis

by glucagon was parallel with the inactivation of PK. The stimulation of gluconeogenesis by the inactivation of pyruvate kinase is mediated by PEP which accumulates and which, by mass action, pushes the intermediate towards glucose. Accordingly, liver PEP concentrations were increased in the ($-P_i$) group (Table I). Liver PEPCK activity also tended to be higher in the ($-P_i$) group (16.56 ± 1.04 vs 18.44 ± 1.38 munits/mg protein), but the difference was not statistically significant. The higher PEP concentration is therefore more likely to be the result of its lesser conversion to pyruvate by PK rather than its increased production by PEPCK.

The fructose 6-phosphate/fructose 1,6-bisphosphate cycle

Another key reaction in gluconeogenesis is catalyzed by fructose-1,6-bisphosphatase and is inhibited by F-2,6-P_2 [21,22]. The concentration of F-2,6-P_2 is determined by the activity of the bifunctional enzyme 6-phosphofructo 2-kinase/fructose 2,6-bisphosphatase. The kinase activity of this enzyme is inactivated and the phosphatase activity is activated by PKA in liver [23,24]. Therefore an increase in cAMP such as observed here in the liver of rats fed with a ($-P_i$) diet should decrease F-2,6-P_2, by a concerted inhibition of its synthesis and stimulation of its degradation. Table I shows that this is indeed the case, since F-2,6-P_2 concentrations were decreased by half in the ($-P_i$) group. The resulting deinhibition of fructose-1,6-bisphosphatase would be in agreement with a stimulation of gluconeogenesis. The fact that F-2,6-P_2 concentration decreased in the ($-P_i$) group suggests that this metabolite does not play a role in the overexpression of G6Pase found in this condition [4], because F-2,6-P_2 is a known stimulator of p36 gene expression [25] .

The glucose/glucose 6-phosphate cycle

The upregulation of G6Pase activity by the ($-P_i$) diet [4] would favor net liver glucose production only if the opposing reaction catalyzed by GK was unchanged or decreased. Experimental data showed that, compared to the ($+P_i$) group, GK activity was not modified in the ($-P_i$) group (7.74 ± 1.53 vs 8.1 ± 0.94 munits/mg protein), thus indicating that enhanced G6Pase activity alone might be responsible, at this ultimate cycle, for increased hepatic glucose production. Given that the mRNA abundance of both the putative G6P transporter [4] and the catalytic subunit [4,9] of G6Pase are stimulated by cAMP, it is probable that the increased cAMP in the liver of the animals fed a low P_i diet is the cause for increased gene expression of the components of G6Pase and increased activity of this enzyme [4].

Glycogen

In order to know if the increase in cAMP observed in the livers of the ($-P_i$) group had also affected glycogen degradation, that is stimulated by cAMP, we measured the liver glycogen content. Fig. 3 shows a linear negative correlation between cyclic AMP and glycogen concentrations in the two groups of rats and that all individual values of cAMP and glycogen were different between the two groups. It appears that the glycogen concentration was decreased almost by half in the livers of rats fed a low P_i diet and that this decrease was associated with the increase in cAMP concentration, suggesting a cAMP-induced glycogenolysis in this group.

Glucoregulatory effects

The effects of the low P_i diet on regulatory steps of gluconeogenesis were manifest at the level of the whole animal as elevated plasma glucose levels during glucose loading. In the fed state, plasma glucose levels were increased (Table I) and after an intravenous glucose load, plasma glucose levels were higher in the ($-P_i$) group as shown in Panel A, Fig. 4, even though the rate of glucose fall (K_G) was similar (Table I). These data suggest a mild state of glucose intolerance in the (-Pi) group. This result is consistent with the observation in [26] which showed a slight tendency to hyperglycaemia during an IVGTT in patients with hypophosphatemia. There was no difference, however, in the plasma glucose or insulin levels following an overnight fast (Table I), indicating a potential compensating effect of fasting to P_i deficiency. Although plasma insulin concentration was substantially lower in the ($-P_i$) group in the fed state (Table I), the insulin response was not significantly different following the glucose bolus in the IVGTT as shown in Panel B, Fig.4. The elevated plasma glucose level during the IVGTT was due to a decreased suppression of endogenous glucose production by the glucose bolus (Panel C, Fig.4). This suggests that the mild glucose intolerance is due to an increase in gluconeogenesis and glycogenolysis by P_i deficiency.

Conclusions

Our previous work indicated that dietary P_i deficiency enhanced liver G6Pase expression and activity [4]. The present observations show in addition that the metabolic liver profile of ($-P_i$)-fed rats is that of enhanced endogenous glucose production resulting from stimulated gluconeogenesis and glycogenolysis. This increased glucose production is most likely triggered by an increase in cAMP

concentration, as documented by the inactivated PK, higher PEP and lower F-2,6-P_2 and glycogen concentrations. Similarly, high cAMP concentration can account for the increased expression of G6Pase. How P_i deficiency affects the liver *in vivo* is unknown. Our data demonstrate that both groups of rats ingested the same amount of food (40.5 ± 6.68 for (+P_i) group vs 41.4 ± 7.75 g for (-P_i) group) during the special diet feeding period, excluding the possibility of lower caloric intake in (-P_i) group. Reduced fed state plasma insulin data suggest that dietary P_i deficiency may alter the insulin/glucagon ratio entering the liver which may in turn affect hepatic cAMP metabolism. With respect to insulin secretion, the effect of phosphate deficiency is not consistent. It has been reported that pancreatic insulin secretion was lower in the rats with phosphate depletion [27]. In contrast, however, serum insulin levels were substantially higher in the hypophosphatemic patients during an IVGTT [26]. Another intriguing possibility would be that hormone(s) associated to phosphate homeostasis, such as the newly discovered phosphaturic hormone phosphatonin [28] or stanniocalcin [29], is regulated by dietary P_i deprivation and affects liver cAMP. It was indeed reported that stanniocalcin was expressed in human pancreatic cells and could affect glucose metabolism [30].

Acknowledgement: This work was supported by Grant MT-10804 from the Medical Research Council of Canada (to G. van de Werve) and by a grant from the Canadian Diabetes Association (to D.T. Finegood). An abstract of this work was presented at the President Poster Session in the 60th American Diabetes Association Conference. Drs Richard Béliveau and Edith Beaulieu (UQAM) are gratefully acknowledged for providing the diets and animal care and Dr Marie-Claire Méchin for helpful discussion. Authors also thank Lily Huang for the animal surgery and Guylaine Gévry for the artwork.

REFERENCES

1. 1 Foster, J.D.F., Pederson, B.A. and Nordlie, R.C. (1997) Glucose-6-phosphatase structure, regulation, and function: an update. Proc. Soc. Exp. Biol. Med. **215**, 314-332
2. 2 Lei, K.J., Shelly, L.L., Pan, C.J., Sidbury, J.B. and Chou, J.Y. (1993) Mutations in the glucose-6-phosphatase gene that cause glycogen storage disease type 1a. Science **262**, 580-583
3. Gerin, I., Veiga-da-Cunha, M., Achouri, Y., Collet, J.F. and Van Schaftingen, E. (1997) Sequence of a putative glucose 6-phosphate translocase, mutated in glycogen storage disease type Ib. FEBS Lett. **419**, 235-238
4. Xie, W.S., Li, Y.Z., Méchin, M.-C. and van de Werve, G. (1999) Up-regulation of liver glucose-6-phosphatase in rats fed with a P(i)-deficient diet. Biochem. J. **343**, 393-396
5. DeFronzo, R.A. and Lang, R. (1980) Hypophosphatemia and glucose intolerance: evidence for tissue insensitivity to insulin. N. Engl. J. Med. **303**, 1259-1263
6. Nowicki, M., Fliser, D., Fode, P. and Ritz, E. (1996) Changes in plasma phosphate levels influence insulin sensitivity under euglycemic conditions. J. Clin. Endocrinology and Metabolism. **81**, 156-159
7. Capparelli, A.W., Roh, D., Dhiman, J.K., Jo, O.D. and Yanagawa, N. (1992) Altered proximal tubule glucose metabolism in X-linked hypophosphatemia mice. Endocrinology. **130**, 328-334

8. Rifas, L., Gupta, A., Hruska, K.A. and Avioli, L.V. (1995) Altered osteoblast gluconeogenesis in X-linked hypophosphatemia mice is associated with a depressed intracellular pH. Calcif. Tissue Int. **57**, 60-63

9. Lange, A.J., Argaud, D., El-Maghrabi, M.R., Pan, W., Maitra, S.R. and Pilkis, S.J. (1994) Isolation of a cDNA for the catalytic subunit of rat liver glucose-6-phosphatase: regulation of gene expression in FAO hepatoma cells by insulin, dexamethasone and cAMP. Biochem. Biophys. Res. Commun. **201**, 302-309

10. Li, Y.Z., Méchin, M.-C. and van de Werve, G. (1999) Diabetes affects similarly the catalytic subunit and putative glucose-6-phosphate translocase of glucose-6-phosphatase. J. Biol. Chem. **274**, 33866-33868

11. McArthur, M.D., You, D., Klapstein, K. and Finegood, D. (1999) Glucose effectiveness is the major determinant of intravenous glucose tolerance in the rat. Am. J. Physiol. **276**, E739-E746

12. Bontemps, F., Hue, L. and Hers, H.-G. (1978) Phosphorylation of glucose in isolated rat hepatocytes. Sigmoidal kinetics explained by the activity of glucokinase alone. Biochem. J. **174**, 603-611

13. Feliu, J.E., Hue, L. and Hers H.-G. (1976) Hormonal control of pyruvate kinase activity and of gluconeogenesis in isolated hepatocytes. Proc. Natl. Acad. Sci. USA. **73**, 2762-2766

14. Chang, H. C. and Lane, M. D. (1966) The enzymatic carboxylation of phosphoenolpyruvate. II. Purification and properties of liver mitochondrial phosphoenolpyruvate carboxykinase. J. Biol. Chem. **241**, 2413-2420

15. Czok, R. and Lamprecht, W. (1983) Methods of enzymatic analysis, edited by Bergmeyer, H. U. et al, Vol.3, 1447-1451

16. Van Schaftingen, E., Lederer, B., Bartrons, R. and Hers, H. G. (1982) A kinetic study of pyrophosphate: fructose-6-phosphate phosphotransferase from potato tubers. Application to a microassay of fructose 2,6-bisphosphate. Eur. J. Biochem. **129**, 191-195

17. Finegood, D.T., Bergman, R.N. and Vranic, M. (1988) Modeling error and apparent isotope discrimination confound estimation of endogenous glucose production during euglycemic glucose clamps. Diabetes, **37**, 1025-1034

18. Hue, L. (1987) Gluconeogenesis and its regulation. Diabetes Metab. Rev. **3**, 111-126

19. Titanji, V.P., Zetterqvist, O. and Engström, L. (1976) Regulation in vitro of rat liver pyruvate kinase by phosphorylation-dephosphorylation reactions, catalyzed by cyclic-AMP dependent protein kinases and a histone phosphatase. Biochim. Biophys. Acta. **422**, 98-108

20. Blair, J.B., Cimbala, M.A., Foster, J.L. and Morgan, R.A. (1976) Hepatic pyruvate kinase. Regulation by glucagon, cyclic adenosine 3'-5'-monophosphate, and insulin in the perfused rat liver. J. Biol. Chem. **251**, 3756-3762

21. Van Schaftingen, E. and Hers, H.-G. (1981) Inhibition of fructose-1,6-bisphosphatase by fructose 2,6-biphosphate.Proc. Natl Acad. Sci. U.S.A. **78**, 2861-2863

22. Pilkis, S.J., El-Maghrabi, M.R., Pilkis, J. and Claus, T.J. (1981) Inhibition of fructose-1,6-bisphosphatase by fructose 2,6-bisphosphate. J. Biol. Chem. **256**, 3619-3622

23. Rousseau, G.G. and Hue, L. (1993) Mammalian 6-phosphofructo-2-kinase/fructose-2,6-bisphosphatase: a bifunctional enzyme that controls glycolysis. Prog. Nucleic Acid Res. Mol. Biol. **45**, 99-127

24. Kurland, I.J. and Pilkis, S.J. (1995) Covalent control of 6-phosphofructo-2-kinase/fructose-2,6-bisphosphatase: insights into autoregulation of a bifunctional enzyme. Protein Sci. **4**,1023-1037

25. Argaud, D., Kirby, T.L., Newgard, C.B. and Lange, A.J. (1997) Stimulation of glucose-6-phosphatase gene expression by glucose and fructose-2,6-bisphosphate. J. Biol. Chem. **272**, 12854- 12861

26. Paula, F.J.A., Plens, A.E.C.M. and Foss, M.C. (1998) Effects of hypophosphatemia on glucose tolerance and insulin secretion. Horm. Metab. Res. **30**, 281-284

27. Zhou, X.J., Fadda, G.Z., Perna, A.F. and Massry, S.G. (1991) Phosphate depletion impairs insulin secretion by pancreatic islets. Kidney Int. **39**, 120-128

28. Drezner, M.K. (2000) PHEX gene and hypophosphatemia. Kidney Int. **57**, 9-18

29. Wong, C.K., Ho, M.A. and Wagner, G.F. (1998) The co-localization of stanniocalcin protein, mRNA and kidney cell markers in the rat kidney. J. Endocrinol. **158**, 183-189

30. Moore, E.E., Kuestner, R.E., Conklin, D.C., Whitmore, T.E., Downey, W., Buddle, M.M., Adams, R.L., Bell, L.A., Thompson, D.L., Wolf, A., Chen, L.,

Stamm, M.R., Grant, F.J., Lok, S., Ren, H. and De Jongh, K.S. (1999) Stanniocalcin 2: characterization of the protein and its localization to human pancreatic alpha cells. Horm. Metab. Res. **31**, 406-414

FIGURE LEGENDS

Figure 1. Effect of a P_i-deficient diet on PK activity

PK was measured in a liver high-speed supernatant as described in the Experimental section. Panel A: assay at low (0.15 mM) PEP that measures the active (dephosphorylated) form of the enzyme. Panel B: assay at high (5.0 mM) PEP that measures the total (phosphorylated + dephosphorylated) form of the enzyme. Activity values at 0.15 mM PEP were statistically different from each other when comparing the two groups. * : $p< 0.01$ (Unpaired Student's *t* test).

Figure 2. Correlation between cAMP concentration and PK activity

Individual values of liver cAMP concentration and the active form of PK, measured as described in the Experimental section, were plotted one against each other.

Figure 3. Correlation between cAMP and glycogen concentration

Individual values of liver cAMP and glycogen concentrations, measured as described in the Experimental section, were plotted one against each other.

Figure 4. Plasma glucose and insulin levels and endogenous glucose production during the IVGTT

The IVGTT was performed with overnight fasted rats as described in the Experimental section. [3-^{3}H]glucose infusion started at time 0 min, the glucose bolus mixed with tracer [3-^{3}H]glucose was injected at 160 min. Results are mean values ± S.E. ($n = 4 - 5$). ○ ($+P_i$) group, ● ($-P_i$) group, * : $p< 0.05$ (Unpaired Student's *t* test).
A. Plasma glucose concentration was measured at each time point during IVGTT. B. Plasma insulin concentration was measured at time points 120, 155, 162, 165, 175 and 250 min. C. Endogenous glucose production parameter, Ra, was calculated from the plasma tracer data and plasma glucose concentration as described in the Methods section.

Table I Effect of a P_i-deficient diet on insulin and metabolites

	(+P_i)	(-P_i)
Plasma P_i (μM)	1.5 ± 0.25	*0.63 ± 0.19
Liver cAMP (nmol/g liver	1.6 ± 0.13	*2.2 ± 0.09
Liver PEP (nmol/g liver)	30 ± 3.2	*48 ± 3.0
Liver F-2,6-P_2 (nmol/g liver)	7.5 ± 0.32	*3.5 ± 0.42
Plasma glucose in the fed state (mM)	6.8 ± 0.3	* 9.2 ± 0.5
Plasma insulin in the fed state (pM)	251 ± 17	*111 ± 5.9
Plasma glucose in the fasted state (mM)	5.07 ± 0.34	¶5.56 ± 0.52
Plasma insulin in the fasted state (pM)	72.1 ± 9.3	¶66.4 ± 6.7
K_G (%/min)	1.9 ± 0.4	¶2.2 ± 0.6

Assays were performed as described in the Experimental section. Samples were from rats fed with a (+Pi) or (-Pi) diet for 48h in the fed or fasted state. K_G, the glucose disapperance rate during the IVGTT, was calculated as described in the Data analysis section. Results are mean values ± S.E. for each group (n = 4-5). * : $p < 0.05$ (Unpaired Student's *t* test). ¶ not significantly different.

Figure 1

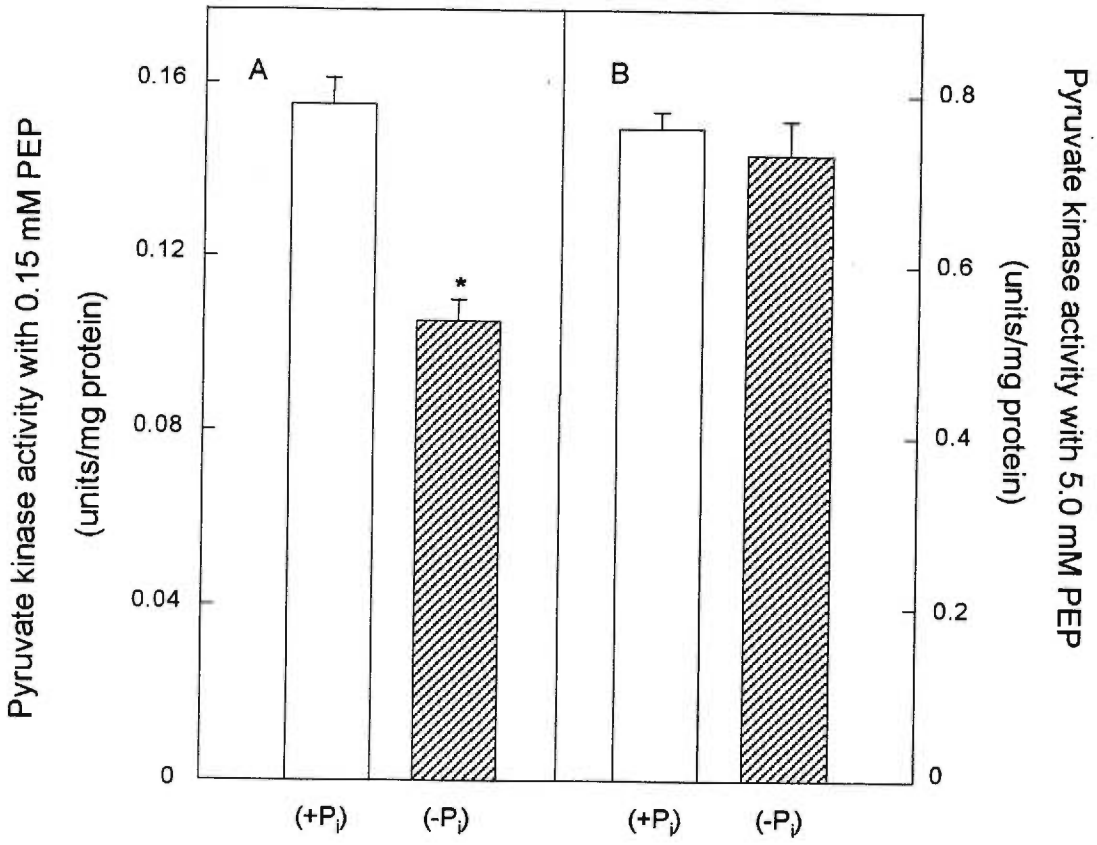
Pyruvate kinase activity with 0.15 mM PEP
(units/mg protein)
Pyruvate kinase activity with 5.0 mM PEP
(units/mg protein)
A
B
0.16
0.12
0.08
0.04
0
0.8
0.6
0.4
0.2
0
*
(+Pi)
(-Pi)
(+Pi)
(-Pi)

Figure 2

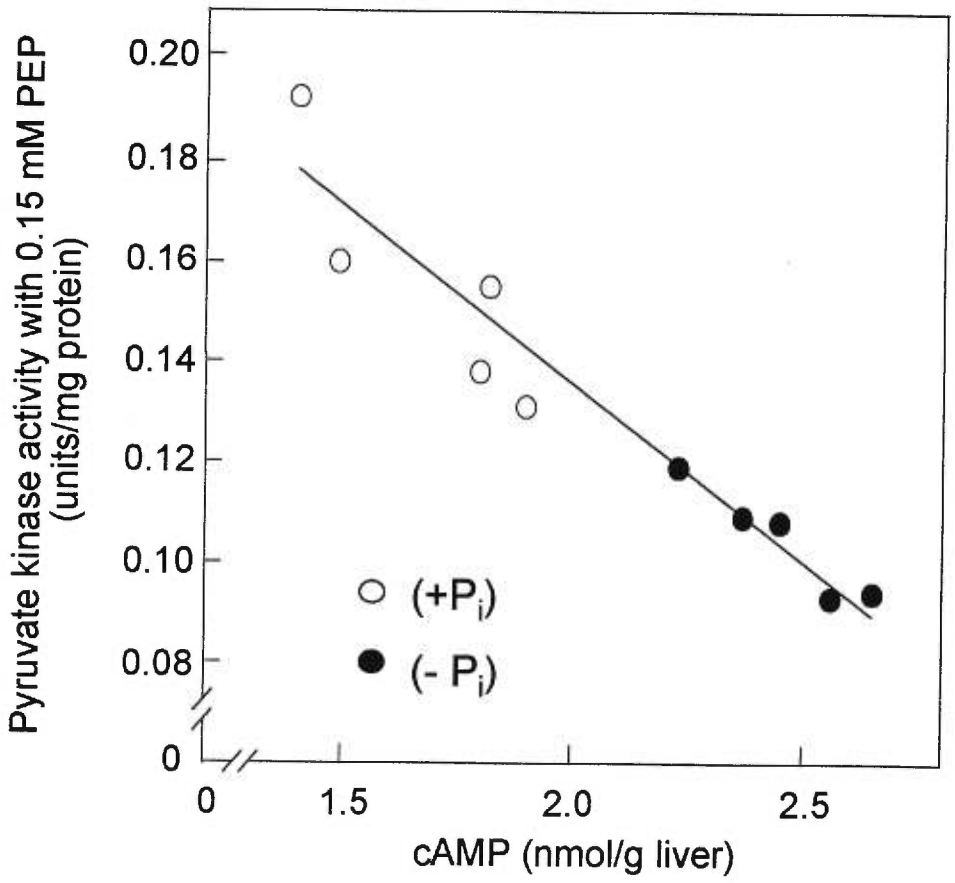
Pyruvate kinase activity with 0.15 mM PEP
(units/mg protein)
0.20
0.18
0.16
0.14
0.12
0.10
0.08
0
0
1.5
2.0
2.5
cAMP (nmol/g liver)
(+P$_i$)
(- P$_i$)

Figure 3

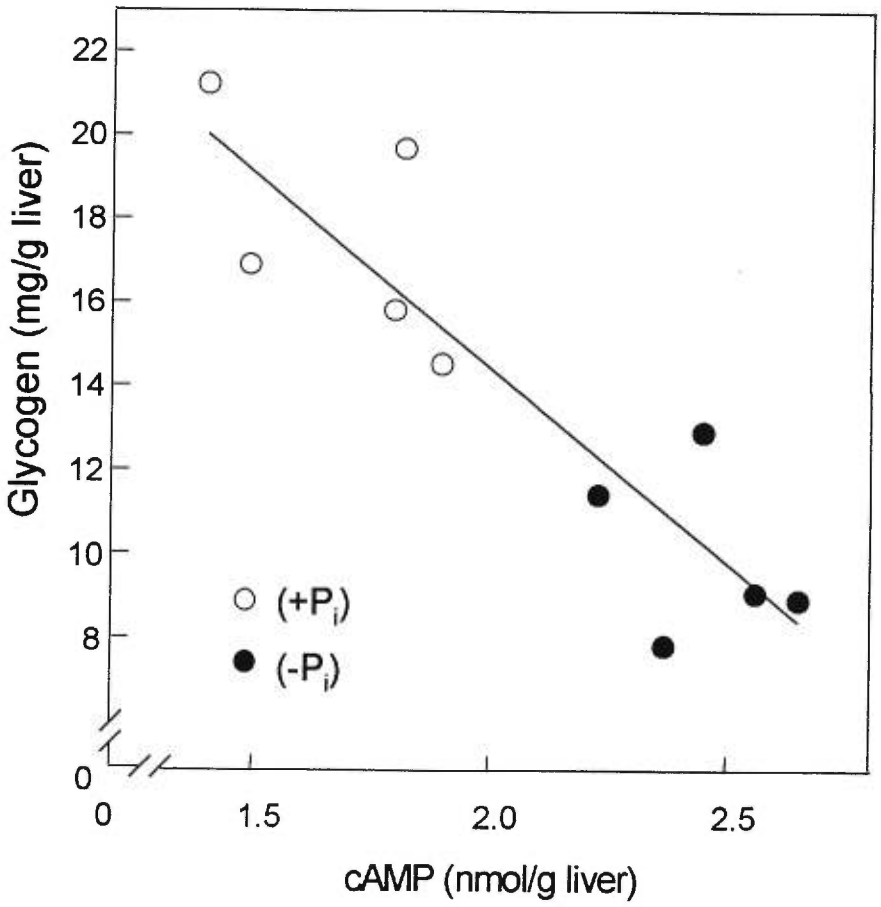
Glycogen (mg/g liver)
22
20
18
16
14
12
10
8
0
0
1.5
2.0
2.5
cAMP (nmol/g liver)
(+P$_i$)
(-P$_i$)

Figure 4

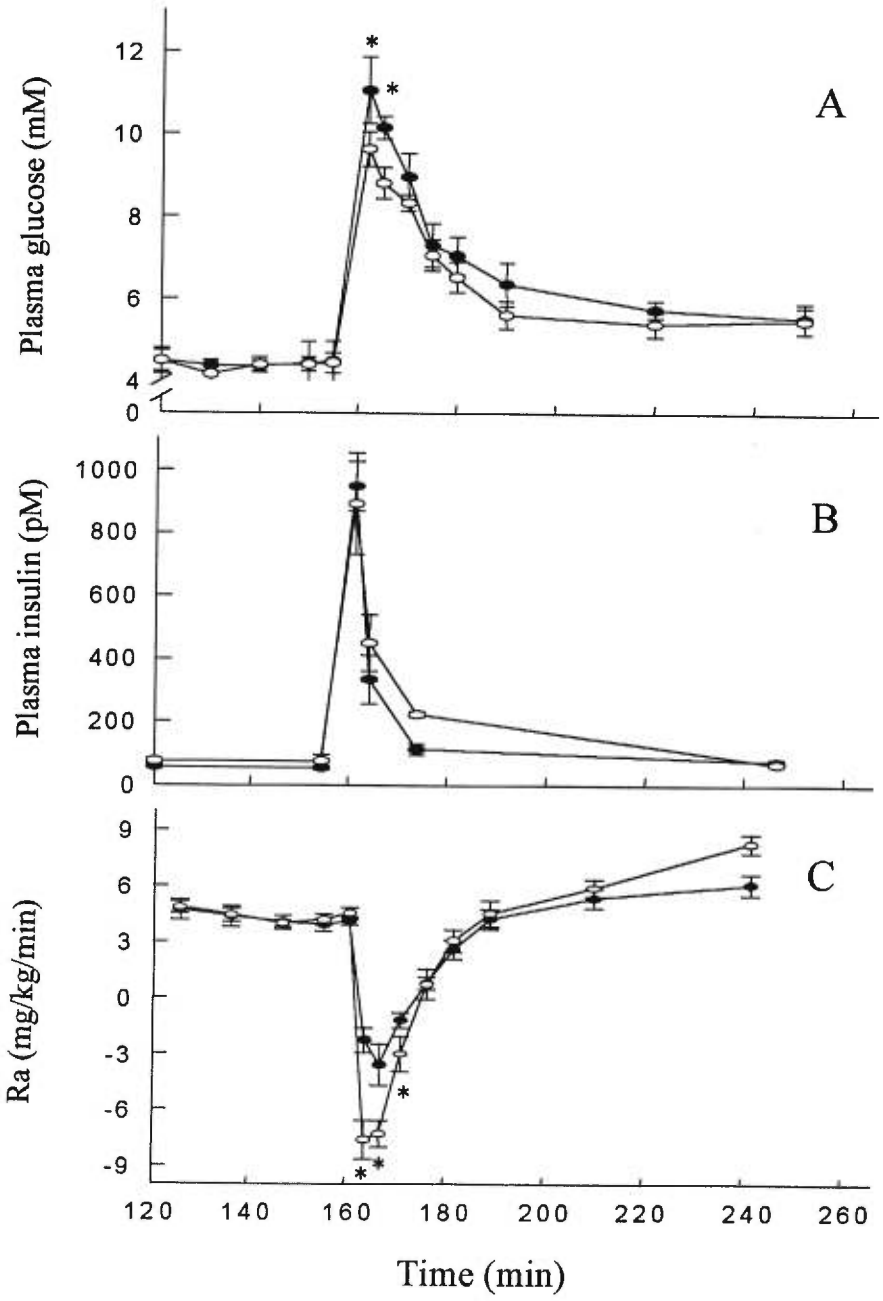
Plasma glucose (mM)
12
10
8
6
4
0
A
Plasma insulin (pM)
1000
800
600
400
200
0
B
Ra (mg/kg/min)
9
6
3
0
-3
-6
-9
C
120
140
160
180
200
220
240
260
Time (min)

IV.3 Article 3

Up-regulation of liver and kidney glucose-6-phosphatase in X-linked hypophosphatemic mice

Wensheng XIE [a], Marie-Claire MÉCHIN [a], Stephanie DUBOIS [b], Daniel LAJEUNESSE [b], Gérald VAN DE WERVE [a, c] *

Departments of Biochemistry [a] and Nutrition [c], Osteoarthritis Research Unit [b], Centre de Recherche du CHUM, University of Montreal, Montreal, QC, Canada H3C 3J7

* Corresponding author. Fax: 514-896-4701

E-mail: [redacted]

Key words: G6Pase, hypophosphatemia, glucose metabolism, mouse liver, mouse kidney

Running title: G6Pase in Hyp mice

Abbreviations: G6P, glucose-6-phosphate; G6Pase, glucose-6-phosphatase; XLH, X-linked hypophosphatemia; Hyp mice, X-linked hypophosphatemic mice; p36, the catalytic subunit of G6Pase; p46, the putative G6P translocase of G6Pase; NaP_i-2, sodium phosphate cotransporter 2

ABSTRACT

We previously showed (Biochem J, 1999, 343, 393-396) that a P_i-deficient diet resulting in hypophosphatemia upregulated the rat liver microsomal glucose-6-phosphatase (G6Pase) system, indicating an association between glucose homeostasis and phosphate homeostasis. In the present study, G6Pase activity of intact or detergent-treated liver and kidney microsomes was found to be increased in X-linked hypophosphatemic mice (Hyp mice). In both tissues, the expression of the catalytic subunit of G6Pase (p36) was upregulated as shown by increased mRNA and protein amounts, while the expression of the putative glucose-6-phosphate translocase (p46) was decreased at the mRNA and protein levels. Taken together, these data indicate that in Hyp mice, increased G6Pase activity is likely due to increased expression of p36, notwithstanding decreased p46 and that distinct mechanisms are involved in the effects of P_i deficiency and the Hyp mutation on the two components of G6Pase system. Increased hepatic and renal G6Pase activity in Hyp mice further support that stimulated glucose production may be responsible for the impaired glucose metabolism documented under hypophosphatemic conditions.

INTRODUCTION

Glucose-6-phosphatase (G6Pase, E.C. 3.1.3.9) catalyzes the hydrolysis of glucose-6-phosphate (G6P) into glucose and inorganic phosphate, hence plays a crucial role in endogenous glucose production [1]. G6Pase is a multiprotein complex located in the endoplasmic reticulum membrane, that is highly expressed in the two gluconeogenic organs, liver and kidney. Until now, two components of G6Pase have been cloned: the catalytic subunit, a 36 kDa protein (p36) [2] and a 46 kDa putative G6P translocase (p46) [3]. The regulation of the expression of p36 gene has been well documented [4], whereas that of p46 was only recently investigated [5, 6]. The p46 gene expression is differently regulated than p36 by insulin, cyclic AMP, and thapsigargin [6].

X-linked hypophosphatemia (XLH) is a disorder of renal phosphate wasting with a hallmark of low serum phosphate concentration resulting from decreased activity of renal sodium-dependent phosphate cotransporter 2 (NaP_i-2) [7]. XLH is characterized by lower extremity deformities, rickets, short stature, bone pain, dental abscesses, and osteomalacia. Hyp mice are the murine homologues to human XLH. The molecular basis of XLH and Hyp mice is the dysfunction of PHEX gene [8], while strong evidence exists for a humoral factor(s) in the regulation of NaP_i-2 and the phosphate homeostasis [9].

It has been reported that hypophosphatemia is associated with impaired glucose tolerance and insulin resistance [10, 11]. We also previously reported that liver G6Pase was upregulated in the rats fed with a phosphate deficient diet [12]. In the

present study, we further investigated the activity and expression of G6Pase in Hyp mice. Results showed that both in Hyp mice liver and kidney, G6Pase activity was increased, the protein amount and mRNA abundance of p36 were increased, while those of p46 were decreased.

MATERALS AND METHODS

Materals

[U-^{14}C]glucose-6-phosphate was from ICN Biomedicals (Montreal, QC) and [α-^{32}P]dCTP was from Pharmacia Biotech (Baie d'Urfé, QC). Glucose-6-phosphate was from Sigma (St-Louis, MI). Molecular markers were purchased from Bio-Rad (Mississauga, ONT). The rabbit polyclonal antiserum against the recombined G6Pase catalytic subunit (antibody against p36) was a kind gift of Dr. Howard Haspel (Denver, CO). The rabbit antiserum against a peptide from the N-terminus of p46 was produced in our laboratory as reported in [12]. The BCIP/NBT stock solutions and the anti-rabbit IgG-AP conjugate were from the Promega Co (Madison, WI). TRI_{ZOL} Reagent was from Gibco BRL (Burlington, ONT).

Animals

Male mice (4-6 weeks old) of the C57BL/6J strain, both normal (C57BL/6J +/Y) and Hyp (C57BL/6J Hyp/Y) were obtained in the laboratory of Dr. Lajeunesse. Hyp mice were identified by their shorter body length, shorter tail length, lower weight and reduced serum phosphorus levels as reported previous [9]. The mice were fed with regular rodent diet (Charles River Rodent, ONT). Animals were anesthesized

with Nembutal before the livers and kidneys were taken for homogenization or frozen in liquid nitrogen pending further analysis. 5 Hyp mice and 4 age matched control mice were used.

Preparation of microsomes and G6Pase assay

Mouse liver or kidney was homogenized using a glass homogenizer in an ice-cold buffer containing 50 mM Hepes-Tris, 250 mM sucrose, pH 7.3. Microsomes were prepared as described in [12]. G6Pase activity was assayed at 0.2 mM and 5 mM G6P at 30°C before and after detergent (Chapso 0.8%) treatment [12].

Western blot analysis

Western blots were performed with 50 μg protein of microsomes as described in [12, 13]. The quantification of each specific band was analyzed by using a Dual Light™ Transilluminator.

Northern blot analysis

Total liver or kidney RNA was individually extracted with TRI_{ZOL} Reagent. Northern blots were performed as previous described [12]. The intensities of the mRNA bands were determined using a densitometer (Dual Light™ Transilluminator) and normalized to 28S RNA intensity.

Data analysis

Statistical analysis was performed according to Students' T test. Difference was considered significant when the p value was less than 0.05.

RESULTS

G6Pase activity

Strong evidence has been reported on the association of hypophosphatemia and glucose intolerance [10, 11]. Since G6Pase is responsible for endogenous glucose production, we measured its activity in liver and kidney of Hyp mice. As shown in Fig. 1A, as compared to control mice, Hyp mice liver G6Pase activity was increased at 0.2 mM and 5 mM G6P before and after detergent treatment. Hyp mice kidney G6Pase activity was also increased at 0.2 mM and 5 mM G6P before and after detergent treatment (Fig.1B). In addition, the activity change is more evident in intact liver microsomes and in chapso-treated kidney microsomes, indicating a difference between hepatic G6Pase and kidney G6Pase. The possibility that G6Pase changes in the Hyp mice tissues were due to modifications in the protein amount was further tested by Western blot analysis.

Western blot analysis of p36 and p46 in liver and kidney

As implied from the results of G6Pase activity, the immunoreactivity of p36 was significantly increased in Hyp mouse liver (Fig.2A), demonstrating that the protein amount of p36 was increased. This result suggests that the enhanced G6Pase activity might be due to an increase in the protein amount of the catalytic subunit of G6Pase. In contrast, the intensity of the specific band of p46 was substantially decreased in the Hyp mouse liver as shown in Fig. 2A, similar results were observed in Hyp mouse kidney (Fig.2B), indicating lower p46 protein amounts in these tissues. These results

suggest that p46 does not participate to increased G6Pase activity in Hyp mice, except if p46 was inhibitory to p36.

Northern blot analysis of p36 and p46 in liver and kidney

Northern blot of both p36 and p46 was performed in order to know whether these changes in protein abundance were due to modified synthesis or degradation. One representative blot of liver p36 and p46 is shown in the upper panel of Fig. 3A. The quantification data are shown in the bar panel. One can see p36 mRNA was substantially stimulated in Hyp mouse liver, in agreement with the Western blot results. Consistent with the immunoreactivity of p46 protein, its mRNA was also markedly decreased in Hyp mouse liver as shown in Fig.3A left panel. Similar results were observed in Hyp mouse kidney, i.e., p36 mRNA was increased while p46 mRNA was decreased in Hyp mice (Fig.3B).

DISCUSSION

We previously reported that liver G6Pase activity was upregulated in rats fed with a P_i-deficient diet for 48h by increased expression of p36 gene. The abundance of p46 mRNA was also increased, but not the protein amount [12]. Consistently, in intact or detergent-treated microsomes, G6Pase activity was increased in Hyp mouse liver and kidney at physiological or saturable substrate concentration. In addition, the activity changes in Hyp mice are more evident in intact liver microsomes than in intact kidney microsomes. This difference may be related to the regulation specificity of G6Pase in liver and kidney [14]. It also indicates that *in vivo* the hepatic G6Pase may contribute more to the impaired glucose metabolism. The increase of G6Pase activity

was very likely due to the stimulated p36 gene expression as demonstrated by Western and Northern results of p36. These results indicate that a common factor linked to P_i deficiency, caused either by a P_i-deficient diet or PHEX gene mutations, may affect p36 gene expression. In contrast to the changes of p46 under P_i-deficient diet conditions, both p46 mRNA and protein were decreased in Hyp mouse liver and kidney. This result suggests that p46 does not participate to increased G6Pase activity in Hyp mice, except if p46 could inhibit the hydrolytic activity. However, no evidence has been shown that p46 is inhibitory to p36. In addition, overexpression of p46 affected glycogen content similarly as p36 overexpression and had an additive effect on p36 overexpression [15]. This result of p46 gene expression suggests that P_i deficiency caused by PHEX gene mutations has a distinct effect on p46 gene expression than that following a P_i-deficient diet. This difference might be explained by a number of characteristics of these two animal models although both cases show hypophosphatemia. In X-linked hypophosphatemic subjects, the expression of renal NaP_i-2 was markedly suppressed, while upregulated under P_i-deficient diet conditions [16]. The parathyroid hormone content and 1,25-dihydroxyvitamin D_3 content were at the same levels in Hyp mice as normal mice, but they are changed by a P_i-deficient diet [17, 18]. All these facts suggest that distinct mechanisms are involved in the effects of P_i deficiency on G6Pase system under P_i-deficient diet conditions or X-linked hypophosphatemia. It also confirms that p36 and p46 are subjected to distinct regulation [6].

The increased G6Pase activity in Hyp mouse liver and kidney further demonstrate that hypophosphatemia could impair glucose metabolism through elevated glucose

production, as we documented before in alimentary P_i deficiency [12]. How P_i deficiency affects G6Pase *in vivo* is unknown. It is unlikely that P_i deficiency per se affects G6Pase system since neither G6Pase activity nor the mRNA levels of p36 was affected in rat primary hepatocytes cultured in P_i depleted medium (Data not shown). Insulin/glucagon ration can be a potential cause for these changes of G6Pase. It was found that plasma insulin concentration was markedly decreased in rats fed with a P_i deficient diet (Data not shown). Whether this is the case in Hyp mice is not certain. Controversial data have been reported about insulin secretion in P_i deficient animals. One study showed that glucose-stimulated insulin secretion was markedly lower in perfused pancreatic islets from rats fed with a P_i-deficient diet [19]. In contrast, serum insulin concentration after glucose loading during an intravenous glucose tolerance test was higher in hypophosphatemic patients [11]. Another possibility would be that hormone(s) linked to phosphate homeostasis, such as stannocalcin [20] and phosphatonin [21], was (were) affected by P_i deficiency or PHEX dysfunction, resulting in changes on G6Pase system.

Acknowledge: This work was supported by Grant MT-10804 from the Medical Research Council of Canada (to G. van de Werve). The authors thank Guylaine Gévry for the artwork.

REFERENCES

1. Foster JDF, Pederson BA, Nordlie RC, 1997, Glucose-6-phosphatase structure, regulation, and function: an update, Proc Soc Exp Biol Med, 215: 314-332
2. Lei KJ, Shelly LL, Pan CJ, Sidbury JB, Chou JY, 1993, Mutations in the glucose-6-phosphatase gene that cause glycogen storage disease type 1a, Science, 262: 580-583
3. Gerin I, Veiga-da-Cunha, Achouri Y, Collet, JF, van Schaftingen E, 1997, Sequence of a putative 6-phosphate translocase, mutation in glycogen storage disease type Ib, FEBS Lett, 419: 235-238
4. van de Werve G, Lange A, Newgard C, Méchin MC, Li Y, Berteloot A, 2000, New lessons in the regulation of glucose metabolism taught by the glucose 6-phosphatase system, Eur J Biochem, 267: 1533-1549
5. Li Y, Méchin M-C, van de Werve G, 1999, Diabetes affects similiarly the catalytic subunit and putative glucose-6-phosphate translocase of glucose-6-phosphatase, J Biol Chem, 274: 33866-33868
6. Li Y, van de Werve, 2000, Distinct hormone stimulation and counteraction by insulin of the expression of the two components of glucose 6-phosphatase in HepG2 cells, Biochem Biophys Res Commun, 272: 41-44
7. Hruska KA, Rifas L, Cheng SL, Gupta A, Halstead L, Avioli L, 1995, X-linked hypophosphatemic rickets and the murine Hyp homologue, Am J Physiol, 268: F357-F362

8. Econs, 1996,Positional cloning of the HYP gene: a review, Kidney Int, 49: 1033-1037

9. Lajeunesse D, Meyer RA Jr, Hamel L, 1996, Direct demonstration of a humorally-mediated inhibition of renal phosphate transport in the Hyp mouse, Kidney Int, 50: 1531-1538

10. DeFronzo RA, Lang R, 1980, Hypophosphatemia and glucose intolerance: evidence for tissue insensitivity to insulin, N Engl J Med, 303: 1259-1263

11. Paula FJ, Plens AE, Foss MC, 1998, Effects of hypophosphatemia on glucose tolerance and insulin secretion, Horm Metab Res, 30: 281-284

12. Xie WS, Li Y, Méchin M-C, van de Werve G, 1999, Upregulation of liver glucose-6-phosphatase in rats fed with a P_i-deficient diet, Biochem J, 343: 393-396

13. Méchin MC, Annabi B, Pegorier JP, van de Werve G, 2000, Ontogeny of the the catalytic subunit and putative glucose-6-phosphate transporter proteins of the rat microsomal liver glucose-6-phosphatase system, Meta, 49: 1-5

14. Voice MW, Scott HM, Watkins SL, Middleditch C, Burchell A, 1996, A comparison of the renal and hepatic microsomal glucose-6-phosphatase enzymes, Arch Biochem Biophys, 330: 380-386

15. An J, Li Y, van de Werve G, Newgard C, 2000, Activity of the hepatic glucose-6-phosphatase system is altered by manipulation of glucose-6phosphate translocase expression, Diabetes Abstract Book of 60th Diabetes Scientific Sessions, San Antonio

16. Kido S, Miyamoto K, Mizobuchi H, Taketani Y, Ohkido I, Ogawa N, Kaneko Y, Harashima S, Takeda E, 1999, Identification of regulatory sequences and binding proteins in the type II sodium/phosphate cotransporter NPT2 gene responsive to dietary phosphate, J Biol Chem, 274: 28256-28263
17. Tenenhouse HS, 1999, X-linked hypophosphataemia: a homologous disorder in humans and mice, Nephrol Dial Transplant, 14: 333-41
18. Bugg NC, Jones JA, 1998, Hypophosphataemia, Anaesthesia, 53: 895-902
19. Zhou XJ, Fadda GZ, Perna AF, Massry SG, 1991, Phosphate depletion impairs insulin secretion by pancreatic islets, Kidney Int, 39 : 120-128
20. Moore EE, Kuestner RE, Conklin DC, Whitmore TE, Downey W, Buddle MM, Adams RL, Bell LA, Thompson DL, Wolf A, Chen L, Stamm MR, Grant FJ, Lok S, Ren H, De Jongh KS, 1999, Stanniocalcin 2: characterization of the protein and its locatization to human pancreatic alpha cells, Horm Metab Res, 31: 406-414
21. Dresser MK, 2000, PHEX gene and hypophosphatemia, Kidney Int, 57: 9-18

FIGURE LEGENDS

Fig.1. G6Pase activity in mouse liver (A) and kidney (B). G6Pase activity was measured at 30°C with 0.2 or 5 mM G6P in intact or detergent-treated microsomes. ☐ represents normal control mice, ■ represents Hyp mice. Results are mean values ± S.E. (n = 4-5). One unit stands one μmol products in one minute under experimental conditions. * $p < 0.05$

Fig.2. Immunoblot analysis of p36 and p46 in mouse liver (A) and kidney (B). The panel with bands is one representative of specific bands of p36 and p46 in control mouse (left band) or Hyp mouse (right band). The panel with bars is the quantification of specific bands of p36 and p46 in control mice (☐) or Hyp mice (■). The control mice were taken as 100%. Results are mean values ± S.E. (n = 4-5). * $p < 0.05$

Fig.3. Northern blot analysis of p36 and p46 in mouse liver (A) and kidney (B). the panel with bands is one representative of specific bands of p36 and p46 in control mouse (left band) or Hyp mouse (right band). The panel with bars is the quantification of specific bands of p36 and p46 in control mice (☐) or Hyp mice (■). The control mice were taken as 100%. Results are mean values ± S.E. (n = 4-5). * $p < 0.05$

Figure 1

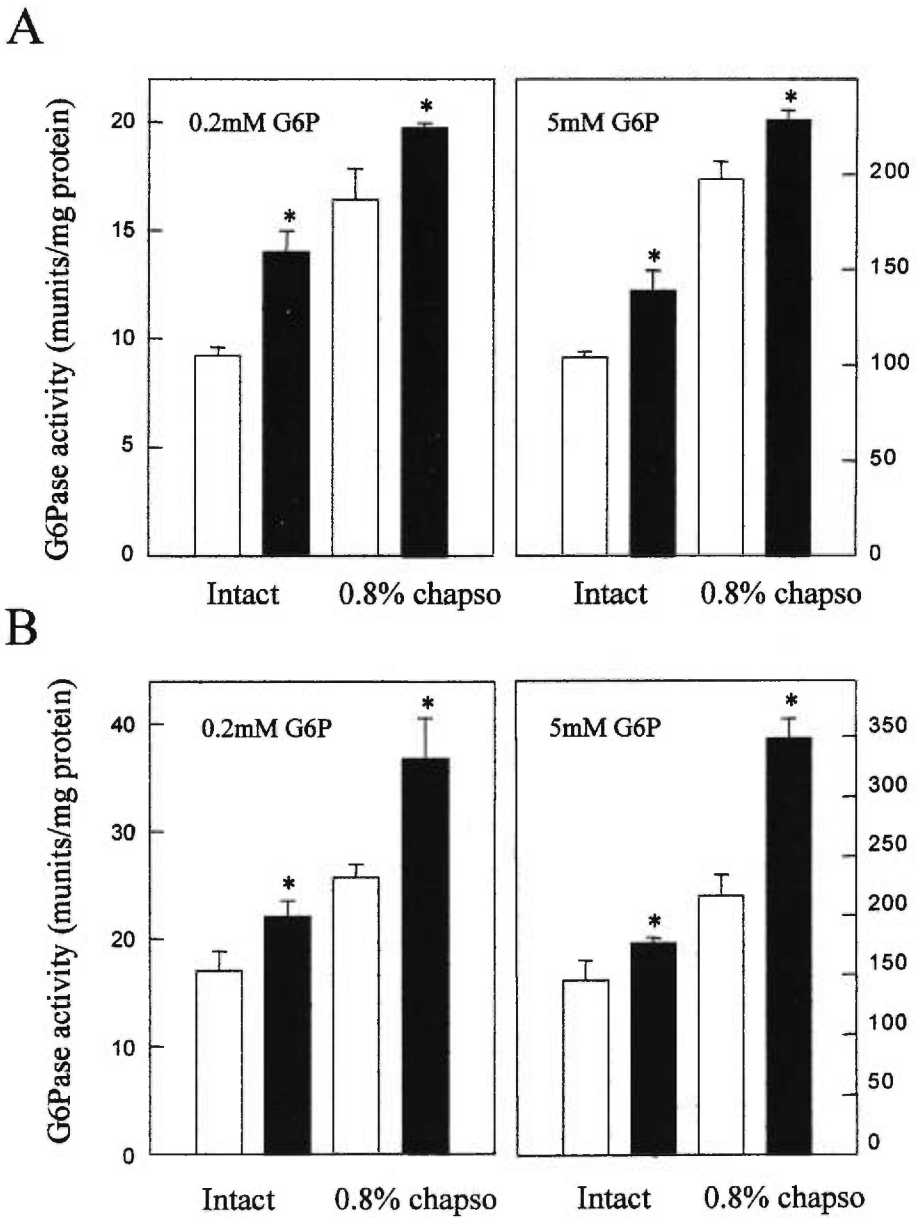
A
G6Pase activity (munits/mg protein)
0.2mM G6P
5mM G6P
Intact
0.8% chapso
Intact
0.8% chapso
B
G6Pase activity (munits/mg protein)
0.2mM G6P
5mM G6P
Intact
0.8% chapso
Intact
0.8% chapso

Figure 2

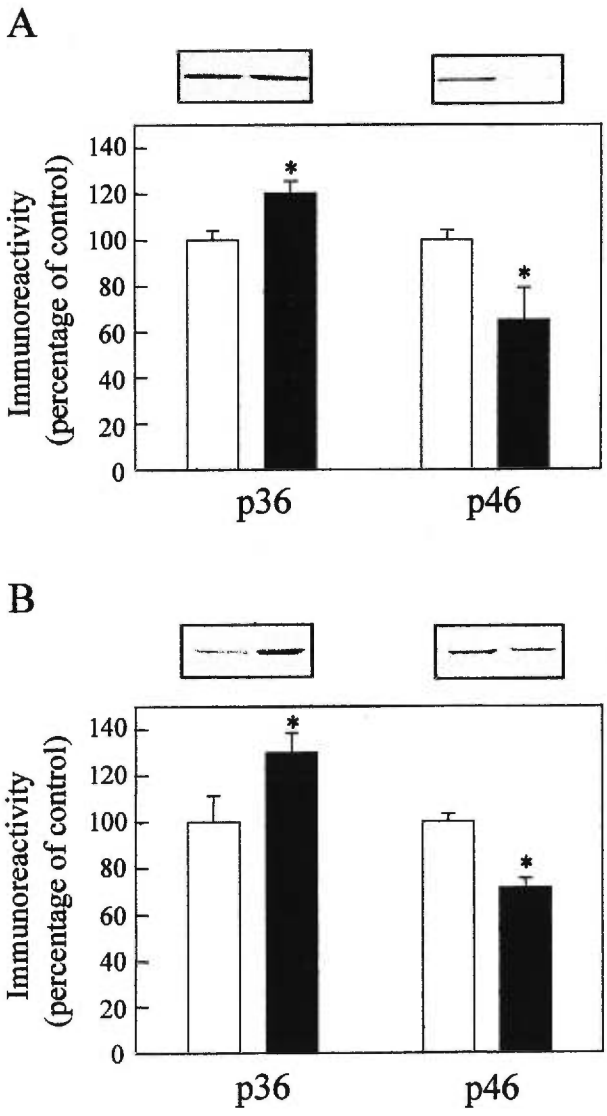
A
Immunoreactivity
(percentage of control)
140
120
100
80
60
40
20
0
*
*
p36
p46
B
Immunoreactivity
(percentage of control)
140
120
100
80
60
40
20
0
*
*
p36
p46

Figure 3

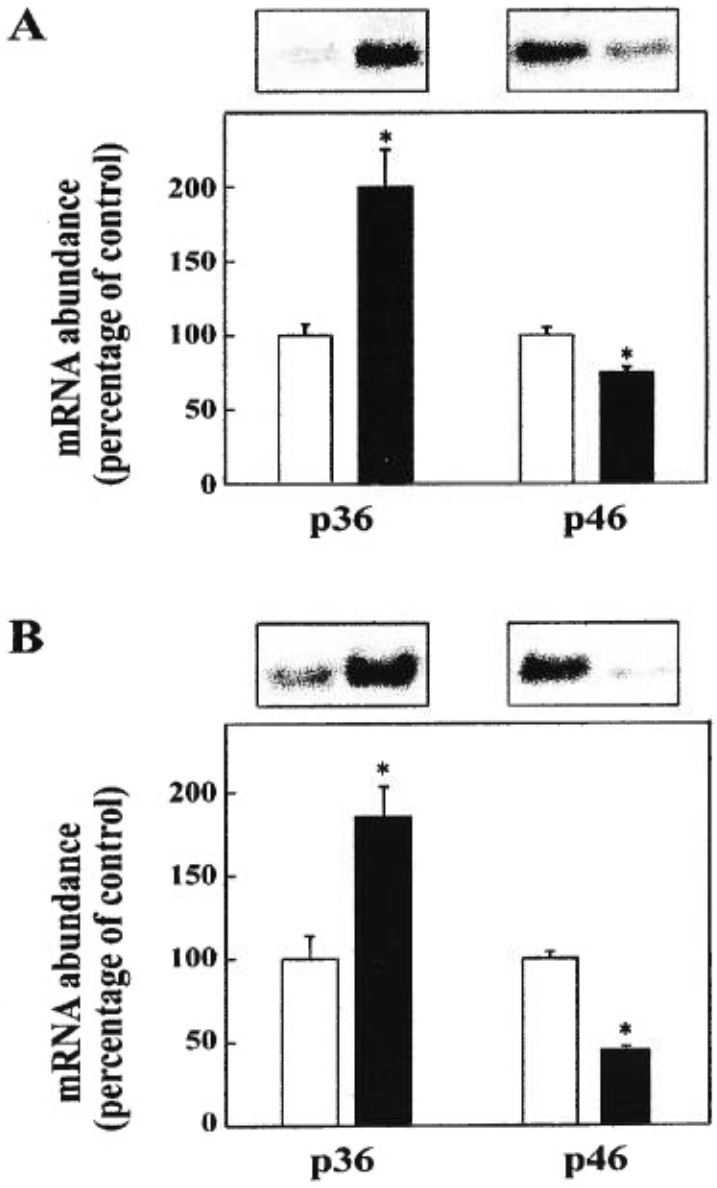
A
mRNA abundance
(percentage of control)
200
150
100
50
0
*
*
p36
p46
B
mRNA abundance
(percentage of control)
200
150
100
50
0
*
*
p36
p46

IV.4 Article 4

An integrated view of the kinetics of glucose/phosphate transport and of glucose 6-phosphate transport/hydrolysis in intact rat liver microsomes

by

Wensheng Xie [a,c], Gérald van de Werve [a,c] and Alfred Berteloot [b*]

Laboratoire d'Endocrinologie Métabolique, Departments of Nutrition and Biochemistry [a] and Physiology [b], Centre de Recherche du CHUM [c] and Groupe de Recherche en Transport Membranaire, Faculty of Medicine, University of Montreal, Montreal, QC, H3C 3J7, Canada

[*]Corresponding author. Tel: +1 (514) 343-5634; Fax: +1 (514) 343-2111.

E-mail: Alfred.Berteloot@umontreal.ca

Key Words: Glucose-6-phosphatase; Rapid kinetics; Vectorial transport; Endoplasmic reticulum

Running title: glucose 6-phosphate transport/hydrolysis

SUMMARY

The structure-function relationships of rat liver glucose 6-phosphatase were investigated in intact microsomes with regard to their compatibility with the substrate transport or conformational models. The kinetics of [^{14}C]D-glucose and [^{32}P]phosphate transport followed single exponential kinetics ($T_{1/2}$ = 40 ± 6 and 23 ± 3 s, respectively), were unaffected by unlabeled substrate concentrations up to 100 mM, and proved insensitive to a variety of potential inhibitors. Tracer equilibration during [^{14}C]- and [^{32}P]glucose 6-phosphate hydrolysis proceeded with $T_{1/2}$ values of 47 ± 5 and 21 ± 1 s, respectively. Similar ratios were observed between the $T_{1/2}$ and the steady-state levels of [^{14}C]glucose vs [^{32}P]phosphate accumulation into the microsomes (2.24 ± 0.35 vs 2.11 ± 0.14) whereas a $T_{1/2}$ value of 21 ± 1 s characterized [^{32}P]phosphate efflux following inhibition of enzyme activity by vanadate. By contrast, similar initial rates of uptake were observed for [^{14}C]glucose and [^{32}P]phosphate, which account for 12-13% only of the steady-state rate of substrate hydrolysis. These results failed to give a consistent integrated view of glucose 6-phosphate transport/hydrolysis and of glucose/phosphate transport when confronted to an exact solution of a simplified substrate transport model. We therefore propose a conformational model whereby glucose 6-phosphate transport/hydrolysis are tightly coupled processes whereas glucose and phosphate share with water and a variety of other organic and inorganic solutes a common pore-like structure accounting for their transport through the microsomal membrane.

Introduction

Glucose 6-phosphatase (G6Pase)[1] catalyzes the hydrolysis of glucose 6-phosphate (G6P) as well as the synthesis of G6P *via* phosphotransferase activity [28,29]. The enzyme protein is tightly linked to the endoplasmic reticulum (ER) membrane in rat liver cells such that microsomes, *i.e.* membrane vesicles enriched in ER, are generally used as an *in vitro* model to study the catalytic and postulated transport functions associated with the G6Pase system [29,38]. In intact preparations, the structure-function relationships of the G6Pase system are still debated and two main concepts have emerged over the last 25 years. The substrate transport-catalytic unit hypothesis proposed by Arion *et al.* [6] depicts the G6Pase system as consisting of a fairly nonspecific catalytic unit with its active site located on the luminal side of the ER, and of at least three transmembrane spanning translocases involved in the transport of substrate (T1, G6P translocase) and products (T2 and T3, phosphate and glucose translocases, respectively) of the hydrolase reaction. Alternatively, the combined conformational flexibility-substrate transport model put forward by Schulze *et al.* [33] and updated by Berteloot *et al.* [12] views the G6Pase system as a multifunctional enzyme embedded deep within the ER membrane and possessing both catalytic and substrate/product transport activities.

The important physiological role of hepatic G6Pase is apparent in type 1 glycogen storage disease (GSD-1) for which different subtypes have been reported that would involve impaired functions of either of the catalytic unit (GSD-1a) or its associated T1 (GSD-1b), T2 (GSD-1c), and T3 (GSD-1d) translocases [15]. The absence of a functional catalytic unit protein, also identified as the p36 protein at the molecular level,

has been confirmed to be the cause of GSD-1a [23]. By contrast, the finding of close chromosomal locations (11q23) and identification of mutations in the same p46 gene from both GSD-1b and GSD-1c patients [1,18] challenge the classical view that G6P and phosphate transport involves separate translocases. A recent report however suggests the existence of a distinct GSD-1c locus [24]. The role of the p46 protein in the functioning of the G6Pase system is still debated but its homology with the products of the bacterial UhpT and UhpC genes suggests that it may act, respectively, as a G6P/phosphate translocase or G6P receptor during G6P hydrolysis [20,38]. Similarly, the existence of a specific glucose-transport protein is controversial. A 52 kDa protein has been isolated from rat liver ER [40], but the putative function of this protein has never been demonstrated directly. Nonetheless, antibodies raised against this protein proved successful in isolating a rat liver cDNA clone (GLUT-7) with sequence similarities to GLUT-2, the liver plasma-membrane facilitative glucose transport (GLUT) protein [41]. However, this former claim has ultimately been recognized as a cloning artefact [16].

So far, most kinetic studies aimed at resolving the structure-function relationships of the G6Pase systems in intact microsomes have been performed under steady-state conditions, the results of which might provide necessary, but in no case sufficient conditions to unequivocally prove the validity of the substrate transport or conformational models. This is so because steady-state kinetics cannot give any useful information on the dynamics of the system, in contrast to rapid kinetics that may allow us to test the fundamental hypotheses which lead to the formulation of these two models. Most particularly relevant in this regard is the previously questioned postulate of the substrate

transport-catalytic unit hypothesis that G6P transport represents an obligatory rate-limitant step to its hydrolysis [12]. However, when measured by incubation of microsomal vesicles with [^{14}C]G6P, the most serious difficulty in the interpretation of rapid kinetic studies is the everpresent G6Pase activity that does not allow us to discriminate between [^{14}C]G6P and [^{14}C]glucose within the intravesicular compartment. Accordingly, ^{14}C uptake in such experiments has been assimilated to represent either [^{14}C]G6P transport [22], [^{14}C]glucose accumulation [12, 13,35], or both [9]. Clearly, then, the most objective answer about the meaning of G6P/glucose uptake data should rely on simulation studies. This approach was pioneered by Berteloot *et al.* [13] but could not be used at that time to propose an integrated view of the kinetics of G6P transport and hydrolysis due to the lack of information regarding the kinetics of glucose/phosphate transport in microsomes. This gap in our knowledge has since been filled in to some extent [8,9,12,19,26,32,35], such that it now seems possible to reassess in depth the validity of the substrate transport and conformational models provided that a number of conflicting results can be resolved in the first place.

As regards glucose transport, the radiotracer studies of Romanelli *et al.* [32] did not demonstrated zero-trans glucose influx whereas those of St-Denis *et al.* [35] showed both [^{14}C]glucose accumulation in the presence of zero-trans concentrations of [^{14}C]G6P and [^{14}C]glucose efflux from actively-loaded microsomes with $T_{1/2}$ values of 30-50 s that proved insensitive to glucose concentrations up to 20 mM. It was concluded that glucose transport appears unidirectional in the absence of G6Pase activity and that the kinetics of glucose efflux are compatible with simple diffusion or facilitative diffusion through a low

affinity system. A putative role of a GLUT-related protein was further ruled out based on the absence of both efflux inhibition by phloretin and accelerated exchange by high concentrations of outside unlabeled glucose. By contrast, the light-scattering measurements of Marcolongo *et al.* [26] demonstrated that D- and L-glucose, as well as a number of other sugar substrates, can all equilibrate across the microsomal membrane with $T_{1/2}$ values in the range 3.5-9.0 s. These studies further suggested the existence of a facilitative transport pathway in the ER membrane on the evidence that glucose transport is saturable and can be partially inhibited by high concentrations of cytochalasin B (250 μM) and pentamidine (50 μM). Yet, a different picture emerged from the studies of Bánhegyi *et al.* [8] reporting that the rate of tracer glucose uptake into microsomes appears much lower than the rate of glucose influx measured by the light-scattering technique and that the initial rate of tracer glucose uptake is hardly saturable over the 0-100 mM range of glucose concentrations. Another difference with the light-scattering technique also included the observation that the radiotracer assay fails to show inhibition of glucose influx by phloretin and cytochalasin B. It was therefore concluded that microsomal vesicles are heterogeneous regarding their glucose-transport properties with both fast (saturable, inhibitor-sensitive) and slow (unsaturable, inhibitor-insensitive) transport systems accounting for approx. 80 and 20 % of total microsomal transport, respectively. According to this view, the slow glucose transport process is bidirectional and is the only one that shows up when using a radiotracer assay due to the loss of the majority of intravesicular glucose from a fast releasable pool during the washing steps inherent to the rapid filtration technique.

The initial approach used by Romanelli *et al.* [32] to measure glucose uptake in rat liver microsomes was adapted from similar studies performed in intestinal brush-border membrane vesicles where mannitol is generally used as a space marker against which specific glucose uptake can be assessed [11]. With the demonstration that D-glucose and D-mannitol can be taken up at similar rates by rat liver microsomes [26], the initial protocol of Romanelli *et al.* [32] needs to be reassessed in the absence of space marker. This was done in the present studies, which also tested the corollary prediction of the glucose transport heterogeneity hypothesis proposed by Bánhegyi *et al.* [8] that total glucose transport should be observable in a radiotracer assay provided that a glucose transport inhibitor like phloretin is included in the wash solutions to block glucose efflux through the fast transport system. It is shown that the results of the radiotracer assay are independent of the presence of phloretin in either of the incubation media or the stop solutions. The present studies also addressed the kinetic mechanism of phosphate transport in parallel experiments, and it is demonstrated that both glucose and phosphate transports may be accounted for by passive diffusion according to the usual criteria. Finally, it was reasoned that if tracer uptake represents G6P transport rather than accumulation of the products resulting from the phosphohydrolase reaction, tracer uptake should be the same whether [^{14}C]G6P or [^{32}P]G6P is used as the starting substrate. This prediction of the G6P transport hypothesis was directly tested in the present studies and it is shown that the rates of tracer uptake and efflux, as well as the levels of intravesicular tracer accumulation, are all directly related to the rates of glucose and phosphate permeation through the microsomal membrane. An exact solution of a simplified substrate

transport model is further used to demonstrate that the substrate transport-catalytic unit concept fails to give a consistent integrated view of G6P transport/ hydrolysis and of glucose/phosphate transport in rat liver microsomes. We therefore propose an updated view of our previous version of a combined conformational flexibility-substrate transport model [12] whereby G6P transport/hydrolysis are tightly coupled processes whereas glucose and phosphate may share with water and a variety of other organic and inorganic solutes a common pore-like structure that would account for their transport through the ER membrane.

Materials and Methods

MATERIALS

[^{32}P]KH_2PO_4 in H_2O (1 Ci/mmol), [U-^{14}C]D-glucose (200 mCi/mmol), and [U-^{14}C]G6P (317 mCi/mmol) were purchased from ICN Biomedicals. [^{32}P]G6P (144 mCi/mmol) was prepared as described in [13]. KH_2PO_4, glucose, G6P, $HgCl_2$, phlorizin, phloretin, chlorogenic acid, 2-hydroxy-5-nitrobenzaldehyde (HNB), and sodium orthovanadate were from Sigma.

PREPARATION OF MICROSOMES

Liver microsomes were isolated from overnight-fasted male Sprague-Dawley rats (approx. 300 g body weight) as described previously [13], except that the homogenization and resuspension buffers were 50 mM Hepes-Tris (pH 7.3) containing 250 mM sucrose. If necessary, microsomes were permeabilized by detergent treatment (0.8% Chapso) as reported in [32].

ASSAYS

G6Pase activity was determined at room temperature as described previously [12,13]. Mannose-6-phosphatase activity was used as an index of microsome integrity [4], and microsomal preparations routinely displayed 95% latency. Protein was assayed as reported in [12].

PHOSPHATE AND GLUCOSE UPTAKE MEASUREMENTS

The kinetics of [U-^{14}C]D-glucose and [^{32}P]KH_2PO_4 uptake were determined at room temperature using a fast-sampling, rapid-filtration apparatus (FSRFA, US patent N° 5,330,717) developed in our laboratory [10] as described previously [32,36]. For each glucose assay, 2.0 μCi of [U-^{14}C]glucose (10 μM) was included in the incubation medium (50 mM Hepes-Tris, 250 mM sucrose, pH 7.3) in the presence or absence of inhibitors as indicated. When 100 mM unlabeled D-glucose was used, the osmolarity was kept constant by adjusting the sucrose concentration in the medium at 150 mM. For phosphate transport, the incubation medium contained different concentrations of potential inhibitors or unlabeled KH_2PO_4 as indicated while keeping the tracer concentration at 10 μM (10 μCi) in 50 mM Hepes-Tris buffer (pH 7.3) containing 250 mM sucrose and 2 mM EGTA. When tested for accelerated exchange, the microsomes were preincubated for 2 min in the same buffer containing 100 mM KH_2PO_4. In all cases, uptake was initiated by the injection of 40 μl of microsomes (approx. 0.8 mg protein) into the incubation chamber of the FSRFA containing 1ml of incubation medium. Uptakes were determined by a 18-point automatic sequential sampling of the uptake mixtures. At each time point, 50 μl was injected into 1 ml of ice-cold stop solution, which consisted of 50 mM Hepes-Tris buffer

(pH 7.3) containing 250 mM sucrose and 0.25 mM phloretin where indicated. The stopped mixture was then filtered through 0.65 μm cellulose nitrate filters, and the filters were washed three times with 1 ml of ice-cold stop solution. The tracer content of the vesicles was then determined by liquid scintillation counting as described previously [32,36].

G6P UPTAKE AND EFFLUX MEASUREMENTS

The kinetics of 0.2 mM G6P uptake were determined at room temperature using 10 μM of [U-^{14}C]- and [^{32}P]G6P and a FSRFA as described above. The incubation medium and stop solution in this case were 50 mM Hepes-Tris buffer (pH 7.3) containing 250mM sucrose. For efflux experiments, 0.2 mM G6P (including 10 μM of [^{32}P]G6P) was incubated with microsomes for 3min at room temperature, then efflux was initiated by the injection of 0.5 mM vanadate into the incubation chamber of the FSRFA.

DATA ANALYSIS

Three to five uptake time courses were run under each of the experimental conditions reported in this paper. Uptake data were analyzed by the Enzfitter or P.Fit softwares (both published and distributed by Biosoft) according to the first-order rate equation

$$U = U_0 + U_\infty (1 - e^{-kt}) \qquad (1)$$

in which U, U_0, and U_∞ stand for the intravesicular amounts of substrate at time t, at zero-time, and at equilibrium, respectively, whereas k is the first-order rate constant of the uptake process. Efflux data were analyzed according to the first-order rate equation

$$U = U_0 e^{-kt} + U_\infty \qquad (2)$$

in which U, U_0 and U_∞ have the same definitions as above while k is the first-order rate constant of the efflux process. The best model fit to the data is shown in each of the figures. The errors associated with the kinetic parameter values reported in this paper represent the standard errors of regression (SER) on these parameters, which result from weighted or unweighted nonlinear regression analysis to the data. The kinetics of glucose and phosphate equilibration across the microsomal membrane are characterized by their $T_{1/2}$ values, which represent the time at which 50% of the process has been completed and can be calculated according to the relationship

$$T_{1/2} = \frac{\text{Ln } 2}{k} \qquad (3)$$

where k is the first-order rate constant derived from Eqs. (1) and (2).

Results

D-[U-^{14}C]GLUCOSE UPTAKE

The recent demonstration that D-glucose and D-mannitol can be taken up at similar rates by rat liver microsomes [26] prompted us to reevaluate the zero-trans influx kinetics of D-glucose transport in the absence of space marker. As depicted in Fig. 1A, zero-trans uptake of 10 μM [U-^{14}C]D-glucose can now be successfully measured; however, under these conditions, the zero-time glucose uptake (y-intercept) assumes a positive value, which represents the dead-space (background) in these experiments. The time course of glucose equilibration across the microsomal membrane is best-described by single

exponential kinetics with a $T_{1/2}$ value as reported in Table 1, which falls within the 30-50 s time range previously estimated by St-Denis *et al.* [35] for the $T_{1/2}$ of [^{14}C]glucose efflux from actively-loaded microsomes. The comparison between these two sets of data gathered at room temperature (22-23 °C) and 30 °C, respectively, also indicates that the glucose transport rates are quite insensitive to changes in the temperature of the assay.

As compared to tracer alone, identical time courses of glucose uptake are observed in the presence of either 100 mM unlabeled glucose or 0.25 mM phloretin in the uptake media (Fig. 1A). Glucose permeation of the microsomal membrane was similarly unaffected by a variety of potential inhibitors used at concentrations known to affect the G6Pase system [3,28] (Table 1). Similarly, glucose efflux was found to be insensitive to phloretin inhibition and did not show any tendency to saturation at glucose concentrations up to 20 mM [35]. Thus, in contratst to our previous conclusion that the ER membrane is not permeable to glucose in the outside to inside direction in the absence of G6Pase activity [12,35], these results clearly demonstrate that glucose transport is in fact bidirectional and symmetrical regarding its rates of influx and efflux.

The present radiotracer data qualitatively agree with those of Bánhegyi *et al.* [8]. Still, according to these authors, the rapid filtration technique would only resolve a slow (unsaturable, inhibitor-insensitive) glucose transport process because the time required by the washing procedure would lead to the loss of the majority of intravesicular glucose from a fast releasable pool. The further proposal that the fast glucose transport process would be sensitive to phloretin inhibition [8] can be tested directly on the rationale that glucose efflux through this putative pathway should be blocked by including this inhibitor

into the stop solutions. However, as reported in Fig. 1B, the inclusion of 1 mM phloretin in the wash solutions significantly affects neither the $T_{1/2}$ of glucose equilibration nor the amplitude of the uptake process (Fig. 1B and Table 1). Interestingly, the glucose space at equilibrium estimated in Figs. 1A and 1B represents an intravesicular volume of 5.3 ± 0.2 and 5.5 ± 0.2 µl/mg protein, respectively, thus equivalent to the total water space of 3.6-4.7 µl/mg protein reported by others [19,26]. Accordingly, the possibility that we might be missing up to 70-90% of the microsomal vesicles with fast glucose transport process can be safely ruled out.

[^{32}P]KH_2PO_4 UPTAKE

Fig. 2 shows that the kinetics of 10 µM [^{32}P]phosphate uptake are best-described by single exponential kinetics with a $T_{1/2}$ value as reported in Table 1. Time-dependent uptake is fully abolished when measured following permeabilization of the microsomal membrane by 0.8% CHAPSO, thus showing that most of the phosphate uptake represents transport into an intravesicular space of 4.2 ± 0.1 µl.mg^{-1} protein as estimated from the amplitude of the uptake process. Moreover, binding to the membrane vesicles appears marginal because the dead-space recorded in these experiments (12.4 ± 3.3 pmol.mg^{-1} protein, mean uptake value ± SEM under CHAPSO conditions in Fig. 2A) is similar to that observed in the case of glucose (10.0 ± 0.9 pmol.mg^{-1} protein, see Fig. 1A). Still, it should be underscored that the presence of EGTA in the uptake media appears essential to prevent phosphate binding because in the absence of this chelator, we found that the radioactive background was very high and similar in untreated or detergent-treated microsomes, thus precluding net [^{32}P]phosphate uptake measurements. This high

background might result from the non-specific binding of phosphate anions to cations such as Ca^{2+}.

The kinetics of phosphate equilibration across the microsomal membrane were found to be similar to those observed in the presence of tracer alone when the concentration of unlabeled phosphate was varied from 0 up to 100 mM (Fig. 2B and Table 1) and when a variety of potential inhibitors was added to the uptake media at concentrations known to affect the G6Pase system [3,28] (Table 1). Moreover, a similar $T_{1/2}$ value of 22 ± 2.0 s (mean ± SEM for 3 experiments) was also estimated for phosphate transport into microsomes preloaded with 100 mM KH_2PO_4, thus indicating the absence of accelerated exchange.

COMPARATIVE KINETICS OF INTRAMICROSOMAL RADIOTRACER INFLUX AND EFFLUX FROM [^{32}P]G6P AND [U-^{14}C]G6P

Previous experiments from our lab have shown that similar $T_{1/2}$ values account for the kinetics of tracer influx into and efflux from intact rat liver microsomes when using 0.2 mM [U-^{14}C]G6P as the sole labeled molecule in the uptake media [35]. Moreover, from the absence of ^{14}C uptake in vesicles whose G6Pase activity was inhibited by saturating concentrations of vanadate, it was concluded that the kinetics of tracer uptake mostly (if not solely) reflect those of [^{14}C]glucose accumulation into and efflux from the vesicles [35]. As shown in Fig. 3A and Table 2, similar results and conclusions also apply when 0.2 mM [^{32}P]G6P is instead used as the starting substrate. Note that the prior inhibition of G6Pase activity by 5 min preincubation of the membrane vesicles with 0.5 mM vanadate abolished the time-dependent uptake, thus showing that most of the ^{32}P uptake

and efflux represents phosphate transport into and out of an intravesicular space. In agreement with this view, note that the $T_{1/2}$ values of ^{32}P influx and efflux reported in Table 2 are identical to those shown in Table 1 for [^{32}P]phosphate equilibration across the microsomal membrane.

For comparison purposes, ^{14}C uptake was also measured in the same membrane preparation using 0.2 mM [^{14}C]G6P as the starting substrate. The time course data could be fit to single exponential kinetics with parameters as reported in Table 2. In agreement with our previous conclusion that ^{14}C uptake mostly (if not solely) reflect those of [^{14}C]glucose accumulation into the vesicles [12,13, 35], note that the $T_{1/2}$ value accounting for ^{14}C influx is within the range of those shown in Table 1 for [^{14}C]glucose equilibration across the microsomal membrane. Interestingly too, the amplitude of ^{14}C influx is about twice that observed for ^{32}P influx and efflux. Moreover, as calculated in Table 2, the $T_{1/2}$ ratio of ^{14}C vs ^{32}P equilibration across the microsomal membrane is not significantly different from the amplitude ratio of ^{14}C uptake vs ^{32}P uptake and efflux. Finally, when the ^{32}P and ^{14}C data are corrected for their respective dead-spaces reported in Table 2, and then plotted together as shown in Fig. 3B, it is readily apparent that identical initial rates of transport (v_i) are observed for the two radiotracers. Numerical values of the latter parameter can be estimated from the following relationship

$$v_i = \left[\frac{dU}{dt}\right]_{(t=0)} = k\,U_\infty \qquad (4)$$

which can be easily established from Eq. (2). Accordingly, from the data shown in Table 2, v_i values of 10.4 ± 1.4 and 11.2 ± 1.0 pmol.s^{-1}.mg^{-1} protein can be calculated for ^{14}C

and ^{32}P uptake, respectively. By contrast, the steady-state rate of G6P hydrolysis measured in the same microsomal preparation amounts to 85.0 ± 3.3 $pmol.s^{-1}.mg^{-1}$ protein.

Discussion

KINETIC MECHANISM OF GLUCOSE AND PHOSPHATE TRANSPORT IN RAT LIVER MICROSOMES

The early studies of Arion *et al.* [5] concluded that glucose permeation through the ER membrane most likely reflects a nonmediated process (simple diffusion) on the following pieces of evidence: i) glucose transport does not appear to be stereospecific, ii) equally rapid rates of permeation were observed with other nonelectrolytes of similar size like D-mannose and glycerol, and iii) access of D-glucose to G6Pase is unaffected by the general inhibitors of facilitative glucose transport, most notably cytochalasin B. The broad substrate specificity and the lack of stereospecificity of sugar uptake were largely confirmed by the light-scattering measurements of Marcolongo *et al.* [26]: D- and L-glucose, D-mannitol, D-mannose, D-fructose, D-galactose, 2-deoxy-D-glucose (DG), 3-O-methyl-D-glucopyranose (OMG) and α-methyl-D-glucopyranose (AMG) were all shown to equilibrate across the ER membrane with $T_{1/2}$ values in the time range of 3.5 to 9.0 s. These properties of sugar transport by rat liver microsomes contrast quite sharply with the kinetic characteristics now established for the different members of the two known families of glucose transport proteins. For example, the GLUT1-4 proteins are highly stereospecific and may accept D-glucose, D-galactose, OMG and DG, but none

of the other sugars, as substrates [31]. Similarly, the SGLT (Na^+-dependent glucose transport) proteins are highly stereospecific for D-glucose and may accept D-galactose, OMG and AMG, but none of the other sugars, as alternative substrates [42]. Accordingly, the ER glucose transport protein, if any, does not seem to qualify as a putative member of the SGLT or GLUT families. In agreement with this view, the classical inhibitors of sugar transport through the SGLT ($HgCl_2$ and phlorizin) and GLUT ($HgCl_2$ and phloretin) proteins failed to affect glucose permeation across the microsomal vesicles (Fig. 1 and Table 1). Moreover, microsomal glucose transport is not saturable up to 100 mM glucose concentrations (Fig. 1A), fails to demonstrate accelerated exchange kinetics [35], appears symmetrical under zero-trans influx and efflux conditions (present studies and [35], does not depend much on the temperature of the assay (these studies compared to [35]), and proves insensitive to a variety of inhibitors of the G6Pase system in intact microsomes like vanadate, chlorogenic acid, and HNB (Table 1).

The kinetic characteristics of phosphate transport by rat liver microsomes appear quite similar to those established for glucose: transport is not saturable up to 100 mM phosphate concentrations (Fig. 2B), appears symmetrical under zero-trans influx (Fig. 2 and Table 1) and efflux (Fig. 3A and Table 2) conditions, does not demonstrate accelerated exchange kinetics (see Results), and is not inhibited by either $HgCl_2$ or other known effectors of the G6Pase system (Table 1).

All together, the above criteria constitute strong evidence that glucose and phosphate transport in the ER occurs by simple diffusion. However, because the rates of sugar and phosphate equilibration across microsomal vesicles appear too fast to support the

hypothesis of passive diffusion through the lipid bilayer, we would rather suggest that a pore-like structure may in fact assume most (if not all) of the glucose and phosphate transport functions attributed to the putative T3 and T2 translocases in intact microsomes. Because of the smaller size of the phosphate anion relative to the sugar molecule, this assumption would in fact provide an easy explanation for the higher rates of phosphate transport relative to glucose, hence the smaller phosphate space at equilibrium relative to glucose. Moreover, the built-up of an opposing membrane potential could be minimized in the case of phosphate transport by the high rates of Na^+ (or K^+) permeation through the ER membrane [19], which might also be accounted for by Na^+ (and K^+) transport through the same pore-like structure.

In our opinion, the proposed existence in the ER membrane of a pore-like structure represents at this time the safest assumption that best accounts for the lack of stereospecificity of glucose transport and for the microsome permeability to a large number of solutes including water molecules. It does not matter much in the following as to whether or not this pore-like structure is constituted by a specific protein or results, as suggested recently [8], from fragmentation of the ER membrane during homogenization. In any event, glucose transport through this structure behaves as pure passive diffusion over the physiological range of sugar concentrations that may need to be considered for the interpretation of kinetic data regarding the functioning of the G6Pase system in intact microsomes. Moreover, the concept of water permeabilty through a pore would help in reconciliating the light-scattering and radiotracer data because it does predict the observation of higher rates of glucose permeation when using

the light-scattering technique as compared to the rapid filtration assay as further discussed below.

COMMENTS ON THE INTERPRETATION OF RADIOTRACER AND LIGHT-SCATTERING DATA

The concept of glucose transport heterogeneity in rat liver microsomal vesicles [8] relies heavily on the comparison of results between the rapid filtration [8,12,35, and present studies] and the light-scattering techniques [8,26] showing that the $T_{1/2}$ values estimated by the two approaches differ by close to one order of magnitude. One may thus need to question to what extent can these $T_{1/2}$ values be compared. In this regard, the questions of whether a solute and water have common permeation pathways and to what extent they interact during transport need to be addressed. This is usually done by considering the reflection coefficient σ of a solute for a given membrane: a σ value equal to 1 indicates separate pathways whereas $0 < \sigma < 1$ reveals solute-solvent interactions through shared pathways [25].

As defined by Kedem and Katchalsky [21], the volume (J_v) and solute (J_s) fluxes per unit area of a porous membrane are related through the following two equations

$$J_v = -L_p(RT\Delta C_m + \sigma RT\Delta C_s) \qquad (5)$$

$$J_s = (1-\sigma)\overline{C_s}J_v + P_s\Delta C_s \qquad (6)$$

where L_p and P_s represent osmotic and solute permeability coefficients, ΔC_m is the total concentration gradient of all impermeable species, ΔC_s accounts for the concentration

gradient of the single permeable solute under study, and

$$\overline{C_s} = \Delta C_s / \mathrm{Ln}\frac{C_{s1}}{C_{s2}} \qquad (7)$$

is a mean value of permeable solute concentration within the membrane (C_{s1} and C_{s2} represent permeable solute concentrations outside and inside of the vesicles, respectively).

Eq. (6) is of primary interest here because the last term contains P_s, whose behavior will indicate whether or not carrier kinetics are involved for the solute being studied [17,25]. Note that the first term in this equation is a solvent drag term, the importance of which when evaluating the solute flux is dictated by the value of the reflection coefficient σ. In the case of radiotracer assays, solute transport can in general be measured under close to isovolumetric conditions (see legend to Fig. 1 for example), hence in the almost complete absence of hydraulic conductance ($J_v \approx 0$). Accordingly, a direct determination of P_s can be achieved from initial rate measurements or curve-fitting to the integrated form of Eq. (6) performed at variable solute concentrations [27]. In the latter case, note that the observation of monoexponential uptake kinetics is the rule for passive diffusion but is not generally expected when dealing with a carrier-mediated process [17]. By contrastt, the light-scattering technique is an indirect approach whereby solute permeation is assessed from the changes in vesicular volume with time following a sudden increase in solute concentration. Accordingly, the simultaneous determination of the three phenomenological coefficients L_p, P_s, and σ is required to characterize completely a particular membrane and solvent-solute combination, which can in theory be accomplished through the combined application of a fast-resolution stopped-flow

apparatus and Eqs. (5-6) [17, 25]. In this respect, Eq. (6) clearly shows that, in the most general case where $0 < \sigma < 1$, J_s measured by the light-scattering technique will always be higher than J_s determined by an isovolumetric radiotracer assay because the glucose and water fluxes both proceed in the same direction. Accordingly, the solvent-drag effect will decrease the apparent $T_{1/2}$ for glucose equilibration. In the case where $\sigma = 1$, Eq. (6) seems to indicate that the light-scattering technique and the radiotracer assay may lead to similar results. However, the determination of initial rates of permeation at the start of the swelling phase is highly sensitive to the refractive index (a parameter that obviously increases at increasing glucose concentrations) of the solutions [37] whereas the integration of Eq. (6) should take into account the volume changes with time [39] and requires a number of explicit assumptions to get simple analytical solutions [27,39].

The conclusion of Marcolongo *et al.* [26] regarding the involvement of a fast carrier-mediated process in glucose transport across the ER membrane relies on the observation that glucose influx is saturable. However, in the experiments reported in Fig 2a of this paper where the osmolarity gradient varied with the tested glucose concentrations, it clearly appears that glucose permeation through the microsomal membrane was assessed under conditions of variable volumes during the swelling phase. Because more water molecules need to be transported with glucose to reach a similar final isoosmotic volume, higher $T_{1/2}$ values (lower apparent glucose fluxes) are expected at higher volume differences (higher glucose concentrations) independently of whether glucose transport is carrier-mediated or occurs through passive diffusion, hence the (apparent) saturation kinetics reported in Fig. 2b of this paper. Note that a thorough interpretation of the latter

figure may also be complicated by the following observation: the maximum in the light intensities recorded at the end of the shrinking phase (see Fig. 2a in this paper) does not seem to be proportional to volume differences, which may arise because the microsomal vesicles do not behave as perfect osmometers and/or because the intensity of the scattered-light does not change linearly with the vesicular volume.

The involvement of a fast carrier-mediated process in glucose transport through the ER membrane also rests on the observation of Marcolongo *et al.* [26] that pentamidine, DIDS, and cytochalasin B reduced the microsomal permeability to various monosaccharides. However, this inhibition was only partial and, with the exception of cytochalasin B, none of the inhibitors tested appear specific to glucose transport through the SGLT or GLUT proteins [31,42]. Because Eq. (6) clearly shows that any reduction of the solvent drag term through decreased J_v would in turn produce an apparent inhibition of J_s, one may question, then, to what extent the experiments of Marcolongo *et al.* [26] do demonstrate partial inhibition of glucose permeation rather than partial inhibition of water fluxes. This question cannot be easily answered from the reported data, and the direct assessment of its relevance to the kinetics of microsomal transport may require the use of a fast-resolution stopped-flow apparatus to analyze the effect of these inhibitors on the shrinking phase when using an impermeant solute like sucrose (such a control experiment may allow one to directly determine the effect of any inhibitor on J_v, see Eqs. (5) and (6) with $\sigma = 1$ and $\Delta C_s = 0$).

An important discrepancy between the results of the present radiotracer studies and those of Bánhegyi *et al.* [8] deals with the glucose space at equilibrium. In this respect,

it was previously determined that glucose efflux over the first 20 s required for the filtration and two washing steps represents approx. 11% of the amount of radioactivity accumulated at zero-time when 0.25 M sucrose was present both inside the vesicles and in the ice-cold stop solutions [13]. Under these experimental conditions, Fig. 1 also demonstrates that, at equilibrium, glucose occupies the entire vesicular water space of 3.6-4.7 $\mu l.mg^{-1}$ protein reported by others [19,26]. These low efflux rates and high glucose spaces contrast with those reported by Marcolongo *et al.* [26) and Bánhegyi *et al.* [8] at 22 °C where up to 80% of the tracer molecules were lost during the filtration and washing steps. In both of the latter studies, the intravesicular medium mostly contained permeant species (100 mM KCl and 20 mM NaCl) while the stop solution was made up of 0.25 M sucrose, an impermeant species. Such conditions should induce vesicle shrinking and lead to high rates of glucose efflux due to the solvent-drag effect through a pore-like structure. Accordingly, then, great care should be taken in the choice of the washing solutions when using a radiotracer assay.

Clearly, a thorough comparison between the rapid filtration and light-scattering techniques does not support the claim of Marcolongo *et al.* [26] that the efflux rates of the permeant sugars are too fast to allow confident measurements by the rapid filtration technique. We therefore challenge the conclusion of these authors that rat liver microsomal vesicles are heterogenous concerning their glucose transport properties when this conclusion rests on an uncritical comparison between the results of light-scattering and radiotracer data, and on efflux experiments that are not representative of an optimum use of the rapid filtration assay. In agreement with this view, the heterogeneity problem

does not show up in the light-scattering studies of Marcolongo *et al.* [26] in which one would have expected to observe both fast and slow kinetics of sugar permeation during the swelling phase.

AN INTEGRATED VIEW OF THE KINETICS OF G6P TRANSPORT AND HYDROLYSIS

The substrate transport-catalytic unit concept

In the original proposal of the substrate transport model by Arion *et al.* [6], it was suggested that the demonstration of a metabolically active pool of G6P within the intramicrosomal space would be definitive for the choice between substrate and group transport, for this feature is unique to the substrate transport-catalytic unit concept. We do not share this view for the following reasons. First, this early statement may need to be reevaluated in the light of the possibility that G6P access to the intraluminally-oriented active center of the p36 protein may involve both direct (channel in the ternary structure of the protein) and indirect (transport through the ER membrane via T1 or any other route) pathways [12]. Second, such studies need to be performed under steady-state conditions in which the intravesicular concentration of G6P may result from a balance between the hydrolytic and synthetic functions of the G6Pase system [29]. Last, the experimental approach is endowed with a number of technical difficulties, some of which can be best illustrated by reference to a recent paper of Bánhegyi *et al.* [9] where a rapid filtration assay was used to assess the presence of an intravesicular G6P pool. In these experiments, DIDS was included in the washing solution on the rationale that this T1-inhibitor would reduce G6P efflux during the washing procedure. However, DIDS was

also shown to induce glucose efflux from actively-loaded microsomes [35] and the composition of the stop solution itself does not minimize glucose efflux (see above). Accordingly, the studies of Bánhegyi *et al.* [9] cannot objectively assess the relative contributions of the coexisting G6P and glucose pools to the kinetics of the G6Pase system in intact microsomes. Moreover, as previously noted by Ballas and Arion [7] who failed to demonstrate any evidence for G6P permeation when the microsomes were isolated from the incubation medium by centrifugal transfer through a layer of silicone fluid that lasted less than 1 s, the most serious limitation in such studies is the everpresent G6Pase activity. In this respect, it is noteworthy that the level of enzyme activity reported by Bánhegyi *et al.* [9] in their microsomal preparation is such as to hydrolyse in no more than 1 to 3 s the totality of the intravesicular G6P pools observed in these studies and that DIDS does not inhibit the catalytic unit of the G6Pase complex [28]. If anything, then, the results of Bánhegyi *et al.* [9] could as well be interpreted to mean that G6P is poorly hydrolyzed from the inside of the microsomes.

In our opinion, the key question at this time is not to determine whether or not G6P can reach the intravesicular space under intact form but, rather, to test whether or not the presence of intravesicular G6P is an obligatory prerequisite to G6P hydrolysis. There is no simple answer to the latter question when addressed by looking at the kinetics of tracer uptake following incubation of the microsomes with [^{14}C]G6P because of the presence of both [^{14}C]G6P and [^{14}C]glucose within the intravesicular compartment. In this regard, there is some confusion in the literature among the proponents of the substrate transport-catalytic unit concept, so that the following discussion aims at emphasizing the limits of

any interpretation of G6P transport and hydrolysis according to this hypothesis.

The most objective answer about the meaning of G6P/glucose uptake data should rely on simulation studies. Such an approach was pioneered by Berteloot *et al.* [13] who derived an exact analytical solution of the substrate transport model under the case where the concentration of G6P in the incubation medium ($G6P_o$) is small as compared to the apparent Km's for transport and hydrolysis. Accordingly, as depicted in Fig. 4, G6P hydrolysis can be considered as an irreversible process for the duration of the assay with rate constant $k_h = V_{maxh} / K_h$ if V_{maxh} and K_h represent the maximum rate and the Michaelis constant for G6P hydrolysis. If we assume an intravesicular volume of 5 μl/mg protein, then a k_h value of 0.374 s^{-1} can be calculated from the steady-state V_{maxh} and K_h values reported by Berteloot *et al.* [12] for G6P hydrolysis in intact microsomes. Similarly under these conditions, G6P transport is equivalent to a passive diffusion process with apparent first-order rate constant k_t _ 0.035 s^{-1} ($T_{1/2}$ _ 20 s, see Fulceri *et al.* [19]). Note that k_t may represent the $V_{m,faxt}/Kt,f$ or $Vm,r_{axt}/Kt,r$ ratios of a carrier-mediated transport system if V_{maxt} and K_t represent, respectively, the maximum rate and the Michaelis constant for G6P transport in the forward (extra indice f) and reverse (extra indice r) directions. However, these two ratios are equal due to the law of microscopic reversibility [17], so that transport appears symmetrical as also occurs with passive diffusion. Finally, as justified experimentally (see above), glucose efflux can be assimilated to a passive diffusion process with apparent first-order rate constant $ke,G = 0.017$ s^{-1} ($T_{1/2} = 40$ s, see Table 1 and [12,35]).

The following equations describe the kinetics of G6P uptake into microsomes ($G6P_i$)

$$(G6P_i) = \frac{k_t (G6P_o)}{k_t + k_h} [1 - e^{-(kSUBt + k_h)t}] \qquad (8)$$

and the time course of intravesicular glucose accumulation (G_i)

$$(G_i) = \frac{k_t k_h (G6P_o)}{k_e^G (k_t + kSUBh)(k_t + k_h - k_e^G)} [(k_t + k_h)(1 - e^{-k_e^G t}) - k_e^G (1 - e^{-(k_t + k_h)t})] \qquad (9)$$

as adapted from Berteloot *et al.* [13] to the model depicted in Fig. 4. Therefore, because $k_t + k_h \gg k_{e,G}$ (see numerical values above), a steady-state $G6P_i$ concentration should be reached rapidly ($T_{1/2} \ll 1.7$ s) as compared to intravesicular G_i accumulation. Accordingly, Eq. (9) rapidly degenerates to the simpler form

$$(G_i) = \frac{k_t k_h (G6P_o)}{k_e^G (k_t + k_h)} (1 - e^{-k_e t}) \qquad (10)$$

and the slow phase of tracer uptake should describe the kinetics of glucose efflux independently of whether or not G6P can also be found into the intramicrosomal compartment. These conclusions are intuitively sound when correlated to the experimental observation that a steady-state rate of G6P hydrolysis is rapidly established in intact microsomes (see for example Berteloot *et al.* [13] and Arion *et al.* [2]), which cannot be fulfilled unless a steady-state G6Pi concentration has also been rapidly reached within the intravesicular compartment. To assume, then, that the slow phase of tracer uptake can be assimilated to G6P transport [22] or to the combined accumulation of G6P and glucose into the intravesicular compartment [9] just simply conflicts with the steady-state hypothesis. In this respect, it should also be emphasized that the question of the rate

limitancy of G6P transport relative to G6P hydrolysis is irrelevant to the functioning of the G6Pase system in intact microsomes: the time period over which a steady-state $G6P_i$ concentration is reached is dictated by the values of both k_t and k_h (see Eq. [8]) and will mostly depend on the k_h value when $k_t \ll k_h$.

These theoretical predictions can be tested directly using the results of the present studies. Indeed, equations similar in form to Eqs. (8-10) can be derived when [^{32}P]G6P rather than [^{14}C]G6P is used as the tracer substrate. Obviously, Eq. (8) is unaffected by the nature of the tracer substrate and ^{32}P uptake would mostly characterize the kinetics of phosphate efflux if P_i (intravesicular phosphate concentration) and ke,P (rate constant of phosphate efflux) are substituted for G_i and ke,G in Eq. (9). In agreement with this view, similar $T_{1/2}$ values were observed for the kinetics of ^{32}P uptake and efflux (Fig. 3A and Table 2) and these $T_{1/2}$ values are identical within the range of the experimental errors to those observed for [^{32}P]phosphate uptake (Fig. 2 and Table1). Moreover, it can be predicted from Eq. (10) that the ratio of [^{14}C]G_i to [^{32}P]P_i accumulated at equilibrium (infinite time) should be described by the following relationship

$$\left[\frac{(G_i)}{(P_i)}\right]_{equilibrium} = \frac{k_e^P}{k_e^G} = \frac{T_{1/2}^G}{T_{1/2}^P} \qquad (11)$$

where $T^G{}_{1/2}$ and $T^P{}_{1/2}$ stand for the $T_{1/2}$ of G_i and P_i efflux, respectively. This prediction is clearly verified by the experiments reported in Fig. 3 and Table 2.

Eqs. (8) and (9) can also be used to demonstrate that

$$\left[\frac{(G6\Pi)}{(G6\Pi)+(Gi)}\right]_{equilibrium} = \frac{k_e^G}{k_h + k_e^G} = 0.044, \qquad (12)$$

hence that the steady-state amount of intravesicular [^{14}C]G6P is independent of G6P transport and represents a tiny fraction only of the total amount of the [^{14}C]-labelled molecules taken up by the microsomes. Accordingly, the combination of the high rate and low amplitude of [^{14}C]G6P uptake relative to the intramicrosomal production of [^{14}C]glucose should normally preclude the resolution of the rapid phase of tracer uptake at the experimental level. In agreement with this view, the rapid phase of tracer uptake has only been observed when using a fast-sampling rapid-filtration apparatus [12,13,35] whereas the slow phase has now been reported by a number of laboratories [9,12,13,22,35]. In view of the low signal over noise ratio predicted by the theory as regards the possibility to observe the rapid phase of tracer uptake, one may thus question to what extent could its resolution by rapid kinetic techniques be compatible with the substrate transport hypothesis. An unambiguous answer to this question can be provided as follows.

The kinetics of tracer G6P/glucose uptake predicted by the substrate transport-catalytic unit concept should be described by the sum of Eqs. (8) and (9), which can be cast under the form of the biexponential function

$$Tracer\ uptake = AMP_1(1 - e^{-k_1 t}) + AMP_2(1 - e^{-kSUB2\,t}) \qquad (13)$$

with the following algebraic expressions of the kinetic parameters.

$$k_1 = k_t + k_h = 0.173\ s^{-1} \qquad (14)$$

$$k_2 = k_e^G = 0.017\ s^{-1} \qquad (15)$$

$$\frac{AMP_1}{(G6\,P_o)} = w\,\frac{k_t(k_t - k_e^G)}{(k_t + k_h)(k_t + k_h - k_e^G)} = 0.91\ pmol.mg^{-1}\ protein \qquad (16)$$

$$\frac{AMP_2}{(G6\,P_o)} = w\,\frac{k_t\,k_h}{k_e^G(k_t + k_h - k_e^G)} = 9.57\ pmol.mg^{-1}\ protein \qquad (17)$$

The numerical values shown on the right-hand-side of Eqs. (14) and (15) correspond to the mean $T_{1/2}$ values of 4 and 40 s reported by St-Denis *et al.* [35] for the fast and slow uptake phases, respectively, whereas those appearing on the right-hand-side of Eqs. (16) and (17) have been calculated from the data published by Berteloot *et al.* [12]. Note that the theoretical volume of the intramicrosomal space (w) has also been introduced in the latter two equations, such that Eqs. (14-17) can be solved simultaneously to give a unique solution in which w = 3.47 µl/mg protein, $k_t = 0.094\ s^{-1}$ ($T_{1/2} = 7.4$ s), and $k_h = 0.080\ s^{-1}$ ($T_{1/2} = 8.7$ s). Interestingly, the calculated volume falls within the expected range [19,26] and the calculated k_t value appears fully compatible with the $T_{1/2}$ value estimated by Fulceri *et al.* [19] for G6P equilibration across the microsomal membrane using the light-scattering technique. However, this k_t value differs by close to one order of magnitude from the k_t value calculated using the V_{max} and K_t estimates reported by Arion *et al.* [4]. Indeed, the latter values were obtained on the premise that G6P hydrolysis was consecutive to G6P transport. In this respect, our calculated k_h and k_t values are almost identical, in which case transport and hydrolysis may occur simultaneously. More importantly, however, the calculated k_h value is close to one order of magnitude lower than expected from the steady-state rate of G6P hydrolysis in intact microsomes ($0.55\ s^{-1}$

as calculated from [12] using the w value above). Clearly, then, for these data to be compatible with the substrate transport hypothesis, one may have to assume that the bulk of G6P hydrolysis occurs outside of the microsomes, so that G6P transport is not an obligatory prerequisite to G6P hydrolysis by intact microsomes.

If one assumes that the rapid phase of tracer uptake partially conforms to the prediction of the substrate transport hypothesis, then a corollary implication is that the glucose produced through the substrate transport pathway should affect in some way the total rate of glucose production (Go) during the initial phase of G6P hydrolysis. The expected behavior for transport-dependent hydrolysis is the observation of a presteady-state delay (lag) in G6Pase activity as shown by the following equation

$$(G_o) = \frac{k_t k_h (G6P_o)}{k_t + k_h} t - \frac{kSUBt\, k_h (G6P_o)}{(k_t + k_h)^2} [1 - e^{-(k_t + k_h)t}] \qquad (18)$$

adapted from Berteloot *et al.* [13] to the model depicted in Fig. 4. This result is intuitively sound because, at subsaturating G6P concentrations, one may expect more and more G6P to be hydrolyzed as more and more G6P gets into the intravesicular space via the transport system until the steady-state is reached. The time period over which one may expect to observe the lag kinetics is dictated by the value of the apparent first-order rate of the fast uptake phase ($T_{1/2}$ = 2 to 4 s, see above) and could not be missed in a realistic experiment. Interestingly, the observation of either burst [13] or linear [2] kinetics during the presteady-state phase of glucose production rules out the latter prediction of the translocase-catalytic unit concept.

A revised version of the combined conformational flexibility-substrate transport model

A detailed analysis of the substrate-transport model clearly shows that the intravesicular glucose and phosphate pools are more relevant than the G6P pool to the understanding of the kinetics of G6P uptake and hydrolysis in intact microsomes. Moreover, the latent form of G6Pase activity can be prevented by histone II-A treatment of the microsomes which, contrary to the previous report by Blair and Burchell [14], does not permeabilize the membrane [30,34]. The "histone-activated" microsomes accumulate glucose produced from [^{14}C]G6P hydrolysis to even greater extent than the native vesicles but the mannose released from [^{14}C]mannose 6-phosphate (M6P) hydrolysis does not accumulate into the vesicular space [34]. Since M6P, in contrast to G6P, does not permeate intact microsomes [19], these important studies thus demonstrate that substrate hydrolysis can occur in the complete absence of substrate transport and that vectorial tracer uptake into the intravesicular space is specific to the glucose product of hydrolysis. Alternatively, then, the rapid phase in tracer uptake could also be interpreted to represent a glucose precursor pool generated close to the active center of the enzyme (G_m), which would thus support the slow phase of glucose uptake once a steady-state rate of G6P hydrolysis has been rapidly achieved [12]. This hypothesis nicely fits within the concept of the combined conformational flexibility-substrate transport model previously proposed by Schulze *et al.* [33]. We therefore suggested an updated version of this model [12] whereby the catalytic site of the p36 protein lies deep within a hydrophilic pocket of an intrinsic membrane protein which is connected to the extra- and intravesicular spaces

through channels with different intrinsic permeabilities to G6P and glucose. This model may now need to be modified further to account for the bidirectionality of glucose transport, which could easily be done as depicted in Fig. 5.

In this model, the following equations

$$\frac{d(G_o)}{dt} = k_{D2}(G_m) + k_e^G(G_i) \qquad (19)$$

$$\frac{d(G_i)}{dt} = k_{D3}(G_m) - k_e^G(G_i) \qquad (20)$$

would describe the steady-state rates of glucose production in the extra- and intramicrosomal compartments, respectively. Accordingly, the steady-state rate of G6P hydrolysis (v_h) can be expressed as

$$v_h = \frac{d(G_o)}{dt} + \frac{d(G_i)}{dt} = (k_{D2} + k_{D3})(G_m) \qquad (21)$$

from which the steady-state glucose concentration within the hydrophilic pocket

$$(G_m) = \frac{v_h}{k_{D2} + k_{D3}} \qquad (22)$$

can be calculated and would mostly account for AMP_1 in Eq. (13). Eq. (22) can in turn be used to establish that

$$v_i^G = k_{D3}(G_m) = \frac{k_{D3}\, v_h}{k_{D2} + k_{D3}} \qquad (23)$$

represents a correct expression of the initial rate of glucose transport into the

intravesicular space. Eq. (20) can be integrated to give

$$(G_i) = AMP_2^G (1 - e^{-k_e^G t}) \qquad (24)$$

where

$$AMP_2^G = \frac{k_{D3}\, v_h}{k_e^G (k_{D2} + k_{D3})} \qquad (25)$$

would account for AMP_2 in Eq. (13). Obviously, Eqs. (22) and (25) are fully compatible with our previous observation that AMP1 and AMP2 demonstrate Michaelis-Menten kinetics relative to (G6Po) with K_m values similar to those observed for the steady-state rate of G6P hydrolysis [12]. Note that the following relationship

$$v_i^G = k_e^G\, AMP_2^G \qquad (26)$$

can also be easily established from Eqs. (23) and (25).

Equations similar in form to Eq. (19-26) could be derived to account for phosphate production during G6P hydrolysis. However, as shown in Fig. 3B, $v_{i,G} = v_{i,P} = v_i$ with mean value of 10.8 ± 0.6 pmol.s^{-1}.mg^{-1} protein (see Results). It can thus be established from Eq. (23) that $(P_m) = (G_m)$ and that identical values of k_{D2} and k_{D3} describe the efflux rates of both [^{14}C]glucose and [^{32}P]phosphate from the hydrophilic pocket. Accordingly, Eq. (7) also applies to the conformational model depicted in Fig. 5 and Eq. (23) allows us to calculate that

$$\frac{k_{D3}}{k_{D2}+k_{D3}} = \frac{v_i}{v_h} = 0.127 \pm 0.012 \qquad (27)$$

using the v_h value of 85 ± 3.3 pmol.s^{-1}.mg^{-1} protein reported under results. Quite obviously, then, the experiments described in Fig. 3 demonstrate once again that G6P transport is not an obligatory prerequisite to G6P hydrolysis because some 87% of the total glucose (and phosphate) produced during the course of the enzyme reaction does not cycle through the intravesicular space.

Eq. (22) can be developed further to establish the relationship

$$\frac{(V_h)_{max}(G6P_o)}{(k_{D2}+k_{D3})[K_h+(G6P_o)]} = \frac{(AMP_1)_{max}(G6P_o)}{K_h+(G6P_o)} \qquad (28)$$

$$k_{D2}+k_{D3} = \frac{(V_h)_{max}}{(AMP_1)_{max}} = 1.7 \pm 0.5\ s^{-1} \qquad (29)$$

from which the value of

can be calculated. Note that the left-hand term in Eq. (28) simply expresses the fact that v_h in Eq. (22) follows Michaelis-Menten kinetics with kinetic parameters $(V_h)_{max}$ and K_h whereas the right-hand term in Eq. (28) takes into account the facts that AMP_1 can replace (G_m) into Eq. (22) and that AMP1 also follows Michaelis-Menten kinetics with kinetic parameters $(AMP_1)_{max}$ and K_h [12]. The numerical value appearing in Eq. (29) results from the $(V_h)_{max}$ and $(AMP_1)_{max}$ values previously published by Berteloot *et al.* [12]. Solving simultaneously Eqs. (27) and (29) thus leads to k_{D2} and k_{D3} values of 1.48 ± 0.6 and 0.22 ± 0.08 s^{-1}, respectively.

SUMMARY AND CONCLUSIONS

The substrate transport (Fig. 4) and the conformational (Fig. 5) models both predict biexponential kinetics of [^{14}C]G6P/glucose uptake whereby the slow phase of tracer uptake accounts for the kinetics of glucose efflux from the microsomes, independently of whether or not G6P can also be found in the intramicrosomal compartment. However, the simultaneous analysis of the kinetics of G6P transport/hydrolysis and of glucose/phosphate transport proves incompatible with the current version of the substrate transport-catalytic unit concept because approx. 90% of the total glucose produced during the course of the enzyme reaction does not cycle through the intravesicular space. By contrast, our revised version of the combined conformational flexibility-substrate transport model is fully compatible with the latter result and all of its microscopic rate constants can be determined. The most notable exception in this respect concerns the rate of G6P access to the active site on the enzyme. As inferred from the analysis of the substrate transport model, this is so because a steady-state rate of G6P hydrolysis ought to be rapidly established within the hydrophilic pocket independently of whether or not G6P transport constitutes the rate-limiting step for G6P hydrolysis. Therefore, the role of the p46 protein in the functioning of the G6Pase system cannot be assessed from kinetic studies of tracer G6P transport/hydrolysis in intact rat liver microsomes.

FOOTNOTES

1. **Abbreviations used:** AMG, α-methylglucose; CHAPSO, 3-[(3-cholamidopropyl)-dimethylammonio]-2-hydroxy-1-propanesulfonate; DG, 2-deoxyglucose; DIDS, 4,4'-diisothiocyanostilbene-2,2'-disulfonic acid; EGTA, ethyleneglycol-bis-(β-aminoethyl ether)N,N,N',N'-tetraacetic acid; ER, endoplasmic reticulum; FSRFA, fast-sampling, rapid-filtration apparatus; G_i, intra microsomal glucose; G_m, glucose in the intramembrane compartment; G_o, extramicrosomal glucose; G6P, glucose 6-phosphate; $G6P_i$, intramicrosomal G6P; $G6P_m$, G6P in the intramembrane compartment; $G6P_o$, extramicrosomal G6P; G6Pase, glucose 6-phosphatase; GLUT, facilitative glucose transport protein; GSD, glycogen storage disease; Hepes, N-[2-hydroxyethyl]piperazine-N'-[2-ethanesulfonic] acid; HNB, 2-hydroxy-5-nitrobenzaldehyde; M6P, mannose 6-phosphate; OMG, 3-O-methylglucose; P_i, intramicrosomal phosphate; P_m, phosphate in the intramembrane compartment; P_o, extramicrosomal phosphate; p36, catalytic subunit of G6Pase; p46, putative G6P transporter; SEM, standard error of the mean; SER, standard error of regression; SGLT, Na^+-dependent glucose transport protein; T1, G6P translocase; T2, phosphate translocase; T3, glucose translocases; Tris, tris-[hydroxymethyl]-aminomethane; UhpC, upper hexose phosphate receptor; UhpT, upper hexose phosphate transport protein.

ACKNOWLEDGEMENTS

The authors thank C. Gauthier for the art work.This research was supported by Grants from the Medical Research Council of Canada (ME-10783 and MOP-37959 to G.v.d.W., and MT-14407 to A.B.). W.X. was supported by a studentship from the GRTM (FCAR-Centres).

REFERENCES

1. Annabi, B., Hiraiwa, H., Mansfield, B.C., Lei, K.J., Ubagai, T., Polymeropoulos, M.H., Moses, S.W., Parvari., R., Hershkovitz, E., Mandel, H., Fryman, M., Chou, J.Y. 1998. The gene for glycogen-storage disease 1b maps to chromosome 11q23. *Am. J. Hum. Gen.* **62:**400-405

2. Arion, W.J., Canfield, W.K., Callaway, E.S., Burger, H.-J., Hemmerle, H., Schubert, G., Herling, A.W., Oekonomopulos, R. 1998. Direct evidence for the involvement of two glucose 6-phosphate-binding sites in the glucose-6-phosphatase activity of intact liver microsomes. *J. Biol. Chem.* **273:**6223-6227

3. Arion, W.J., Canfield, W.K., Ramos, F.C., Schindler, P.W., Burger, H.-J., Hemmerle, H., Schubert, G., Below, P., Herling, A.W. 1997. Chlorogenic acid and hydroxynitro-benzaldehyde: new inhibitors of hepatic glucose 6-phosphatase. *Arch. Biochem. Biophys.* **339:**315-322

4. Arion, W.J., Lange, A.J., Ballas, L.M. 1976. Quantitative aspects of relationship between glucose 6-phosphate transport and hydrolysis for liver microsomal glucose 6-phosphate system. *J. Biol. Chem.* **251:**6784-6790

5. Arion, W.J., Lange, A.J., Walls, H.E., Ballas, L.M. 1980. Evidence for the participation of independent translocases for phosphate and glucose 6-phosphate in the microsomal glucose 6-phosphatase system. *J. Biol. Chem.* **255:**10396-10406

6. Arion, W.J., Wallin, B.K., Lange, A.J., Ballas, L.M. 1975. On the involvement of

a glucose 6-phosphate transport system in the function of microsomal glucose 6-phosphatase. *Mol. Cell. Biochem.* **6:**75-83

7. Ballas, L.M., Arion, W.J. 1977. Measurement of glucose 6-phosphate penetration into liver microsomes. *J. Biol. Chem.* **252:**8512-8518

8. Bánhegyi, G., Marcolongo, P., Burchell, A., Benedetti, A. 1998. Heterogeneity of glucose transport in rat liver microsomal vesicles. *Arch. Biochem. Biophys.* **359:**133-138

9. Bánhegyi, G., Marcolongo, P., Fulceri, R., Hinds, C., Burchell, A., Benedetti, A. 1997. Demonstration of a metabolically active glucose-6-phosphate pool in the lumen of liver microsomal vesicles. *J. Biol. Chem.* **272:**13584-13590

10. Berteloot, A., Malo, C., Breton, S. Brunette, M. 1991. A fast sampling, rapid filtration apparatus: principal characteristics and validation from studies of D-glucose transport in human jejunal brush-border membrane vesicles. *J. Membrane Biol.* **122:**111-125

11. Berteloot, A., Semenza, G. 1990. Advantages and limitation of vesicles for the characterization and the kinetic analysis of transport systems. *Meth. Enzymol.* **192:**409-437

12. Berteloot, A., St-Denis, J.-F., van de Werve, G. 1995. Evidence for a membrane exchangeable glucose pool in the functioning of rat liver glucose-6-phospharase. *J. Biol. Chem.* **270:**21098-21102

13. Berteloot, A., Vidal, H., van de Werve, G. 1991. Rapid kinetics of liver microsomal glucose 6-phosphatase. *J. Biol. Chem.* **266:**5497-5507

14. Blair, J.N.R., Burchell, A. 1988. The mechanism of histone activation of the hepatic microsomal glucose-6-phosphatase system: a novel method to assay glucose-6-phosphatase activity. *Biochim. Biophys. Acta* **964:**161-167

15. Burchell, A. 1990. Molecular pathology of glucose-6-phosphatase. *FASEB J.* **4:**2978-2988

16. Burchell, A. 1998. A re-evaluation of GLUT7. *Biochem. J.* **331:**973

17. Eilam, Y., Stein, W.D. 1974. Kinetic studies of transport across red blood cell membranes. *In:* Methods in Membrane Biology. E.D. Korn editor. Vol. 2, Chap. 5, pp. 283-354. Plenum Press, New-York

18. Fenske, C.D., Jeffery, S., Weber, J.L., Houlston, R.S., Leonard, J.V., Lee, P.J. 1998. Localization of the gene for glycogen storage disease 1c by homozygosity mapping to 11q. *J. Med. Genet.* **35:**269-272

19. Fulceri, R., Bellomo, G., Gamberucci, A., Scott, H.M., Burchell, A., Benedetti, A. 1992. Permeability of rat liver microsomal membrane to glucose 6-phosphate. *Biochem. J.* **286:**813-817

20. Kadner, R.J., Webber, C.A., Island, M.D. 1993. The family of organo-phosphate transport proteins includes a transmembrane regulatory protein. *J. Bioenerg. Biomemb.* **25:**637-645

21. Kedem, O., Katchalsky, A. 1958. Thermodynamic analysis of the permeability of biological membranes to non-electrolytes. *Biochim. Biophys. Acta* **27:**229-246

22. Lei, K.-J., Chen, H., Pan, C.-J., Ward, J.M., Mosinger, B., Jr., Lee, E.J., Westphal, H., Mansfield, B.C., Chou, J.Y. 1996. Glucose-6-phosphatase

dependent substrate transport in the glycogen storage disease type-1a mouse. *Nature Genetics* **13:**203-209

23. Lei, K.-J., Shelly, L.L., Pan, C.-J., Sidbury, J.B., Chou, J.Y. 1993. Mutations in the glucose-6-phosphatase gene that cause glycogen storage disease 1a. *Science* **262:**580-583

24. Lin, B., Hiraiwa, H., Pan, C.J., Nordlie, R.C., Chou, J.Y. 1999. Type-1c glycogen storage disease is not caused by mutations in the glucose-6-phosphate transporter gene. *Hum. Gen.* **105:**515-517

25. Macey, R.I., Wadzinski, L.T. 1974. Mathematical models and membrane permeability. *Fed. Proc.* **33:**2323-2326

26. Marcolongo, P., Fulceri, R., Giunti, R., Burchell, A., Benedetti, A. 1996. Permeability of liver microsomal membranes to glucose. *Biochem. Biophys. Res. Commun.* **219:**916-922

27. Mild, K.H., Lovtrup, S. 1985. Movement and structure of water in animal cells. Ideas and experiments. *Biochim. Biophys. Acta* **822:**155-167

28. Nordlie, R.C. 1982. Kinetic examination of enzyme mechanisms involving branched reaction pathways - A detailed consideration of multifunctional glucose-6-phosphatase. *Meth. Enzymol.* **87:**319-353

29. Nordlie, R.C., Foster, J.D., Lange, A.J. 1999. Regulation of glucose production by the liver. *Annu. Rev. Nutr.* **19:**379-406

30. Pederson, B.A., Foster, J.D., Nordlie, R.C. 1998. Histone II-A activates the glucose-6-phosphatase system without microsomal membrane permeabilization.

Arch. Biochem. Biophys. **357:**173-177

31. Pessin, J.E., Bell, G.I. 1992. Mammalian facilitative glucose transporter family: structure and molecular regulation. *Annu. Rev. Physiol.* **54:**911-930

32. Romanelli, A., St-Denis, J.-F., Vidal, H., Tchu, S., van de Werve, G. 1994. Absence of glucose uptake by liver microsomes, an explanation for the complete latency of glucose dehydrogenase. *Biochem. Biophys. Res. Commun.* **200:**1491-1497

33. Schulze, H.-U., Nolte, B., Kannler, R. 1986. Evidence for changes in the conformational status of rat liver microsomal glucose-6-phosphate:phosphohydrolase during detergent-dependent membrane modification. *J. Biol. Chem.* **261:**16571-16578

34. St-Denis, J.-F., Annabi, B., Khoury, H., van de Werve, G. 1995. Histone II-A stimulates glucose-6-phosphatase and reveals mennose-6-phosphatase activities without permeabilization of liver microsomes. *Biochem. J.* **310:**221-224

35. St-Denis, J.-F., Berteloot, A., Vidal, H., Annabi, B., van de Werve, G. 1995. Glucose transport and glucose 6-phosphate hydrolysis in intact rat liver microsomes. *J. Biol. Chem.* **270:**21092-21097

36. St-Denis, J.-F., Comte, B., Nguyen, D.K., Seidman, E., Paradis, K., Lévy, E., van de Werve, G. 1994. A conformational model for the human liver microsomal glucose-6-phosphatase system: evidence from rapid kinetics and defects in glycogen storage disease type 1. *J. Clin. Endocrinol. Metab.* **79:**955-959

37. Van der Goot, F., Ripoche, P., Corman, B. 1989. Determination of solute

reflection coefficients in kidney brush-border membrane vesicles by light-scattering: influence of the refractive index. *Biochim. Biophys. Acta* **979:**272-274

38. Van de Werve, G., Lange, A., Newgard, C., Méchin, M.-C., Li, Y.Z., Berteloot, A. 2000. New lessons in the regulation of glucose metabolism taught by the glucose 6-phosphatase system. Eur. J. Biochem., **267:**1533-1549

39. Verkman, A.S., Ives, H.E. 1986. Water permeability and fluidity of renal basolateral membranes. *Am. J. Physiol.* **250:**F633-F643

40. Waddell, I.D., Scott, H., Grant, A., Burchell, A. 1991. Identification and characterization of a hepatic microsomal glucose transport protein. T_3 of the glucose 6-phosphatase system? *Biochem. J.* **275:**363-367

41. Waddell, I.D., Zomerschoe, A.G., Voice, M.W., Burchell, A. 1992. Cloning and expression of a hepatic microsomal glucose transport protein. *Biochem. J.* **286:**173-177

42. Wright, E.M. 1993. The intestinal Na^+/glucose ion-coupled cotransporter. *Annu. Rev. Physiol.* **55:**575-589 Berteloot, A. and Semenza, G. (1990) Methods Enzymol. 192, 409-437

Table 1. Effect of potential inhibitors on glucose and phosphate equilibration across the microsomal membrane

	$T_{1/2}$ values of substrate equilibration (s)	
Experimental conditions	Glucose	Phosphate
Tracer alone	33 ± 3 (Fig. 1A)	21 ± 1 (Fig. 2A)
	46 ± 3 (Fig. 1B)	24 ± 2 (Fig. 2B)
$HgCl_2$ (10 μM)	42 ± 4	22 ± 2
Vanadate (200 μM)	32 ± 4	19 ± 1
Phlorizin (5 mM)	39 ± 6	26 ± 1
Chlorogenic acid (5 mM)	45 ± 7	24 ± 1
HNB (5 mM)	45 ± 2	20 ± 1
Mean values ± SEM	40 ± 6	23 ± 3

Experimental conditions and analyses were as described in the legends to Fig. 1A and 2A for glucose and phosphate transport, respectively. $T_{1/2}$ values ± SER are shown under control and test conditions.

Table 2. Kinetic parameters of radiotracer accumulation and efflux from [^{32}P]- or [^{14}C]G6P in rat liver microsomes

Experimental conditions	Kinetic parameters		
	$T_{1/2}$ (s)	U_∞ (pmol.mg^{-1} protein)	U_0 (pmol.mg^{-1} protein)
[^{32}P] uptake	21 ± 1	333 ± 10	120 ± 3
[^{32}P] efflux	21 ± 1	128 ± 19	335 ± 9
[^{14}C] uptake	47 ± 5	701 ± 24	63 ± 10
$T^{G}_{1/2} / T^{P}_{1/2}$	2.24 ± 0.35	-	-
$[(G_i)/(P_i)]_{equilibrium}$	-	2.11 ± 0.14	-

Experimental conditions and analyses were as described in the legend to Fig. 3. The kinetic parameters U_∞ and U_0 correspond to those appearing in Eqs. (1) and (2) for influx and efflux conditions, respectively, whereas the $T_{1/2}$ values have been calculated using Eq. (3) in the text. Numerical values ± SER are shown. The kinetic parameters $T^{G}_{1/2}$ and $T^{P}_{1/2}$, as well as the $[(G_i)/(P_i)]_{equilibrium}$ ratio correspond to those appearing in Eq. (11) in the text.

LEGENDS TO FIGURES

Fig. 1. Kinetics of [U-^{14}C]D-glucose uptake into rat liver microsomes. Rat liver microsomes were resuspended in 50 mM Hepes-Tris buffer (pH 7.3) containing 250 mM sucrose. Uptakes were measured at room temperature using a FSRFA as described in "Materials and Methods". The uptake medium contained (final concentrations in 1 ml): (A) 50 mM Hepes-Tris buffer (pH 7.3), 10 μM [U-^{14}C]D-glucose, 250 (●, □) mM sucrose or 150 mM sucrose plus 100 mM unlabeled D-glucose (○), and either 0.25 mM phloretin (□) or other potential inhibitors as indicated in Table 1; (B) 50 mM Hepes-Tris buffer (pH 7.3), 10 μM [U-^{14}C]D-glucose, and 250 mM sucrose. The stop solution in (A) and (B) was 50 mM Hepes-Tris buffer (pH 7.3) containing 250 mM sucrose but also included 0.25 mM phloretin (◊) in (B). Each data point represents the mean ± SEM of 3 to 5 determinations using the same microsomal preparation. Missing error bars were smaller than the symbol size. Lines shown are the best-fit curves corresponding to Eq. (1) in the text whereas the $T_{1/2}$ of glucose equilibration are reported in Table 1.

Fig. 2. Kinetics of [^{32}P]KH_2PO_4 uptake into rat liver microsomes. Rat liver microsomes were resuspended in 50 mM Hepes-Tris buffer (pH 7.3) containing 250 mM sucrose. (A) Uptakes were measured at room temperature, in the absence (●) or presence (▲) of 0.8% CHAPSO in the uptake medium, using a FSRFA as described in "Materials and Methods". The uptake medium contained (final concentrations in 1 ml): 50 mM Hepes-Tris buffer (pH 7.3), 250 mM sucrose, 2 mM EGTA, and 10 μM [^{32}P]KH_2PO_4. The stop solution was 50 mM Hepes-Tris buffer (pH 7.3) containing 250 mM sucrose. Each data point represents the mean ± SEM of 4 determinations using the same microsomal preparation. Missing error bars were smaller than the symbol size. The line shown for control is the best-fit curve corresponding to Eq. (1) in the text whereas the $T_{1/2}$ of phosphate equilibration is reported in Table 1. The line shown for CHAPSO indicates the mean of all data points. (B) Experimental conditions were as described in (A) except that the uptake media also contained unlabeled phosphate to reach the indicated concentrations. The corresponding uptake time courses were fit to Eq. (1) in the text. The data shown are the $T_{1/2}$ values of phosphate equilibration calculated according to Eq. (3) in the text. Each data point represents the mean ± SEM of 3 determinations using the same microsomal preparation. The line shown indicates the mean of all data points, which is also reported in Table 1.

Fig. 3. Kinetics of radiotracer accumulation and efflux from [^{32}P]G6P and [U-^{14}C]G6P in rat liver microsomes. Rat liver microsomes were resuspended in 50 mM Hepes-Tris buffer (pH 7.3) containing 250 mM sucrose. Uptakes were measured at room temperature using a FSRFA as described in "Materials and Methods". The stop solution was 50 mM Hepes-Tris buffer (pH 7.3) containing 250 mM sucrose. (A) The uptake medium contained (final concentrations in 1 ml): 50 mM Hepes-Tris buffer (pH 7.3), 250 mM

sucrose, and 0.2 mM of [^{32}P]G6P. The line shown for control influx (▲) is the best-fit curve corresponding to Eq. (1) in the text. Alternatively: microsomes were first preincubated for 5 min in the presence of 0.5 mM vanadate (●), in which case the solid and extrapolated dotted lines indicate the mean of all data points, or uptake was run for 3 min before the addition of 0.5 mM vanadate as indicated by the arrow, in which case the line shown for the efflux data (◊) is the best-fit curve corresponding to Eq. (2) in the text. (B) Experimental conditions were as described in (A) (▲) or 0.2 mM [U-^{14}C]G6P was substituted for [^{32}P]G6P (□). The ^{32}P and ^{14}C data shown have been corrected for their respective dead-spaces reported in Table 2 to clearly demonstrate that identical initial rates of uptake are observed for the two radiotracers. The lines shown are the best-fit curves corresponding to Eq. (1) in the text. In both (A) and (B), each data point represents the mean ± SEM of 3 to 5 determinations using the same microsomal preparation. Missing error bars were smaller than the symbol size whereas the kinetic parameters of influx and efflux are reported in Table 2.

Fig. 4. Simplified substrate transport model. In this model, the complete system involves a fairly nonspecific catalytic unit (G6Pase) with its active site located on the luminal side of the microsomes, and at least three transmembrane spanning translocases to ensure transport of the substrate (T1, G6P translocase) and products (T2 and T3, phosphate and glucose translocases, respectively) of the hydrolase reaction. At low G6P concentrations relative to the apparent Km's for transport and hydrolysis, all transport processes behave as passive diffusion and appear symmetrical with regard to their rates of influx and efflux, whereas the phosphohydrolase activity can be assimilated to represent a first-order, irreversible reaction (see justifications in the text and further considerations in [13]). Accordingly, the first-order rate constants k_t, k_h, ke,G, and ke,P can be used to describe, respectively, G6P transport and hydrolysis as well as glucose and phosphate efflux. G6P, G, and P represent glucose 6-phosphate, glucose, and phosphate, while indices o and i refer to the incubation medium and the intramicrosomal space, respectively.

Fig. 5. Revised version of the combined conformational flexibility-substrate transport model. As done previously [12], microsomal G6Pase is depicted as a transmembrane protein with the catalytic site lying in a hydrophilic pocket deep inside of the protein where glucose 6-phosphate (G6P) hydrolysis occurs at rate V_h. The access to and exit from the hydrophilic pocket are controlled by outer and inner channels with different intrinsic permeabilities to G6P (k_{D1}), glucose, and phosphate (k_{D2} and k_{D3}). Glucose (G) and phosphate (P) exchanges between the extra- and intravesicular spaces are also made possible through a pore-like structure that would account for most (if not all) of the glucose (first-order rate constant ke,G) and phosphate (first-order rate constant ke,P) transport functions usually attributed to the putative T3 and T2 translocases in intact microsomes (see justifications in the text). Indices o, m, and i refer to the incubation medium, the hydrophilic pocket, and the intramicrosomal space, respectively.

Figure 1

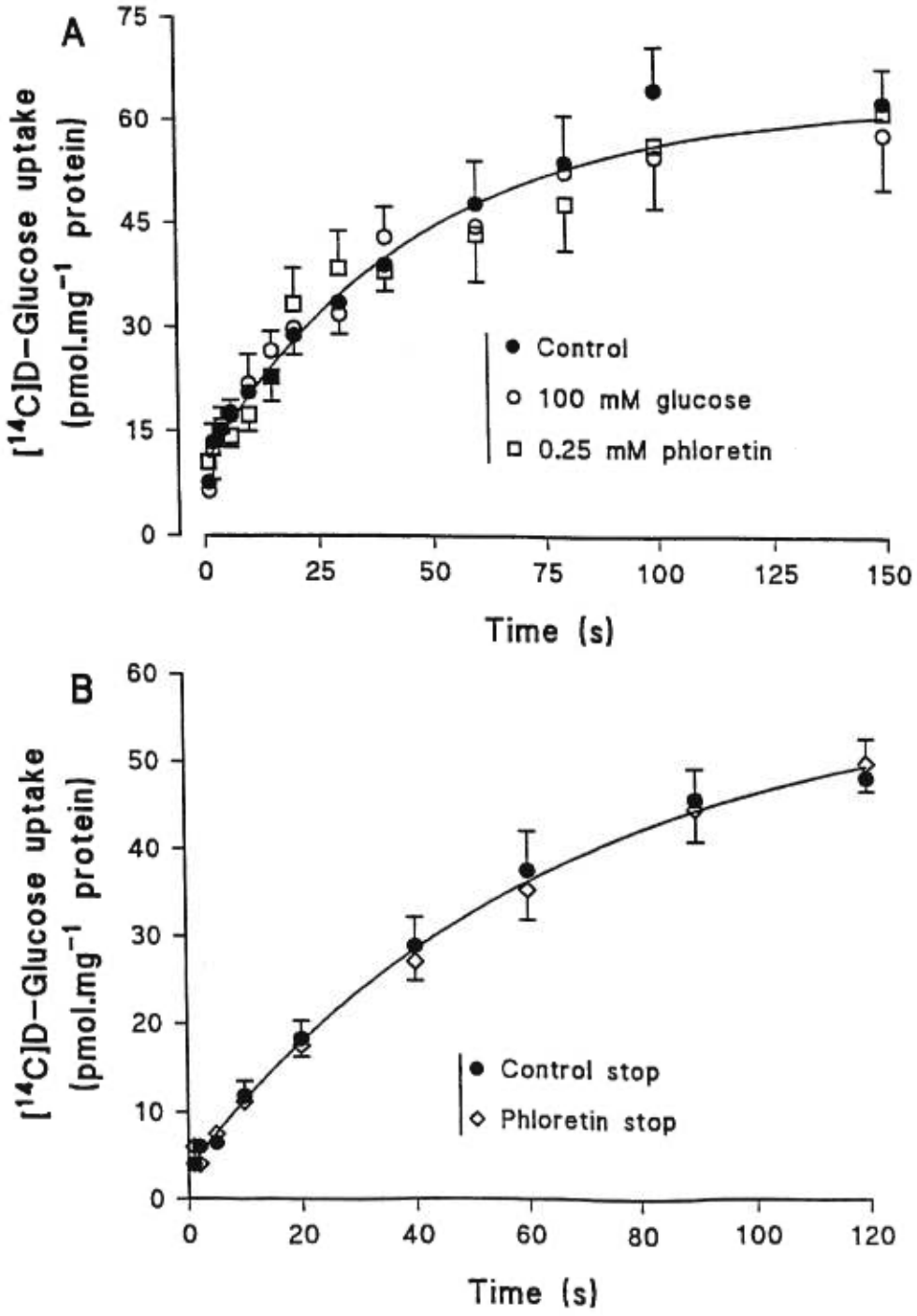
A
[14C]D-Glucose uptake
(pmol.mg-1 protein)
75
60
45
30
15
0
0
25
50
75
100
125
150
Time (s)
Control
100 mM glucose
0.25 mM phloretin
B
[14C]D-Glucose uptake
(pmol.mg-1 protein)
60
50
40
30
20
10
0
0
20
40
60
80
100
120
Time (s)
Control stop
Phloretin stop

Figure 2

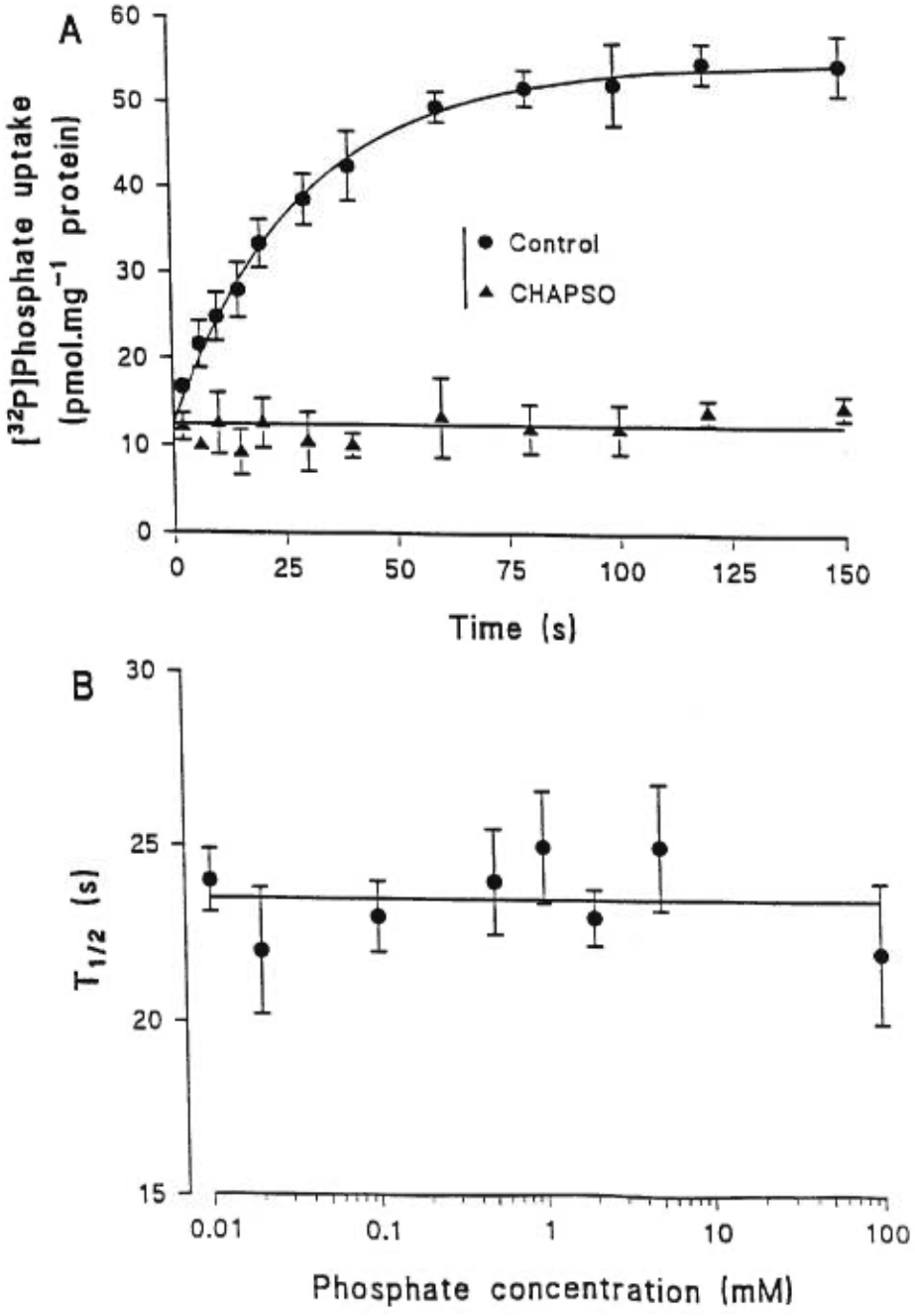
A
[32P]Phosphate uptake
(pmol.mg-1 protein)
60
50
40
30
20
10
0
Control
CHAPSO
0
25
50
75
100
125
150
Time (s)
B
T1/2 (s)
30
25
20
15
0.01
0.1
1
10
100
Phosphate concentration (mM)

Figure 3

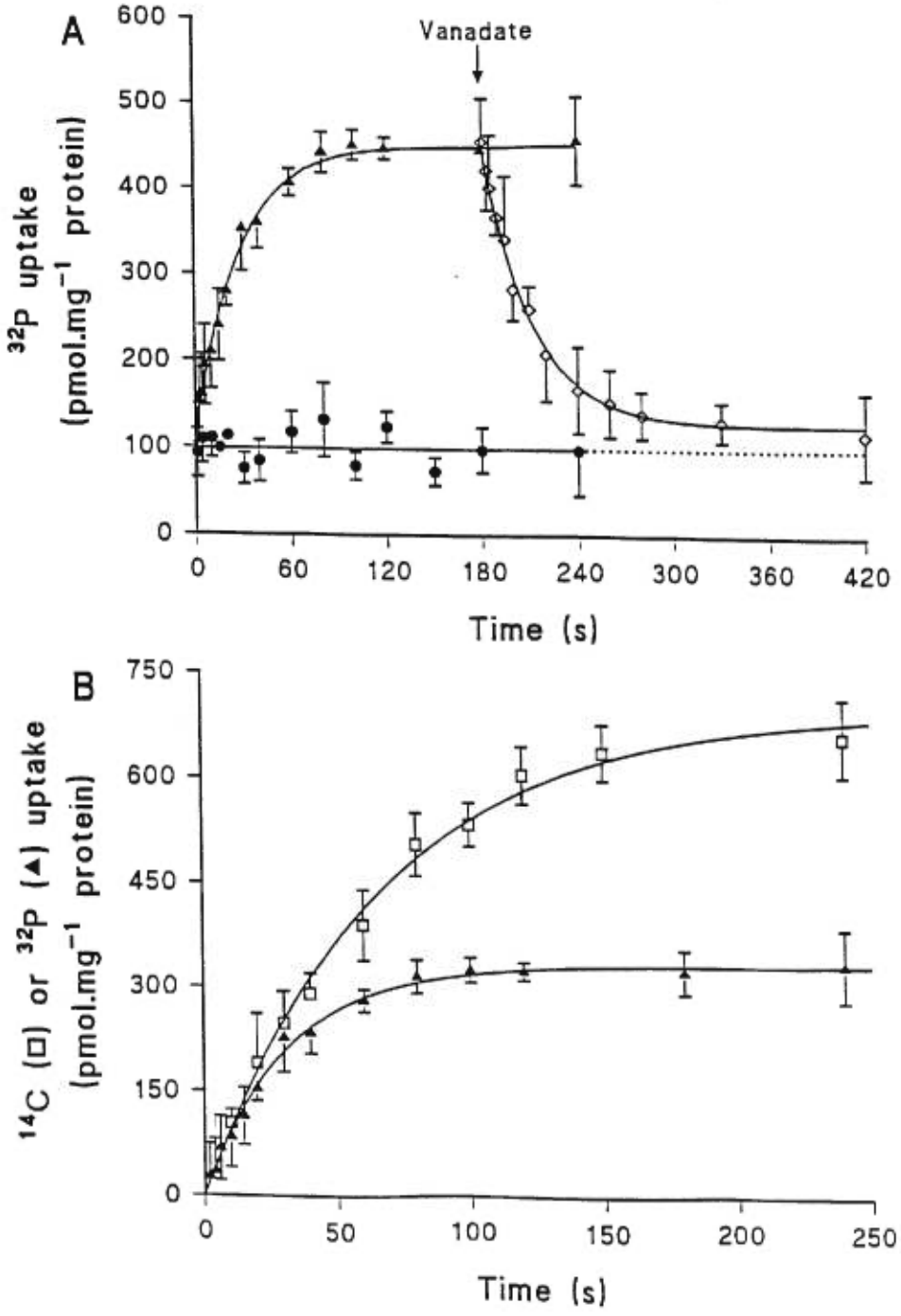
A
Vanadate
^{32}P uptake
(pmol.mg^{-1} protein)
600
500
400
300
200
100
0
0
60
120
180
240
300
360
420
Time (s)
B
^{14}C (□) or ^{32}P (▲) uptake
(pmol.mg^{-1} protein)
750
600
450
300
150
0
0
50
100
150
200
250
Time (s)

Figure 4

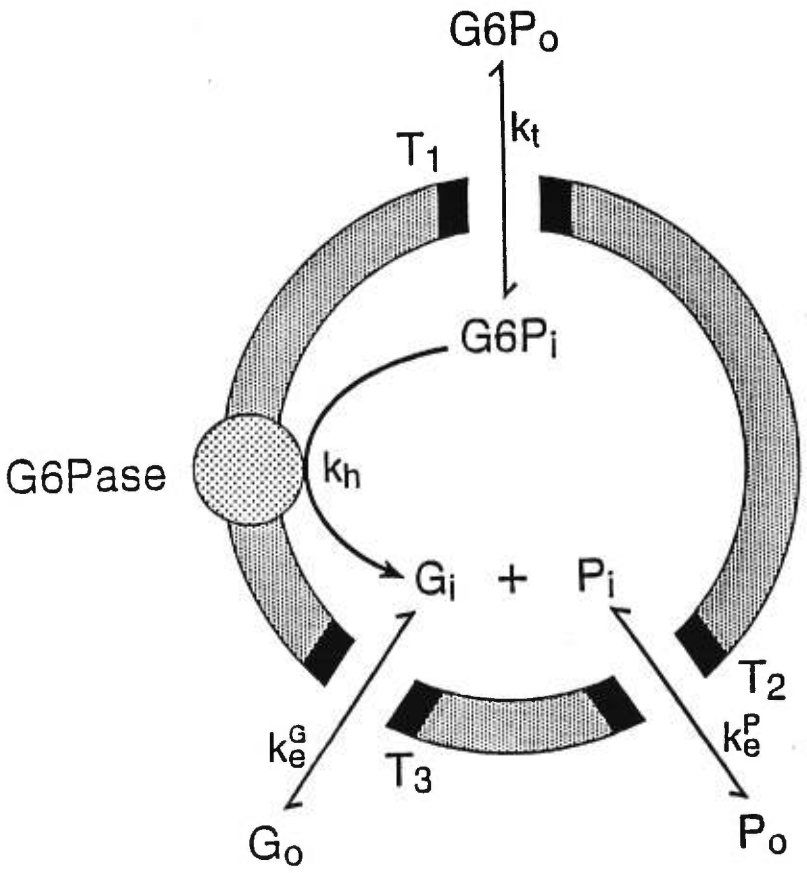

Figure 5

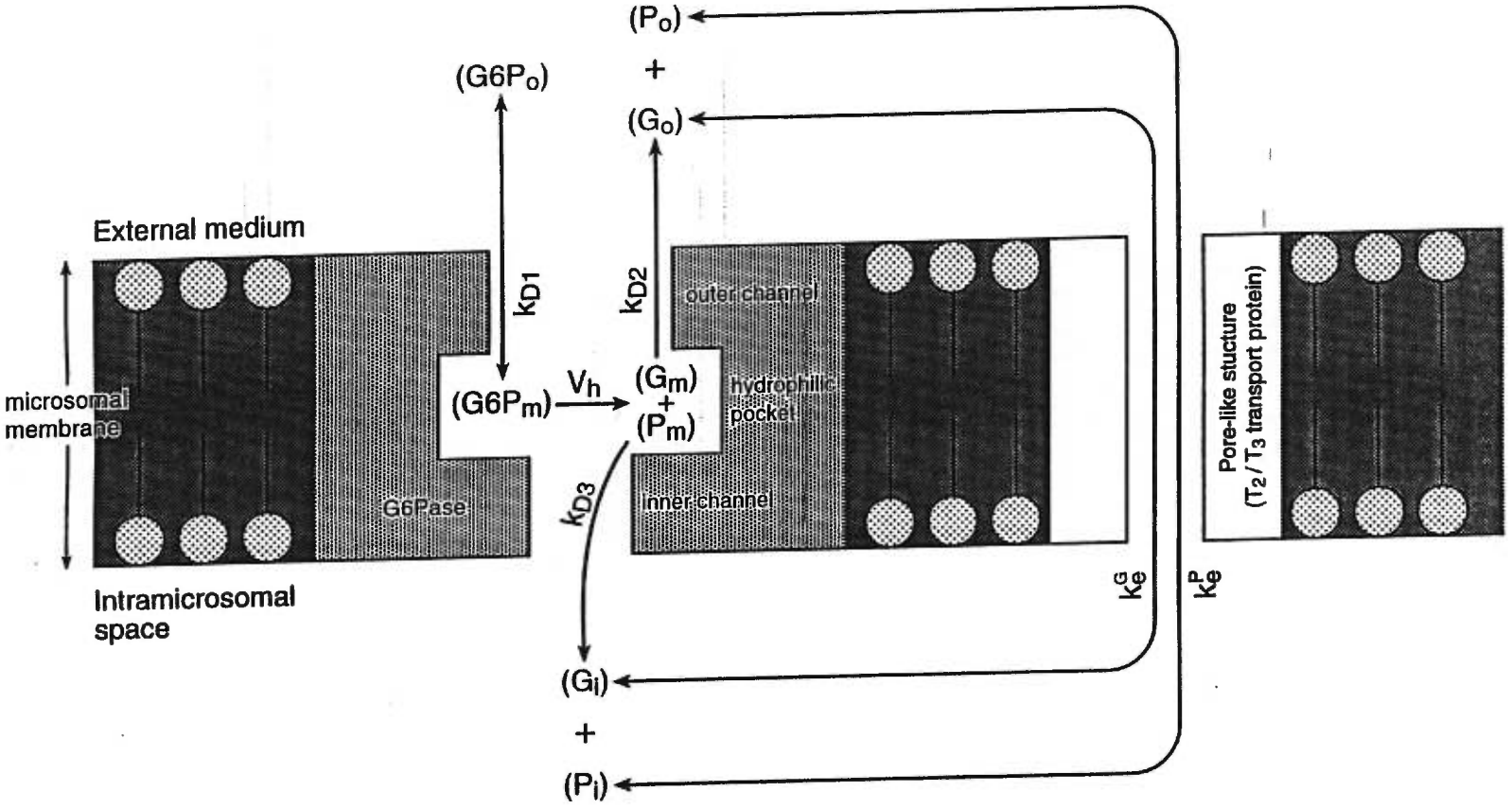
External medium
microsomal membrane
Intramicrosomal space
G6Pase
(G6Po)
(G6Pm)
kD1
Vh
(Po)
+
(Go)
kD2
outer channel
hydrophilic pocket
(Gm)
+
(Pm)
inner channel
kD3
(Gi)
+
(Pi)
kGe
kPe
Pore-like stucture
(T2 / T3 transport protein)

IV.5 Article 5

Further transport kinetic studies on rat liver microsomal glucose-6-phosphatase system

Wensheng XIE [a,c], Alfred BERTELOOT [b] and Gérald VAN DE WERVE [a,c,*]

Laboratoire d'Endocrinologie Métabolique, Departments of Nutrition and Biochemsitry [a] and Physiology [b], Centre de Recherche du CHUM [c] and Group de Recherche en Transport Membrane, faculty of Medicine, University of Montreal, Montreal, QC, H3C 3J7, Canada

* Corresponding author. Tel: +1 (514) 2816000 ext. 7237; Fax: +1 (514) 8964701

E-mail: [redacted]

Key Words: kinetic properties, glucose-6-phosphate transport, glucose-6-phosphatase, rat liver microsomes

Running title: G6P transport in liver microsomes

Abbreviations used: G6P, glucose-6-phosphate; G6Pase, glucose-6-phosphatase; P_i, inorganic phosphate, GSD, glycogen storage disease; p36, the catalytic subunit of G6Pase; p46, the putative G6P transporter; CHL, chlorogenic acid.

Abstract

Previous studies of our laboratory (J Biol Chem, 1995, 270, 21092-21097) showed that radioactivity accumulation into liver microsomes from [U-^{14}C]glucose-6-phosphate (G6P) was tightly associated with the hydrolytic activity of microsomal glucose-6-phosphatase (G6Pase) and a combined-conformational flexibility model was proposed to explain G6Pase system. In the present study, radioactivity accumulation into liver microsomes from [^{32}P]G6P was studied at different concentration of unlabelled G6P. Results showed the steady-state level of radioactivity accumulation from [^{32}P]G6P was dependent on the concentration of unlabelled G6P, but with identical $T_{1/2}$ values around 23s. This process was suppressed in the presence of inhibitors of G6Pase. Radioactivity efflux from microsomes preincubated with [^{32}P]G6P was observed with the addition of unlabelled G6P or KH_2PO_4. Kinetic parameters of efflux were identical to those of radioactivity accumulation from [^{32}P]G6P. Data also showed no exchanging transport between G6P and glucose/phosphate, excluding the possibility that G6P and glucose/phosphate may be anti-transported via a common transporter. Taken together, these results demonstrated that G6P transport and hydrolysis were tightly coupled processes, and the G6P transporter, if any, did not transport glucose or phosphate. It was also indicated that functions of two components of G6Pase were required for the uptake process.

Introduction

Liver glucose-6-phosphatase (G6Pase) plays a crucial role in glucose metabolism by hydrolyzing glucose-6-phosphate (G6P) into glucose and inorganic phosphate (P_i) [1]. G6Pase is located in endoplasmic reticulum and highly expressed in liver and kidney. Until now, two components of G6Pase have been cloned, the catalytic subunit p36 [2] and the putative G6P translocase p46 [3]. It has been proposed that the dysfunction of p36 causes the glycogen storage disease Ia (GSD Ia), while that of p46 causes GSD Ib, and dysfunctions of the transport of products, phosphate and glucose, cause GSD Ic and Id, respectively [1]. Even though G6Pase system has been studied for several decades and great progress has been made to understand this enzyme [4], its functional mechanism is still in debate. The relation between p36 and p46, the transport characters of the substrate and products are uncertain. Our laboratory previously studied the kinetics of [U-^{14}C]G6P accumulation into rat liver microsomes and demonstrated that the radioactivity accumulation from [U-^{14}C]G6P was tightly coupled with the hydrolytic activity of G6Pase [5]. A combined-conformational flexibility model was proposed to explain G6Pase system [5,6], namely, p36 forms a channel-like structure through which G6P could access to the active site and the products go to the cytosol. Despite of these studies, the kinetic properties of [^{32}P]G6P accumulation is still open, hence no data are available for the description of phosphate properties in this model. In regard to the phosphate transport, it has been reported that mutations in p46 gene were found both in GSD Ib and GSD Ic patients [7, 8], initiating the possibility that p46 might be responsible for

the transport of G6, phosphate and glucose simultaneously. In contrast, another study showed no mutation in p46 gene in one GSD Ic patient and suggested a distinct locus of phosphate transporter [9].

In the present study, the radioactivity accumulation into liver microsomes from [^{32}P]G6P was studied at different concentration of unlabelled G6P with or without inhibitors of G6Pase. The possibility of exchanging transport between G6P and glucose/phosphate was also investigated. Data showed the radioactivity accumulation from labelled G6P was linked to the hydrolytic activity of G6Pase, and no exchanging transport occurred between G6P and the hydrolytic products. These data further support the combined-conformational flexibility model and provide more information to understand G6Pase system.

Materials and Methods

Materials

[U-^{14}C]G6P (317 mCi/mmol) was from ICN Biomedicals (Montreal, QC). [^{32}P]G6P (144 mCi/mmol) was prepared as described in [9]. KH_2PO_4, glucose, G6P, mannose-6-phosphate, phlorizin, chlorogenic acid and sodium orthovanadate were from Sigma (St-Louis, MO).

Liver microsomal preparation

Liver microsomes were prepared from overnight fasted male Sprague-Dawley rats (around 300g body weight) as described previously [10], except the buffer was 50

mM Hepes-Tris, 250 mM Sucrose, pH 7.3. The intactness of microsomes was indicated by microsomal mannose-6-phosphatase activity and large than 90% intactness was obtained.

G6Pase hydrolytic activity

G6Pase activity was determined at room temperature as described previously [5].

Radioactivity uptake and efflux from [^{32}P]G6P

Radioactivity uptake and efflux from [^{32}P]G6P was determined using a fast-sampling, rapid-filtration apparatus (FSRFA) [11] at room temperature as described before [5]. For the uptake experiments, 10 μM [^{32}P]G6P was constantly kept in the incubation medium (50 mM Hepes-Tris, 250 mM sucrose, pH 7.3) with different concentration of unlabelled G6P, in the presence or absence of G6Pase inhibitors. 40 μl microsomes (20 mg protein/ml) were injected into the chamber to initiate the uptake. The mixture was sampled at each time point to the filter and washed with 1 ml ice-cold buffer (the same content as above). The radioactivity was determined by liquid scintillation counting. For efflux experiments, 10 μM [^{32}P]G6P was incubated with microsomes for 3 min in the incubation chamber, then efflux was initiated by the injection of unlabelled G6P or KH_2PO_4. Other steps were performed similarly as above.

Exchanging transport measurements

The exchanging transport between G6P and glucose/phosphate was measured using FSRFA. Microsomes were preincubated with 50 mM glucose or KH_2PO_4 for 3 min at room temperature, then injected into the chamber containing 10 μM [U-

^{14}C]G6P or [^{32}P]G6P to initiate the reaction. The mixture was sampled and handled as described above.

In order to suppress the hydrolytic activity of G6Pase, microsomes were treated with 200 μM vanadate for 3 min at room temperature, then preloaded with 50 mM glucose or phosphate. After that, similar steps were performed as above.

Data analysis

Four to five rounds were performed for each condition. Uptake data were analyzed by the Enzfitter software according to the first-order rate equation:

$$U = U_0 + U_\infty (1 - e^{-kt}) \qquad (1)$$

in which U, U_0 and U_∞ stand for the intravesicular amounts of substrate at time t, 0 and equilibrium, respectively, whereas k is the first-order rate constant of the uptake process.

Efflux data were analyzed according to the first order-rate equation:

$$U = U_0 e^{-kt} + U_\infty \qquad (2)$$

in which U, U_0 and U_∞ have the same definitions as above while k is the first-order rate constant of the efflux process.

The kinetics of uptake and transport were characterized by the $T_{1/2}$ value, which represents the time at which 50% of the process has been completed. $T_{1/2}$ was calculated according to the following equation

$$T_{1/2} = Ln2 / k \qquad (3)$$

where k is from equation (1) or (2).

Results and Discussion

1. Radioactivity accumulation from [^{32}P]G6P

As shown in Fig.1, the steady-state level of radioactivity accumulation from [^{32}P]G6P was dependent on the concentration of unlabelled G6P, while the $T_{1/2}$ value at each concentration was all around 23s (Table 1). This result implied that the radioactivity accumulation was dependent on the hydrolysis of G6P rather than on the G6P transport process because in the later case, $T_{1/2}$ value should increase parallelly to unlabelled G6P concentration. This result also indicated that the accumulated radioactivity was mainly the product, P_i, rather than G6P. The lower steady-state level at high concentration of unlabelled G6P was due to the decrease of the specific activity of [^{32}P]G6P, which resulted in less labelled P_i via G6Pase hydrolytic activity.

Effects of inhibitors of G6Pase on the uptake more convincingly demonstrated that there was no radioactivity accumulation in the absence of G6Pase hydrolytic activity. Vanadate is an inhibitor of G6Pase via competitive binding to the catalytic subunit p36 [12]. In the presence of 200 μM vanadate, the radioactivity accumulation was almost fully suppressed as shown in Fig.2. The small amount of accumulation in the presence of vanadate could be accounted for by the remained G6Pase activity since there was still 6% hydrolytic activity in the presence of 200 μM vanadate (0.3 vs 5 nmol/min/mg protein at 0.2 mM G6P), or by the non-specific phosphatase activity. This result is in agreement with the report that no G6P uptake was observed in liver microsomes from p36 knockout mice [13]. It demonstrated that the function of p36

was required for the uptake of radioactivity from labelled G6P. Chlorogenic acid (CHL) has been reported to be a G6Pase inhibitor by its specific binding to p46 [14]. In the presence of 5 mM CHL, the radioactivity uptake was completely suppressed. The fact that dysfunction of p46 impaired G6P uptake suggested both p36 and p46 be required for the full activity of G6Pase. This result is consistent to the observation in showing that only coexpression of p36 and p46 together in COS-1 cells resulted in [^{14}C]G6P uptake in physiological range[15]. Phloridzin, another inhibitor of G6Pase, similarly suppressed the uptake as shown in Fig.2.

2. Radioactivity efflux from microsomes preincubated with [^{32}P]G6P

In the experiments illustrated in Fig.3, microsomes were incubated with 10 μM [^{32}P]G6P for 3 min to reach a steady-state of intramicrosomal [^{32}P]. The subsequent addition of unlabelled G6P (1-10 mM) caused a decrease in radioactivity within vesicles. The efflux was dose-dependent and similar steady-state levels and $T_{1/2}$ values were observed under symmetrical conditions of G6P concentrations during uptake and efflux (Fig.3 and Table 1). The observation of efflux demonstrated that the same molecules, either G6P or phosphate, existed in *cis*- and *trans*-sides of microsomes. KH_2PO_4 also caused [^{32}P] efflux with similar kinetic parameters (Fig.3 and Table 1). This fact strongly suggested that the accumulated radioactivity was mainly the product, inorganic phosphate, rather than G6P.

3. Exchanging transport

If one transport protein can transport G6P and phosphate via an anti-transport mechanism, efflux or exchanging transport between G6P and phosphate could be also observed and one of them would accelerate the transport of the other. This is obviously not the case as demonstrated by the exchanging transport experiment. As shown in Fig.4, one can see the uptake was even lower in the microsomes preloaded with glucose or phosphate. This result was not compatible with exchanging transport which should be accelerated. The lower steady-state level in the presence of glucose or phosphate was due to their inhibition on G6Pase hydrolytic activity. In order to avoid the interference of the hydrolytic process, microsomes were treated with vanadate before preloading of 50 mM glucose or phosphate. Under these conditions, no exchanging transport was observed, either (Fig.4, solid symbols). Fig.5 showed the radioactivity uptake from [^{32}P]G6P was also lower when microsomes were preloaded with 50mM phosphate. This result is of importance in that it not only excluded the exchanging transport between G6P and phosphate, but also showed no accelerated phosphate transport. The later fact further supported our other kinetic studies showing that there was no specific phosphate transport protein in the ER membrane (Data not shown). The conclusion drawn from the kinetic studies is also consistent to gene mutation studies which showed that mutations were all found in p46 gene in GSD Ib, Ic and Id patients [7, 8]. Based on those mutation results, it was recently proposed that there appeared to be only two types of GSD, GSD Ia and GSD Ib, which was caused by the mutations of p36 and p46 gene, respectively [16]. This

propose is obviously consistent to our observation that no specific phosphate transport protein existed in the ER membrane.

When comparing the radioactivity accumulation from [^{32}P]G6P and [U-^{14}C]G6P (Fig.1 and Fig.4, control condition), one can see that they displayed distinct kinetic parameters, i.e., $T_{1/2}$ values were 21 and 45 s, the steady-state levels were 50 and 90 pmol/mg protein, respectively. These differences further suggested that tracer accumulation inside microsomes was mainly the products, rather than labelled G6P. If it was the later case, the steady-state levels and $T_{1/2}$ values should be the same, irrespective of the nature of the tracer, [U-^{14}C]G6P or [^{32}P]G6P.

Taken together, results from uptake, efflux and exchanging transport all consistently demonstrated that the accumulated radioactivity inside microsomes from labelled G6P was mainly the product, rather than G6P. These data indicated that G6P uptake/hydrolysis were tightly coupled processes. It was also demonstrated that without the function of p36, p46 alone could not transport G6P. Furthermore, the G6P transporter in ER membrane, if any, did not transport phosphate or glucose.

Acknowledge: This work was supported by Grants ME-10783 and MT-10804 from the Medical Research Council of Canada (to G.v.d.W.).

References:

1. Foster JDF, Pederson BA, Nordlie RC, 1997, Glucose-6-phosphatase structure, regulation, and function: an update. Proc Soc Exp Biol Med, 215: 314-332
2. Lei KJ, Shelly LL, Pan CJ, Sidbury JB, Chou JY, 1993, Mutations in the glucose-6-phosphatase gene that cause glycogen storage disease type 1a. Science, 262: 580-583
3. Gerin I, Veiga-da-Cunha M, Achouri Y, Collet JF, van Schaftingen E, 1997, Sequence of a putative glucose-6-phosphate translocase, mutated in glycogen storage disease type Ib. FEBS Lett, 419: 235-238
4. Van de Werve G, Lange A, Newgard C, Méchin M-C, Li Y, Berteloot A, 2000, New lessons in the regulation of glucose metabolism taught by the glucose 6-phosphatase system. Eur J Biochem, 267: 1533-1549
5. St-Denis, J-F., Berteloot A., Vidal, H., Annabi, B., van de Werve, G., 1995, Glucose transport and glucose-6-phosphate hydrolysis in intact rat liver microsomes. J. Biol. Chem. 270: 21092-21097
6. Berteloot A, St-Denis J-F, van de Werve G, 1995, Evidence for a membrane exchangeable glucose pool in the functioning of rat liver glucose-6-phosphatase. J Biol Chem, 270: 21098-21102
7. Galli L, Orrico A, Marcolongo P, Fulceri R, Burchell A, Melis D, Parini R. Gatti R, Lam C-W, Benedetti A, Sorrentino V, 1999, Mutations in the glucose-6-phosphate transporter (G6PT) gene in patients with glycogen storage disease type 1b and 1c. FEBS Lett, 459: 255-258

8. Veiga-da-Cunha M, Gerin I, Chen YT, Lee PJ, Leonard JV, Maire I, Wendel U, Vikkula M, van Schaftingen E, 1999, The putative glucose 6-phosphate translocase gene is mutated in essentially all cases of glycogen storage disease type I non-a, Eur J Hum Genet, 7: 717-723
9. Lin B, Hiraiwa H, Pan CJ, Nordlie RC, Chou JY, 1999, Type-1c glycogen storage disease is not caused by mutations in the glucose-6-phosphate transporter gene, Hum Genet, 105: 515-517
10. Berteloot A, Vidal H, van de Werve G, 1991, Rapid kinetics of liver microsomal glucose 6-phosphatase. J Biol Chem, 266: 5497-5507
11. Berteloot A, Malo C, Breton S, Brunette M, 1991, A fast sampling, rapid filtration apparatus: principal characteristics and validation from studies of D-glucose transport in human jejunal brush-border membrane vesicles. J Membrane Biol, 122: 111-125
12. Singh J, Nordlie RC, Jorgenson RA, 1981, Vanadate: a potent inhibitor of multifunctional glucose-6-phosphatase. Biochim Biophys Acta, 678: 477-82
13. Lei KJ, Chen H, Pan CJ, Ward JM, Mosinger B, Lee EJ, Westphal H, Mansfield BC, Chou JY, 1996, Glucose-6-phosphatase dependent substrate transport in the glycogen storage disease type-1a mouse, Nat Genet, 13: 203-209
14. Arion WJ, Canfield WK, Ramos FC, Schindler PW, Burger HJ, Hemmerle H, Schubert G, Below P, Herling AW, 1997, Chlorogenic acid and hydroxynitrobenzaldehyde: new inhibitors of hepatic glucose 6-phosphatase. Arch Biochem Biophys, 339: 315-22

15. Hiraiwa H, Pan C-J, Lin B, Moses SW, Chou JY, 1999, Inactivation of the glucose 6-phosphate transporter causes glycogen storage disease type 1b. J Biol Chem, 274: 5532-5536

16. Veiga-da-Cunha M, Gerin I, van Schaftingen E, 2000, How many forms of glycogen storage disease type I?, Eur J Pediatr, 159: 314-318

Figure legends

Fig.1. Time course of tracer [^{32}P] uptake into microsomes at different concentrations of unlabelled G6P. Experiments were performed as described in the Methods section with constant 10 μM of [^{32}P]G6P in the incubation medium containing unlabelled G6P. Control condition stands only 10 μM of [^{32}P]G6P. For the background, microsomes were treated with 0.8% chapso for 5 minutes at 4°C and uptake was measured with 10 μM of [^{32}P]G6P. Results shown are mean values ± S.E. of 5 repeats at each condition.

Fig.2. Effect of inhibitors of G6Pase on [^{32}P] uptake into microsomes. Experiments were performed in the presence of 10 μM of [^{32}P]G6P with (•, ■, ▲) or without (o) inhibitors. Results shown are mean values of 5 repeats at each condition.

Fig.3. Time-course of [^{32}P] efflux from microsomes preincubated with [^{32}P]G6P. Microsomes were preincubated with 10 μM [^{32}P]G6P for 3 min at room temperature. Efflux was initiated by the addition of buffer (○) or unlabelled G6P (● 1 mM, ■ 5 mM, ▼10 mM) or 20 mM KH_2PO_4 (▲). Data shown are 4-5 repeats at each condition.

Fig.4. Effect of preloading microsomes with phosphate or glucose on [^{14}C] uptake. Microsomes were preincubated with buffer (○, ●), 50 mM glucose (Δ, ▲) or 50 mM phosphate (□, ■) for 3 min at room temperature before injected into the chamber containing 10 μM [U-^{14}C]G6P. For the solid symbols (●, ▲, ■), microsomes were treated with 200 μM vanadate for 3 min before the preincubation. Data shown are 4-5 repeats at each condition.

Fig.5. Effect of preloading microsomes with phosphate on [^{32}P] uptake. Microsomes were preincubated with buffer (○) or 50 mM KH_2PO_4 (●) for 3 min at room temperature before injected into the chamber containing 10 μM [^{32}P]G6P. Results are mean values of 5 rounds at each condition.

Table 1 $T_{½}$ values of [^{32}P]G6P uptake and efflux at different concentrations of unlabelled G6P or KH_2PO_4

Conditions	$T_{½}$ (s)	
	Uptake	efflux
Control (10 μM [^{32}P]G6P)	21 ± 1.12	
+ 0.2 mM G6P	21 ± 1.20	
+ 1 mM G6P	26 ± 1.22	30 ± 8.95
+ 5 mM G6P	20 ± 2.66	25 ± 3.51
+ 10 mM G6P	18 ± 3.27	22 ± 9.93
+ 20 mM KH_2PO_4		23 ± 4.14

Experiments were performed at room temperature. Results are mean values ± SE for at least 5 rounds of experiments, $p \geq 0.1$ for all conditions compared with control values.

Figure 1

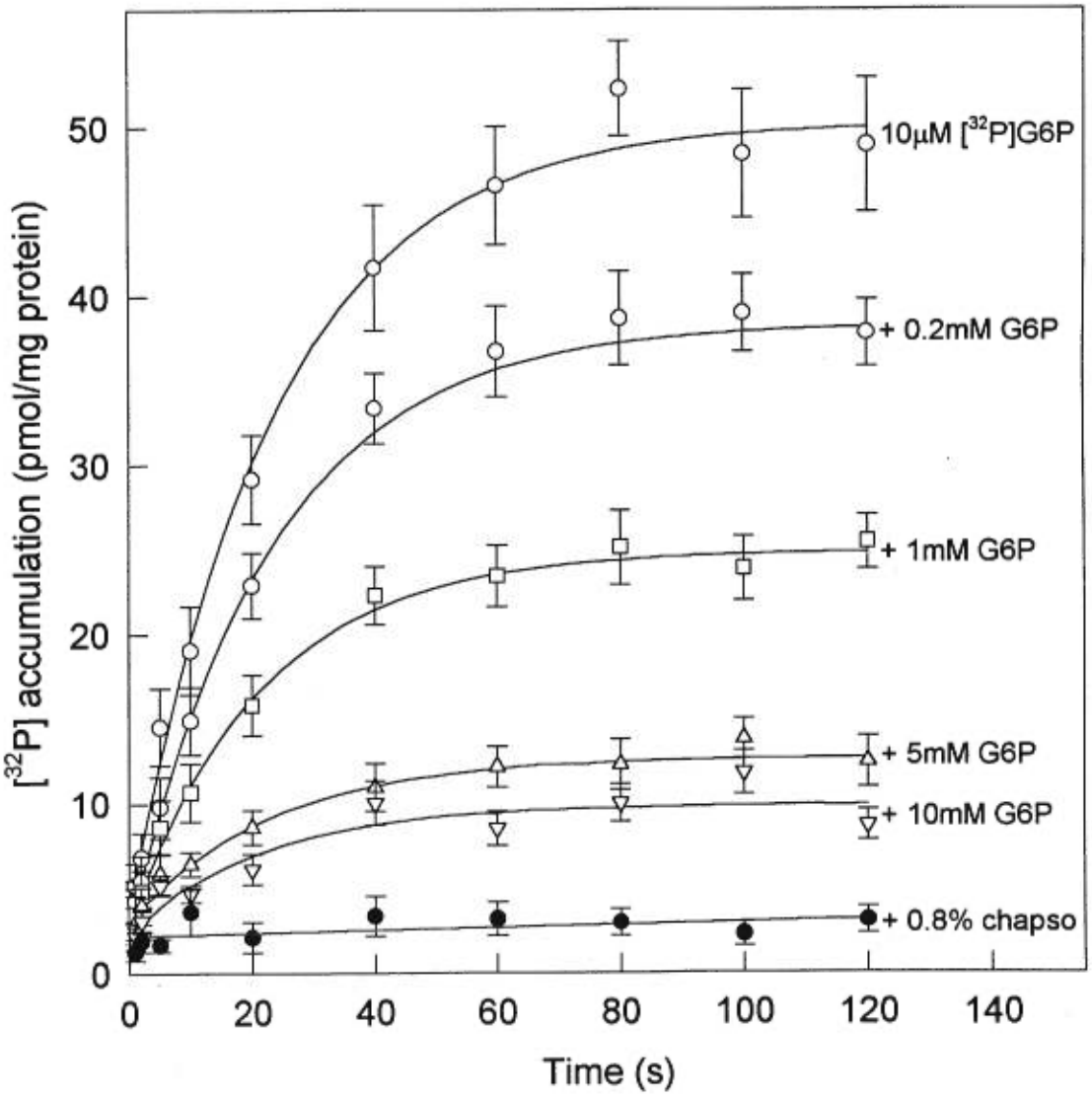
[32P] accumulation (pmol/mg protein)
Time (s)
0
10
20
30
40
50
0
20
40
60
80
100
120
140
10μM [32P]G6P
+ 0.2mM G6P
+ 1mM G6P
+ 5mM G6P
+ 10mM G6P
+ 0.8% chapso

Figure 2

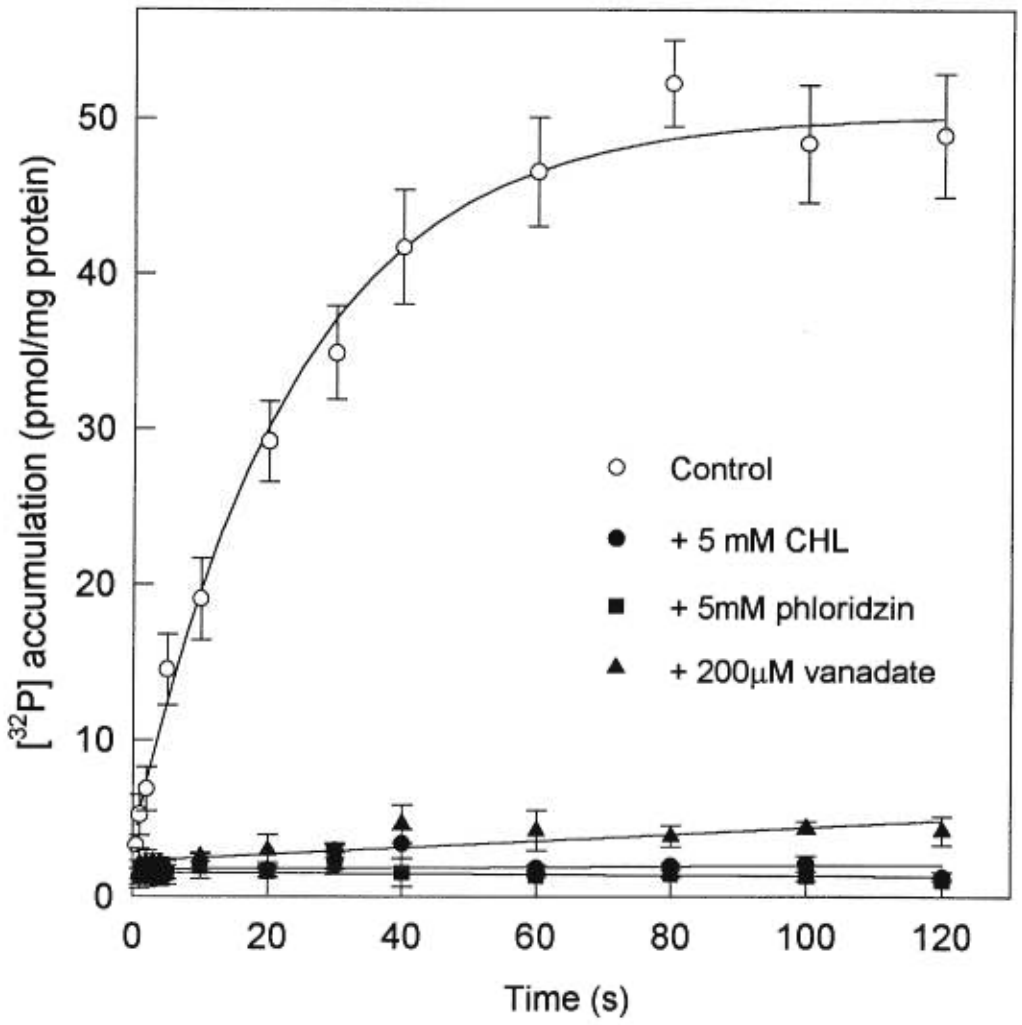
[32P] accumulation (pmol/mg protein)
0
10
20
30
40
50
0
20
40
60
80
100
120
Time (s)
Control
+ 5 mM CHL
+ 5mM phloridzin
+ 200μM vanadate

Figure 3

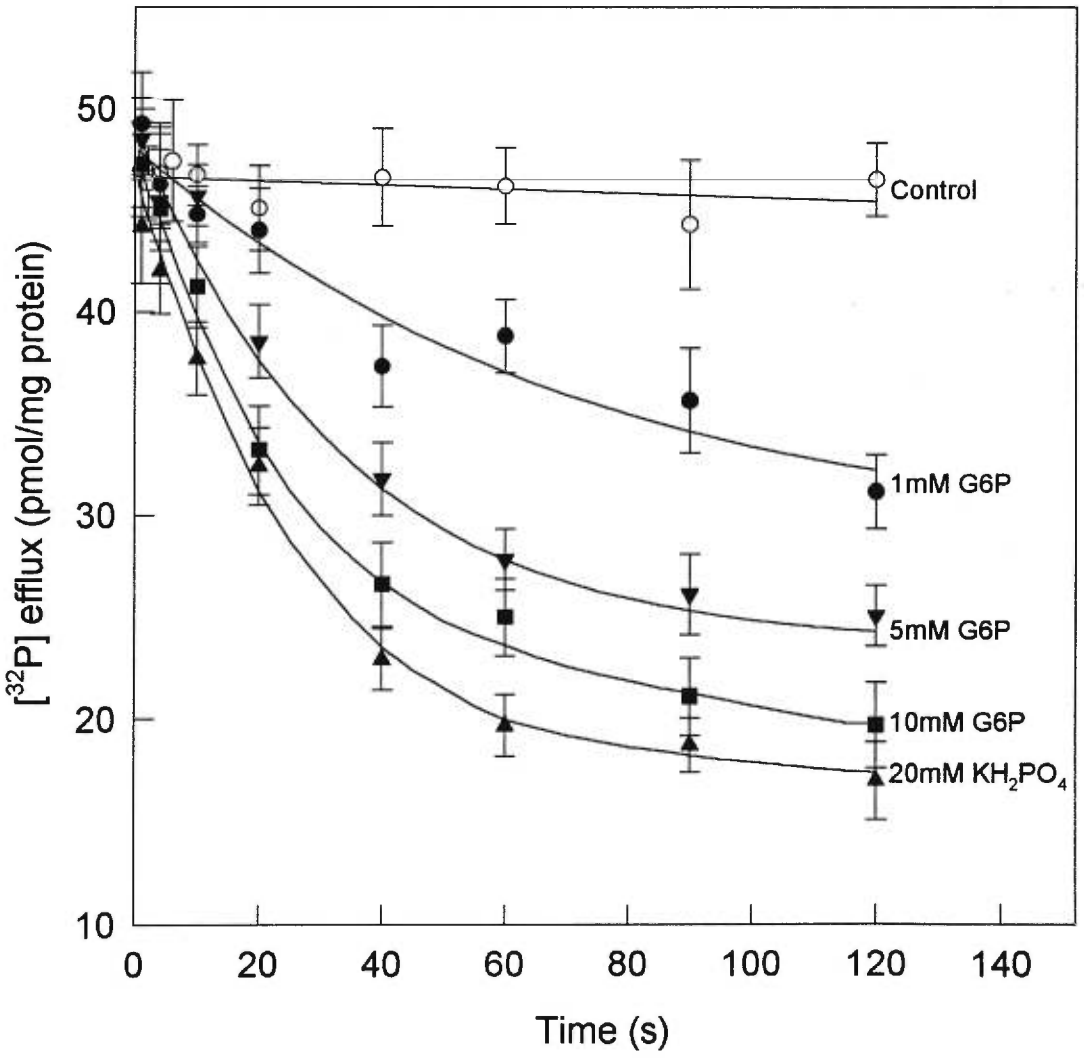
50
40
30
20
10
0
20
40
60
80
100
120
140
[32P] efflux (pmol/mg protein)
Time (s)
Control
1mM G6P
5mM G6P
10mM G6P
20mM KH2PO4

Figure 4

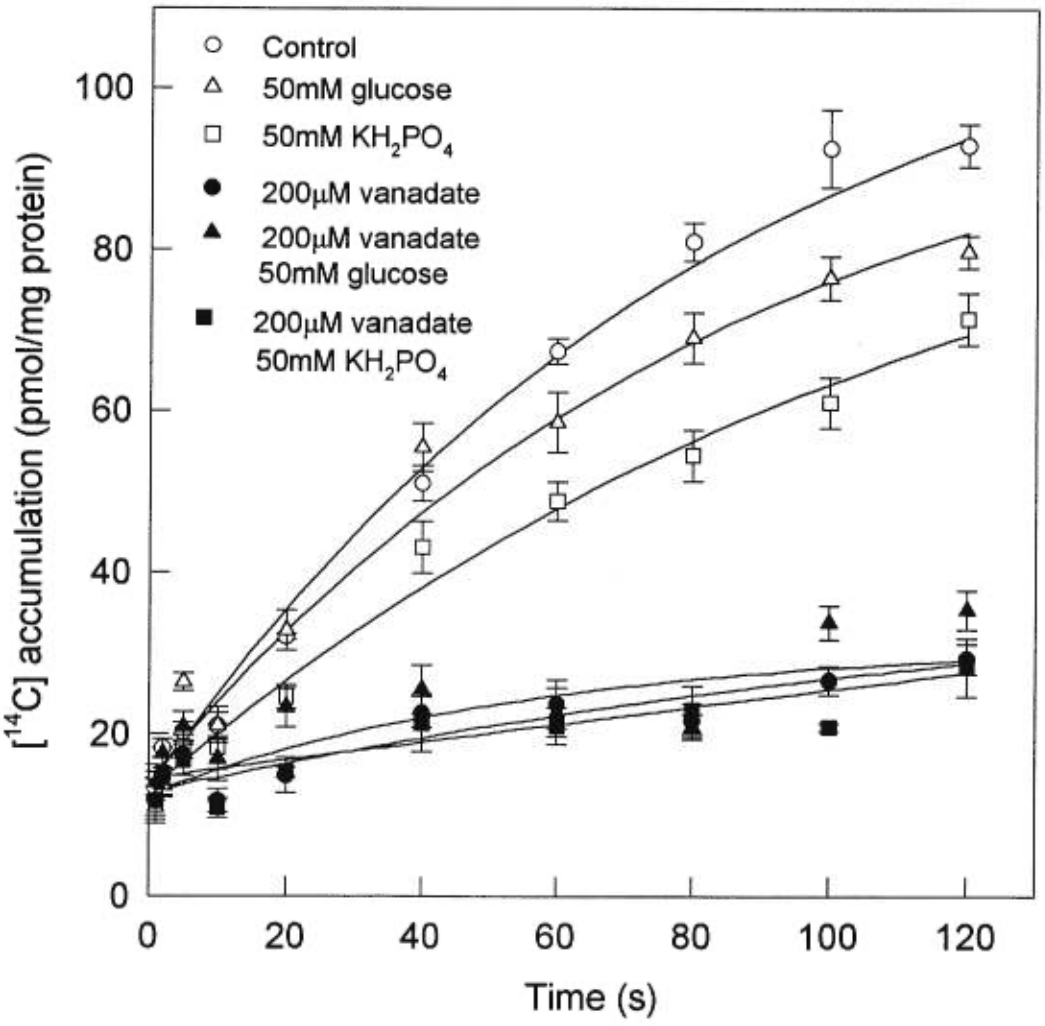
Control
50mM glucose
50mM KH2PO4
200μM vanadate
200μM vanadate
50mM glucose
200μM vanadate
50mM KH2PO4
[14C] accumulation (pmol/mg protein)
Time (s)
0
20
40
60
80
100
120

Figure 5

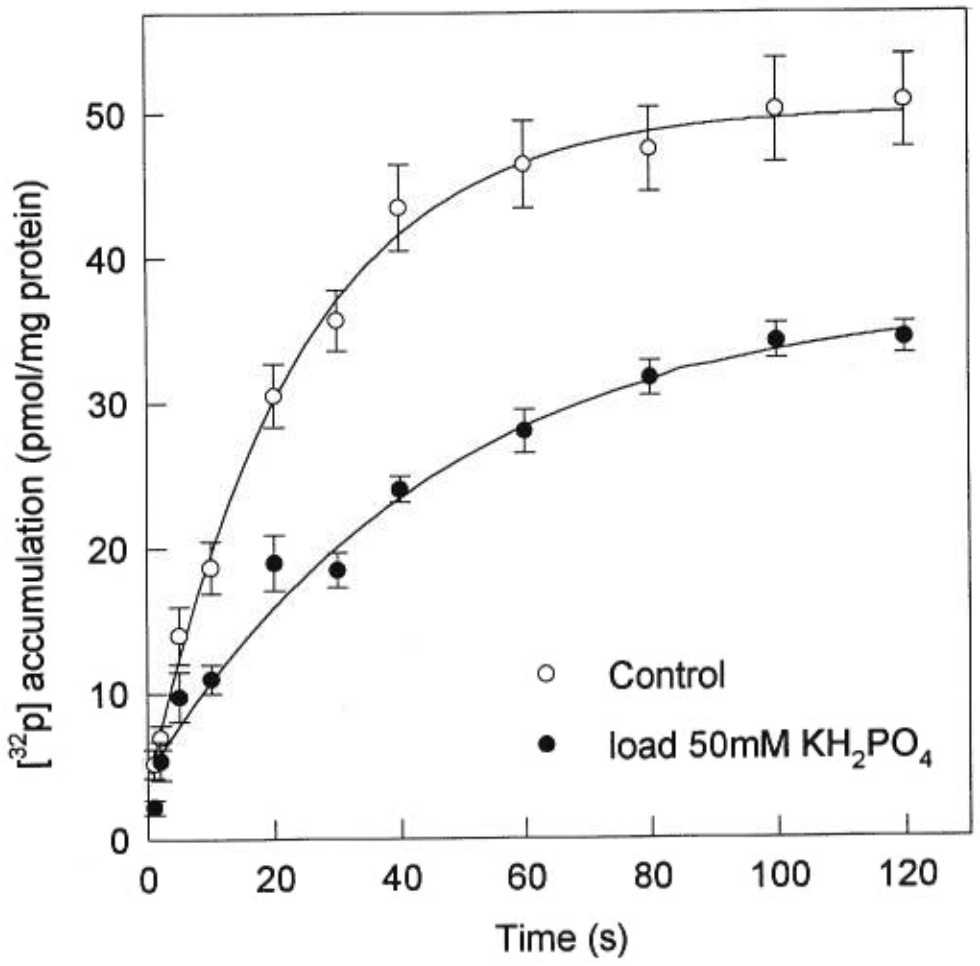
[32p] accumulation (pmol/mg protein)
0
10
20
30
40
50
0
20
40
60
80
100
120
Time (s)
Control
load 50mM KH2PO4

IV.6 Other results

IV.6.1 G6Pase activity and cAMP content in cultured primary hepatocytes

	Control medium	P_i depleted medium
G6Pase activity at 0.2mM G6P (μunits/mg protein)	5.9 ± 0.45	6.7 ± 0.52
G6Pase activity at 5 mM G6P (μunits/mg protein)	37.8 ± 2.1	30.0 ± 1.3
Intracellular cAMP content (fmol/10^4 cells)	120 ± 15	100 ± 12

Primary hepatocytes were cultured with MEM or P_i depleted MEM for 24 h, then harvested for microsomal preparation or for cAMP measurement.

IV.6.2 Northern blot results of p36 and p46 from cultured primary hepatocytes

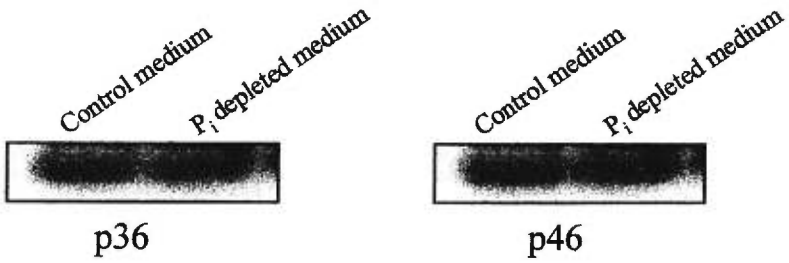

Primary heparocytes were cultured with MEM or P_i depleted MEM for 24h, then harvested for totale RNA extraction.

Chapter VI Discussion

VI.1 Effects of phosphate deficiency on glucose metabolism

Experimental data showed that, compared to a control diet ($+P_i$), feeding rats with a P_i-deficient diet ($-P_i$) for 48h resulted in a substantial decrease in plasma phosphate concentration. Consequently, G6Pase was upregulated via stimulation of both mRNA and protein levels of the catalytic subunit, p36, but only p46 mRNA in the ($-P_i$) group. In the fed state, liver gluconeogenic key steps were stimulated, liver glycogen content was decreased and plasma glucose concentration was increased in the ($-P_i$) group. Endogenous glucose production in the ($-P_i$) group was less suppressed by a glucose bolus during the IVGTT performed with overnight fasted rats. Although the glucose fall rates and plasma insulin concentrations were not significantly different in both groups, a tendency to hyperglycemia after the glucose bolus was observed in the ($-P_i$) group. Consistently, in the fed state, liver cAMP, a stimulator of G6Pase, gluconeogenesis and glycogenolysis, increased; and plasma insulin concentration was decreased in the ($-P_i$) group. For the first time, these results integrally demonstrate that *in vivo*, P_i deficiency severely affects glucose metabolism and elevated glucose production may be responsible for the impaired glucose metabolism in the condition of hypophosphatemia. Results also showed that both in liver and kidneys, G6Pase activity was stimulated in X-linked hypophosphatemic (Hyp) mice at physiological

and saturating substrate concentrations. In Hyp mouse liver and kidneys, p36 mRNA and protein were upregulated, whereas those of p46 were downregulated.

Increase of G6Pase activity per P_i-deficient diet or in Hyp mice is more probably due to the stimulated expression of the catalytic subunit (p36). This is more obvious in P_i-deficient diet experiment since V_{max} values were increased but K_m values were unaffected both in intact and detergent-treated microsomes, excluding the change of enzyme affinity to its substrate. Changes of p46 do not seem to be responsible for the increase of G6Pase activity since the protein amount of p46 was unaffected in the P_i-deficient diet experiment or even decreased in Hyp mice. It is still a question whether the increase of p36 mRNA abundance occurs at the transcriptional or post-transcriptional level. It has been reported that PTH mRNA stability was decreased in P_i-deficient diet conditions due to the effects of a P_i-deficient diet on RNA-protein interaction [Moallem et al., 1998]. It can be deduced from this report that the P_i-deficient diet could affect RNA binding proteins, resulting in effects on mRNA stability. On the other hand, a dietary phosphate response sequence was recently identified in the NaP_i-2 gene and its binding factors were also described [Kido et al., 1999], indicating the transcriptional level could be also affected by the P_i-deficient diet. However, neither p36 nor p46 gene promoter possesses a similar sequence. Hence, it is less likely the transcription of p36 or p46 gene would be affected. To investigate the mechanism for the changes in G6Pase gene expression via P_i deficiency should provide information to understand how P_i deficiency affects G6Pase *in vivo*.

Although p46 mRNA increased, the p46 protein was not affected by the P_i-deficient diet for 48h, indicating the translation step was slowed down or p46 protein stability was decreased. In contrast to the case of the P_i-deficient diet, p46 mRNA and detectable protein amount per anti-p46 N-terminus antibody were substantially decreased in Hyp mice. The decreased p46 mRNA level would result in less p46 protein amount. However, it does not exclude the possibility that p46 protein stability may be decreased, too. This possibility is implied via comparing the results of western blot and northern blot in Hyp mice. In Hyp mice, changes in liver p46 protein amount are larger than those in p46 mRNA levels, moreover, p46 protein amount in one Hyp mouse was undetectable, while its liver p46 mRNA was at the same level as other Hyp mice. These results imply that the post-translational level of p46 might be also affected by P_i deficiency. This is consistent to the observation that p46 protein level was unchanged but p46 mRNA level was stimulated in the P_i-deficient diet experiment. The fact that the P_i-deficient diet and Phex mutations had different effects on p46 gene expression can be explained via the differences caused by a P_i-deficient diet and Phex mutations. Even though serum phosphate decreases in both cases, a number of parameters change in an opposite direction. In the P_i-deficient diet conditions, NaP_i-2 gene expression is upregulated, while downregulated in X-linked hypophosphatemic mice. PTH decreased, serum Ca^{2+} and vitamin D increased in the P_i-deficient diet experiment, but all of these parameters are at normal levels in Hyp mice compared to control normal mice. More importantly, the Phex gene is mutated in Hyp mice, but has a normal function in the P_i-deficient diet condition. Taken together, it is logical to deduce that some common factors linked to the P_i deficient

state, caused either by a P_i-deficient diet or PHEX/Phex gene mutations, affect p36 gene expression, whereas special effectors in X-linked hypophosphatemia affect p46 gene expression. The results of p46 gene expression reflect not only the difference of X-linked hypophosphatemia from the P_i-deficient diet, but also demonstrate distinct regulations of p36 and p46 gene expression, as already observed in the studies of hormonal regulations of p36 and p46 gene expression [Li & van de Werve, 2000]. It has also been proposed in that study that hepatic glucose production is related to changes in the catalytic subunit of G6Pase, rather than in p46.

Even though X-linked hypophosphatemia had a distinct effect on p46 gene expression, G6Pase activity was still increased in Hyp mice, in agreement with the observation in P_i-deficient diet experiment. The enhanced G6Pase activity in the two gluconeogenic organs in Hyp mice supports that glucose production in Hyp mice would be also elevated as demonstrated in P_i-deficient diet conditions. In rats fed with a P_i-deficient diet, even though PEPCK and GK activities were unaffected, changes in G6Pase and PK activities, Fru-2,6-P_2 and glycogen contents as well as PEP concentration are all compatible with stimulated liver gluconeogenesis and glycogenolysis. These changes could control the metabolite flux toward glucose producing. Less suppressed endogenous glucose production during the IVGTT in the (-P_i) group further supports this conclusion. All of these changes resulted in increased plasma glucose concentration in the (-P_i) group in the fed state. Although the glucose fall rates and insulin secreting responses during the IVGTT were not significantly different in both groups, there was indeed a tendency to hyperglycemia in the (-P_i) group after the glucose bolus. This higher glucose concentration indicates a mild

glucose intolerance state in the ($-P_i$) group. Glucose tolerance is dependent on three physiological factors, i.e., insulin secretion, tissue sensitivity to insulin and glucose effectiveness. From the results of similar plasma insulin concentration and higher glucose concentration, it is indicated that tissue insensitivity to insulin may exist in the ($-P_i$) group. On the other hand, one would also suggest that glucose effectiveness, namely, the ability of glucose to promote its own uptake and suppress endogenous glucose production, might be lower in the ($-P_i$) group. Although the plasma glucose and insulin concentrations are markedly different in ($+P_i$) and ($-P_i$) group, their differences are lessened in the fasted state. It seems likely that fasting could compensate some effects of P_i deficiency, although plasma phosphate concentration was still lower and G6Pase was upregulated in the fasted ($-P_i$) group. It has indeed been reported that fasting could increase serum phosphorus [Jara et al., 1999], supporting a potential compensating effect of fasting on dietary P_i deficiency. This compensating effect of fasting could account for the insignificant difference in glucose fall rates during the IVGTT in both groups. It could also provide an explanation for the controversial reports about the effect of P_i deficiency on insulin secretion. In the study of Zhou et al. [1991], it was shown that glucose-stimulated insulin secretion of perfused pancreatic islets from P_i depleted rats was markedly reduced, while another report showed a higher serum insulin concentration during an IVGTT in the fasted hypophosphatemic patients [Paula et al., 1998]. These controversies could result from the experimental conditions, such as nutritional states.

Enhanced liver cAMP provided a potential cause for the alterations in gluconeogenesis and glycogenolysis. From this result, one would easily expect that

circulating insulin concentration might be lower in the (-P_i) group, which was indeed the case. Therefore, it is likely that change in insulin/glucagon ratio accounted for the elevated liver cAMP and the resultant stimulated glucose production. There is no evidence about whether insulin gene is affected by P_i deficiency or the secretion process itself is suppressed per P_i deficiency. It has been reported that both the first phase and the second phase of glucose stimulated insulin secretion was reduced in pancreatic islets from P_i depleted rats [Zhou et al., 1991]. Therefore, both insulin gene expression and insulin secretion process could be affected *in vivo* by P_i deficiency. Insulin secretion was, however, not significantly different in INS-1 cells cultured in P_i depleted medium. This result does not indicate that P_i deficiency per se affects insulin secretion. It is unlikely that P_i depletion per se affects the G6Pase system or liver cAMP amount since they were not changed in primary hepatocytes cultured in P_i depleted medium. It is either unlikely that PTH is responsible for the elevated cAMP because it has been demonstrated that PTH decreased in P_i-deficient diet conditions, from which a lower cAMP content would be deduced. Changes in vitamin D and/or serum calcium could be potential cause(s) for the impaired glucose metabolism and insulin secretion since both of them are increased in the P_i-deficient diet condition and calcium is a potential regulator of G6Pase. Although this is possible in the case of the P_i-deficient diet, it would hardly explain the changes in G6Pase activity in Hyp mice via these factors because serum Ca^{2+} and vitamin D are at the same levels in Hyp mice as normal mice.

It is likely that some unknown factors are involved in the association of P_i deficiency with glucose metabolism. The newly discovered hormone, stanniocalcin,

which acts as a regulator of calcium and phosphate homeostasis and has an autocrine/paracrine endocrine role [Lu et al., 1994; Yoshiko et al., 1999], is possibly one of these factors. Two mammalian homologues of stanniocalcin were identified so far, stanniocalcin 1 [Olsen et al., 1996] and stanniocalcin 2 [Ishibashi et al., 1998]. It has been reported that kidney is a possible site of synthesis for stanniocalcin 1 [Olsen et al., 1996], while recently, it was reported that the primary site of human stanniocalcin 2 production was the pancreas [Moore et al., 1999]. Using double immunostaining assay, it was shown that stanniocalcin 2 protein was found in the pancreatic α cells, but not β cells [Moore et al., 1999]. The authors of that study speculated that stanniocalcin 2 might play a role in glucose homeostasis. P_i deficiency, caused either by a P_i-deficient diet or PHEX/Phex gene mutations, possibly affects the expression or function of stanniocalcin 2, which further affects the function of pancreas and alters insulin/glucagon ratio or other related factors. These changes result in stimulated G6Pase and impaired glucose metabolism. Another putative hormone related to phosphate homeostasis, phosphatonin, may also participate in these changes. Compared to stanniocalcin 1, phosphatonin is proposed to inhibit renal phosphate reabsorption. The characteristics of phosphatonin are less clear. Neither its gene has been cloned nor the protein has been identified. Since the regulations and exact physiological functions of these two hormones are undefined at this stage, more investigation is needed to elucidate their effects on glucose metabolism. In the case of Hyp mice, more complications occur. The primary cause of Hyp mice is the dysfunction of the PHEX/Phex gene which has been demonstrated

to code for an endopeptidase. It is likely that the dysfunction of PHEX/Phex may impair other protein(s)' function related to gene regulation, resulting in down regulation of p46 gene regulation.

VI.2 Roles of p36 and p46 in the G6Pase system

It has been fully accepted that p36 is the catalytic subunit of G6Pase even though its active site and conformational structure are still unclear. Our results are consistent with this concept. When p36 protein is upregulated, G6Pase activity increases, more convincingly in the conditions of detergent-treated microsomes and saturating substrate concentration. However, the role of p46 is less clear. According to the substrate-transport model, p46 is proposed to be a G6P transporter and this process is the rate-limiting step during the hydrolysis of G6P. Our results showed this might not necessarily be the case since the p46 protein amount is unchanged in the P_i-deficient diet experiment or even decreased in Hyp mice, while G6Pase activity still increased as long as p36 protein amount was increased. It has indeed been documented that inhibition and stimulation of G6Pase hydrolytic activity are related to changes in the catalytic subunit of G6Pase rather than in p46 [Li & van de Werve, 2000]. Considering this aspect together with the fact that p46 is expressed in tissues without p36 [Li & van de Werve, unpublished results] as well as no G6P uptake in p36 knockout mice [Lei et al., 1996], one can reasonably think that the physiological function(s) of p46 may be not only in relation with G6Pase. As reported in the study of Méchin & van de Werve [2000b], p46 is homologous to both UhpT and UhpC, implying p46 could function as a G6P sensor and regulate other processes. G6P is an

important metabolite leading to glucose storage and oxidation, also a regulator of several enzymes, such as phosphorylase kinase and glycogen synthase. Interestingly, G6P stimulates the ATP-dependent uptake of Ca^{2+} into isolated microsomes, whereas neutrophils and monocytes from patients with p46 deficiency are unable to efficiently sequester Ca^{2+} [Kilpatrick et al., 1990]. This evidence strongly suggests that p46 may participate in the control of Ca^{2+} uptake in microsomes by G6P. The regulation of p46 gene expression also supports this possibility. Although it has been reported that glucose, cAMP and insulin affect p46 gene expression in the same direction as that of the p36 gene [Li et al., 1999], it is clearly shown here that p46 mRNA and protein levels decreased while p36 mRNA and protein levels increased in Hyp mice. This result indicates a distinct regulation of p46 gene expression from that of the p36 gene. In fact, it has been documented in the study of our laboratory [Li & van de Werve, 2000] that hormonal changes compatible with increased hepatic glucose production essentially modify the expression of the catalytic subunit of G6Pase, p36, without a significant effect on that of p46. In general, regulation of gene expression is associated with the physiological function of the protein. Hence, distinct regulation of p46 gene expression supports that p46 has some other functions than G6P transport.

Rapid kinetic studies also indicates that p46 may not necessarily be responsible for G6P transport. Since radioactivity accumulation from [U-^{14}C]G6P and [^{32}P]G6P showed distinct kinetic parameters, it is unquestionable that the radioactivity accumulation is mainly the products, rather than the substrate G6P. Because if it was only the substrate accumulation, the steady-state level and $T_{1/2}$ value of G6P uptake would be the same whether it was [U-^{14}C]G6P or [^{32}P]G6P. Even though it was not

excluded that there might be a small amount of G6P accumulated, kinetic analysis of the radioactivity uptake obviously demonstrates that G6P transport step, if any, is not the rate-limiting step during the G6P hydrolysis. The effect of vanadate on [^{32}P]G6P uptake and the dose effect of unlabelled G6P demonstrated that the radioactivity uptake from labelled G6P was dependent on the hydrolytic activity of G6Pase. This is in agreement with the observation of no G6P uptake in liver microsomes from p36 knockout mice [Lei et al., 1996]. It demonstrates that p46 alone has no G6P transport function and function of p36 is required for the radioactivity uptake from labeled G6P. The fact that no G6P hydrolytic activity and G6P uptake occurred in the presence of CHL, an inhibitor of p46, indicates that the function of p46 is also required for the G6Pase full activity. All of these results support that G6P transport/hydrolysis are tightly coupled processes. In other words, functions of both p36 and p46 are required for G6Pase activity and p46 alone does not transport G6P. It is implied that p36 and p46 have a coupling interaction which could affect their functions.

Glucose transport and inorganic phosphate transport parameters are not compatible with specific glucose or phosphate facilitative transport protein. Theoretically, facilitative transport process has saturable effect, specific inhibitors and accelerated transport effect. Our data showed glucose uptake into liver microsomes had no saturable effect even at 100 mM glucose concentration. Specific inhibitors of classical glucose transporters, such as phloretin, had no effect on glucose uptake into liver microsomes. All of these data indicate there is no specific glucose transporter in ER membrane. Using light-scattering technique, a very rapid glucose transport

process ($T_{1/2}$ 3-9s) was reported and a potential saturable effect was observed when glucose concentration was higher than 100 mM [Marcolongo et al., 1996]. Moreover, it was also observed in that study that all L-glucose, ascorbic acid, D-mannitol, D-fructose, D-galactose and other compounds permeated microsomes in a fashion similar to D-glucose. Specific inhibitors of glucose transporter, such as cytochalasin B, only partially inhibited the transport. These results could be explained by experimental artefacts resulted from the effect of osmolarity on the vesicle volume. The addition of high concentration of glucose into a low osmolarity medium used in that experiment would cause the efflux of intravesicular water and interfere the uptake of glucose, resulting in a rapid influx of glucose and saturating effect. The lack of stereospecificity of the substrate and no full inhibitory effect do not support their conclusion of facilitative transport. In contrast, these results are compatible with our observation and support the above explanation. Similarly, phosphate uptake into liver microsomes had neither saturable effect nor accelerated transport. All of the potential inhibitors showed no effect, too. The results of exchanging transport exclude the possibility that glucose or phosphate may be anti-transported via G6P transport. All of these results indicate that the concepts of phosphate transporter and glucose transporter in G6Pase system may need to be re-evaluated. Consistent to our kinetic studies, gene mutation studies also initiate the similar idea. Based on the results that mutations were found in p46 gene in GSD Ib, Ic and Id patients, it was recently proposed that there appears to be only two types of GSD I, type Ia and type Ib which is caused by mutations of p36 gene and p46 gene, respectively [Veiga-da-Cunha et al., 2000]. This proposal is obviously consistent to the idea that no glucose

or phosphate transport protein exists in G6Pase system. It is also of importance to note that the accumulated radioactivity inside microsomes only presents 10% of the total product, as shown by comparison of the initial transport rate with the initial intact hydrolytic activity of G6Pase under similar conditions. This result indicates that most of the products are directly exported to the outside of microsomes, in agreement with concepts of the conformational model.

Taken together, these results demonstrate that G6P transport is tightly coupled to G6Pase hydrolytic activity and G6P transport step is not the rate-limiting step during G6P hydrolysis. The products, glucose and inorganic phosphate, are exported by a diffusion process rather than via a facilitative transport protein. Based on these data, the combined-conformational flexibility model of the G6Pase system is further modified in the following aspects. In this model, as proposed previously [Berteloot et al., 1995], the catalytic subunit, p36, is an intrinsic membrane protein and spans the ER membrane to form a channel-like structure with the active site embedded in a hydrophilic pocket. G6P could access to the active site through the channel and hydrolysis process take place at the hydrophilic pocket. 90% products, both glucose and phosphate, are directly exported to the cytosol, 10% of the two products are accumulated inside the lumen. The function of p46 could be related to binding and transport of G6P into the active site. The binding of G6P to p46 could affect the conformation of p46, which would further affect the conformation of p36 via their coupling interaction. This protein-protein interaction may account for the hysteretic transition of G6Pase during the hydrolysis of G6P [Berteloot et al., 1995]. Since kinetic parameters of phosphate transport and glucose transport were neither

compatible with facilitative transport nor passive diffusion which would be much slower, a pore-like structure is proposed to be responsible for the diffusion of glucose and inorganic phosphate across the ER membrane. L-glucose, mannitol and other glucose analogues can also pass through this structure. The pore-like structure may contribute to the putative T2 and T3 translocase in intact microsomes. Because of the smaller size of the phosphate anion compared to the glucose molecule, the rate of phosphate transport is higher than that of glucose, hence, resulting in the smaller phosphate intravesicular space. The opposing membrane potential could be minimized in the case of phosphate transport by the high rates of K^+ (or Na^+) permeation. This pore-like structure can be composed of proteins or a specific phospholipid structure, which have a kind of size specificity so that G6P does not pass through. When considering the nuclear pore and mitochondrial membrane pore structure, one will not be surprised at the existence of a pore-like structure in the ER membrane which is the continuation with nuclear membrane. Small invaginations or caves which are termed as 'caveolae' exist in the plasma membrane in many cell types. Caveolae are found to be important for the extra/intra-cellular communiction as well as responsible for the transport of small molecules [Shaul et al., 1998]. It would be interesting to investigate whether the similar structure exists in the ER membrane to represent the pore-like structure proposed in our new model. In fact, a similar idea was proposed in the study of Bànhegy et al. [1998]. It was documented in that study that glucose transport properties could be explained by assuming that the ER contains a limited number of highly permeable structures. This pore-like structure is compatible with most of the experimental data obtained up to date, such as the

unsaturable effect, a large range of substrates, the lack of stereospecificity, no specific inhibitors as well as the failure of glucose transporter gene cloning [Burchell 1999]. However, its existence has to be further demonstrated; its structure and function need to be investigated in more detail.

VI.3 Perspectives

The present studies demonstrate that G6Pase activity up-regulated by P_i deficiency is potentially caused by the increased liver cAMP and decreased plasma insulin concentration. At this stage, the mechanism(s) for the changes in liver cAMP and plasma insulin concentration remain to be established. These aspects can be interesting and important points to elucidate the mechanism of impaired glucose mechanism by P_i deficiency. Since it appears that P_i deficiency per se has no direct effect on these parameters, there should be some factors, such as hormones, which are related to P_i homeostasis and affect glucose metabolism. To identify these factors and their characteristics is an essential issue. Stanniocalcin 2, which is expressed primarily in pancreatic α cells [Moore et al., 1999], is a possible mediator between glucose metabolism and P_i homeostasis. Studies on the potential effect of stanniocalcin 2 on insulin or glucagon secretion are necessary and may bring out exciting results. Although insulin secretion was studied in pancreas from P_i depleted rats [Zhou et al., 1991], it is still worth to study the effect of P_i deficiency on insulin gene expression.

Phosphate, glucose and G6P transport in rat liver microsomes was relatively detailed by classical transport studying means in the present studies. On the other hand, since PP_i and carbamyl-P are also the substrates of G6Pase, it can be an essential issue to address their transport/hydrolysis kinetic characteristics in liver microsomes. Since it has been a failure to clone the glucose transporter in liver ER membrane [Burchell, 1998], it sounds uninteresting to do it again or try to clone the phosphate transport protein in liver ER membrane. On the other hand, the new combined-conformational model of G6Pase has no way to be fully described at this moment. For this aspect, it is crucial to study the exact function of p46, which is also the focus in G6Pase field. There are difficulties in this aspect in terms of means. Studies on its crystal structure can be a good way. Studies on the effect of p46 on other processes, such as Ca^{2+} uptake, should also provide implications. Besides the function of p46, it is also necessary to investigate the pore-like structure proposed in this thesis. This proposal is a relative new idea and needs more data to demonstrate the existence of the pore-like structure which can be composed of proteins (such as caveolin, the marker protein for caveolae) or just a special phospholipid structure. Therefore, molecular cloning of the ER membrane proteins and the structure of liver ER membrane are the targets for this purpose.

References

Annabi B, van de Werve, 1997, Evidence that the transit of glucose into liver microsomes is not required for functional glucose-6-phosphatase, Biochem Biophys Res Commun, 236: 808-813

Ajzannay A, Minassian C, Riou JP, Mithieux G, 1993, Glucose-6 phosphate phosphohydrolase of detergent-treated liver microsomal membranes exhibits a specific kinetic behaviour towards glucose-6-phosphate, Eur J Biochem, 212: 335-338

Ajzannay A, Minassian C, Riou JP, Mithieux G, 1994, Glucose-6-phospahtase specificity after membrane solubilization by detergent treatment, J Biochem, 116: 1336-1340

Ajzannay A, Mithieux G, 1996, Glucose-6-phosphate and mannose-6-phosphate are equally and more actively hydrolyzed by glucose-6-phosphatase during hysteretic transition within intact microsomal membrane than after detergent treatment, Arch Biochem Biophys, 326: 238-242

Arden SD, Zahn T, Steegers S, Webb S, Bergman B, O'brien RM, Hutton JC, 1999, Molecular cloning of a pancreatic islet-specific glucose-6-phosphatase catalytic subunit-related protein, Diabetes, 48: 531-542

Argaud D, Zhang Q, Pan W, Maitra S, Pilkis S, Lange AJ, 1996, Regulation of rat liver glucose 6-phosphatase gene expression in different nutritional and hormonal states, Diabetes, 45: 1563-1571

Argaud D, Kirby TL, Newgard CB, Lange AJ, 1997, Stimulation of glucose-6-phosphatasse gene expression by glucose and fructose-2,6-bisphosphate, J Biol Chem, 272: 12854-12861

Arion WJ, Wallin BK, Lange AJ, Ballas LM, 1975, On the involvement of a glucose-6-phosphate transport system in the function of microsomal glucose-6-phosphatase, Mol Cell Biochem, 6: 75-83

Arion WJ, Lange AJ, Ballas LM, 1976, Quantitative aspects of relation between glucose-6-phosphate transport and hydrolysis for liver microsomal glucose 6-phosphatase system, J Biol Chem, 251: 6784-90.

Arion WJ, Lange AJ, Walls HE, Ballas LM, 1980, Evidence of the participation of independent translocases for phosphate and glucose-6-phosphate in the microsomal glucose 6-phosphatase system, J Biol Chem, 255: 10396-10406

Arion WJ, Canfield WK, Ramos FC, Schindler PW, Burger HJ, Hemmerle H, Schubert G, Below P, Herling A, 1997, Chlorogenic acid and hydroxynitrobenzaldehyde: new inhibitors of hepatic glucose 6-phosphatase, Arch Biochem Biophy, 339: 315-322

Arion WJ, Canfield WK, Callaway ES, Burger HJ, Hemmerle H, Schubert G, Herling A, Oekonomopulos R, 1998, Direct evidence for the involvement of two glucose 6-phosphate-binding sites in the glucose-6-phosphatase activity of intact liver microsomes, J Biol Chem, 273: 6223-6227

Arnaud CF, Glorieux F, Scriver C, 1971, Serum parathyroid hormone in X-linked hypophosphatemia, Science, 173: 845-847

Bànhegyi G, Marcolongo P, Burchell A, Benedetti A, 1998, Heterogeneity of glucose transport in rat liver microsomal vesicles, Arch Biochem Biophys, 359: 133-138

Bashan N, Potashnik R, Peist A, Peleg N, Moran A, Moses SW, 1993, Deficient glucose phosphorylation as a possible common denominator and its relation to abnormal leucocyte function, in glycogen storage disease 1b patients, Eur J Pediatr 152 (Suppl 1): S44-S48

Baranowska B, Terlecki g, Baranowski T, 1984, The influence of inorganic phosphate and ATP on the kinetics of bovine heart muscle pyruvate kinase, Mol Cell Biochem, 64: 45-50

Beck L, Soumounou Y, Martel J, Krishnamurthy G, Gauthier C, Goodyer CG, Tenenhouse HS, 1997, Pex/PEX tissue distribution and evidence for a deletion in the 3' region of the Pex gene in X-linked hypophosphatemic mice, J Clin Invest, 99: 1200-1209

Berner YN, Shike M, 1988, Consequences of phosphate imbalance, Annu Rev Nutr, 8: 121-148

Berteloot A, Vidal H, van de Werve G, 1991a, Rapid kinetics of liver microsomal glucose-6-phosphatase, J Biol Chem, 266: 5497-5507

Berteloot A, Malo C, Breton S, Brunette M, 1991b, Fast sampling, rapid filtration apparatus: principal characteristics and validation from studies of D-glucose transport in human jejunal brush-border membrane vesicles, J Membr Biol, 122: 111-25

Berteloot A, St-Denis JF, van de Werve G, 1995, Evidence for a membrane exchangeable glucose pool in the functioning of rat liver glucose-6-phosphatase, J Biol Chem, 270: 21098-21102

Bevington A, Kemp GJ, Graham R, Russell G, 1992, Phosphate-sensitive enzymes: a possible molecular basis for cellular disorders of phosphate metabolism, Clin Chem Enzym Comms, 4: 235-257

Biber J, Custer M, Magagnin S, Hayes G, Werner A, Lotscher M, Kaissling B, Murer H, 1996, Renal Na^+/Pi-cotransporters, Kidney Intern, 49: 981-985

Bontemps F, Hue L, Hers HG, 1978, Phosphorylation of glucose in isolated rat hepatocytes. Sigmoidal kinetics explained by the activity of glucokinase alone, Biochem J, 174: 603-11

Boyer CJC, Xiao Y, Dugré A, Vincent É, Delisle MC, Béliveau R, 1996, Phosphate deprivation induces overexpression of two proteins related to the rat renal phosphate cotransporter NaPi-2, Biochim Biophys Acta, 1281: 117-123

Brautbar N, Carpenter C, Baczynski R, Kohan R, Massry SG, 1983, Impaired energy metabolism in skeletal muscle during phosphate depletion, Kidney Int, 24: 53-57

Bruni N, Rajas F, Montano S, Chevalier-Porst F, Maire I, Mithieux G, 1999, Enzymatic characterization of four new mutations in the glucose-6-phosphatase (G6PC) gene which cause glycogen storage disease type 1a, Ann Hum Genet, 63: 141-146

Bugg NC, Jones JA, 1998, Hypophosphataemia. Pathophysiology, effects and management on the intensive care unit, Anaesthesia, 53: 895-902

Burchell A, Gibb L, 1991, Diagnosis of type IB and IC glycogen storage disease, J Inherit Metab, 14: 305-307

Burchell A, 1998a, Glycogen storage diseases and the liver, Baillière's Clinical Gastroenterology, 12: 337-354

Burchell A, 1998b, A re- evaluation of GLUT 7, Biochem J, 331: 973

Cai Q, Hodgson SF, Kao PC, Lennon VA, Klee GG, Zinsmiester AR, Kumar R, 1994, Brief report: inhibition of renal phosphate transport by a tumor product in a patient with oncogenic osteomalacia, N Engl J Med, 330: 1645-1649

Capparelli AW, Roh D, Dhiman JK, Jo OD, Yanagawa N, 1992, Altered proximal tubule glucose metabolism in X-linked hypophosphatemic mice, Endocrinology, 130: 328-334

Carayannopoulos MO, Chi MM, Cui Y, Pingsterhaus JM, McKnight RA, Mueckler M, Devaskar SU, Moley KH, 2000, GLUT8 is a glucose transporter responsible for insulin-stimulated glucose uptake in the blastocyst, Proc Natl Acad Sci, USA, 97: 7313-7318

Chalew SA, Lovchik JC, Brown CM, Sun CC, 1996, Hypophosphatemia induced in mice by transplantation of a tumor-derived cell line from a patient with oncogenic rickets, Pediatr Endocrinol Metab, 9: 593-597

Change HC, Lane MD, 1966, The enzymatic carboxylation of phosphoenolpyruvate, J Biol Chem, 241: 2413-2420

Chasiotis D, 1983, The regulation of glycogen phosphorylase and glycogen breakdown in human skeletal muscle, Acta Physiol Scand Suppl, 518: 1-68

Chevalier-Porst F, Bozon D, Bonardot AM, Bruni N, Mithieux G, Mathieu M, Maire I, 1996, Mutation analysis in 24 French patients with glycogen storage disease type 1a, J Med Genet, 33: 358-60

Chou JY, Mansfield BC, 1999, Molecular genetics of type 1 glycogen storage diseases, TEM, 10: 104-113

Collins JF, Bulus N, Ghishan KF, 1995a, Sodium-phosphate transporter adaptation to dietary phosphate deprivation in normal and hypophosphatemic mice, Am J Physiol, 268: G917-G924

Collins JF, Scheving LA, Ghishan FK, 1995b, Decreased transcription of the sodium-phosphate transporter gene in the hypophosphatemic mouse, Am J Physiol, 269: F439-F448

Cowgill LD, Goldfarb S, Lau K, Slatopolsky E, Agus ZS, 1979, Evidence for an intrinsic renal tubular defect in mice with genetic hypophosphatemic rickets, J Clin Invest, 63: 1203-1210

Czok R, Lamprecht W, 1983, Pyruvate, phosphoenolpyruvate and D-glycerate-2-phosphate, in Methods of enzymatic analysis, edited by Bergmeyer HU et al., 3: 1447-1451

Daniele N, Bordet JC, Mithieux G, 1997, Unsaturated fatty acids associated glycogen may inhibit glucose-6phosphatase in rat liver, J Nutr, 127: 2289-2292

Daniele N, Rajas F, Payrastre B, Mauco G, Zitoun C, Mithieux G, 1999, Phosphatidylinositol 3-kinase translocates onto liver endoplasmic reticulum and may account for the inhibition of glucose-6-phosphatase during refeeding, J Biol Chem 274: 3597-601

Decaux JF, Antoine B, Kahn A, 1989, Regulation of the expression of the L-type pyruvate kinase in diabetic rat liver by insulin and dietary fructose, J Biol Chem, 260: 14393-14397

DeFronzo R, Lang R, 1980, Hypophosphatemia and glucose intolerance: evidence for tissue insensitivity to insulin, N Engl J Med, 27: 1259-1263

Dousa TP, 1996, Modulation of renal Na-Pi cotransport by hormones acting via genomic mechanism and by metabolic factors, Kidney Int, 49: 997-1004

Drezner MK, 2000, PHEX gene and hypophosphatemia, Kidney Int, 57: 9-18

Du L, Desbarats M, Viel J, Glorieux FH, Cawthorn C, Ecarot B, 1996, cDNA cloning of the murine Pex gene implicated in X-linked hypophosphatemia and evidence for expression in bone, Genomics, 36: 22-28

Dudman NPB, de Maine MM, Benkovie SJ, 1978, Fructose 1,6-bisphosphate. Kinetics of hydrolysis catalyzed by rabbit liver neutral fructose-1,6-bisphosphatase with Mn2+, J Biol Chem, 253: 5712-5718

Ecarot B, Glorieux FH, Desbarats M, Travers R, Labelle l, 1992, Defective bone formation by Hyp mouse bone cells transplanted into normal mice: evidence in favor of an intrinsic osteoblast defect, J Bone Miner Res, 7: 215-220

Ecarot B, Desbarats M, 1999, 1,25-$(OH)_2D_3$ down-regulates expression of Phex, a marker of the mature osteoblast, Endocrinology, 140: 1192-1199

Ecarot-Charrier B, Glorieux FH, Travers R, Desbarats M, Bouchard F, Hinek A, 1988, Defective bone formation by transplanted Hyp mouse bone cells into normal mice, Endocrinology, 123: 768-773

Econs MJ, Drezner MK, 1994, Tumour-induced osteomalacia--unveiling a new hormone, N Engl J Med, 330: 1679-1681

Econs MJ, 1996, Positional cloning of the HYP gene. A review, Kidney Int, 49: 1033-1037

Econs MJ, 1999, New insights into the pathogenesis of inherited phosphate wasting disorders, Bone, 25: 131-135

Eicher EM, Southard JL, Scriver CR, Glorieux FH, 1976, Hypophosphatemia: mouse model for human familial hypophosphatemic (vitamin D-resistant) rickets, Proc Natl Acad Sci U S A, 73: 4667-4671

Essig M, Friedlander G, 1998, Regulation of phosphate homeostasis and hypophosphatemia, La Revue du Practicien, 48: 1218-1225

Feldman F, Butler LG, 1972, Protein-bound phosphoryl histidine: a probable intermediate in the microsomal glucose-6-phosphatase-inorganic pyrophosphatase reaction, Biochim Biophys Acta, 268: 698-710

Feliu JE, Hue L, Hers HG, 1976, Hormonal control of pyruvate kinase activity and of gluconeogenesis in isolated hepatocytes, Proc Natl Acad Sci U S A, 73: 2762-2766.

Finegood DT, Bergman AR, 1983, Optimal segments: a method for smoothing tracer data to calculate metabolic fluxes, Am J Physiol, 244: E472-E479

Foster JD, Pederson BA, Nordlie RC, 1997, Glucose-6-phosphase structure, regulation, and function: an update, Proc Soc Exp Biol Med, 215: 314-332

Francis F, Strom TM, Hennig S, Boddrich A, Lorenz B, Brandau O, Mohnike KL, Cagnoli M, Steffens C, Klages S, Borzym K, Pohl T, Oudet C, Econs MJ, Rowe PS, Reinhardt R, Meitinger T, Lehrach H, 1997, Genomic organization of the human PEX gene mutated in X-linked dominant hypophosphatemic rickets, Genome Res, 7: 573-585

Gardner LB, Liu Z, Barrett EJ, 1993, The role of glucose-6-phosphatase in the action of insulin on hepatic glucose production in the rat, Diabetes, 42: 1614-1620

Gerin I, Veiga-da-Cunha M, Achouri Y, Collet JF, van Schftingen E, 1997, Sequence of a putative glucose 6-phosphate translocase, mutated in glycogen storage disease type Ib, FEBS Lett, 419: 235-238

Ghishan FK, Rebeiz R, Honda T, Nakagawa N, 1993, Characterization and expression of a novel Na^+-inorganic phosphate transporter at the liver plasma membrane of the rat, Gastroenterology, 105: 519-526

Gishan FK, Rebeitz R, Honda T, Nakagawa N, 1993, Characterization and expression of a novel Na(+)-inorganic phosphate transporter at the liver plasma membrane of the rat, Gastroenterology, 105: 519-526

Gray RW, Haasch ML, Brown CE, 1983, Regulation of plasma 1,25-$(OH)_2$-D_3 by phosphate: evidence against a role for total or acid-soluble renal phosphate content, Calcif Tissue Int, 35: 773-777

Green J, Luong KV, Kleeman CR, Ye LH, Chaimovitz C, 1993, 1,25-Dihydroxyvitamin D3 inhibits Na(+)-dependent phosphate transport in osteoblastic cells, Am J Physiol, 264: C287-C295

Groen AK, Vervoorn RC, Van der Meer R, Tager JM, 1983, Control of gluconeogenesis in rat liver cells. I. Kinetics of the individual enzymes and the effect of glucagon, J Biol Chem, 258: 14346-14353

Hanson RW, Reshef L, 1997, Regulation of phosphoenolpyruvate carboxykinase (GTP) gene expression, Annu Rev Biochem, 66: 581-611

Hattenhauer O, Traebert M, Murer H, Biber J, 1999, Regulation of small intestinal Na-P(i) type IIb cotransporter by dietary phosphate intake, Am J Physiol, 277: G756-G762

Hemrika W, Wever R, 1997, A new model for the membrane topology of glucose-6-phosphatase, the enzyme involved in von Gierke disease, FEBS Lett, 409: 317-319

Hilfiker H, Hattenhauer O, Traebert M, Foster I, Murer H, Biber J, 1998, Characterization of a murine type II sodium-phosphate cotransporter expressed in mammalian small intestine, Proc Natl Acad Sci U S A, 95: 14564-14569

Hiraiwa H, Pan CJ, Lin B, Moses SW, Chou JY, 1999, Inactivation of the glucose 6-phosphate transport causes glycogen storage disease type 1b, J Biol Chem, 274: 5532-5536

Holm IA, Huang X, Kunkel LM, 1997, Mutational analysis of the PEX gene in patients with X-linked hypophosphatemic rickets, Am J Hum Genet, 60: 790-797

Horl WH, Kreusser W, Rambausek M, heidland A, Ritz E, 1983, Glycogen metabolism in phosphorus-depleted rats, Miner Electrolyte Metab, 9: 113-118

Hruska KA, Cheng FSL, Gupta A, Halstead L, Avioli L, 1995, X-linked hypophosphatemic rickets and the murine Hyp homologue, Am J Physiol, 268: F357-F362

Hue L, Bontemps F, Hers HG, 1975, The effects of glucose and of potassium ions on the interconversion of the two forms of glycogen phosphorylase and of glycogen synthetase in isolated rat liver preparations, Biochem J, 152: 105-114

HYP Consortium, 1995, A gene (PEX) with homologies to endopeptidases is mutated in patients with X-linked hypophosphatemic rickets. Nat Genet, 11: 130-136

Ihara K, Ryuichi K, Hara T, 1998, Genomic structure of the human glucose-6-phosphatase and novel mutations in the gene of a Japanese patient with glycogen storage disease type Ib, Hum Genet, 103: 493-496

Ishibashi K, Miyamoto K, Taketani Y, Morita K, Takeda E, Sasaki S, Imai M, 1998, Molecular cloning of a second human stanniocalcin homologue (STC2), Biochem Biophys Res Commun, 250: 252-258

Jara A, Lee E, Stauber D, Moatamed F, Felsenfeld AJ, Kleeman CR, 1999, Phosphate depletion in the rat: effect of bisphosphonates and the calcemic response to PTH, Kidney Int, 55: 1434-1443

Katai K, Segawa H, Haga H, Morita K, Arai H, Tatsumi S, Taketani Y, Miyamoto K, Hisano S, Fukui Y, Takeda E, 1997, Acute regulation by dietary phosphate of the sodium-dependent phosphate transporter (NaP(i)-2) in rat kidney, J Biochem (Tokyo), 121: 50-55

Katai K, Miyamoto K, Kishida S, Segawa H, Nii T, Tanaka H, Tani Y, Arai H, Tatsumi S, Morita K, Taketani Y, Takeda E, 1999, Regulation of intestinal Na+-dependent phosphate co-transporters by a low-phosphate diet and 1,25-dihydroxyvitamin D3, Biochem J, 343: 705-712

Kato K, Bishop JS, 1972, Glycogen synthetase-D phosphatase. I. Some new properties of the partially purified enzyme form rabbit skeletal muscle, J Biol Chem, 247: 7420-7429

Kavanaugh MP, Kabat D, 1996, Identification and characterization of a widely expressed phosphate transporter/retrovirus receptor family, Kidney Int, 49: 959-963

Keller KM, Schutz M, Podskarbi T, Bindl L, Lentze MJ, Shin YS, 1998, A new mutation of the gucose-6-phosphatase gene in a 4-year-old girl with oligosymptomatic glycogen storage disease type Ia, J Pediatr, 132: 360-361

Kempson SA, Lotscher M, Kaissling B, Biber J, Murer H, Levi M, 1995, Parathyroid hormone action on phosphate transporter mRNA and protein in rat renal proximal tubules, Am J Physiol, 268: F784-F791

Khandelwal RL, Kasmani SA, 1980, Studies on inactivation and reactivation of homogeneous rabbit liver phosphoprotein phosphatase by inorganic pyrophosphate and divalent cations, Biochim Biophys Acta, 613: 95-105

Kido S, Ken-ichi M, Mizobuchi H, Taketani Y, Ohkido I, Ogawa N, Kaneko Y, Harashima S, Takeda E, 1999, Identification of regulatory sequences and binding proteins in the type II sodium/phosphate cotransporter NPT2 gene responsive to dietary phosphate, J Biol Chem, 274: 28256-28263

Kilav R, Silver J, Naveh-Many T, 1995, Parathyroid hormone gene expression in hypophosphatemic rats, J Clin Invest, 96: 327-333

Kilpatrick l, Garty BZ, lundquist KF, hunter K, et al., 1990, J Clin Invest, 86: 196-202

Klein P, Kanehisa M, DeLisi C, 1985, The detection and classification of membrane-spanning proteins, Biochim Biophys Acta, 815: 468-76

Kos CH, Tihy F, Econs MJ, Murer H, Lemieux N, Tenenhouse HS, 1994, Localization of a renal sodium-phosphate cotransporter gene to human chromosome 5q35, Genomics, 19: 176-177

Kountz PD, McCain RW, Raafat El-Maghrabi M, Pilkis SJ, 1986, Hepatic 6-phosphofructo-2-kinase/fructose-2,6-bisphosphatase: phosphate dependence and effects of other oxyanions, Arch Biochem Biophy, 251: 104-113

Kramer R, 1996, Structural and functional aspects of the phosphate carrier from mitochondria, Kidney Intern, 49: 947-952

Kraus-Friedmann N, 1984, Hormonal regulation of hepatic gluconeogenesis, Physiol Rev, 64: 170-259

Kurland IJ, Pilkis S, 1995, Covalent control of 6-phosphofructo-2-kinase/fructose-2,6-bisphosphatase: insights into autoregulation of a bifunctional enzyme, Protein Sci, 4: 1023-1037

Lajeunesse D, Meyer RA, Jr., Hamel L, 1996, Direct demonstration of a humorally-mediated inhibition of renal phosphate transport in the HYP mouse, Kidney Int, 50: 1531-1538

Lam CW, But WM, Shek CC, tong SF, Chan YS, Choy KW, Tse WY, Pang CP, hjelm NM, 1998, Glucose-6-phosphatase gene (727G-T) splicing mutation is prevalent in Hong Kong Chinese patients with glycogen storage disease type 1a, Clin genet, 53: 184-190

Lange AJ, Argaud D, el-Maghrabi MR, Pan W, Maitra SR, Pilkis SJ, 1994, Isolation of a cDNA for the catalytic subunit of rat liver glucose-6-phosphatase, regulation of gene expression in FAO hepatoma cells by insulin, dexamethasone and cAMP, Biochem Biophys Res Commun, 201: 302-309

Lee WJ, Lee HM, Chi CS, Shu SG, Lin LY, Lin WH, 1996, Genetic analysis of the glucose-6-phosphatase mutation of type 1a glycogen storage disease in a Chinese family, Clin Genet, 50: 206-211

Lei KJ, Shelly LL, Pan CJ, Sidbury JB, Chou JY, 1993, Mutations in the glucose 6-phosphatase gene that cause glycogen storage disease type 1a, Science, 262: 580-583

Lei KJ, pan CJ, Shelly LL, Liu JL, Chou JY, 1994, Identification of mutations in the gene for glucose-6-phosphatase, the enzyme deficient in glycogen storage disease type Ia, J Clin Invest, 93: 1994-1999

Lei KJ, Shelly LL, Pan CJ, liu JL, Chou JY, 1995a, Structure-function analysis of human glucose-6-phosphatase, the enzyme deficient in glycogen storage disease type 1a, J Biol Chem., 270: 11882-11886

Lei KJ, Chen YT, Chen H, Wong LJ, Liu JL, McConkie-Rosell A, Van Hove JL, Ou HC, Yeh NJ, Pan LY, Chou JY, 1995b, Genetic basis of glycogen storage disease type 1a: prevalent mutations at the glucose-6-phosphatase locus, Am J Hum Genet, 57: 766-771

Lei KJ, Chen H, Pan CJ, Ward JM, Mosinger B Jr, Lee EJ, Westphal H, Mansfield BC, Chou JY, 1996, Glucose-6-phosphatase dependent substrate transport in the glycogen storage disease type-1a mouse, Nat Genet, 13: 203-209

Levi M, Lotscher M, Sorribas V, Custer M, Arar M, Kaissling B, Murer H, Biber J, 1994, Cellular mechanisms of acute and chronic adaptation of rat renal P(i) transporter to alterations in dietary P(i), Am J Physiol, 267: F900-F908

Li H, Onwochei M, Ruch RJ, Xie Z, 1996, Regulation of rat Na/Pi cotransporter-1 gene expession: the roles of glucose and insulin, Am J Physiol, 271: E1021-E1028

Li Y, Mèchin MC, van de Werve G, 1999, Diabetes affects similarly the catalytic subunit and putative glucose-6-phosphate translocase of glucose-6-phosphatase, J Biol Chem, 274: 33866-33868

Li Y, van de Werve G, 2000, Distinct hormone stimulation and counteraction by insulin of the expression of the two components of glucose 6-phosphatase in HepG2 cells, Biochem Biophys Res Commun, 272: 41-44

Lin B, Morris DW, Chou JY, 1997, The role of HNF1α, HNF3γ, and cyclic AMP in glucose-6-phosphatase gene activation, Biochemistry, 36: 14096-14106

Lin B, Annabi B, Hiraiwa H, Pan CJ, Chou JY, 1998a, Cloning and characterization of cDNAs encoding a candidate glycogen storage disease type 1b protein in rodents, J Biol Chem, 273: 31656-31660

Lin B, Morris DW, Chou JY, 1998b, Hepatocyte nuclear factor 1α is an accessory factor required for activation of glucose-6-phosphatase gene transcription by glucocorticoids, DNA Cell Biol, 17: 967-74

Lin B, Hiraiwa H, Pan CJ, Nordlie RC, Chou JY, 1999, Type-1c glycogen storage disease is not caused by mutations in the glucose-6-phosphate transporter gene, Hum Genet, 105: 515-517

Lipman ML, Panda D, Bennett HP, Henderson JE, Shane E, Shen Y, Goltzman D, Karaplis AC, 1998, Cloning of human PEX cDNA. Expression, subcellular localization, and endopeptidase activity, J Biol Chem, 273: 13729-13737

Lotscher M, Scarpetta Y, Levi M, Halaihel N, Wang H, Zajicek HK, Biber J, Murer H, Kaissling B, 1999, Rapid downregulation of rat renal Na/P(i) cotransporter in response to parathyroid hormone involves microtubule rearrangement, J Clin Invest, 104: 483-494

Lu M, Wagner GF, Renfro JL, 1994, Stanniocalcin stimulates phosphate reabsorption by flounder renal proximal tubule in primary culture, Am J Physiol, 267: R1356-R1362

Lucius RW, Waddell ID, Burchell A, Nordlie RC, 1993, The hepatic glucose-6-phosphatase system in Ehrlich-ascites-tumour-bearing mice, Biochem J, 290: 907-911

Lucius RW, Waddell ID, Burchell A, Nordlie RC, 1995, An altered T2β translocase of the glucose-6-phosphatase system in the membrane of the endoplasmic reticulum from livers of Ehrlich-ascites-tumour-bearing mice, Biochem J, 311: 537-540

Lyon MF, Scriver CR, Baker LR, Tenenhouse HS, Kronick J, Mandla S, 1986, The Gy mutation: another cause of X-linked hypophosphatemia in mouse, Proc Natl Acad Sci U S A, 83: 4899-4903

Marcolongo P, Fulceri R, Giunti R, Burchell A, Benedetti A, 1996, Permeability of liver microsomal membranes to glucose, Biochem Biophys Res Commun, 219: 916-922

Marcolongo P, Barone V, Priori G, Pirola B, Gilglio S, Biasucci G, Zammarchi E, Parenti G, Burchell A, Benedetti A, Sorrentino V, 1998, Structure and mutation analysis of the glycogen storage disease type 1b gene, FEBS Lett, 436: 247-250

Massillon D, Barzilai N, Chen W, Hu M, Rossetti L, 1996, Glucose regulates *in vivo* glucose-6-phosphatase gene expression in the liver of diabetic rats, J Biol Chem, 271: 9871-9874

Massillon D, Barzilai N, Hawkins M, Prus-Wertheimer D, Rossetti L, 1997, Induction of hepatic glucose-6-phosphatase gene expression by lipid infusion, Diabetes, 46: 153-157

Matschinsky FM, 1996, A lesson in metabolic regulation inspired by the glucokinase glucose sensor paradigm, Diabetes, 45: 223-241

McArthur MD, You D, Klapstein K, Finegood DT, 1999, Glucose effectiveness is the major determinant of intravenous glucose tolerance in the rat, Am J Physiol, 276: E739-E746

Méchin MC, van de Werve G, 2000a, G6P transporter and receptor functions of the glucose 6-phosphatase system analyzed from a consensus defined by multiple alignments, Protein, in press

Méchin MC, Annabi B, Pegorier JP, van de Werve G, 2000b, Ontogeny of the catalytic subunit and putative glucose-6-phosphate transporter proteins of the rat microsomal liver glucose-6-phosphatase system, Meta, 49: 1-5

Mersmann HJ, Segal HL, 1967, An on-off mechanism for liver glycogen synthetase activity, Proc Natl Acad Sci USA, 58: 1688-1695

Meyer RA Jr, Meyer MH, Gray RW, 1989, Parabiosis suggests a humoral factor is involved in X-linked hypophosphatemia in mice, J Bone Miner Res, 4: 493-500

Middleditch C, Clottes E, Burchell A, 1998, A different isoform of the transport protein mutated in the glycogen storage disease 1b is expressed in brain, FEBS Lett, 433: 33-36

Minassian C, Zitoun C, Mithieux G, 1996, Differential time course of liver and kidney glucose-6 phosphatase activity during long-term fasting in rat correlates with differential time course of messenger RNA level, Mol Cell Biochem, 155: 37-41

Mithieux G, Bordeto JC, Minassian C, Ajzannay A, Mercier I, Riou JP, 1993, Characteristics and specificity of the inhibition of liver glucose-6-phosphatase by arachidonic acid. Lesser inhibitability of the enzyme of diabetic rats, Eur J Biochem, 213: 461-466

Mithieux G, Zitoun C, 1996, Mechanisms by which fatty-acyl-CoA esters inhibit or activate glucose-6-phosphatase in intact and detergent-treated rat liver microsomes, Eur J Biochem, 235: 799-803

Mithieux G, Daniele N, Payrastre B, Zitoun C, 1998, Liver microsomal glucose-6-phosphatase is competitively inhibited by the lipid products of phosphatidylinositol 3-kinase, J Biol Chem, 273: 17-19

Moallem E, Kilav R, Silver J, Naveh-Many T, 1998, RNA-Protein binding and post-transcriptional regulation of parathyroid hormone gene expression by calcium and phosphate, J Biol Chem, 273: 5253-5259

Moore EE, Kuestner RE, Conklin DC, Whitmore TE, Downey W, Buddle MM, Adams RL, bell LA, Thompson DL, Wolf A, Chen L, Stamm MR, Grant FJ, Lok S, Ren H, De Jongh KS, 1999, Stanniocalcin 2: characterization of the protein and its location to human pancreatic alpha cells, Horm Metab Res, 31: 406-414

Murer H, Werner A, Reshkin S, Wuarin F, Biber J, 1991, Cellular mechanism in proximal tubular reabsorption of inorganic phosphate, Am J Physiol, 260: C885-C889

Murer H, Forster I, Hernando N, Lambert G, Traebert M, Biber J, 1999, Posttranscriptional regulation of the proximal tubule NaPi-II transporter in response to PTH and dietary Pi, Am J Physiol, 277: F676-F684

Nelson AE, Namkung HJ, Patava J, Wilkinson MR, Chang AC, Reddel RR, Robinson BG, Mason RS, 1996, Characteristics of tumor cell bioactivity in oncogenic osteomalacia, Mol Cell Endocrinol, 124: 17-23

Nesbitt T, Coffman TM, Griffiths R, Drezner MK, 1992, Crosstransplantation of kidneys in normal and Hyp mice. Evidence that the Hyp mouse phenotype is unrelated to an intrinsic renal defect, J Clin Invest, 89: 1453-1459

Nesbitt T, Econs MJ, Byun JK, Martel J, Tenenhouse HS, Drezner MK, 1995, Phosphate transport in immortalized cell cultures from the renal proximal tubule of normal and Hyp mice: evidence that the HYP gene locus product is an extrarenal factor, J Bone Miner Res, 10: 1327-1333

Noguchi T, Inoue H, Tanaka T, 1985, Transcriptional and post-transcriptional regulation of L-type pyruvate kinase in diabetic rat liver by insulin and dietary fructose, J Biol Chem, 260: 14393-14397

Nordlie RC, Lygre DG, 1966, The inhibition by citrate of inorganic pyrophosphate-glucose phosphotransferase and glucose 6-phosphatase, J Biol Chem, 241: 3136-3141

Nordlie RC, Jorgenson RA, 1981, Latency and inhibitability by metabolites of glucose-6-phosphatase of permeable hepatocytes from fasted and fed rats, J Biol Chem, 256: 4768-4771

Nordlie RC, Sukalski KA, Munoz JM, Baldwin JJ, 1983, Type Ic, a novel glycogenosis. Underlying mechanism, J Biol Chem, 258: 9739-9744

Nordlie RC, Scott HM, Waddell ID, Hume R, Burchell A, 1992, Analysis of human hepatic microsomal glucose-6-phosphatase in clinical conditions where the T2 pyrophosphate/phosphate transport protein is absent. Biochem J, 281: 859-863

Nouspikel T, Iynedjian PB, 1992, Insulin signaling and regulation of glucokinase gene expression in cultured hepatocytes, Eur J Biochem, 210: 365-373

Nowicki M, Fliser D, Fode P, Ritz E, 1996, Changes in plasma phosphate levels influence insulin sensitivity under euglycemic conditions, J Clin Endo Met, 81: 156-159

Ochs RS, Lardy HA, 1983, Catecholamine stimulation of hepatic gluconeogenesis at the site between pyruvate and phosphoenolpyruvate, J Biol Chem, 258: 9956-9962

Olsen HS, Cepeda MA, Zhang QQ, Rosen CA, Vozzolo BL, 1996, Human stanniocalcin: a possible hormonal regulator of mineral metabolism, Proc Natl Acad Sci U S A, 93: 1792-1796

Olson AL, Pessin JE, 1996, Structure, function, and regulation of the mammalian facilitative glucose transporter gene family, Annu Rev Nutr, 16: 235-256

Pan CJ, Lei KJ, Annabi B, Hemrika W, Chou JY, 1998, Transmembrane topology of glucose-6-phosphatase, J Biol Chem, 273: 6144-6148

Pan CJ, Lin B, Chou JY, 1999, Transmembrane topology of human glucose 6-phosphate transport, J Biol Chem, 274: 13865-13869

Paula FJA, Plens AECM, Foss MC, 1998, Effects of hypophosphatemia on glucose tolerance and insulin secretion, Horm Metab Res, 30: 281-284

Pederson BA, Foster JD, Nordlie RC, 1998a, Histone II-A activates the glucose-6-phosphatase system without microsomal membrane permeabilization, Arch Biochem Biophy, 357: 173-177

Pederson BA, Foster JD, Nordlie RC, 1998b, Low-K_m mannose-6-phosphatase as a criterion for microsomal integrity, Biochem Cell Biol, 76: 115-124

Pederson BA, Nordlie MA, Foster JD, Nordlie RC, 1998c, Effects of ionic strength and chloride ion on activities of the glucose-6-phosphatase system: regulation of the biosynthetic activity of glucose-6-phosphatase by chloride ion inhibition/deinhibition, Arch Biochem Biophys, 353: 141-151

Pfister MF, Lederer E, Forgo J, Ziegler U, Lotscher M, Quabius ES, Biber J, Murer H, 1997, Parathyroid hormone-dependent degradation of type II Na+/Pi cotransporters, J Biol Chem, 272: 20125-20130

Pfister MF, Ruf I, Stange G, Ziegler U, Lederer E, Biber J, Murer, 1998, Lysosomal degradation of renal type II Na/Pi cotransporte, a novel principal in the regulation of membrane transport, Proc Natl Acad Sci USA, 45: 1909-1914

Popovetzer MM, 1981, Tumor-induced hypophosphatemic osteomalacia (TUO): evidence for a phosphaturic cyclic AMP-independent action of tumour extract, Clin Res, 29: 418A

Puskàs F, Marcolongo P, Watkins SL, Mandl J, Allan BB, Houston P, Burchell A, Benedetti A, Banhegyi G, 1999, Conformational change of the catalytic subunit of glucose-6-phosphatase in rat liver during the fetal-to-neonatal transition, J Biol Chem, 274: 117-122

Rake JP, ten Berge AM, Verlind E, Visser G, Niezen-koning KE, Buys CH, Smit GP, Scheffer H, 1999, Glycogen storage disease type Ia. Four novel mutations (175delGG, R170X, G266V and V338F) identified, Mutations in brief no.220. Online, Hum Mutat, 13: 173

Ravenscroft AJ, Valentine JMJ, Knappett PA, 1999, Sever hypophosphataemia and insulin resistance in diabetic ketoacidosis, Anaesthesia, 54: 198

Rifas L, Gupta A, Hruska KA, Avioli LV, 1995, Altered osteoblast gluconeogenesis in X-linked hypophosphatemic mice is associated with a depressed intracellular pH, Calcif Tissue Int, 57: 60-63

Rowe PSN, 1998, The role of the PHEX gene (PEX) in families with X-linked hypophosphataemic rickets, Curr Opin Nephrol Hypertens, 7: 367-376

Schmoll D, Wasner C, Hinds CJ, Allan BB, Walther R, Burchell A, 1999, Identification of a cAMP response element within the glucose- 6-phosphatase hydrolytic subunit gene promoter which is involved in the transcriptional regulation by cAMP and glucocorticoids in H4IIE hepatoma cells, Biochem J, 338: 457-463

Schulze HU, Nolte B, Kannler R, 1986, Evidence for changes in the conformational status of rat liver microsomal glucose-6-phosphate: phosphohydrolase during detergent-dependent membrane modification, J Biol Chem, 261: 16571-16578

Seoane J, Trinh K, O'Doherty RM, Gomez-foix AM, Lange AJ, Newgard CB, Guinovart JJ, 1997, Metabolic impact of adenovirus-mediated overexpression of the gucose-6-phosphatase catalytic subunit in primary hepatocytes, J Biol Chem, 272: 26972-26977

Sestoft L, Bartels PD, 1981, Regulation of metabolism by inorganic phosphate, In: Short-term regulation of liver metabolism, edited by L Hue and G van de Werve, pp. 427-452, Amsterdam: Elservier/North Holland Biomedical Press

Shaul PW & Anderson RW, 1998, Role of plasmalemmal caveolae in signal transduction, Am J Physiol, 275: L843-L851

Shelly LL, Lei KJ, Pan CJ, Sakata SF, Ruppert S, Schutz G, Chou JY, 1993, Isolation of the gene for murine glucose 6-phosphatase, the enzyme deficient in glycogen storage disease type 1a, J Biol Chem, 268: 21482-21485

Spagnoli D, Dobrosielski-Vergona K, Widnell CC, 1983, Effects of hormones on the activity of glucose-6-phosphatase in primary cultures of rat hepatocytes, Arch Biochem Biophys 226: 182-189

St-Denis JF, Comte B, Nguyen DK, Seidman E, Paradis K, Levy E, van de Werve, 1994, A conformational model for the human liver microsomal glucose-6-phosphatase system: evidence from rapid kinetics and defects in glycogen storage disease type Ia, Journal of Clinical Endocrinology and Metabolism, 79: 955-959

St-Denis JF, Berteloot A, Vidal H, Annabi B, van de Werve G, 1995a, Glucose transport and glucose-6-phosphate hydrolysis in intact rat liver microsomes, J Biol Chem, 270: 21092-21097

St-Denis JF, Annabi B, Khoury H, van de Werve G, 1995b, Histone II-A stimulates glucose-6-phosphatase and reveals mannose-6-phosphatase activities without permeabilization of liver microsomes, Biochem J, 310: 221-224

Streeper RS, Svitek CA, Chapman S, Greenbaum LE, Taub R, O'Brien RM, 1997, A multicomponent insulin response sequence mediates a strong repression of mouse glucose-6-phosphatase gene transcription by insulin, J Biol Chem, 272: 11698-11701

Strom TM, Francis F, Lorenz B, Boddrich A, Econs MJ, Lehrach H, Meitinger T, 1997, Pex gene deletions in Gy and Hyp mice provide mouse models for X-linked hypophosphatemia, Hum Mol Genet, 6: 165-171

Stroppiano M, Regis S, DiRocco M, Caroli F, Gandullia P, Gatti R, 1999, Mutations in the glucose-6-phosphatase gene of 53 Italian patients with glycogen storage disease type Ia, J Med Genet, 33: 358-360

Taketani Y, Segawa H, Chikamori M, Morita K, Tanaka K, Kido S, Yamamoto H, Iemori Y, Tatsumi S, Tsugawa N, Okano T, Kobayashi T, Miyamoto K, Takeda E, 1998, Regulation of type II renal Na^+-dependent inorganic phosphate transporters by 1,25-dihydroxyvitamin D3. Identification of a vitamin D-responsive element in the human NAPi-3 gene, J Biol Chem, 273: 14575-14581

Tenenhouse HS, Scriver CR, McInnes RR, Glorieux FH, 1978, Renal handling of phosphate in vivo and in vitro by the X-linked hypophosphatemic male mouse: evidence for a defect in the brush border membrane, Kidney Int, 14: 236-244

Tenenhouse HS, Werner A, Biber J, Ma S, Martel J, Roy S, Murer H, 1994, Renal Na(+)-phosphate cotransport in murine X-linked hypophosphatemic rickets. Molecular characterization, J Clin Invest, 93: 671-676

Tenenhouse HS, Martel J, Biber J, Murer H, 1995, Effect of Pi restriction on renal Na^+-Pi cotransporter mRNA and immunoreactive protein in X-linked Hyp mice, Am J Physiol, 268: F1062-F1069

Tenenhouse HS, 1999, X-linked hypophosphataemia: a homologous disorder in humans and mice, Nephrol Dial Transplant, 14: 333-341

Trinh K, Minassian C, Lange A, O'Doherty RM, Newgard CB, 1997, Adenovirus-mediated expression of the catalytic subunit of glucose-6-phosphatase in INS-1 cells. Effects on glucose cycling, glucose usage, and insulin secretion, J Biol Chem, 272: 24837-24842

Trinh KY, O'Doherty RM, Anderson P, Lange AJ, Newgard CB, 1998, Perturbation of fuel homeostasis caused by overexpression of the glucose-6-phosphatase catalytic subunit in liver of mormal rats, J Biol Chem, 273: 31615-31620

Trioche P, Francoual J, Chalas J, Capel L, Bernard O, Labrune P, 1999, Identification of three novel mutations (Q54P, W70X and T108I) in the glucose-6-phosphatase gene of patients with glycogen storage disease type Ia, Mutation in brief no. 256 Online, Hum Mutat, 14: 91

Tsuboi KK, Fukunaga K, 1965, Inorganic phosphate and enhanced glucose degradation by the intact erythrocyte, J Biol Chem, 240: 2806-2810

Tyynismaa H, Kaitila I, Nanto-Salonen K, Ala-Houhala M, Alitalo T, 2000, Identification of fifteen novel PHEX gene mutations in Finnish patients with hypophosphatemic rickets, Hum Mutat (Online), 15: 383-384

van de Werve, Lange A, Newgard C, Méchin MC, Li Y, Berteloot A, 2000, New lessons in the regulation of glucose metabolism taught by the glucose 6-phosphatase system, Eur J Biochem, 267: 1533-1549

van Schaftingen E, Lederer B, Bartrons R, Hers HG, 1982, A kinetic study of pyrophosphate: fructose-6-phosphate phosphotransferase from potato tubers. Application to a microassay of fructose 2,6-bisphosphate, Eur J Biochem, 129: 191-195

van Schaftingen E, Vandercammen A, Detheux M, Davies DR, 1992, The regulatory protein of liver glucokinase, Adv Enzyme Regul, 32: 133-148

Vargas AM, Sola MM, Lange AJ, Poveda G, Pilkis SJ, 1994, cAMP-independent synergistic effects of insulin and dexamethasone on fructose 2,6-bisphosphate metabolism in H4IIE cells, Diabetes, 43: 792-799

Vaulont S, Munnich A, Decaux JF, Kahn A, 1986, Transcriptional and post-transcriptional regulation of L-type pyruvate kinase expression in rat liver, J Biol Chem, 261: 7621-7625

Veiga-da-Cunha M, Gerin I, Chen YT, Lee PJ, Leonard JV, Maire I, Wendel U, Vikkula M, van Schaftingen E, 1999, The putative glucose 6-phosphate translocase gene is mutated in essentially all cases of glycogen storage disease type I non-a, Eur J Hum Genet, 7: 717-723

Veiga-da-Cunha M, Gerin I, Van Schaftingen E, 2000, How many forms of glycogen storage disease type I?, Eur J Pediatr, 159: 314-318

Vidal H, Berteloot A, Larue MJ, St-Denis JF, van de Werve G, 1992, Interaction of mannose-6-phosphate with the hysteretic transition in glucose-6-phosphate hydrolysis in intact liver microsomes, FEBS Lett, 302: 197-200

Voice MW, Scott HM, Watkins SL, Middleditch C, Burchell A, 1996, A comparison of the renal and hepatic microsomal glucose-6-phosphatase enzymes, Arch Biochem Biophys 330: 380-386

Waddell ID, Lindsay JG, Burchell A, 1988, The identification of T2; the phosphate/pyrophosphate transport protein of the hepatic microsomal glucose-6-phosphatase system, FEBS Lett, 229: 179-182

Waddell ID, Scott H, Grant, Burchell A, 1991, Identification and characterization of a hepatic microsomal glucose transport protein. T3 of the glucose-6-phosphatase system?, Biochem J, 275: 363-367

Waddell ID, Zomerschoe AG, Voice MW, Burchell A, 1992, Cloning and expression of a hepatic microsomal glucose transport protein, Biochem J, 286: 173-177

Wagner GF, Vozzolo BL, Jaworski E, Haddad M, Kline RL, Olsen HS, Rosen CA, Davidson MB, Renfro JL, 1997, Human stanniocalcin inhibits renal phosphate excretion in the rat, J Bone Min Res, 12: 165-171

Werner A, Moore ML, Mantel N, Biber J, Semenza G, Murer H, 1991, Cloning and expression of cDNA for a Na/Pi cotransport system of kidney cortex, Proc Natl Acad Sci USA, 88: 9608-9612

White TK, Wilson JE, 1990, Binding of nucleoside triphosphates, inorganic phosphate, and other polyanionic ligands to the N-terminal region of rat brain hexokinase: relationship to regulation of hexokinase activity by antagonistic interactions between glucose 6-phosphate and inorganic phosphate, Arch Biochem Biophys, 277: 26-34

Wu S, Finch J, Zhong M, Slatopolsky E, Grieff M, Brown AJ, 1996, Expression of the renal 25-hydroxyvitamin D-24-hydroxylase gene: regulation by dietary phosphate, Am J Physiol, 271: F203-F208

Yoshiko Y, Son A, Maeda S, Igarashi A, Takano S, Hu J, Maeda N, 1999, Evidence for stanniocalcin gene expression in mammalian bone, Endocrinology, 140: 1869-1874

Zhou XJ, Fadda GZ, Perna AF, Massry SG, 1991, Phosphate depletion impairs insulin secretion by pancreatic islets, Kidney Int, 39: 120-128

Zingone A, Hiraiwa H, Pan CJ, Lin B, Chen H, Ward JM, Chou JY, 2000, Correction of glycogen storage disease type 1a in a mouse model by gene therapy, J Biol Chem, 275: 828-832